A study of the Microtubule associated protein family, MAP65, in Arabidopsis

Kaloriti, Despina

A study of the Microtubule Associated Protein family, MAP65, in *Arabidopsis*

By Despina Kaloriti

Submitted in accordance with the requirements for the degree of Doctor of Philosophy

University of Durham

School of Biological and Biomedical Sciences

September 2004

Declaration

The material contained in this thesis has not been submitted for another degree on the University of Durham or any other University. Unless otherwise stated, all original research within this thesis is the candidates own.

Statement of Copyright

Acknowledgements

I am extremely grateful to Prof. Patrick Hussey for his excellent supervision, constructive criticism and his generous support throughout this work. I would also like to express my gratitude to Dr Andrei Smertenko for his never-ending patience teaching me since I was an undergraduate student in the lab and for his advice throughout my PhD project. The MAP65 phylogenetic tree in chapter 3 was constructed in co-operation with Dr Andrei Smertenko, who also provided me with the AtMAP65-1 and AtMAP65-5 proteins. Many thanks to Dr Mike Deeks for his advice on the yeast two hybrid technique, for proof reading chapters of this manuscript and for being a great friend. I would also like to thank Dr Stepan Fenyk for his advice on the 2D-PAGE gels and Mr Andrej Hlavacka and Mr Tim Hawkins for their co-operation in preparing *Arabidopsis* cDNA samples from various tissues. Thank you also to Dr Safina Khan for providing me with *AtMAP65-3* and *AtMAP65-9* PCR plasmids.

My thanks to all the past and present members of the lab for their friendship and for offering endless advice; particularly, to Dr Luísa Camacho for support and inspiration during long late-hours in the lab, to Ms Cecília Rodrigues and Ms Hsin-Yu Chang for encouragement during my writing, to Dr Hisako Igarashi, Dr Ellen Allwood, Dr Tijs Ketelaar and Mr Simon Dimmock. My appreciation is extended to Prof. Keith Lindsey for providing me the p-Δ-GUS-Bin19 plasmid and to the members of his lab for useful discussions on the *GUS* reporter gene technology. I would also like to thank Prof. Tony Slabas for providing me with *Arabidopsis* tissue culture cells.

Many thanks to Katerina Mattheou, Alessandra Badari, Daniel Price and Demetrios Vassilakos for their endless encouragement, to Mark Knell for constant support and for keeping up my morale and, to my past and present housemates in Palatine House who have all made Durham an enjoyable place to be.

Finally, and by no means least, I am indebted to my parents, Stamatios and Aggeliki and to my sister Myrsini for their moral and financial support throughout my education. This thesis is dedicated to them.

Abstract

Microtubules (MTs) play a key role in cell division and morphogenesis. Plant cells form four distinct MT arrays through the cell cycle; the interphase cortical array, the preprophase band, the spindle and the phragmoplast. The cortical array, the preprophase band and the phragmoplast are unique to plant cells. Microtubule Associated Proteins (MAPs) must be involved in the organisation of the MT structures. The most abundant plant MAPs are the MAP65 proteins. A database search has revealed the presence of nine *MAP65* genes in the *Arabidopsis* genome. Homologues of MAP65 proteins are present in vertebrates and yeast. Using prediction servers, putative phosphorylation and post-translation modification sites were identified in AtMAP65 protein sequences and transcription regulatory elements in *AtMAP65* promoter sequences.

The temporal and spatial expression of all nine AtMAP65 proteins was examined by transforming *Arabidopsis* with AtMAP65 promoter::GUS reporter gene transcriptional fusion constructs. The data revealed that the *AtMAP65* isoforms were expressed differentially in *Arabidopsis* seedling and flower tissues. The abundance of the each of the *AtMAP65* transcripts in various *Arabidopsis* tissues was investigated by Reverse Transcription-PCR.

The full length of *AtMAP65-6* coding sequence was cloned by screening cDNA libraries and subsequently, it was expressed in *E.coli*. The recombinant AtMAP65-6 protein was shown to bind MTs and to increase the turbidity of MT solutions. The possible protein-protein interactions between AtMAP65-1, AtMAP65-6 and AtMAP65-5 were assessed with yeast two hybrid assays and it was shown that AtMAP65-6 interacts with itself. An antibody was raised against AtMAP65-6 and used for investigating the AtMAP65-6 localisation to MT structures through the cell cycle. AtMAP65-6 does not bind to cortical MTs, however localises to preprophase band, anaphase spindle and phragmoplast. The anti-AtMAP65-6 antibody recognises three isoforms on a western blot of a 2D SDS-PAGE gel of total protein extract of *Arabidopsis* tissue culture cells.

List of Abbreviations

aa	amino acid
Ab	antibody
Ag	*Anopheles gambiae*
At	*Arabidopsis thaliana*
ABRC	*Arabidopsis* Biological Resource Center
AD	activation domain
APC	adenomatous polyposis coli
Agrobacterium	*Agrobacterium tumefaciens*
APS	ammonium persulphate
Arabidopsis	*Arabidopsis thaliana*
Ase1	Anaphase spindle Elongation factor 1
AtMAP65	*Arabidopsis thaliana* microtubule associated protein of 65 kilo Daltons
ATP	adenosine triphosphate
ATK1	*Arabidopsis thaliana* kinesin 1, Formally known as KATA
AtPAKRP1	*Arabidopsis thaliana* phragmoplast associated kinesin related protein 1
Bis-acrylamide	bis (N,N'- methylene-bis-acrtlamide)
BAC	Bacterial Artificial Chromosome
BD	binding domain
BIMC	block in mitosis C
BLAST	Basic Alignment Search Tool
bot1	*botero1*
BY2	bright yellow 2
bp	base pare
BSA	bovine serum albumin
^{o}C	degrees centigrade
Cc	critical concentration
cAMP	cyclic adenosine mono-phosphate

cDNA	complementary DNA
cdk	cyclin-dependent kinase
cGMP	cyclic guanosine mono-phosphate
CHAPS	3-[(3-Cholamidopropyl) dimethylammonio]-1-propanesulfonate
Ci	currie
CLIP170	cytoplasmic linker protein 170
CM	conserved motif
Col-0	Columbia 0
C-Terminal	Carboxy-Terminal
Dc	*Daucus carota*
DcMAP65	*Daucus carota* microtubule associated protein 65 of 65 kilo Daltons
DcKRP120	*Daucus carota* kinesin-related protein of 120 kilo Daltons
DEPC	diethyl pyrocarbonate
Dm	*Droshophila melanogaster*
DMSO	dimethylsulphoxide
CPAMs	cell plate assembly matrixes
DNA	deoxyribonucleic acid
ds	double stranded
DTT	dithiothreitol
EB1	end binding 1
ECL	enhanced chemiluminescence
E.coli	*Escherichia coli*
EDTA	ethylenediaminetetraacetic acid
EF1α	elongation factor 1α
EGTA	ethylene-glycol-bis (β-aminoethylether)-NNN'N'-tetra-acetic acid
E.indica	*Eleusine indica*
EST	expressed sequence tag

EtOH	ethanol
erh3	*ectopic root hair*
FITC	Fluorescein isothiocyanate
fra2	*fragile fibre*
FRAP	fluoresence recovery after photobleaching
GDP	guanosine diphosphate
gem1	*gemini pollen 1* (mutant)
GFP	green fluoresence protein
GTP	guanosine triphosphate
GUS	β-glucuronidase
h	hour
Hs	*Homo sapiens*
HSP90	heat shock protein 90
hik	*hinkel* (mutant)
IF	intermediate filament
IPTG	isopropyl-β-d-thiogalactoside
KCBP	kinesin-like calmodulin binding protein
KIC	KCBP interacting $Ca^{=2}$ binding protein
KIF2	kinesin superfamily protein 2
KINI	Kinesin, Internal motor
KIPK	KCBP-interacting protein kinase
kbp	kilobase pair
kDa	kilo Dalton
L	litre
LB	Luria-Bertani (culture medium)
LiAc	Lithium Acetate
MAP	Microtubule Associated Protein
MAPK	mitogen-activated protein kinase
MCAK	mitotic centromere-assiciated kinesin
Min	minute
Mm	*Mus musculus*

MOR1	microtubule organisator one
MOPS	3-(N-morpholino)propanesulfonic acid
mRNA	messenger ribonucleic acid
MS	Murashige and Skoog medium
MT	microtubule
MTOCs	microtubule organisation centres
MTSB	Microtubule stabilising buffer
MW	molecular weight
NACK1	NPK activating kinase-like proteins
Nc	*Neurospora crassa*
NCBI	National Centrer for Biotechnology Information
NLS	Nuclear localisation signal
NPK1	nucleus and phragmoplast-localised protein kinase 1
NQK1	negative kinase 1
Nt	*Nicotiana tabacum*
N-Terminal	Amino-Terminal
NtMAP65	*Nicotiana tabaccum* microtubule associated protein of 65 kilo Daltons
OD_{260}	optical density at a wavelenght of 260 nanometers
O/N	overnight
Os	*Oryza sativa*
PAGE	poly acrylamide gel electrophoresis
PBS	phosphate-buffered saline
pI	isoelectric point
PIPES	piperazine-N,N'-bis(2-ethansulphonic acid)
PKA	protein kinase A
PKC	protein kinase C
PLD	phospholipase D
PPB	preprophase band
PRC1	Protein Regulating Cytokinesis 1
PCR	polymerase chain reaction

PFS	planar fenestrated sheet
PGZ	peripheral growth zone
Ple	*pleiade* (mutant)
rcf	relative centrifugal force
Rn	*Rattus norvegicus*
RNA	ribonucleic acid
rpm	revolutions per minute
*rsw*1	*radial swelling* 1 (mutant)
RT	reverse transcription
RT-PCR	reverse transcriptase polymerase chain reaction
SD	Synthetic dropout
SDS	sodium dodecyl sulphate
SDS-PAGE	sodium dodecyl sulphate poly-acrylamide gel Electrophoresis
Sc	*Saccharomyces cerevisiae*
Sec	second
Sp	*Schizosaccharomyces pompe*
Spc98p	spindle pole body component 98 kDa, protein of
SPR	*SPIRAL*
ss	single stranded
SSC	saline sodium citrate or standard saline citrate
TAE	Tris-Acetate + EDTA
TAN1	TANGLED 1
Taq	*Thermus aquaticus*
TBS	tris-buffered saline
TE	Tris/EDTA
TEMED	*N,N,N,'N'*-tetramethylethylenediamide
TKRP125	tobacco kinesin-related polypeptide of 125 kDa
TMBP200	*tobacco* microtubule bundling protein
TN	tubular network
TOGp	Tumour Overexpressing Gene, Protein of

Tris	tris-(hydroxymethyl)-aminomethane
TRITC	Tetramethylrhodamine isothiocyanate
TUA	alpha-tubulin gene
TVN	Tubular-vesicular networks
UTR	untranslated region
UV	ultraviolet light
v/v	volume for volume
WT	wild type
w/v	weight for volume
Y2H	yeast two hybrid
Xl	*Xenopus laevis*
XKCM1	*Xenopus* kinesin catastrophe modulator 1
X-Gal	5-bromo-4-chloro-3-indoyl-β-D-galactoside
X-Gluc	5-bromo-4-chloro-3-indoyl-β-D-glucuronic acid
YPDA	Yeast peptone dextrose adenine

TABLE OF CONTENTS

List of Figures

List of Tables

Chapter 1

Introduction

1.1 Cytoskeleton

The cytoskeleton is an important component of all eukaryotic cells. It is a dynamic network of protein filaments that extends throughout the cytoplasm and is involved in many processes such as nuclear and cell division, organelle movement and secretion, cell expansion and deposition of cell wall. The cytoskeletal organisation is responsible for the differentiation and growth of eukaryotic cells. Plant cells are surrounded by a rigid cell wall and are immobile. The development of tissues and organs is dependent on the balance of cell division and cell expansion and in particular on the positioning of the internal crosswalls in cytokinesis. Therefore, the cytoskeleton is important for both direction of division and cell shape. This makes it a key element for plant morphogenesis.

1.2 Microtubule Cytoskeleton

The plant cytoskeleton mainly consists of microtubules (MTs) and actin filaments. A third cytoskeletal element, intermediate filaments, was also found in plant cells (Shaw *et al.*, 1991). MTs are dynamic filamentous polymers and their ability to grow and shorten rapidly allows the rapid re-formation of MT structures, for example the conversion of interphase cortical array to mitotic spindles. Hence, before the description of the MT structures the assembly and disassembly of MTs will be discussed first, as they are key factors in the function of the MT cytoskeleton.

1.2.1 Tubulin

The α- and β-tubulin heterodimer is 8nm in length and heterodimers associate head to tail to form a protofilament. MTs normally consist of 13 linearly aligned protofilaments in the

form of a hollow tube with an internal diameter of 14 nm and an external diameter of 25 nm. MTs consist mainly of tubulin (Mw = 100,000), a heterodimeric protein of α and β subunits. A third tubulin subunit is γ-tubulin, which was found to be located at MT Organising Centres (MTOCs) (Liu *et al.*, 1993; Panteris *et al.*, 2000). The α-, β-, and γ-tubulins share 35% - 40 % identity with each other and their primary sequences are conserved between different organisms. All plants express multiple isoforms of both α- and β-tubulins that are distinct but related proteins encoded in multigene families (Hussey *et al.*, 1990). *Arabidopsis thaliana* has at least fifteen expressed tubulin genes, six α and nine β (Kopczak *et al.*, 1992, Snustad *et al.*, 1992). In addition to tubulin genetic complexity, more diversity within the cell may be generated at the protein level. Post-translation modifications of both α- and β-tubulins exist, such as acetylation, detyrosination, phosphorylation and glutamylation (Mandelkow *et al.*, 1995; Wymer and Lloyd, 1996).

1.2.2 MT Dynamics

The tubulin dimer binds to two molecules of the nucleotide guanine trisphosphate (GTP). One GTP molecule is bound to the α-tubulin subunit and it seems to have structural function, while the second GTP molecule binds to the β-tubulin subunit and is exchangeable (Burns and Surridge, 1994). At high concentrations of un-polymerised GTP-bound tubulin, the rate of addition of tubulin to the MT plus end is faster than the rate of hydrolysis of the GTP bound in the MT. Thus, a GTP cap is formed and the MT grows as only MTs whose terminal tubulin is associated with GTP are stable and can serve as primers for polymerisation of additional tubulin. After the tubulin dimer is incorporated onto the plus end of the MT, GTP bound to β-tubulin is hydrolysed to GDP and hence, the middle body of the MT contains GDP in the exchangeable site on β-tubulin. GTP binds to tubulin in a Mg^{2+} dependent manner, although GDP binding is Mg^{2+} independent. The GDP molecules are

only exchanged for GTP after MT disassembly. At low concentrations of unpolymerised GTP-bound tubulin, the rate of GTP hydrolysis at MT ends exceeds the rate of addition of tubulin and a GDP cap is formed. As the GDP cap is unstable, the MT end peels apart to release tubulin subunits.

MTs do not disassemble totally and each individual MT undergoes transitions between periods of rapid growth and shrinking, a function termed as MT dynamic instability. The transition between MT elongation and shortening is termed catastrophe, while the transition between shortening and elongation is called rescue. A MT undergoing rapid shortening has a certain probability of sudden transition to the elongation phase, which is called the rescue frequency. Equivalently, the probability of MT sudden transition from elongation to shortening phase is called catastrophe frequency. The dynamic instability is considered to have a main role in MTs conformation changes. The interphase plant MTs grow at 5 μm/min, shrink at 20 μm/min, and display catastrophe and rescue frequencies of 0.02 and 0.08 events/sec respectively, exhibiting faster turnover than the mammalian MTs (Dhonukshe *et al.*, 2003). The proteins located at microtubule plus ends could regulate dynamic instability (Howard and Hyman, 2003). For instance, the MT plus end binding EB1 protein increases the MT rescues and decreasing the catastrophes, resulting in an increase of MT polymerisation (Tirnauer *et al.*, 2002).

Recent studies in *Arabidopsis* cells transformed with GFP tubulin revealed that new MTs are initiated at the cell cortex and exhibit dynamics at both ends (Shaw *et al.*, 2003). The plus end undergoes polymerisation-biased dynamic instability, while the minus end undergoes slow depolymerisation. The balanced addition and removal of subunits at the MT ends results in MT migration across the cell cortex by a hybrid treadmilling mechanism. In

addition, MT bundles were observed to grow by incorporation of migrating MTs through treadmilling motility. The treadmilling MTs appeared to be common and long-lived in *Arabidopsis* cells and it was suggested treadmilling motility plays a key role in the organisation of the cortical array (Shaw *et al.*, 2003).

MT dynamics are essential for a variety of functions in living cells. As shown by fluoresence recovery after photobleaching (FRAP), MT turnover is approximately 20 times faster in mitotic compared to interphase arrays (Saxton *et al.*, 1984). This increase in MT turnover mediates the dramatic reorganisation of the long interphase MT arrays to form the generally shorter and close-packed MTs of the mitotic spindle. The extent of tubulin subunit incorporation into the mitotic spindle affects not just the dynamics of individual MTs but also the reorganisation of the entire mitotic spindle. For example, tubulin incorporation in the spindle midzone is associated with spindle elongation at mid- to late-anaphase stage (Wadsworth and Shelden, 1990). Any disruption or suppression of MT dymanics inhibits MT-dependent cellular functions.

1.3 Tubulin mutants effect plant growth and morphology

1.3.1 Herbicide Resistance

An example of how single mutations of plant tubulin can alter MTs properties comes from the herbicide resistance of *Eleusine indica* and transgenic maize calli against dinitroaniline (Anthony *et al.*, 1998, Anthony and Hussey, 1999). The *E. indica* resistance is caused by Thr239 substitution by Ile239 in α-tubulin. This position is close to the site of interaction between tubulin dimers in the protofilament (Anthony *et al.*, 1998). The same mutation can cause resistance in transgenic maize but also a substitution of Met268 to Thr268 also in α-tubulin has similar results (Anthony and Hussey, 1999). Double mutants of both α-tubulin

substitutions in transgenic maize increase the herbicide resistance phenotype, suggesting that these mutations are likely to act independently of each other. They probably act by changing the tubulin conformation so that herbicide binding is less effective and/or by stabilising the MT dimer-dimer interactions against the destabilising effect of the herbicide (Anthony and Hussey, 1999).

Plant MTs show different stability to anti-MT agents than animal MTs. Different mechanisms within plant and animal cells may result in their different response against de-stabilising agents. Even minor conformation differences between plant and animal α-, β-tubulin are likely to affect the herbicide's binding capacity. For example, plant MTs are more resistant to colchicine, which results in MT breakdown (Morejohn *et al.*, 1991). In contrast, dinitroaniline and phosphorothioamidate inhibit *in vitro* assembly of plant tubulin but do not effect animal MTs (Hugdahl and Morejohn, 1993). Cortical MTs are less sensitive to both these herbicides, while spindle and phragmoplast MTs are affected the most. The dinitroaniline and phosphorothioamidate herbicides result in inhibition of mitosis in plant cells.

1.3.2 Lefty Phenotype

Another example of how a mutation of plant tubulin can effect plant properties comes from the *lefty* phenotype in *Arabidopsis thaliana* (Thitamadee *et al*, 2002; Hashimoto T., 2002). Thitamadee and co-workers showed dominant negative mutations in the α-tubulins genes *TUA4* and *TUA6* caused left-handed helical growth and clockwise twisting in elongating organs. The *lefty* mutation results from a serine replacement by phenylalanine in the α-tubulin gene. Interestingly, the point where the mutation exists is predicted to be located at the contact region with β-tubulin within tubulin dimers (Thitamadee *et al*, 2002).

1.4 MT structures in plant cell cycle

The MT assemblies formed in higher plant cells are different from those in the animal cell. The plant MTs form four basic arrays during the cell cycle: the cortical MT array, preprophase band (PPB), mitotic spindle and phragmoplast (figure 1.1; Alberts *et al.*, 1994). The cortical array, the PPB and the phragmoplast are present only in plant cells.

1.4.1 Interphase cortical array

The interphase cortical array aids the alignment of cellulose microfibrils in the cell wall, and is important in determining the direction of cell expansion. However there is some controversy over the exact relationship between MTs, cellulose microfibrils and growth polarity (Wasteneys, 2000). The fact is the cortical MTs reorientate as the direction of growth changes due to environmental and hormonal factors (Lloyd and Hussey, 2001). Additionally, depending on the stage of the cell cycle, MTs may emerge from the nuclear surface and radiate toward the cell periphery. These nucleus associated MTs are prominent when the new interphase array is formed (post-cytokinesis) and during preprophase. It has been suggested that perinuclear MTs and actin filaments are not only actively involved in the realignment of pre-existing cortical MTs but integrate into, or may form, the PPB (Lambert and Lloyd, 1994).

Cortical MTs regulate the direction in which cellulose is deposited and so mediate directional cell growth. It has been suggested that parallel MTs provide tracks for cellulose synthases. As the cellulose arrangement controls the direction of cell growth a connection has been proposed between cortical MTs and microfibrils alignment and that the orientation of these microfibrils are in parallel to the orientation of the MTs (Hable *et al.*, 1998; Kost *et*

Figure 1.1
MT arrays through the cell cycle

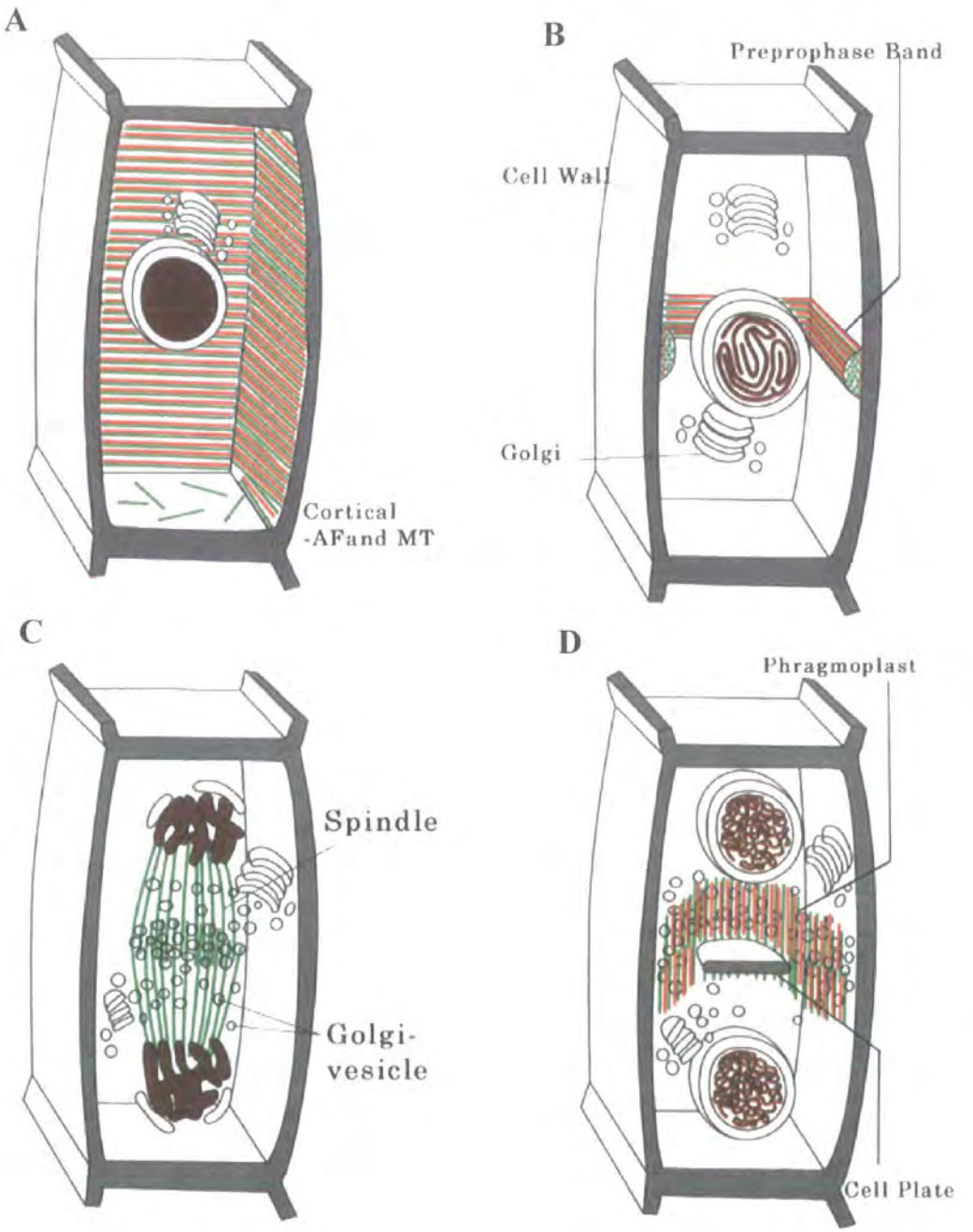

Figure 1.1: The MT organisation in the interphase cortical array (**A**), in the Preprophase Band (**B**), in the mitotic spindle (**C**) and in the cytokinetic phragmoplast (**D**). (Image by Alberts *et al.*, 1994)

al., 1999). Still, it is not clear to what extent this is true but unorganised cortical MTs result in disorganised cell wall formation as it was proved by the *mor1/gem1* mutant (Whittington *et al.*, 2001; Twell *et al.*, 2002). MTs are not always parallel to the microfibrils, after the cells leave the elongation state the MT arrays rotate and adopt helical conformations, which could be in different direction than microfilaments alignment (Baskin *et al.*, 2001). The classical hypothesis of cellulose-MT 1:1 relationship has been brought into doubt by studying the cellulose-deficient radial swelling mutant (*rsw1*; Arioli *et al.*, 1998) in *Arabidopsis*. Sugimoto and co-workers observed that microfibrils lose their transverse alignment in radially swollen *rsw1* epidermal cells while MTs remain transversely arranged, indicating that cellulose microfibrils do not use MTs as orientation template (Sugimoto *et al.*, 2001).

1.4.2 Preprophase band

PPB is a ring of MTs, which predicts the plane in which the cell will divide. The PPB and the interphase array temporally overlap. Hence, it is possible that the PPB is made by re-utilisation of the existing cortical MTs. The PPB starts forming among the interphase cortical array at the end of the S phase. Its development continues through G2 to a mature, narrow PPB. It coexists briefly with the prophase spindle, which forms around the nucleus (Mineyuki and Gunning, 1990). It has been also suggested that perinuclear MTs may integrate and form the PPB (Staiger *et al.*, 1991). A variety of molecules, such as cyclin-dependent kinases (Stals *et al.*, 1997), γ-tubulin (Liu *et al.*, 1993) and kinesin-like proteins (Asada *et al.*, 1997; Bowser and Reddy, 1997) have been detected at the PPB site. The mechanism by which these molecules could contribute to cell plate positioning is uncertain. In a mutant of the *Arabidopsis TONNEAU2* gene, which encodes a putative novel protein phosphatase 2A regulatory subunit, the plant cells were unable to form the PPB (Camilleri *et*

al., 2002). In addition, concentration of Golgi stacks at the site where the future cell plate will be positioned was observed (Nebenfuhr *et al.*, 2000). Dixit *et al.*, 2002, investigated the possibility of Golgi secretion to be involved in marking the PPB site (Dixit *et al.*, 2002). However, inhibition of Golgi secretion by brefeldin A during PPB formation did not prevent the phragmoplast formation at the predicted from the PPB site, indicating Golgi stacks do not have a functional role in determing the cell division site.

Dhonukshe and co-workers using MT plus-end labelling with the yellow fluorescent protein CLIP170 (Cytoplasmic Linker protein 170), suggested that the altered MT dynamic instability influences PPB formation and proposed a model for PPB formation (Dhonukshe *et al.*, 2003). Based to this model the PPB formation was resolved into four stages: PPB initiation, narrowing, maturation and breakdown. In PPB initiation, a broad PPB forms, which overlaps almost two-thirds of the cell length. At this stage, the catastrophe frequency increases gradually resulting in MTs depolymerisation and increase of tubulin pool. During PPB narrowing, PPB contains newly formed MTs. The cycle of gradual increase in catastrophe frequency and subsequently increased growth rate results in the increasingly dynamic MTs of the mature PPB. During the final PPB breakdown, the catastrophe frequency reaches an even higher level that cannot be overcome by the increased growth rate and the PPB collapse. Dhonukshe and co-workers also suggested that the PPB MTs are more dynamic and shorter than the cortical MTs (Dhonukshe *et al.*, 2003).

1.4.3 Mitotic Spindle

The prophase spindle that forms around the nuclear envelope is succeeded by the mitotic spindle, which separates the daughter chromosomes. As the prophase spindle is formed before nuclear envelope breakdown, the prophase spindle could be a consequence of MT

nucleating activity at the nuclear surface (Smirnova *et al.*, 1992). The PPB is disassembled by metaphase at the latest. This results in an increase in the cytosolic tubulin pool and can be correlated with the increased growth rate of nuclear envelope-originating MTs that contributes to the development of spindle fibres (Dhonukshe *et al.*, 2003). The nuclear surface predicts the future formation of spindle poles and it has been shown that the nuclear surface is associated with calmodulin, which is later distributed to the polar regions during mitosis of most animal or plant cell types (Lambert and Lloyd, 1994). This observation suggests that some of the regulatory mechanisms involved in spindle formation and chromosome movement may be similar in plant and animal cells. The anaphase spindle exhibits similar organisation to the animal one but at the same time is also different in certain aspects. For example, its poles are broader without centrosomes and it does not form astral MTs (Lloyd and Hussey, 2001). Despite the absence of a centrosome, prophase mitotic MTs in plants demonstrate similar dynamic properties to astral arrays in animal cells. Calmodulin was shown to associate with kinetochore MTs only in plants, which suggests a calmodulin plant specialised role in the regulation of kinetochore MT dynamics (Schmit A.C., 2002). Mitotic processes are likely to involve protein kinase activity and the presence of calmodulin suggests a putative calcium/calmodulin regulation of MT dynamics during the plant cell cycle. It has been reported that the calcium/ calmodulin complex depolymerise MTs by some form of interaction with MT Associated Proteins (Cyr R.J., 1991a).

1.4.4 Phragmoplast

The phragmoplast appears during late anaphase, when the sister chromatids have separated to the opposite sites of the mitotic plane and it is present in telophase. It appears first as a MT bundle, a remnant of the anaphase spindle, and starts to grow centrifugally with the MT

plus ends overlapping at the midline. While it grows, it directs secretory vesicles to the midzone. The secretory vesicles are fused and form then new cell plate at the site vacated previously by the PPB. Sequi-Simarro and co-workers using a combination of cryofixation/freeze-substitution and electron tomography techniques investigated the process of somatic-type cytokinesis and proposed a model of plant cytokinesis illustrated at figure 1.2 (Sequi-Simarro *et al.*, 2004). This model divides the cytokinetic process into four phases. In phase A, during late anaphase, phragmoplast initials arise from the opposite sets of polar spindle MTs. Vesicles travel toward the cell plate assembly sites, defined by the presence of cell plate assembly matrixes (CPAMs). Projecting from the vesicles are "Y" shaped structures reminiscent of exocyst complexes. The vesicles fuse and are transformed into dumbbell shapes, presumably through the action of dynamin-like springs (plane A). Tubular-vesicular networks (TVN) form. As a result, a TVN cell plate arises within the CPAM that forms the solid phragmoplast (plane B). During the transition phase C, the central CPAM and the associated MTs disassemble, while a new CPAM with MTs arises in the cell plate periphery, giving rise to the ring-shaped phragmoplast and peripheral growth zone (PGZ). In the central region, the TVN is converted to a tubular network (TN) by callose deposition (plane C). In phase D, the TN forms a planar fenestrated sheet (PFS). Secondary CPAMs and associated MTs reform over the PFS to fill the "holes". The now ring-shaped phragmoplast and CPAM define the peripheral growth zone (PGZ). The PGZ expands centrifugally until the cell plate reaches and fuses with the mother cell walls (plane D). (Sequi-Simarro *et al.*, 2004)

1.5 MT Organising Centres (MTOCs)

In animal cells, most if not all, MTs emerge from the one centrosome in interphase and from two centrosomes at the opposite poles during mitosis, with the minus end of MTs attached at

Figure 1.2
Model of Plant Somatic-Type Cytokinesis

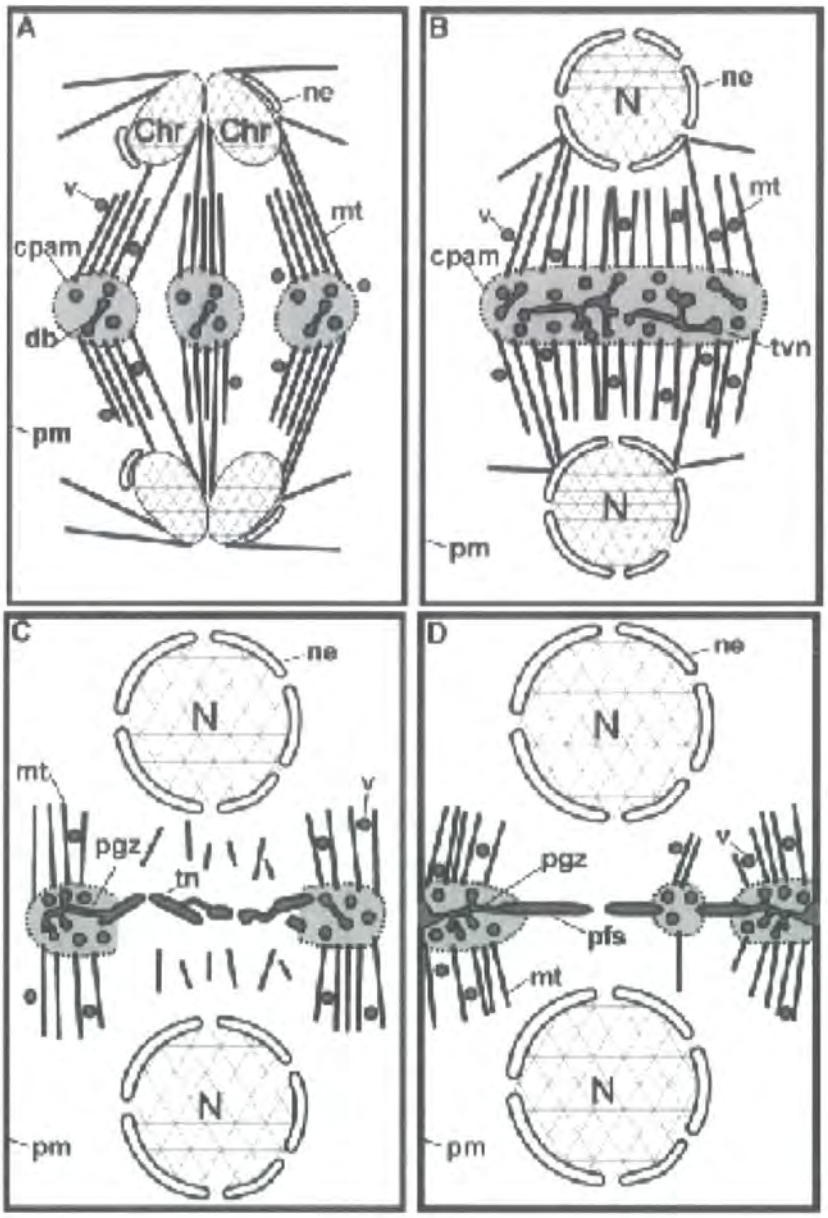

Sequi-Simarro *et al.*, 2004

Figure 1.2:
A. The phragmoplast assembly phase during late anaphase. (ne, nucleus envelope; Chr,chromosome; v, vesicle; cpam, cell plate assembly matrix; mt, microtubule; db,dumbbell-shaped vesicle; pm, plasma membrane)
B. Solid phragmoplast phase. (tvn, tubular-vesicular membrane network)
C. Transitional phragmoplast phase. (pgz, peripheral growth zone; tn, tubular network)
D. Ring-shaped phragmoplast phase. (pfs, planar fenestrated sheet)

the centrosome. On the other hand, in plants there are no centrosomes and MTs arise from MT Organisation Centres (MTOCs) which could be multiple, independent nucleation sites activated only at specific times during the cell cycle. So, while the cytoplasmic MTs of animal cells extend to the periphery from the centrosome, cortical MTs do not radiate from a specific point but are dispersed over the cortex in a parallel arrangement (Lloyd and Chan, 2004). Multiple and mobile MT nucleating sites revealed in *Arabidopsis* by labelling the cortical MTs with the MT end-binding protein, EB1 (Chan *et al.*, 2003).

The plant nuclear surface has been proposed as a putative MTOC site at interphase and during PPB and spindle formation (Liu *et al.*, 1993; Schmit *et al.*, 2002). Stoppin and co-workers has also shown that isolated plant cell nuclei support MTs growth (Stoppin *et al.*, 1994). However, Shaw and co-workers observed that new MTs could born at nucleating sites over the cortex of interphase cells (Shaw *et al.*, 2003).

1.5.1 Gamma tubulin is located at MTOC sites

γ-tubulin nucleates MTs in plants and appears to be localised at MTOCs (Schmit, 2002). It is part of a multi-protein group and forms a ring that acts as template for the addition of α and β tubulin dimers, from which protofilaments initiate and grow. Gamma tubulin has been used as a marker for the minus ends of MTs (Job *et al.*, 2003). Antibodies to γ-tubulin label sites around the nucleus surface and over the entire cortical array (Panteris *et al.*, 2000). The cortical labelling pattern of γ-tubulin could be a result of the dispersed arrangement of MT minus ends or it could indicate a more general role of γ-tubulin in MT stabilisation. Thus gamma tubulin has not proved a good marker of MTOCs in plant cells. The Spc98p is another component of the γtubulin ring complex located at MTOCs (Erhardt *et al.*, 2002). Its antigen was shown to inhibit the ability of isolated tobacco nuclei to polymerise tubulin.

Spc98p antigen was also found at the cortex but is not known if marks the MT initiation sites.

1.6 MT Associated Proteins (MAPs)

Tubulin dimers upon self-assembly to form the basic 25 nm MT filament. *In vitro* highly purified tubulin is capable of forming MTs with only GTP and Mg^{2+} present. However, the MTs formed from tubulin alone have limited function. Biochemically, the MT behaviour is enhanced by MT Associated Proteins (MAPs). MAPs define a class of proteins, which after binding to a MT affect its behaviour. In a sense, MAPs act to enhance the biochemical repertoire of tubulin and MTs. While tubulin is highly conserved in animal and plants (biochemically, genetically and immunologically), not all animal MAPs are conserved in plants. However, plant MAPs have orthologues in animals (Lloyd *et al.*, 2004) with the exception of Spiral 1 (Furutani *et al.*, 2000) and MAP190 (Hussey *et al.*, 2002).

1.6.1 Role of MAPs in MT assembly and disassembly

Those MAPs involved in regulation of MT assembly and stabilisation, are called structural MAPs. One of the most important activities of structural MAPs is to lower the critical concentration (Cc) of tubulin necessary for assembly by 40 folds. At tubulin dimer concentrations above the critical concentration, MTs polymerise, while at concentrations below the Cc, MTs depolymerise. At concentrations near the Cc, some MTs elongate while others shrink. The Cc of pure tubulin alone is 40-80 μM, while in the presence of MAPs it is 1-20 μM (Bayley *et al.*, 1994). The Cc is important for both MT nucleation and stabilisation. As plants do not have defined centrosomes, it has been hypothesised that MTOCs not only locate at the MTs nucleation regions but they could also be associated with a MAP, which

lowers the Cc at that region. As MT seeds are unstable, MAPs probably stabilise and promote seed assembly by decreasing the Cc (Cyr, 1991α).

On the other hand, MAPs can also be involved into MT disassembly. It has been reported that phosphorylation of brain MAPs inhibits MTs polymerisation probably by decreasing the MAPs affinity for MTs (Hoshi *et al.*, 1992). This fact indicates MAP binding to MTs is dependent on the phosphorylation-state of the MAP. Kinases being components of transduction pathways could affect MAPs phosphorylation/ dephosphorylation (Verde *et al.*, 1990, Diaz-Nido *et al.*, 1990; Mandelkow *et al.*, 1993). Cyr showed that in lysed carrot protoplasts MT stability is calcium/ calmodulin dependent via MAPs (Cyr, 1991b). This observation indicates MAPs are involved in MTs depolymerisation by acting as intracellular receptors of second messengers, such as calcium. MAPs may also induce or inhibit tubulin polymerisation in reponse to signals developed intracellulary like by gibberelic acid (Lloyd *et al.*, 1996) and by environmental factors like gravity (Himmelspach *et al.*, 1999).

1.7 Isolation of Plant MAPs

In plants, in contrast to brain tissues, the concentration of tubulin in the cytoplasm is low and there is a high concentration of phenolics and hydrolases in the plant vacuole, both of which preclude easy isolation of tubulin. The first plant MAPs were isolated *in vitro* through several rounds of temperature induced polymerisation/ depolymerisation using Taxol-stabilised brain MTs as affinity matrix (Cyr and Palevitz, 1989), thus were initially characterised as proteins that co-polymerise with MTs during tubulin assembly/ disassembly cycles. This original term is no longer accepted as many proteins can "stick" to MTs and not all the associations are meaningful. The tubulin-associated proteins could have MAP properties, could be enzymes or even irrelevant basic proteins, which bind to negatively

charged MTs (Lloyd *et al.*, 2003). So, for a protein to be termed as a MAP its *in vivo* localisation and activity it should be examined as well. The advantage of using taxol is that tubulin is polymerised more efficiently. MTs treated with taxol are usually resistant to depolymerisation but can be disassembled using a combination of cold and Ca^{+2}.

1.7.1 MAP 76kDa

Cyr and Palevitz, 1989, after several rounds of MTs polymerisation/ depolymerisation isolated a group of polypeptides from carrot cultured cells (*Daucus carota*), which could bundle MTs and support assembly of tubulin *in vitro*. Immunofluoresence microscopy using Ab against one of these polypeptides of MW 76 kDa proved that plant MAPs can co-localise with cortical MTs (Cyr and Palevitz, 1989).

1.7.2 MAPs 32-170kDa

Taxol stabilised brain MTs were also used as an affinity matrix for the isolation of several maize polypeptides between 32 and 170 kDa. These putative MAPs were able to initiate and promote MT polymerisation and to induce bundling of both plant and neural MTs (Vantard *et al.*, 1991). One of those, of about 83 kDa, could cross-react with an antibody raised against the mammalian MAP tau (Vantard *et al.*, 1991).

1.8 Tobacco MAP65 family

Jiang and Sonobe, 1993, succeeded in isolating a group of MAP proteins from evacuolated protoplasts (miniprotoplasts) of tobacco BY-2 cells (Jiang and Sonobe, 1993). They used taxol to promote MTs polymerisation in the cells and subsequently with cold treatment in presence of Ca^{2+} and high salt forced MTs to disassemble (Jiang and Sonobe, 1993). After three cycles of MTs assembly/ disassemly SDS-PAGE analysis showed the presence of 120

kDa, 110 kDa and a group of 60-65 kDa proteins in addition to tubulin. The MT protein mixture was fractionated by anion exchange chromatography. Each fraction was examined for MT bundling activity and only the fractions, which contained the 65 kDa protein were proved to bundle MTs. The purified 65 kDa protein was also shown to form 10-12 nm crossbridges between MTs *in vitro* (Jiang and Sonobe, 1993). Western blotting analysis with the anti-MAP65 antibody of whole-cell extracts from BY2 cells, pea, azuki bean, *Arabidopsis*, maize roots, rice root tips, barley root tips, *Dichotosiphon tuberosus thalli* and carrot roots revealed the 65 kDa protein was widely distributed in the plant kingdom. The anti-MAP65 antibody cross-reacted with polypeptides of about 65 kDa in all plants examined. Antibodies which raised against animal MAPs failed to identify the 65 kDa protein (Jiang and Sonobe, 1993). The tobacco anti-MAP65 antibody stained the cortical MTs in interphase and the MT arrays during mitosis and cytokinesis.

1.8.1 NtMAP651a

Smertenko and co-workers used anti-MAP65 antibody raised to biochemically purified tobacco MAP65 to screen a cDNA expression library from tobacco BY2 cells (Smertenko *et al.*, 2000). Three similar MAP 65 cDNAs were cloned which encode a protein with relative MW of about 65 kDa. First, NtMAP651a was isolated. Protein sequencing revealed no significant identity of NtMAP651a with previously cloned animal MAPs. However, there is some homology with a few other proteins. Anaphase Spindle Elongation factor (Ase1) from *Saccharomyces cerevisiae* (Pellman *et al.*, 1995) and vertebrate Protein Regulating Cytokinesis (PRC1; Jiang *et al.*, 1998) show 16% and 18% identity with NtMAP651a. Subsequently, NtMAP651b and NtMAP651c were isolated from a rescreen and shown to be 85% similar to NtMAP651a. NtMAP651b shows 96% identity with NtMAP651c. The set of proteins encoded by NtMAP65-1 cDNAs represents the NtMAP65-1 protein. The

recombinant Nt-MAP65-1 binds MTs *in vitro*. The anti-MAP65 antibody after a round of MTs disassembly/assembly decorates MTs of tobacco BY2 cells once they are polymerised, indicating that this MAP is unlikely to be involved in the initial promotion of MT polymerisation (Smertenko *et al.*, 2000). However NtMAP65-1 was not found to bind to all the stable MTs in BY-2 cells treated with taxol but decorated certain regions of the MT arrays. By immunolocalisation studies, the NtMAP65-1 protein was found to associate with a subset of cortical MTs, the preprophase band and overlapping anti-parallel MTs in the anaphase spindle and phragmoplast. (Smertenko *et al.*, 2000).

1.8.2 NtMAP651b

Recently, it was shown NtMAP65-1b has no effect on MT polymerisation rate (Wicker-Planquart *et al*, 2004). However, it could induce MTs bundling. NtMAP651b was also shown to stabilise MTs against depolymerisation induced by cold but not against katanin-induced destabilisation (Wicker-Planquart *et al*, 2004).

1.9 Carrot MAP65 family

Chan and co-workers used taxol-stabilised MTs to isolate a MAP fraction from detergent-extracted cytoskeletons prepared from carrot suspension cells. The MAP fraction contained a 120 kDa MAP and a group of MAP65 proteins, which was constituted by a 60/ 62 kDa doublet and a 68 kDa protein (Chan *et al.*, 1996). Turbidimetric assays showed the MAP fraction stimulated tubulin polymerisation at sub-critical concentrations. The antibodies against the 60/62 kDa doublet recognised the 68 kDa band, indicating that the three polypeptides are antigenically related, and for this reason the three polypeptides could referred to as the "MAP65 family". The antibodies raised against the MAP65 were shown to

stain all the MT structures through the cell cycle (Chan *et al.*, 1996). So, MAP65 staining in carrot cells was the same with the one described in tobacco cells (Jiang and Sonobe, 1993).

From the carrot MAP65 fraction, constituted by the 60/62 and 68 kDa proteins, the single 60 kDa protein was chromatographically isolated and shown to promote MTs assembly *in vitro* although not at sub-critical concentrations (Rutten *et al.*, 1997). Furthermore the MAP60 protein was shown to protect brain MTs against the depolymerisation effects of cold and Ca^{2+} but did not exhibit any bundling activity (Rutten *et al.*, 1997). However, the mixture of the 60, 62 and 68 kDa MAPs, isolated from the 120 kDa MAP by sucrose density gradient centrifugation, was shown to promote bundle formation of parallel MTs providing an MT-MT spacing of 25-30 nm but not to induce tubulin polymerisation (Chan *et al.*, 1999). Interestingly, 25 nm bridges were seen to crosslink MTs during interphase in plant cells (Lancelle *et al.*, 1986). As MAP60 was shown not to bundle MTs (Rutten *et al*, 1997) and MAP68 was not very abundant in the fraction, MAP62 seems to be responsible for the bundling activity.

Indications for developmental control of MAP65 expression comes from Barroso and co-workers who observed in carrots that the 68 kDa band disappears from the MAP65 triplet when the cells go into the elongation phase and stop dividing (Barroso *et al.*, 2000). Chan and co-workets observed that when carrot suspension cells stop dividing only the 62 kDa band from the MAP triplet appears on a 1D SDS page gel (Chan *et al.*, 2003). This is very interesting, as the 62 kDa MAP was also the only one from the MAP65 triplet indicated to bundle MTs and make cross-bridges (Chan *et al.*, 1999). The 62 kDa MAP presence at the elongation-state of cells, where only cortical MTs are present, is another indication of its possible importance in maintaining the inter-MT spacing of the cortical array. On the other

hand, the MAP120 (DcKRP120) was proved to have kinesin-like characteristics (Barroso *et al.*, 2000).

1.10 Azuki beans MAP65 family

The physiological role of the 65 kDa MAP was also examined in azuki beans epicotyls (*Vigna angularis*). Sawano and co-workers analysing the changes in MAP65 content and localisation in plant cell demonstrated that the expression of the MAP65 gene in cortical MTs was proportional to the growth activity of the seedlings (Sawano *et al.*, 2000). MAP65 protein in azuki beans appeared as a single band when visualised by 1D SDS page gel and its expression seemed to be cell cycle dependent, as the MAP65 band was increased when cells were elongating (Sawano *et al.*, 2000). The above observations indicated involvement of MAP65 in regulation of the elongation growth of azuki beans epicotyls.

1.11 MAP65 studies during Programmed Cell Death

Smertenko and co-workers investigated the involvement of cytoskeleton in plant embryo development (Smertenko *et al.*, 2003). The model system used was the somatic embryogenesis of the gymnosperm, *Picea abies* (Von Arnold *et al.*, 2002). It has been established that successful embryogenesis is dependent on programmed cell death (Filonova *et al.*, 2000 and 2002). The possible role of the MAP65 in *Picia abies* somatic embryogenesis lines during programmed cell death was analysed by immunolocalisation studies and western blots of 1D gels of total protein extracts from the cell lines. In a developmentally arrested cell line MAP65 did not bind cortical MTs and it was present only in the cytoplasm. However, at the equivalent time point at a normal embryonic cell line MAP65 was bound to MTs (Smertenko *et al*, 2003). So, the binding of MAP65 to MTs is probably important in embryo development and differentiation. The most abundant MAP

isoform in the normal embryonic cell line was the 63 kDa, while at the developmental arrested line was the 65 kDa. This observation raised the possibility that a critical amount of the 63 kDa isoform is required for the cell to go through a normal developmental cycle and embryogenesis (Smertenko *et al*, 2003). Another example of a MAP involved in embryo development comes from animal MAP1b. Animals without MAP1b do not produce any embryos and in cases of insufficient amounts of MAP1b the embryo suffers from severe abnormalities (Edelmann *et al.*, 1996).

1.12 *Arabidopsis* MAP65 proteins

1.12.1 AtMAP65-1

Searching an *Arabidopsis thaliana* database for MAP65 reveals nine genes with high identity to *Nicotiana tabacum* MAP65 genes. AtMAP65-1 was shown not to promote polymerisation of brain MTs and not to stabilise them against cold-induced MT depolymerisation. However, it could induce MT bundling *in vitro* and form 25nm cross-bridges between MTs (Smertenko *et al.*, 2004). In addition, it was shown the MT binding region locates at the C-terminal half of the protein and the Ala 409 and 420 amino acids are essential for MT binding. Interestingly, Ala 420 is conserved among the AtMAP65 family and its mutation to Valine causes the cytokinesis-defective phenotype of the AtMAP65-3/PLEADE gene (Muller *et al.*, 2002 and 2004), as it will be discussed in section 1.12.2. AtMAP65-1 was also shown to form dimers and the region responsible for this activity was found in the N-terminus of the protein (Smertenko *et al.*, 2004). Smertenko and co-workers suggested that the fprmation of dimers is necessary for MT bundling, as the MT binding region alone could not produce MT crossbridges. Immunolocalisation studies revealed

AtMAP65-1 was expressed in all MT arrays in a cell cycle dependent manner (Smertenko *et al.*, 2004). The expression programme of AtMAP65-1 in various tissues and organs was analysed and its presence in all plant organs and tissues was revealed with the exception of anthers and petals (Smertenko *et al.*, 2004).

1.12.2 AtMAP65-3

The importance of the MAP65 family in plant development was shown by recessive mutations in *AtMAP65-3/PLEADE* gene (Muller *et al.*, 2002, 2004). AtMAP65-3 was revealed to be synonymous with *PLEADE* gene (*PLE*) (Muller *et al.*, 2004). Single, recessive mutations in *PLEADE* gene (*ple*) showed defects in root and embryo development, and resulted in enlarged multinucleated cells with incomplete cross walls, indicating that the defect is in cytokinesis (Sorensen *et al.*, 2002, Sollner *et al.*, 2002, Muller *et al.*, 2002). In addition, these mutations were shown to cause C-terminal truncations and as a result the MT binding activity of AtMAP65-3/PLEIADE was abolished (Muller *et al.*, 2004). This observation agrees with the suggestion that the conserved MT binding region in AtMAP65 proteins locates at their C-terminus (Smertenko *et al.*, 2004). AtMAP65-3/PLE localises in the midzone of overlapping MTs during cell division (Muller, 2004). Immunolocalisation studies revealed AtMAP65-3/PLEIADE was not present in interphase cortical arrays. However, AtMAP65-3/PLEIADE antibodies stained the PPB and the midzone of the late anaphase spindle and phragmoplast. Immunofluoresence studies also showed that the phragmoplast in *ple* mutants was abnormal in size. It was wider and its midzone unusually expanded (Muller *et al.*, 2004). The staining of AtMAP65-3/PLEIADE in metaphase spindles was faint and this could explain why the mitotic spindle shape appeared normal in *ple* mutants and the karyokinesis was not disrupted (Muller *et al.*, 2004). In conclusion, the

ple phenotypes together with the cellular localisation of AtMAP65-3/PLE indicate AtMAP65-3/PLE has an essential role in cytokinesis completion.

1.13 MAP65 animal and yeast orthologues

There are relatives of MAP65 in other organisms, Ase1p in yeast and PRC1 in animal cells, which are essential to maintain the mitotic spindle midzone (Schuyler *et al.*, 2002; Mollinari *et al.*, 2001). The loss of Ase1p resulted in premature spindle disassembly in mid-anaphase (Schuyler *et al.*, 2002). On the other hand, the complete suppression of PRC1 by siRNA caused failure of MT interdigitation between the spindle sets (Mollinari *et al.*, 2001).

1.14 Mor1/Gem1

Another protein, which bundles MTs is Mor1/ Gem1. Mor1/ Gem 1 is the *Arabidopsis* homologue of human TOGp and Xenopus MAP125 (XMAP125). XMAP125 promotes MT assembly and turnover (Vasquez *et al.*, 1994). The observation of the *Arabidopsis mor1* and *gem1* phenotypes indicates MOR1/ GEM1 organises and stabilises cortical MTs. Whittington and co-workers observed using *Arabidopsis*, temperature sensitive, *mor1* allele that the cortical MTs at the restrictive temperature (above 28 °C) were shorter than usual and were lacking a parallel alignment. At the permissive temperature (21 °C) the mutant phenotype was lost and the recovery of normal MT organisation was rapid (Whittington *et al.*, 2001). However, the MT mitotic arrays were not affected in the *mor1* mutant (Twell *et al.*, 2002). Two alleles of *Arabidopsis gemini pollen 1*, *gem1-1* (Park *et al.*, 1998) and *gem1-2* (Twell *et al.*, 2002) were identified. Genetic complementation of the cytokinesis-defective *gem1-1* mutation with the *MOR1* gene shows *MOR1* is synonymous to *GEM1*. The homozygotes of *gem1* mutants are lethal and up to 50 % of the heterozygotes do not form a cell plate during pollen mitosis I. In both the *gem1-1* and *gem1-2* mutants the carboxy-

terminus of MOR1/GEM1 is missing, indicating the importance of the C-terminus in phragmoplast organisation. In contrast, the temperature sensitive *mor1* mutants have point mutations at the N-terminus HEAT repeat indicating the importance of the N terminus and of the HEAT motif in specific for the maintenance of cortical array stability (Whittington *et al.*, 2001).

The stabilising effect of XMAP125 was proven to antagonise the activity of motor kinesin XKCM1 (*Xenopus* kinesin catastrophe modulator; Tournebize *et al.*, 2000). XMAP125 stabilise MTs (Kinoshita *et al.*, 2001) and also has the ability to stimulate MT nucleation and anchor elongating MTs via their minus ends (Popov *et al.*, 2002), an activity which could also be found at *MOR1/GEM1*. Hussey and Hawkins using bioinformatics and protein structural studies of *MOR1/ GEM1* proposed two hypothetical models based on which the N-terminal region of MOR1/ GEM1 could hold the key for the antagonising effect of a putative destabilising kinesin (Hussey and Hawkins, 2001). The MOR1/GEM1 antagonising action against kinesin could be mediated by either binding directly to it or by competing for the MT binding site. Based on the first proposed model, at the permissive temperature (21°C) a Kin1-like kinesin would bind to MOR1/GEM1 at the N-terminus HEAT repeat resulting in reduced or abolished activity of Kin1-like kinesin. At the restrictive temperature (29°C), the *mor1/gem1* mutation would not allow the kinesin association at the HEAT repeat, allowing the destabilising activity of the catastrophic kinesin to predominate, which leads to short disorganised cortical MTs. Based to the second hypothesis, the *mor1/gem1* mutation, at the restrictive temperature, should cause the protein-protein interaction between the N-terminal HEAT repeat and MTs to be lost. The release of the MOR1/GEM1 N-terminus might expose kin1-like kinesin binding sites. The binding of kin1-like kinesin to MTs could then allow the destabilising activity of Kin1-like kinesin and result to short disorganised cortical MTs (figure 1.3; Hussey and Hawkins, 2001). The tobacco homologue

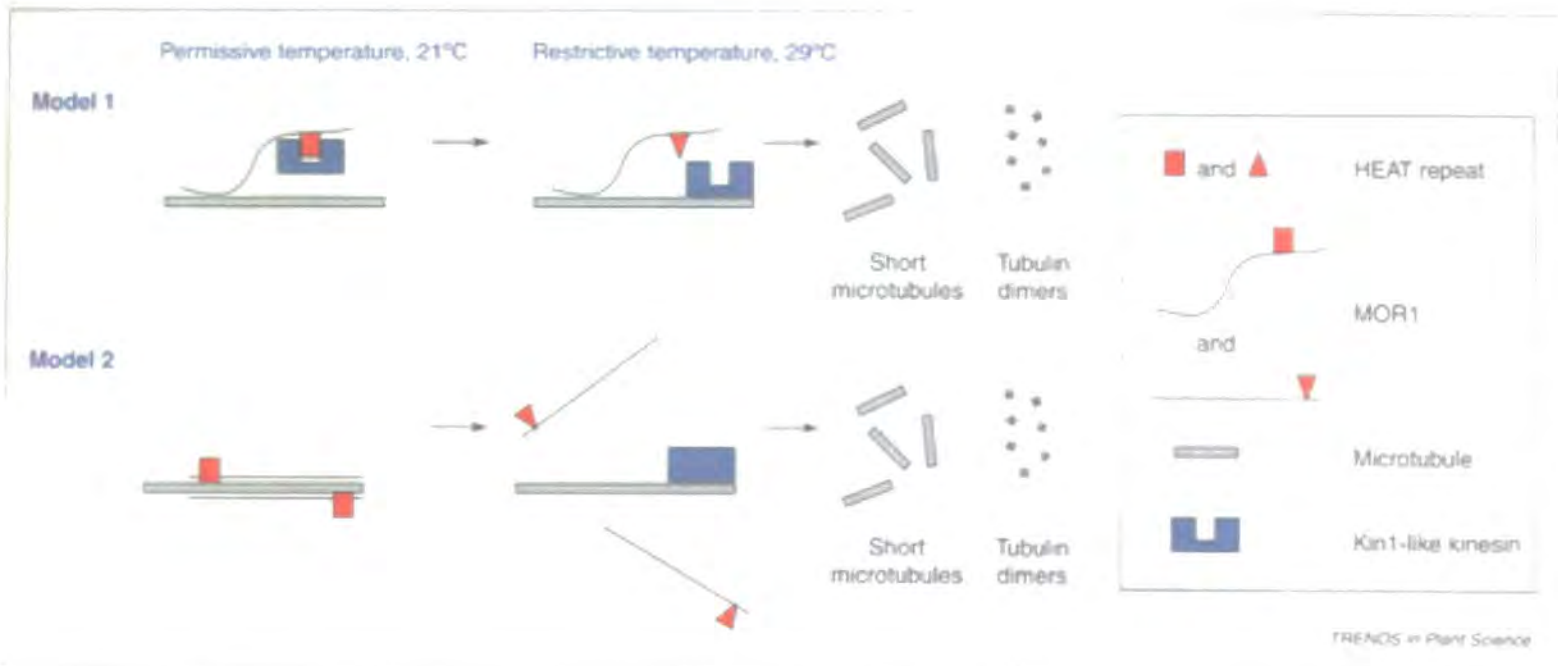

Figure 1.3
***mor1/gem1* and MT dynamics**

Figure 3.2: The MOR1/GEM1 could have antagonising effect on a putative destabilising plant kinesin. Based on the models 1 and 2 the *mor1/gem1* mutation allows the binding of the putative destabilising kinesin with the MTs, which results in short and disorganised MTs. (Image by Hussey and Hawkins, 2001)

of MOR1/GEM1, TMBP200, isolated from telophase cells, made cross bridges between MTs of about 10 nm long. It has been suggested TMBP200 is involved in the formation of MT bundles in phragmoplasts (Yasuhara *et al.*, 2002).

1.15 Motor MAPs

There are two classes of MTs motors, kinesin and dynein. A large family of kinesins are present in plants; 61 kinesins have been identified in the *Arabidopsis* genome (Reddy and Day, 2001). Dynein moves cargo to the MT minus ends. In plants, only homology to dynein heavy chains has been found (Moscatelli *et al.*, 1995; King *et al.*, 2002).

Motor MAPs, using the energy of ATP hydrolysis, are responsible for moving MT polymers or objects along them. They provide the motive force for MT sliding. The MT binding domain localises to either the N or C terminus of the motor MAPs, transporting cargo to the plus or the minus end respectively. Motor MAPs are capable of carrying out vesicular transport at interphase, they are involved in chromosomal movement at karyokinesis and move vesicles along the phragmoplast at cytokinesis (Vale and Fletterick, 1997).

1.15.1 Motor MAPs move cargo on cortical arrays

Several plant kinesins or kinesin-like proteins have been isolated. A 90 kDa protein with kinesin-like characteristics was biochemically isolated from tobacco pollen tubes (Cai *et al.*, 2000). It was shown to induce MT gliding in motility assays *in vitro* and immunolocalisation studies revealed binding between the 90 kDa protein and organelles associated with cortical MTs. So, the 90 kDa motor could be involved in their movement across the cortical array in pollen tubes. Another kinesin-like calmodulin-binding protein has been detected on cortical MTs but its role is not known yet (Preuss *et al.*, 2003).

1.15.2 Motor MAPs in mitosis and cytokinesis

There are indications that plant motors are involved in mitosis. Reddy and Day, 2001 through bioinformatics analysis of the *Arabidopsis* genome identified several proteins with homology to animal kinesins, which operate mitotic functions such as spindle formation and chromosome movement (Reddy and Day, 2001).

1.15.3 KAT A/B/C

The first plant kinesins to be identified were the *Arabidopsis KAT* genes, which encode an 89 kDa (KATA), an 82kDa (KATB) and an 84kDa (KATC) protein (Mitsui *et al.*, 1993; Mitsui *et al.*, 1994). KATA is also named as ATK1. The C-terminal motor proteins KATA/B/C have minus-end directed activity. It was shown KATA supports MT movement in an ATP-dependent manner although it does not move itself along the spindle MTs (Marcus *et al*, 2002). So, its role is probably to generate forces at the minus-end of spindle and to control MT dynamics at that site. In addition, Liu and co-workers had shown KATA localises to the spindle midzone from metaphase through anaphase and at the phragmoplast midzone (Liu *et al*, 1996). Using antibodies generated against truncated proteins expressed by *KATB* and *KATC*, a 85 kDa kinesin like protein, termed KatB/C, was detected in BY-2 cells. The amount of KatB/C in synchronous BY-2 cultures was increased during M phase of the cell cycle (Mitsui *et al.*, 1996). The *atk1-1* mutant of *Arabidopsis ATK1* (formally known as *KATA*) was found to have defective spindle organisation and meiotic chromosome segregation (Chen *et al.*, 2002).

1.15.4 KCBP

The kinesin-like calmodulin binding protein, KCBP, was found in the prophase and metaphase spindles of *Haemanthus* endosperm to label the kinetochore fibres (Smirnova *et al.*, 1998). By mid-anaphase the protein was accumulated at the spindle poles. KCBP was also shown to localise at the phragmoplast and cell plate (Smirnova *et al.*, 1998). KCBP is also known to be the gene product of *ZWICHEL*, detected during an analysis of *Arabidopsis* trichome mutants (Oppenheimer *et al.*, 1997). In *zwickel/kcbp* mutants the trichomes have shorter stalk and fewer branches. KCBP during cytokinesis does not exhibit a similar minus end activity as in the mitotic spindle. In contrast, KCBP locates to the phragmoplast midzone, where the MT plus ends overlap (Vos *et al.*, 2000). Calcium, through calmodulin, has been shown to inhibit the interaction of KCBP with MTs and the extent of inhibition was dependent on calcium and calmodulin concentration (Deavours *et al.*, 1998). This is another example of the effect of calcium/ calmodulin on MT structures. Vos *et al.*, 2000, suggested during prophase and metaphase the KCBP is involved in spindle formation, while at metaphase and telophase KCBP activity is down-regulated. Vos *et al.*, 2000, also proposed that ER systems close to the spindle and phragmoplast could regulate calcium concentrations in a cell cycle dependent manner, affecting KCBP activity. A protein kinesin, KCBP-interacting protein kinase (KIPK) was found to interact specifically with KCBP and its catalytic domain was shown to be capable of phosphorylation (Day *et al.*, 2000). The association of KCBP with KIPK suggests that phosphorylation could be another regulating factor of KCBP function.

Yeast-two-hybrid screens in *Arabidopsis* revealed KCBP interacts with a KCBP-interacting Ca^{+2} binding protein (KIC) in a Ca^{+2} dependent manner (Reddy *et al.*, 2003). KIC binds to Ca^{+2} with its single EF-hand motif. KIC inhibits KCBP microtubule-binding activity like

calmodulin. However, inhibition of KCBP microtubule-stimulated ATPase activity by KIC requires a threefold lower concentration of Ca^{+2} than that required for calmodulin. KIC-related Ca^{+2} binding proteins failed to regulate KCBP activity, indicating that KIC and calmodulin are specific regulators of KCBP. Reddy and co-workers also showed that overexpression of KIC in *Arabidopsis* results in trichomes with less branches as in *zwickel/kcbp* phenotype (Reddy *et al.*, 2003).

1.15.5 KRP125

Motor MAPs are also involved in phragmoplast structure, such as the TKRP125 (tobacco kinesin-related polypeptide of 125 kDa) and DcKRP120-2. Both of them group with the Block in Mitosis C (BimC) family, whose members have plus end directed activity. TKRP125 was purified from isolated phragmoplasts from synchronised tobacco BY2 cells (Asada *et al.*, 1994). Both DcKRP120-1 and DcKRP120-2 kinesin like proteins constitute a 120kDa MAP isolated from carrot protoplast extracts (Barroso *et al.*, 2000). DcKRP120-1 is homologous to the motor region of TKRP125. TKRP125 is distributed along MTs at the cortical array and PPB (Asada *et al.*, 1997), while the anti-DcKRP120-2 antibody labels them only weekly (Barroso *et al.*, 2000). Both stain the spindle and phragmoplast, but only DcKRP120-2 accumulates at the phragmoplast midzone. It has been suggested DcKRP120-2 is probably involved in stabilising the mitotic and cytokinetic structures (Barroso *et al.*, 2000).

1.15.6 AtPAKRP1

Another plus end-directed kinesin related protein, AtPAKRP1 (*Arabidopsis thaliana* phragmoplast-associated kinesin-related protein 1) is possibly also involved in establishing and maintaining of the phragmoplast bipolar structure (Lee and Liu, 2000). It concentrates in

the spindle midzone during late anaphase and at the phragmoplast mid-line during cytokinesis. This specific localisation was suggested to be due to cycle-specific phosphorylation. Lee and co-workers identified AtPAKRP2, which in contrast to AtPAKRP1, appears in a punctuate pattern along phragmoplast MTs with more concentrated distribution near the division site (Lee *et al.*, 2001). AtPAKRP2 involvement has been hypothesised in the transport of Golgi-derived vesicles in phragmoplast.

1.15.7 NPK

Other kinesin-like proteins are also involved in cytokinesis, such as the NPK which regulates the expansion of the cell plate (Nishihama *et al.*., 2002). The tobacco NPK activating kinase-like proteins 1 and 2 (NACK1 and NACK2) activate a MAP kinase cascade (Soyano *et al.*, 2003). NACK1 and NACK2 localise the MAPKKK NPK1 (nucleus and phragmoplast-localised protein kinesin 1) to the cell plate assembly site. The NPK1 activates the MAPKK, NQK1. Overexpression of NQK1 results to multinucleate cells with incomplete cell walls (Soyano *et al.*, 2003). The *Arabidopsis* homologue of NACK1 is called AtNACK1 and it is identical to HINKEL kinesin-like protein (Strompen *et al.*, 2002). Both the *Arabidopsis hinkel* (*hik*) mutants and NACK knock-out exhibit incomplete cell walls.

1.16 MT severing proteins

1.16.1 Katanins

Katanin is a heterodimeric ATPase found in animal centrosomes, where it is thought to cut MTs free from their minus end anchorage (McNally *et al.*, 1996). It has a 60 kDa catalytic subunit and an 80 kDa regulatory subunit. An homoloque of the 60 kDa subunit has been identified in *Arabidopsis* and it was shown to be active *in vitro* (Stoppin-Mellet *et al.*, 2002).

It initally appeared there was no homoloque of the 80 kDa subunit in *Arabidopsis* genome but by a yeast-two-hybrid cDNA screen using *Arabidopsis* katanin as bait a p80 subunit was identified (Bouquin *et al.*, 2003).

The *Arabidopsis* katanin mutant, *fragile fiber* (*fra2*) illustrates the importance of katanin in cell elongation. In *fra2* mutants the parallel arrangement of cortical MTs is disrupted and the cell walls have reduced cellulose (Burk *et al.*, 2001). A similar phenotype has been observed in the *Arabidopsis* mutant *botero 1*, which is allelic to *fra2* (Bichet *et al.*, 2001). Burk and Ye showed that, in *fra2/bot1* mutants, the cellulose deposition is disrupted and abnormal bundles of cellulose are formed (Burk and Ye, 2002). Another katanin mutant, the ectopic root-hair mutant *erh*3, has been identified in *Arabidopsis* (Webb *et al.*, 2002). *ERH3* encodes a p60 katanin protein. In *erh*3 mutants the root hairs emerge from the cells at unpredicted sites. The development of hair and non-hair cells is established during position-dependent cell differentiation in the root epidermis and, hence, it has been suggested that katanins are essential in the specification of cell identities in the *Arabidopsis* root (Webb *et al.*, 2002). A semi-dwarf *Arabidopsis* mutant *lue*1, which is allelic to *fra*2, *bot*1 and *erh*3, was identified in a screen designed to identify mutations affecting the gibberellin biosynthesis (Bouquin *et al.*, 2003). In *lue*1 mutants the cortical MTs lose their parallelism and are arranged randomnly. Bouquin and co-workers suggested that katanins could be involved in modulation of gibberellin biosynthesis (Bouquin *et al.*, 2003).

The study of katanin proteins showed the importance of MT severance in the formation of parallel MT arrays and cell elongation. Wasteneys has proposed a model of how katanin and the MT nucleation are linked with dispersed MT arrays (Wasteneys, 2002). It has been hypothesised that katanin severs the minus end of the cortical MT and the minus end is

transferred to the plus end of the severed microtubule. The transport is most probably mediated by plus-end-directed kinesin-related proteins. According to this model, the katanins produce new MT-nucleating templates by severing MT minus ends, providing in this way a continual supply of MTs for the growing cell (Wasteneys, 2002).

1.16.2 Catastrophic Kinesins

The members of the kinesin subfamily, KinI (termed so for the Internal location of the motor domain) have MT-destabilising effects (Hertzer *et al.*, 2003). MT depolymerisation is involved in establishment and maintenance of the mitotic spindle and in chromosome segregation during cell division (Walczak *et al.*, 1996 a and b; Rogers *et al.*, 2004). MT-depolymerising activity has been identified in KinI kinesins that localise to the kinetochore during mitosis in *Xenopus* (*Xenopus* kinesin catastrophe modulator, XKCM1; Kline-Smith and Walczak, 2002) and in mammals (mitotic centromere-associated kinesin, MCAK; Hunter *et al.*, 2003). Kinesin superfamily protein 2 (KIF2), whose members include KinI kinesin type proteins, was found in murine brain (Aizawa *et al.*, 1992) and it was shown to depolymerise MTs *in vitro* (Desai *et al.*, 1999). Homma and co-workers suggested KIF2 plays a nonmitotic role in the development of the nervous system by suppressing extension of neuron branches at the cell edge (Homma *et al.*, 2003).

The fourth member of the *KAT* family, KATD, has its motor domain in the central region of the protein. Further studies are needed to investigate if acts as a motor, like KATA/B/C, or as a MT destabiliser, like other kinases with their motor domain located in the central region. KATD lacks the α-helical coiled-coil region, which is typical of kinesin heavy chains, and probably work as a monomeric protein (Tamura *et al.*, 1999). KATD was shown to bind MTs and have a microtubule-stimulated ATPase activity.

1.17 MAPs mediate MTs linking to other cell components

1.17.1 MAPs involved in MT linking with Actin

MAPs may link MTs with other cytoskeletal components or organelles. Actin microfilaments and MTs often co-localise in plant cells (Schmit and Lambert, 1990) and, as pure MTs and actin do not associate with themselves, the presence of a MAP co-linker can be a possibility. MAP 190 has been suggested as a candidate for linking actin to MTs (Igarashi *et al.*, 2000). It was isolated from tobacco BY2 cells through cycles of tubulin polymerisation/ depolymerisation and it was also found to bind filamentous actin. It was detected in the nucleus, spindle and phragmoplast only. Hence, it was suggested MAP190 protein has a cell cycle-regulated activity (Igarashi *et al.*, 2000). As it has an endoplasic reticulum retention signal in the N-terminus and a calmodulin-like domain in the C-terminus Hussey and co-workers suggested MAP190 could link MTs, actin and ER in the phragmoplast in a calcium dependent manner (Hussey *et al.*, 2002).

Durso and Cyr isolated a 50 kDa protein, homologue of elongation factor 1α using tubulin affinity chromatography (Durso and Cyr, 1994). GFP-EF-1α shows MT like staining only in presence of weak lipophilic acids (Moore and Cyr, 2000) and EF-1 seems to be a downstream target for calcium and lipid-mediated signal transduction cascades. (Ransom-Hodgkins *et al.*, 2000). The protein showed bundling activity of taxol-stabilised MTs and its activity was stimulated by the addition of Ca^{2+} and calmodulin (Durso *et al.*, 1996). It was also found to bind and bundle actin. Hence, EF-1α could act as a protein transferring signals between MTs and the actin network (Murray *et al.*, 1996).

Another protein found to interact with both MTs and actin filaments is the importin α, which is a nuclear localisation signal (NLS) receptor. It is involved in the nuclear import of proteins containing nuclear localisation signals and its interaction with the cytoskeleton indicates cytoskeletal involvement in intracellular transport pathways (Smith and Raikhel, 1998). Some MAPs could serve as linkers between MTs and Intermediate Filaments. Cell localisation of IF antibodies in plant cells are similar with those of MTs (Shaw *et al.*, 1991).

1.17.2 MAPs involved in MT linking with Plasma membrane

Another hypothesis is that MAPs can link MTs to other organelles and to the plasma membrane. A number of MAPs were isolated from both a membrane and cytosolic fraction of tobacco culture (Marc *et al.*, 1996). The polypeptides from both the fractions bind MTs, induce MT bundling and promote tubulin polymerisation. The membrane fraction in contrast to the cytosolic contains unique MAP proteins of 75, 90 and 98 kDa. Immunological studies illustrate that raised antibody against MAP 90 co-localises with cortical MTs in protoplast ghosts (Marc *et al*, 1996). Gardiner and co-workers proved that MAP 90 is a phospholipase D (PLD) and that its labelling remained in dots along the plasma membrane even when MTs were depolymerised by cold treatment in the presence of calcium. It was proposed MAP90 is a membrane associated phospholipase D transferring hormonal and environmental signals to MT network (Gardiner, *et al.*, 2001). These signals could be originated by various second messengers, which activate PLD, such as calcium (Wang, 1999). Dhonukshe and co-workers showed that PLD activation by *n*-butanol PLD activators triggered plant MTs reorganisation (Dhonukshe *et al.*, 2003). However, only the MTs associated with membranes (plasma or Golgi) were susceptible to PLD-activating treatments and the spindle MTs were unaffected. The MTs were first released from the membrane and subsequently. fragmented

Another indication for the involvement of MTs at plant cell morphogenesis comes from the lefty phenotype (Thitamadee *et al.*; 2002, Hashimoto, T., 2002). The MTs angle in mutant cells was observed to be offset to the long axis compared to wild type. This angle offsetting of MTs angle may re-orientate the cell wall microfibrils angle as well, resulting to the twisting cell shape which causes the lefty phenotype (Hussey, P.J., 2002; Lloyd and Chan, 2002). In *spiral1* and *spiral2* mutants, *Arabidopsis* plants grow with a right-handed twist instead of straight (Furutani *et al.*, 2000). Sedbrook and co-workers showed SPR1 protein functions as a microtubule-interacting protein that preferentially localises to the plus ends of cortical MTs. Hence, it was hypothesised that SPR1 is involved in directional cell expansion by regulating the growth of the plus ends of MTs (Sedbrook *et al.*, 2004).

1.18 MT Interacting Proteins

Some proteins have MAP characteristics but it is difficult to be characterised as structural, motor or cross-linking MAPs. An alternative and general characterisation that could be used is "Microtubule-Interacting Proteins". An example is the 41 kDa TAN1 (TANGLED 1) protein. It shares homology with basic regions of vertebrate adenomatous polyposis coli (APC) proteins, which bind MTs (Smith *et al.*, 2001). TAN1 binds MTs and antibodies against TAN1 label the PPB, spindle and phragmoplast (Smith *et al.*, 2001). This observation could explain the maize *tan1* mutant phenotype, in which PPBs and phragmoplasts are structurally normal but frequently mis-oriented (Cleary and Smith, 1998). Thus, TAN1 function could aid in the proper orientation of cell wall, guiding the PPB and phragmoplast at the correct site in the cell cortex.

Several other plant MAPs have been also identified. Nick and co-workers isolated two proteins of 100 kDa and 50 kDa each from maize suspension culture. Both are capable of

binding neuro-MTs, to co-assemble with endogenous tubulin and are immunologically related to neuronal MAP τau (Nick, 1995). MAP50 co-localises with cortical MTs but exclusively in elongating cells. In contrast, the 100 kDa protein was not found to bind cortical MTs and it was suggested it belongs in the heat shock protein 90 family of chaperones (Nick *et al*, 1995). HSP90 behaves as a MT-binding protein *in vitro* associated with polymerised MTs and tubulin dimers (Freudenreich and Nick, 1998). Immunologically, HSP90 decorates the nuclear envelope, PPB and phragmoplast (Petrasek *et al.*, 1998). It was also shown to co-localise with cortical MTs at further studies but the staining pattern was not continuous.

The eukaryotic initiation factor elF (iso) 4F could transfer signals to MT cytoskeleton. It is composed by p28 and p86 subunits. The p86 subunit was shown to bind and bundle MTs *in vitro* and decorate cortical MTs in patches (Bokros *et al.*, 1995). As elF (iso) 4F is component of the protein translational machinery it was suggested it might indicate linkage of protein translational mechanism to the MT network.

1.19 Project aims and objectives

Searching at *Arabidopsis* genome has revealed 9 MAP65 genes. The deduced amino acid sequences share 28-81% identity with each other and their molecular weight, on the other hand, varies from 62.7 to 80.3 kDa (Chapter 3). The differences between the amino acid sequences of the AtMAP65 family suggest different roles for these proteins within cells. The aim of this project is to compare the biochemical properties, cellular localisation and expression programme of the different AtMAP65 isoforms. First, the temporal and spatial expression of all nine AtMAP65 proteins in *Arabidopsis* plant is compared. Then, in order to continue the functional dissection of the *Arabidopsis* MAP65 proteins, which

Smertenko and Muller and their co-workers started with studies in AtMAP65-1 and AtMAP65-3 respectively (Smertenko *et al.*, 2004, Muller *et al.*, 2004), I focus on a single isoform, AtMAP65-6. At this project the AtMAP65-6 biochemical properties, *in vivo* and *in vitro* expression and cellular immunolocalisation are investigated and compared to other members of the MAP65 family.

Chapter 2

Materials and Methods

All chemical and reagents were supplied by either BDH Chemicals Ltd or Sigma Chemical Company; unless stated otherwise. The enzymes supplied either from MBI Fermentas or Promega; unless stated otherwise. Oligonucleotides were synthesised by either Sigma Genosys or TAGN Ltd (International Centre for Life, Newcastle).

2.1 *Arabidopsis* line used

Columbia-0, obtained from LEHLE SEEDS

2.2 *E.coli* strains used (obtained from Stratagene)

XL1-Blue MRF'Strain

*(mcr*A) *183 (mcrCB-hsdSMR-mrr) 173 endA1 supE44 thi-1recA1 gyrA96 relA1 lac* [F′ *proAB lacI* q *Z M15* T*n10* (Tet^r)]

SOLR™ Strain

e14 – (McrA –) *(mcrCB-hsdSMR-mrr) 171 sbcC recB recJ uvrCumuC::*T*n5* (Kan r) *lac gyrA96 relA1 thi-1 endA1* R [F′ *proAB lacI* q *Z M15*] Su$^-$

DH5α Strain

F-*f*80d*lac*ZDM15 D(*lac*ZYA-*arg*F)U169 *deo*R, *rec*A1 *end*A1 *hsd*R17(rk- mk+ *pho*A *sup*E44 l- *thi*-1 *gyr*A96 *rel*A1

DB3.1 Strain

F$^-$ *gyrA462 endA1 Δ(sr1-recA) mcrB mrr hsdS20 supE44 ara-14 galK2 lacY1 proA2 rpsA2 rpsL20 xyl-5 λ$^-$ leu mtl-1*

2.3 Yeast strains used (Causier and Davies, 2002)

AH109

MATα, trp1-901, leu2-3, 112, ura3-52, his3-200, gal4Δ, gal80Δ, LYS2 : : $GAL1_{UAS}$-$GAL1_{TATA}$-HIS3, MEL1 $GAL2_{UAS}$-$GAL2_{TATA}$-ADE2, URA3::$MEL1_{UAS}$-$MEL1_{TATA}$-lacZ

Y187

MATα, ura3-52, his3-200, ade 2- 01, trp 1-901, leu 2- 3, 112, gal4Δ, met, gal80Δ, URA3 : : $GAL1_{UAS}$-$GAL1_{TATA}$-lacZ, MEL1

2.4 *Agrobacterium* strain used (Topping *et al.*, 1991)

C58C3

Industrial strain of C58 background with resistance in Nalidixic acid acid and streptomycin. Its specific genotype is unknown.

2.5 Molecular Biology Techniques

The molecular biology techniques proceeded based on protocols in Molecular Cloning: A Laboratory Manual (Sambrook and Russell, 2001); unless stated otherwise. In general, all equipment and solutions used for DNA work were sterilised by autoclaving. The equipment used for RNA work were treated with 0.1% (v/v) diethyl pyrocarbonate (DEPC) overnight at 37°C and then autoclaved.

Centrifuges

Centrifuges used: Jouan, CR 422; for spin up to 5000 rpm, eppendorf 5415 R; for spin up to 13,000 rpm with cooling system, eppendorf 5415 D; for spin up to 13,000rpm at room temperature; Bechman J2-HC; for spin up to 18,000 rpm.

2.5.1 Polymerase Chain Reaction (PCR)

PCR reactions of 50 µl were set up on ice. The PCR reactions consisted of DNA template (10-100 ng), gene specific oligonucleotide primers at 0.2 µM, 2.5 mM $MgCl_2$, 0.2 mM each of dATP, dGTP, dCTP and dTTP, 1 x reaction buffer and 1 Unit of BIOTAQ Red DNA Polymerase (Bioline). (One unit is defined as the amount of enzyme that incorporates 10nmoles of dNTPs into acid-insoluble form in 30 min at 72°C.) The reactions were performed using a HYBAIDO mn-E thermal cycler with a heated lid. The PCR mixtures were first heated at 94°C for 1 minute. Then 35 cycles were followed at denaturation temperature of 94°C for 1 minute, at annealing temperature of 50-65°C for 1-2 minutes and at extension temperature of 72°C for 2 minutes. The reactions were completed with 10 minutes at the extension temperature of 72°C. The annealing temperature was determined empirically for each primer combination based on the oligonucleotides melting temperature (Tm). The extension time was calculated based to the predicted product size (1 minute per kb).

2.5.2 Restriction digests

A typical restriction endonuclease digestion mixture was constituted as follows: 1 µg DNA, 2 units of enzyme, 1 x enzyme buffer and sterile H_2O up to 20 µl. The reaction was carried out at the enzyme optimal temperature for two hours. Occasionally, digestion mixtures were scaled up to 50-100 µl and they were incubated at temperature control ovens overnight, following the manufacturer's instructions.

2.5.3 DNA purification

DNA fragments from PCR and other enzymatic reactions were cleaned up and eluted in H_2O using the QIAquick PCR Purification kit from Qiagen.

2.5.4 DNA Extraction by Phenol: chloroform / Ethanol Precipitation

An alternative way used to purify DNA from an enzymatic or PCR mixture without using the Qiagen kit was the phenol: chloroform extraction / ethanol precipitation method. Equal volume of Phenol: chloroform: isoamyl alcohol solution (25:24:1, V:V:V), pH 8 was added to the DNA sample. The mixture, after vigorous vortexing, was centrifuged at maximum speed for 3 minutes. The supernatant was transferred to a fresh tube. An equal volume of chloroform was added and the mixture was vortexed and centrifuged again at maximum speed for 3 minutes. The supernatant was transferred to a fresh eppendorf tube. An equal volume of propanol and 0.1 volume of 3M Potassium acetate (pH 5.4) were added and mixed. The mixture was incubated at -20°C for 30 minutes and then centrifuged at maximum speed for another half an hour. The pellet was washed in 70% (v/v) ethanol and centrifuged at the top speed for 1 minute. The pellet afterwards was allowed to dry on air, resuspended in H_2O and heated at 55°C for 10 min.

2.5.5 Agarose Gel Electrophoresis

Mixtures of DNA were separated by size in agarose gels by electrophoresis. The gel was prepared by boiling, in a microwave, 0.8% (w/v) agarose (Sigma) in 1 x TAE buffer (20 mM glacial acetic acid, 40M Tris acetate, 1mM EDTA, pH 7.2). Afterwards, the agarose solution was cooled down to 50°C and ethidium bromide was added at 0.5 μg/ml final concentration. The solution was poured into gel trays with suitable combs and was left to solidify for 20 minutes. Then the gels were submerged in 1 x TAE buffer in electrophoresis tank. DNA samples were mixed with 6 x loading buffer (0.25 % (w/v) Fast dye, 15 % (w/v) Ficoll, Pharmacia). Electrophoresis was carried out at 50-100 V. DNA fragments were visualised under ultraviolet light. Size markers (HyperLadder, *Bioline)* were run alongside

DNA samples. The ethidium bromide stained gels were viewed using a Bio-Rad Gel Doc 1000 imaging system and images were captured on a PC running Quantity One software (Bio-Rad).

2.5.6 DNA recovery from agarose gels

DNA was extracted from agarose gel after electrophoresis using either the QIAquick gel extraction kit (Qiagen) or the Ultrafree-DA column (Millipore) following the manufacturer's instructions.

2.5.7 Nucleic Acid Quantification

The nucleic acids concentration was determined by optical density (OD) readings at 260 nm using a Helios β spectophotometer. The ratio of the readings at 260 nm and 280 nm provided an estimate of the nucleic acid purity to contaminants that absorb in the UV, such as protein.

2.5.8 DNA ligation reactions

The ratio between DNA vector and insert for optimum ligation varied and for each experiment a range of vector to insert ratios were tried in the range from 1:2 to 1:5. The relative concentration of vector and insert were estimated by agarose gel electrophoresis. PCR products were cloned directly into T/A cloning vector pGMT-E (Promega) and then transferred from pGMT-E to other destination vectors. pGMT-E has an overhanging T compatible with the A nucleotide which Tag polymerase adds at PCR products. In order to increase the efficiency of the ligation 2 extra A residues were added at the forward PCR primer and 2 extra T residues at the reverse PCR primer. A typical ligation reaction contained the vector (50 ng), insert DNA (100ng), 1 x T4 ligase buffer, 3 units of T4 DNA

ligase (Promega) and sterile H_2O to make the volume up to 10 µl. The ligation reaction was performed at 4°C overnight.

2.5.9 Dephosphorylation of linear DNA

Dephosphorylation was necessary to preventing self-ligation of DNA vector when was digested by a single enzyme. Dephosphorylation removes phoshate groups from the 5' termini. It was carried out by treating DNA with alkaline phosphatase (calf intestinal mucosa) from Pharmacia based on the manufacturer's instructions. The alkaline phosphatase was removed from the DNA by phenol: chloroform extraction and ethanol precipitation or by using the PCR Purification kit from Qiagen.

2.5.10 GATEWAY Cloning Technology

GATEWAY technology (from Life Technology/Invitrogen) facilitates cloning that relying on a site specific recombination reactions rather than restriction digest and ligation reactions. The system uses the same mechanism that bacteriophage λ uses to integrate its DNA into specific sites within the *E.coli* genome. The sites labeled L, R, B and P are respectively the *att*L, *att*R, *att*B and *att*P recombination sites for bacteriophage lambda in *E.coli* (figure 2.1; GATEWAY™ Cloning Technology Manual, Life Technologies). These sites are specifically recognised by the recombination proteins that constitute the CLONASE Enzyme Mix. GATEWAY-tagged PCR products (flanked by *att*B recombination sites) were cloned into the Entry vectors using the recombination reaction (BP). The *att*B1 primer sequence used was: 5'-GGGG-ACA-AGT-TTG-TAC-AAA-AAA-GCA-GGC-TTG-ACC-specific sequence-3'. The *att*B2 primer sequence used was: 5'-GGGG-AC-CAC-TTT-GTA-CAA-GAA-AGC-TGG-GTC-specific sequence-3'. The BP

reaction was mediated by BP CLONASE mix of recombination proteins, followed the manufacturer's protocol.

From the Entry vector a series of other vectors can be generated. These Destination vectors were generated in a recombination reaction (LR) between the Entry clone and the Destination vector, which contained a toxic gene (*ccd*B, the toxic gene resistance strain is DB3.1). The result was that a gene sequence from the Entry clone was transferred into a Destination Vector. A by-product plasmid containing the toxic gene *ccd*B was also generated, which gives rise to no colonies in *E.coli* strain DH5α. The LR reaction was mediated by the LR CLONASE mix of recombination proteins, following the manufacturer's protocol. The orientation of the gene is maintained throughout the subcloning, because *att*L1 reacts only with *att*R1, and *att*L2 reacts only with *att*R2.

Figure 2.1: GATEWAY Cloning Technology

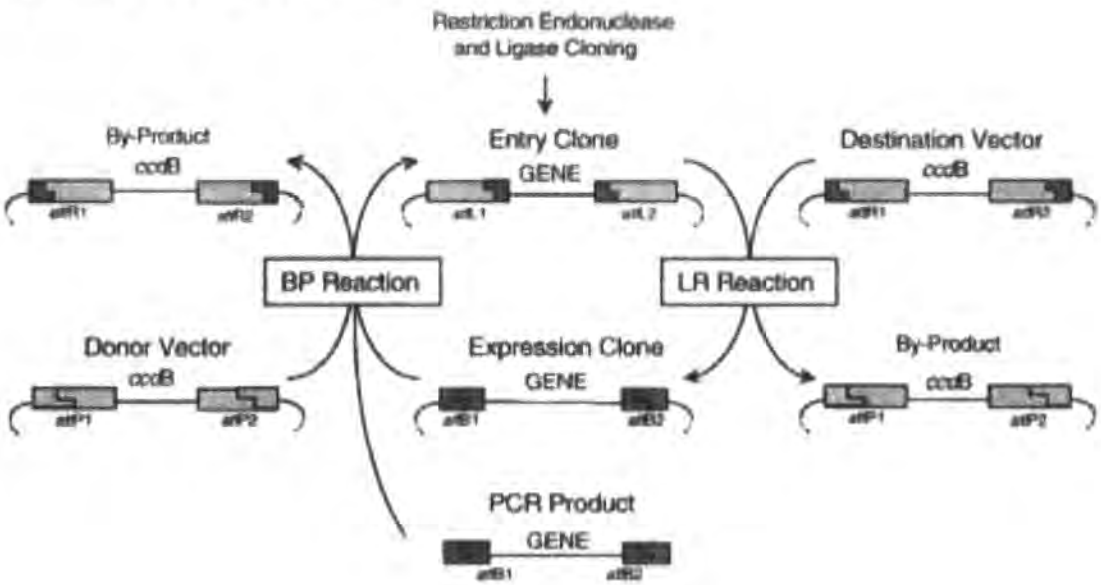

2.5.11 Preparation of Competent *E.coli* cells

The procedure followed as described at Sambrook and Russell, 2001, which is a variation of the method used by Cohen and co-workers to transform bacteria with plasmid DNA (Cohen *et al.*, 1972)

2.5.11.1 Rubidium Chloride method

XL1-Blue MRF' and DH5α strain of *E.coli* were used for preparing competent cells. 1 ml overnight culture of XL1-Blue MRF' cells in LB medium (Luria-Bertaki, 10 g/L NaCl, 10g/L Tryptone, 5 g/L Yeast Extract, pH 7.0) in presence of tetracyclin (100 µg/ ml final concentration) was inoculated in 100 ml Psi broth (5 g/ L Bacto yeast extract, 20 g/ L Bacto Tryptone, 5 g/ L Magnesium Sulfate, pH: 7.6) and grown at 37°C with aeration to A_{550}: 0.45. The cells were kept on ice for 15 minutes before centrifugation at 3000 g for 5 min. The pellet was resuspended in 0.4 volume TfbI (Potassium Acetate 30 mM, Rubidium Chloride 100 mM, Calcium Chloride 10 mM, Manganese chloride 50 mM, glycerol 15 % (v/v), pH: 5.8) and kept on ice for 15 minutes. The cells were pelleted as before, resuspended in 0.04 volume TfbII (MOPS 10mM, Calcium Chloride 75 mM, Rubidium Chloride 10 mM, glycerol 15 % (v/v), pH: 6.5) and either were used immediately or quick frozen at liquid Nitrogen for storage in -80°C. Frozen competent cells were thawed on ice just before use and ligated DNA was added to them quickly.

2.5.11.2 Transformation of Competent *E.coli* cells

Typically, 100 µl of competence cells were transformed with 5 µl of a ligation reaction. The mixture was incubated on ice for 30 minutes and then heat-shocked at 42°C for a minute. The cells were then immediately chilled on ice for 2 minutes and afterwards 800µl

of room temperature LB Broth was added. The cells were allowed to recover at 37°C for 1 hr. The culture was pelleted by spinning for 2 minutes at 4000 rpm in a microcentifuge and then resuspended in 150 µl LB Broth. Transformed cells were spread onto LB agar (LB broth + 20 g/L agar) Petri dishes containing the appropriate antibiotic for the resistance gene in the transformed plasmid. Generally, the antibodies were used in 100 µg/ml concentration. In cases were blue-white selection was applicable (when a vector contained β-galactosidase coding sequence was used) X-GAL was added in the LB medium at 80 µg/ ml concentration and IPTG of 0.5 mM final concentration.

2.5.11.3 Preparation of *Agrobacterium tumefaciens* electrocompetent cells

The preparation and electrotransformation of *Agrobacterium tumefaciens* electrocompetent cells was followed by the protocols described by Topping *et al.*, 1991.

The *Agrobacterium tumefaciens* strain used was C58C3. A single colony grown at 30°C on LB agar plate in presence of 100 µg/ml streptomycin and 25 µg/ml Nalidixic acid was inoculated with aeration in 5 ml LB (100 µg/ ml streptomycin and 25 µg/ ml Nalidixic acid) at 30°C overnight. 100 µl of this culture was inoculated into 50 ml of 2YT (16 g/L pepton, 10 g/L yeast extract, 5 g/L NaCl, pH: 7.2) supplemented with 100 µg/ ml streptomycin and 25 µg/ ml Nalidixic acid and was allowed to grow at 30°C with aeration until the $O.D._{600}$ reached 0.45. When culture reached the target O.D., it was immediately chilled on ice. The cells were then centrifuged at 4000g for 10 minutes at 4°C and resuspended in 50 ml of ice cold 10% (v/v) glycerol. Afterwards, they were spoun at 4000g for other 10 minutes at 4°C and resuspended in 25 ml (0.5 volume) of ice cold glycerol. Cells were again centrifuged as before and resuspended in 1 ml (0.02 volume) of ice cold 10% (v/v) glycerol. The same centrifuge step was repeated and the cells were resuspended again in 1 ml of ice-cold

glycerol. A final centifuge step was occurred at 4000g for 10 minutes at 4°C and cells were resuspended in 0.5 ml of 10% (v/v) ice cold glycerol. Finally, cells were aliquoted into 40 µl volume, snap-frozen in liquid nitrogen and stored at -80°C.

2.5.11.4 Electrotransformation of *Agrobacterium tumefaciens*

Plasmid DNA (2 µl) was added to 40 µl of thawed electrocompetent cells and were mixed gently on ice. The cells were transferred to chilled cuvettes and were "electroporated" with a pulse of 1440 V for 5 ms using Electroporator 2510 (Eppendorf). The cells were then transferred in chilled LB Broth and recovered at 30°C for 3 hours. The culture was then pelleted and resuspended in 150 µl LB broth. The cells were spread onto LB agar *Petri* dishes contained 25 µg/ ml Nalidixic acid, 100 µg/ ml streptomycin and the antibiotic for the resistance gene in the transformed plasmid in 100 µg/ ml concentration. The cell colonies were allowed to grow at 30°C for 48 hours.

2.5.12 Plasmid minipreps, midipreps and maxi preps

Purification of up to 20 µg high-copy plasmid DNA from 1-5 ml overnight cultures of *E.coli* grown in LB medium as carried out using either the QIAprep spin Miniprep kit (Qiagen), or the GeneElute plasmid Miniprep kit (Sigma) or the Wizard DNA purification System (Promega). Purification of low-copy plasmids and preparation of up to 100 µg or 500 µg high copy plasmids midi and maxi preps were occurred accordingly the manufacturer's protocols (Qiagen kit).

2.5.13 Glycerol stocks

E.coli clones were grown overnight in LB broth in the presence of appropiate antibiotic(s) at the specified concentration for the plasmid. An equal volume of the overnight culture

was mixed with 80% (v/v) steriled glycerol up to make the volume up to 1 ml in sterile eppendorfs. The eppendorfs were frozen in liquid nitrogen and then transferred to –80^{0}C for long-term storage.

2.5.14 Automated DNA Sequencing

The DNA sequencing reactions were carried out by the Sequencing Facility Team (Dept. of Biological and Biomedical Sciences, University of Durham) using BigDye terminator with AmpliTaq DNA polymerase (ABI Biosciences). Reaction products were analysed on automated sequencers (ABI Prism 373 STRETCH and ABI Prism 377 XL; DBS Genomics). The sequence data was analysed using the DNASIS-Mac v3.5 software and the BLAST web site (http://www.ncbi.nlm.nih.gov/BLAST/).

2.5.15 Plant genomic DNA extraction

Plant tissues, immediately after harvesting, were frozen in liquid nitrogen and could be stored at - 80 ^{0}C for later processing. Genomic DNA was isolated from plant tissues with the Dneasy Plant mini or maxi kit (Qiagen) based on the manufacturer's instructions.

2.5.16 RNA extraction from plant tissues and tissue culture cells

Total RNA was isolated from *Arabidopsis* plant tissues and tissue culture cells using Rneasy Plant kits (Qiagen) following the manufacturers instructions. The extracted RNA from each sample was treated with DNAase and subsequently the enzyme was removed running the RNA extracts through Qiagen plant RNAeasy mini kit columns. The concentration of RNA was determined by measuring the absorbance at A_{260} nm in a Helios β spectophotometer.

2.5.17 RNA visualisation by electrophoresis

The integrity and size distribution of total RNA purified was checked using agarose gel electrophoresis and ethidium bromide staining. For running RNA on agarose gels TBE buffer (10.8 g/L Tris base, 2.76 g/L boric acid, 0.74 g/ L EDTA) was used.

2.5.18 Reverse Transcription-PCR (RT-PCR)

Total RNA was reverse transcribed into first strand cDNA. Poly-$T_{(24)}$primer (0.5 µg) was mixed with 2 µg of total RNA in a volume of 24 µl. The mixture was heated at 70°C for 10 minutes (in order for RNA secondary structure to be melted) and then transferred in ice for 5 minutes. 5 x reaction buffer, DTT (10mM final concentration) dNTPs (0.5 mM final concentration) and H_20 were added in ice in total volume of 40 µl and the mixture was heated at 42^{0}C for 2 minutes. Then 200 units Superscript II RT (Invitrogen) was added and the mixture was heated at 42°C for 60 minutes for the production of the first strand of cDNA. (One unit incorporates 1 nmole of dNTP into an acid-precipitable material in 10 min at 37°C). The reaction was terminated by incubating the mixture at 70°C for 15 minutes. To remove RNA complementary to the cDNA, 2 units of *E.coli* RNAase were added and the mixture was incubated at 37°C for 20 minutes. RNAase was removed by using the plant RNAeasy mini kit columns.

2.6 Library screening

The procedure followed as described at Sambrook and Russell, 2001, which is a variation of the method used by Singh *et al.*, 1988 and Vinson *et al.*, 1988.

The cDNA libraries, obtained from *Arabidopsis* Biological Resource Center (ABRC, Columbus, USA), were constructed from poly(A)$^+$mRNA isolated from various

Arabidopsis tissues. The bacteriophage lambda (λ) has been used as a cloning vehicle for the cDNA libraries. For this study the *E.coli* host strain XL1-Blue MRF' was used. The XL1-Blue MRF' cells, grown overnight in LB medium (supplemented with 0.2% (w/v) maltose, 10 mM $MgSO_4$) were resuspended and diluted in 10 mM $MgSO_4$ to obtain OD_{550}: 0.5. XL1-Blue MRF' cells were then mixed with the library. After infection with the libraries, cells were incubated at 37°C for 2 hours to allow the cell lysis to occur. The cells were then mixed with NZY top agar (5 g/L NaCl, 2 g/L $MgSO_4$ x 7 H_2O, 5 g/L yeast extract, 10 g/L NZ amine, 0.7 % (w/v) agarose) and plated on NZY plates (5 g/L NaCl, 2 g/L $MgSO_4$ x 7 H_2O, 5 g/L yeast extract, 10 g/L NZ amine,15 g/L Agar, pH: 7.5). Plaques, areas of lysed bacteria, were formed after 6-8 hours. Then the plates were chilled at 4°C for a minimum of 2 hours.

The next step was to transfer some of the phage DNA from the plaques to two replica nitrocellulose membranes (Zeta-Probe GT Genomic Tested Blotting Membrane; BIO-RAD). The plaques were transferred onto the first membrane for 2 minutes and onto the second membrane for 4 minutes. The DNA on the membranes was denaturated with alkali to produce single strands. More specifically, the membranes were immersed in a denaturation solution of 1.5 M NaCl and 0.5 M NaOH for 2 minutes. Then they were transferred into a neutralization solution of 1.5 M NaCl and 0.5 M Tris-HCL (pH 8.0) for 5 minutes and afterwards they were submerged in a 0.2 M Tris-HCL (pH 7.5) and 2x SSC solution (17.5 g/L NaCl, 8.82 g/L sodium citrate, pH: 7.0) for no more than 30 sec. The membranes were blotted on a Whatman 3MM filter paper and the DNA single strands were cross-linked to the membrane by UV irradiation or baking (at 80°C for 2 hours).

Prehybridization solution (50 % (v/v) deionised formamide, 2 X PIPES buffer, 0.5 % (v/v) SDS, blocking agent 100 µg/ml final concentration) was heated up to 50°C. Then, boiled salmon sperm DNA was added after it was boiled for 10 min. (10 x PIPES: 4 M NaCl; 0.1 M PIPES buffer, pH 6.5.) The membranes were placed into prehybridization tubes with the required amount of prehybridization solution (~ 25ml per 4-6 membranes) and were prehybridized for at least 2 hours at 42°C by rotating the tubes in the hybridization oven. The prehybridisation solution reduces unspecific absorption of the radiolabelled probe.

The DNA template used as a probe was first denaturated after boiling for 3 minutes. Immediately after boiling it was chilled on ice for at least 2 min. Then it was labelled with 50µCi of P^{32} using the Amersham Pharmacia Labelling kit, following the manufacturer's instructions. Unincorporated nucleotides were removed using ProbeQuant G-50 micro columns (Amersham Pharmacia). The radioactive probe was mixed with hybridisation solution and the mixture replaced the prehybridisation solution. For each reaction 50ng of probe was used. The membranes were incubated with the hybridisation solution at 42^0C overnight to allow the probe to hybridise to its complementary sequence. After hybridisation, the membranes were washed extensively to remove unhybridised probe. In detail, the membranes were initially washed with 2 x SSC and 0.1% (v/v) SDS solution for 20 min with shaking at 50°C. Then they were washed twice with 0.2 x SSC and 0.1% (v/v) SDS solution for 20 min each at the same temperature. (20 x SSC: 175.3/L NaCl; 88.2/L sodium citrate; pH 7) Afterwards, the membranes were bag sealed and placed in autoradiography cassettes with intensifying screens in contact with X-ray film (Hyperfilm, Amersham Pharmacia) and stored at -70^0C. The X-ray film was exposed and the regions where the probe has hybridised was visualised. By comparing the membrane with the original dish and lining up the regions of hybridisation, the positive plaques were identified.

If membranes were to be screened using a different probe, they were washed in boiling 0.1% (v/v) SDS solution before the subsequent hybridization.

The isolated positive plaques after each screening were stored in 0.5 ml SM buffer (5.8 g/L NaCl, 2.0 g/L $MgSO_4$ x 7 H_2O, 50 mM Tris-HCL of pH:7.5, 0.01 % (w/v) gelatin) with 20 µ l of chloroform at 4°C. For long term storage, supernatant of the isolates was supplemented with and 7% (v/v) of Dimethyl Sulphoxide (DMSO) can be stored at -80°C. The positive plaques were re-plated at a much lower density, and the hybridisation process repeated until a single individual clone was isolated. For the first round of screening, 75,000 plaques per plate were obtained. For the second and third rounds, 5,000 and 500 plaques per plate were obtained respectively. The titer of the cDNA libraries titer was calculated at each step in order to achieve these numbers per plate.

2.6.1 *In vivo* Excision

The recombinant phagemid isolated from a single plaque was converted to a SK (+/-) pBluescript phagemid plasmid. First, XL1-Blue MRF' cells were infected by the isolated phage, in the presence of ExAssist helper phage. This stage resulted in the formation of excised pBluescript phagemid packaged as filamentous phage particles. In the second stage, SOLR cells were transformed with the excised phagemid. Firstly, SOLR cells, grown overnight in LB medium, at an OD_{600} of 1.0 in 10 mM $MgSO_4$ were mixed with the excised pBluescript phagemid. Then the mixture was plated on agar-amplicillin (50 µg/µl) plates and incubated at 37°C overnight. Bacterial colonies grew and DNA was isolated and sequenced.

2.7 Protein analysis

The protein analysis protocols described below are variations of the protein techniques described in previous plant MAP studies (Jiang and Sonobe, 1993, Chan *et al.*, 1996, Smertenko *et al.*, 2000)

2.7.1 Protein expression

The full length of the cDNA was cloned into pET 28α vector (Novagen). The appropriate restriction sites were added to the insert by PCR. The sequence of the clone was verified by sequencing. The cDNA was expressed in *E.coli* BL21(DE3), BL21(DE3)PlysS and BL21(DE3)PlysS STAR (Invitrogen) and the recombinant plasmid was incorporated a 6xHis tag on the N-terminus. Single colonies were incubated at 37°C/200 rpm overnight in LB medium supplemented with kanamycin (50 ng/ml) in final volume 20 ml. Next morning the overnight culture was scaled up to 800 ml of LB + kanamycin (25 ng/ml final concentration. The cells were grown until the culture reached an optical density of 0.5-0.6 measured at 600 nm. Then protein expression was induced by the addition of IPTG in a final concentration 1mM. Cells, after induction, were incubated at 30°C/ 200rpm for 3-4 hours.

2.7.2 Protein Purification

The bacteria cultures were then centrifuged at 4,000 g for 10 min. The pellet was resuspended in ice cold protein extraction buffer (50 mM NaH_2PO_4 of pH 8.0, 300 mM NaCl, 5 mM β-mercaptoethanol) containing protease inhibitors. The protenase inhibitors used were Leupeptin hemisulphate (10 μg/ml), Pepstatin A (10 μg/ml) and Phenylmethylsulfonyl fluoride (PMSF; 1mM). Afterwards the resuspended pellet was sonicated (Soniprep 150, MSF, UK: 10 pulses at amplitude of 26 μm, the length of each

pulse was 1sec/ml of extraction buffer). The bacterial lysates were centrifuged for 10 min at 30,000 g, filtered through 20µm nitrocellulose membrane and applied to columns containing 2 ml of Ni-NTA agarose resin (Qiagen, UK). The Ni-NTA columns were equilibrated with 2 ml of protein extraction buffer. The protein extract was mixed with the resin by shaking the columns for 20 min in ice. The columns were washed three times with protein extraction buffer containing 20 mM, 40 mM and 60 mM imidazole respectively. The washing buffer was constituted of 50 mM NaH_2PO_4, pH 8.0; 0.3 M NaCl and the appropriate concentration of the imidazole buffer at pH 7.0). Four protein extracts of 1 ml each were eluted by elution buffer (50 mM NaH_2PO_4 of pH; 8.0, 300 mM NaCl, 250 mM Imidazole). Ni-NTA column were regenerated by washings with water, 0.2 M Hydrochloric Acid, 30% (v/v) glyceroll and 30% (v/v) EtOH. The column were stored in 30% (v/v) EtOH at 4°C before next use.

2.7.3 Protein Quantification

The protein sample was quantified by Bradford assay using the spectophotometer (Helios, Thermospectronic) at 595 nm. The BIO-RAD protein assay liquid was diluted 5 times. 1 ml diluted assay liquid was mixed with 5 µl protein sample. As blank 5 µl of protein extraction buffer into 1 ml diluted assay liquid was used.

2.7.4 Protein concentration

For protein concentration centrifugal filters were used; vectaspin ™ 3 (Whatman) and vivaspin 2 (VIVASCIENCE) based to manufacturers instructions.

2.7.5 Changing protein buffer for using the protein to raise Antibody

The proteins were dialysed overnight at 4°C against 1 x PBST (570 mg/L NaH_2PO_4, 212 mg/L KH_2PO_4, 8 g/L NaCl, 0.1 ml/L Tween 20, pH: 7.0) supplemented with 1mM DTT. (The tubes used for dialysis had been previously boiled for 30 min in 1 mM EDTA. Then they were washed with dH_2O and stored in 30% (v/v) EtOH.) Alternatively, the protein was run through either PD-10 column (Amersham Pharmacia) or self-made sephadex column. The PD-10 column was used following the manufacturer instructions and equilibrated with 1 X PBST supplemented with 1mM DTT. After use the column was washed with dH_2O and was kept at room temperature until next use. Sephadex column preparation: A 2.5 ml syringe was placed into a 12 ml centrifuge tube and at its bottom was inserted glass wool. In a flask was mixed sephadex G-25 (Sigma) with 3 X volume PBST + 1 mM DTT and then poured into the syringe up to 2.5 ml volume. The syringe was equilibrated by centrifugation at 3,000 rpm for 3 min. 150 µl maximium volume of protein solution was added and the syringe was centrifuged at 3,000 rpm for 3 min. The elution contained the protein in PBST buffer.

2.7.6 Protein renaturation after precipitation

Protein solution after changing buffer was centrifuged at 5,000 rpm. Supernatant contained the soluble protein was going through a centrifugal filter for protein concentration (vectaspin or vivaspin). In order to solubilise the remaining precipitated protein, 50 µl 1 X PBST, 1 mM DTT and 4mM urea were added into the pellet and were mixed thoroughly by vortexing. Afterwards, the mixture was centrifuged at 13,000 rpm for 2 min. The soluble protein at supernatant was going through concentration and the formed pellet was renaturated by the same way.

2.7.7 Protein preparation for immunisation

The soluble protein was used to immunise mice and was administrated in three fortnightly injections of 100μg protein. Prior immunisation 1 X PBST was added to the protein up to 250 μl volume. The solution was mixed with 1:1 (v/v) Freunds incomplete adjuvant (Sigma) and vortexed for 10 min. The protein solution was afterwards divided between 3 mice, which were immunised at both sides of their tummy.

2.7.8 Protein purification specifically for biochemical analysis

AtMAP65-6 in order to be used for biochemical analysis had to be transferred from immidazole elution buffer into MT stabilising buffer, MTSB, (80 mM Pipes of pH 6.8, 1 mM $MgCl_2$, 1 mM EGTA of pH: 6.8, 30 % (v/v) glycerol, 50 mM $NaCl_2$ 3 mM DTT). But as AtMAP65-6 proved to degrade easily during purification and to precipitate through solution changes, a few alternations in the purification protocol were followed. Firstly, DTT at 3mM final concentration was added to each of the washing buffers. Secondly, in order to avoid the buffer-changing step, AtMAP65-6 was not eluted in the usual immidazole elution buffer but in MTSB supplemented with 250 mM immidazole. AtMAP65-6 was concentrated by centrifugation at 13,000 rpm through vivaspin concentrators. Through this step the immidazole was removed from the protein solution.

2.7.9 One Dimensional Polyacrylamide Gel (1D PAGE)

Before the proteins run at 1D PAGE gel, they were mixed 1:1 with 2 x SDS PAGE sample buffer (0.050 M Tris base, 3.8M Glycine, 0.2 % (v/v) SDS) and then boiled at 100°C for 3 min.

The glass plates used for the 1D PAGE apparatus (ATTO CORPORATION) were cleaned with distilled H_2O and ethanol before being assembled. The resolving gel medium was constituted from 6 to 15 % (v/v) acrylamide/ bisacrylamide (Protogel), depending on the protein size, 0.1 % (v/v) SDS, 0.375 M Tris solution of pH: 8.8, 0.1 % (v/v) APS, 0.1 x 10^{-3} volume Temed. The medium was poured 1.5 cm from the top of the plates and covered with ethanol until to solidify. Ethanol overlay was then poured off and the surface was washed with distilled H_2O. Stacking gel (3 to 5 % (v/v) acrylamide/ bisacrylamide; 0.1 % SDS; 0.125 M Tris solution of pH: 6.8; 0.1 % (v/v) APS, 0.1 x 10^{-3} volume Temed) was poured on the top of the desolving gel at the presence of comb. After gel solidification the comb was removed and the wells were washed with distilled H_2O. Protein samples were loaded and gel was run in 1 x SDS PAGE sample buffer at 20 mV until the bromophenol dye had reached the bottom of the resolving gel. Gel was then stained with coomassie solution (25 % (v/v) Methanol, 1 % (v/v) Acetic acid, 12.4 g/L coomassie Brilliant Blue R-250) or it was used for electroblotting. In the case where coomassie staining was used, gel was distained with the fast gel distaining solution (25 % (v/v) Methanol, 1 % (v/v) Acetic acid) or with the normal gel distaining solution (1 % (v/v) Methanol, 1 % (v/v) Acetic acid).

2.7.10 Two Dimensional SDS - Polyacrylamide Gel Electrophoresis (2D PAGE)

In the first dimension of 2D gel electrophoresis, the proteins were separated according to isoelectric point by isoelectric focusing using the Immobiline DryStrip (Pharmacia Biotech), following the manufacturer's instructions. The Immobiline DryStrip gels were rehydrated prior to use in rehydrating solution containing ampholines with matching pH. The strips used in this study were 11 cm long and their pH range was 4-7. The rehydration solution used was constituted by Urea 7.5 M, Tiourea 2M, CHAPS 2% (v/v), ampholines

pH 4-7 (Pharmacia) and DTT 20mM. The amersham pharmacia Biotech Electrophoresis power supply (EPS 3501 XL) was used for the isoelectric focusing. The programme used was for the first step, 300 V for 10 minutes, at second step 3500 V for 1h and 30 min and for the third step 3h and 30 min. The Multi Temp™ III (amersham biosciences) was used to circulate constant temperature liquid to the Isofocusing Electrophoresis system and was set to keep the gels at 16°C during the run.

After the isoelectric focusing step, the strips were washed in Equilibration solution (Urea 72g/200 ml, SDS 2g/200ml, Tris-HCl , glycerol 60ml/200ml). For the first 10 min-wash in Equilibration solution, 100 mg DTT were added. For the second 10 min-wash, 450 mg iodoacetamide were added plus a few grains of the pH indicator Bromophenol Blue. Then second dimension electrophoresis was processed, during which the proteins were separated on the basis of their molecular weight using SDS-PAGE gel. In specific, the Ettan™ DALT*six* Electrophoresis system (Amersham Pharmacia) was used for the second dimension electrophoresis, based to the manufacturer's instructions and the amersham biosciences electrophoresis power supply EPS 601. The programme used was 40 mA for overnight run.

2.7.11 Western blotting

Proteins were transferred from the gel onto Blotting membrane-nitrocellulose (BDH Electran) at 20 V O/N or alternatively at 400 mA at 2 hrs. (The protein blot system was from BDH and the power supply used was the BIORAD PAC 300.) The transfer buffer used was constituted by 38 mM Glycine, 48 mM Tris, 0.037 % (v/v) SDS, 20 % (v/v) methanol. Then, the membrane was stained with 100 diluted Amido black solution (1 %

(w/v) Naphtol blue black in 5 % (v/v) acetic acid) to check transfer. Afterwards, the membrane was washed in distilled H_2O and dried in air.

2.7.12 Immunochemical localisation of proteins on western blots

The NC membrane was blotted in TBST buffer (10 mM Tris of pH: 7.4, 150 mM NaCl, 0.5 ml/L Tween 20) + 5 % (w/v) fat free milk powder for 30 minutes. Then it was incubated with primary antibody diluted in TBST + milk medium for 1 hour. After 3 washes in TBST for 10 minutes each, secondary horseradish conjugated antibody diluted in TBST + milk was added for 45 minutes. 2 washes in TBST were followed for 10 minutes each and the immunochemical reaction was detected by the ECL western blotting analysis system (Amersham Pharmacia) on X-ray film (Amersham Pharmacia).

2.8 Microtubule Co-Sedimentation Assay

Pig brain tubulin was rapidly defrosted from –80 °C to 4°C using a 42°C heating block. Then it was transferred into ice immediately. Both tubulin and recombinant proteins were centrifuged at 200,000 rpm for 10 min at 2^0C to remove any aggregates. The supernatants were collected and the pellets were washed and resuspended in SDS-PAGE sample buffer. The MTs were polymerised with 10 μM taxol in presence of 1mM GTP by incubation at 32°C for 20 min. (The taxol was diluted in DMSO from 10mM stock.) Then the taxol stabilised MTs were mixed with recombinant protein in 1:2 molar ratio and 1 X MTSB. In the negative controls, when MTs were not added in the mixture, the reaction mixture was supplemented with MTSB buffer containing 10 μM taxol. The mixtures were incubated for 10 min at 32°C and centrifuged at 100,000 g for 30 min at 32°C. Supernatants and pellets were loaded on 1D SDS-PAGE.

2.9 Microtubule Turbidometric Assay

Pig brain tubulin was rapidly defrosted from –80 °C to 37°C using a 37°C heating block, was incubated on ice for 5 min and centrifuged at 200,000 g for 10 min to pellet tubulin aggregates. The supernatant was diluted to a 30 μM tubulin solution in MTSB. Then GTP was added to a final concentration of 1 mM and recombinant protein in 1:2 molar ratio with tubulin. The final reaction volume was adjusted to 150 μl with MTSB and the turbidity of the reaction was monitored at 350 nm and at 32°C using a Helios β spectrophotometer equipped with Unicam Peltier temperature control unit (Thermospectronic, UK). In the control experiment, in absence of recombinant protein, the reaction mixture was supplemented with MTSB buffer.

2.10 *Arabidopsis thaliana* cell cultures

An *Arabidopsis thaliana* suspension cell culture variety Erecta was a gift from Professor Tony Slabas. The culture was maintained at 27^{0}C with shaking at 120 rpm (in a 16 hour photoperiod regime). The cells were subcultured into fresh medium (30 g/L sucrose, 4.43 g/L Murashige and Skoog medium (GibcoBRL), 0.5 mM napthalene acetic acid, 0.05 mM kinetin, pH: 5.7) once every week.

2.11 Protein extraction from *Arabidopsis* tissues and tissue culture cells

Cells were ground in liquid N_2. One part of the tissue was mixed with nine parts of boiling SDS-PAGE sample buffer and the mixture was boiled for 5-6 minutes. Then it was centrifuged for 10 minutes at 13000 rpm and its supernatant was mixed with eight parts of Acetone. The mixture was kept at –20^{0}C for 30 minutes and subsequently centrifuged for 5 minutes at 3000 rpm. The supernatant was thrown away and the pellet was washed with 70% (v/v) aceton. The pellet was then air-dried for 15 minutes and 100 μl of Lysis buffer

(0.5 M Tris, pH 6.8, 8M Urea, 4% (v/v) CHAPS and 65 mM DTE) were added in it. The mixture was centrifuged at 13000 rpm for 10 minutes. The supernatant was run on 2D SDS-PAGE gel.

NOTE:

SDS-PAGE sample buffer could be removed from the protein sample using a sephadex column. A 2.5 ml syringe a piece of glass wool was placed at its bottom. Sephadex 25 was added in Tris buffer, pH 7.5 (1: 3 v/v) and placed into the syringe. The syringe was spound at 3000 rpm for 3 minutes for equilibration and then about 50 µl of the protein sample was added and spinned at the same conditions. The-flow through was collected and could be used for Bradford assays.

From tissue culture cells

Protein extraction from tissue culture cells followed the same procedures as in plant tissues case. About 2 ml of packed cell volume was used.

2.12 Microtubule Immunolocalisation in *Arabidopsis* tissue culture cells

The protocols followed was a variation from the immunolocalisation procedures described by Smertenko *et al.*, 2000.

Arabidopsis suspension tissue culture cells were separated from the tissue culture media using 100 mesh nylon cloth and fixed for 30 minutes in freshly prepared fixative (4 % (w/v) paraformaldehyde in 0.1M PIPES, pH: 6.8; 5 mM EGTA; 2 mM $MgSO_4$; 0.4 % (v/v) Triton X-100). Then after two washings for 5 minutes each in PBS buffer (570 mg/L NaH_2PO_4, 212 mg/L KH_2P0_4, 8 g/L NaCl, pH: 7.0), the cells were treated at room temperature with enzyme mixture (0.8 % (w/v) Macerosyme R-10; 0.2 % (w/v) Pectolyase

Y-23; 0.4 M Mannitol; 5 mM EGTA; 15 mM MES, pH: 5.0) in presence of protease inhibitors (1mM PMSF, 10 μg/ μl Leupeptine, 10 μg/ μl Pepstatin A). The cells were washed twice at PBS buffer for 5 minutes each time and afterwards attached onto coverslips coated with 1 mg/ml solution of poly-L-lycine for 5-10 minutes. (The coverslips before the poly-L-lycine applied on them were washed in detergent and after rinsing with dH2O were washed in chromic acid overnight. Afterwards were intensively washed in dH2O and stored in 50 % (v/v) ethanol; 50 % (v/v) ether solution) Coverslips with attached cells were incubated in PBS+2% (v/v) bovine serum albumine (BSA) for 30 minutes. (Alternatively, coverslips could be stored at 4°C in presence of 0.02 % (w/v) sodium azide). For immunostaining, coverslips were incubated for 1h in primary antibody or antibody mixtures and then were washed 3 times in PBS for 7 minutes each. Finally coverslips were incubated in secondary antibody or antibodies for 1h and were mounted in Vectashield (Vector Laboratories) after washing them briefly in PBS. In case of nuclei staining, coverslips were incubated for 10 minutes in PBS containing DAPI before mounting in Vectashield. The primary antibodies used were the mouse anti-AtMAP65-6 diluted 1:200 in PBS+2% (v/v) BSA and the sheep anti-β1 tubulin antibody (Smertenko *et al.*, 1998) diluted 1:500 in PBS+2% (v/v) BSA. The secondary antibodies used were the anti-mouse Tritc conjugate developed in goat, and the anti-sheep FITC conjugate developed in donkey (both secondary antibodies were provided from Sigma). Single images and z-stacks of the cells were acquired using a Zeiss Axioskope microscope (Carl Zeiss Ltd.) fitted with a Bio-Rad Radiance 2000 laser scanning system. The red and green channels were acquired sequentially using a HeNe laser for the red channel and an Argon laser for the green channel. The FITC fluoroform was excited at 494 nm and emmited at 520 nm. The Tritc fluoroform was excited at 554 nm and emitted at 576 nm.

2.13 Gus fusions

The gene promoters were cloned into the binary vector pΔ-GUS-Bin19 (Topping *et al.*, 1991), which was a gift by Prof. Keith Lindsey, and the *Agrobacterium tumefaciens* strain C58C3 was used for tranforming *Arabidopsis* plants. The protocols followed as described by Topping *et al.*, 1991.

2.14 Plant transformation (dipping method)

2.14.1 Plant material

*Arabidopsis thaliana (*variety Columbia) were grown in soil in pots (6-7 plants per pot) with plastic mesh placed over the soil. After 3-4 weeks when they are about 10-15 cm tall and have a few of unopened flower puds are ready for dipping. One day before dipping open flowers and young siliques were removed to eliminate background.

2.14.2 *Agrobacterium* cultures

Agrobacterium colonies containing promoter and P-Δ-GUS-Bin19 fusions were grown for 48 hours at 30 ^{0}C in presence of 25 μg/ml Nalidixic acid, 100 μg/ml streptomycin and 50 μg/ml of the appropriate antibiotic to the transformation vector. Single colonies were inoculated at 200 ml LB supplemented with the same antibiotics used for the colonies incubation. Cultures were pelleted by centrifugation and resuspended in 1 litre of freshly made 5% (w/v) sucrose solution. Then Silwett L-77 was added to a final concentration of 0.05% (v/v).

2.14.3 Dipping Procedure

Plants were fully dipped and gently agitated for 15 seconds into the *Agrobacterium* solution (mesh prevents plants falling out). Afterwards the plants were placed in trasparent bags to

keep humidity and placed in a shaded position overnight. Next day the plants were taken out from the bag and were left to grow at normal greenhouse conditions. The dipping procedure was repeated after a week with fresh grown bacteria and then plants were left to set seed and dry out. (Plants were placed in large photographic negative bags to prevent cross contamination between pots.) Seeds were collected from individual pots over a period of 2-4 weeks as seeds gradually mature.

The seeds of the second generation plants were collected from each line using the ARASYSTEM aracons (LEHLE SEEDS) to prevent seed mixing between the lines.

2.15 *Arabidopsis* seeds sterilisation and storage

Seeds were initially washed at 70% (v/v) EtOH for 2 minutes and then incubated in 5% (v/v) sodium hypochloride (BDH) and 0.05% Tween-20 solution for 10 minutes. After 3 times washings with steriled dH_2O could kept at 4 ^{0}C for a week. For long term seeds should be stored dry without sterilisation.

2.16 Selection of antibiotic resistant seeds

Seeds were germinated on 0.6 % plant agar (Duchefa) plates with 1/2 Murashige and Skoog medium (Duchefa) and 200 μg/ml augmentin (SmithKline Beecham Pharmaceuticals). Seed selection occurred with supplementation of the appropriate antibiotic to the transformation vector in 50 μg/ml final concentration. Antibiotic resistance plants were transferred to soil and their seeds were tested for segregation on selective plates.

2.17 Histochemical GUS analysis

Plant samples were placed into appropriate size tubes and covered with substrate solution (100mM phosphate buffer contained Na_2HPO_4 and NaH_2PO_4 at 1.5 : 1 v/v ratio, 10 mM EDTA of pH: 8.0, 0.1 % (v/v) Triton X-100, 0.5 mM potassium ferricyanide, 0.5 mM potassium ferrocyanide, pH 7.0) supplemented with X-Gluc in 1mM final concentration. Samples were vacuum-infiltrated and then incubated at 37°C from a few hours to overnight depended on the signal strengthen.

2.17.1 Clearing Plant tissues

2.17.1.1 Ethanol treatment

The simplest way to clean tissues from chlorophyll was to wash them in 70% (v/v) ethanol repeatedly for a few hours (the blue precipitate was remained stable)

2.17.1.2 Chlorallactophenol treatment

A most effective way for tissues clearance was followed using chlorallactophenol as was described by N.Barthels *et al.*, 1997. Plants were treated for 30 minutes with 90% (v/v) ice-cold acetone followed by several washes with 0.1 M sodium phosphate (pH 7.0). Then incubation with GUS substrate was followed as described above in paragraph 2.17. Plants were afterwards fixed with 2.5% (v/v) glutaraldehyde at 4°C for several hours. Plant fixation prevented GUS product diffusion to adjacent tissues during incubation to chlorallactophenol (2:1:1 v/v mixture of chloral hydrate: lactic acid: phenol). Incubation of plants in chlorallactophenol was removing all pigments and phenolics and GUS staining resulted in a clear signal.

2.17.2 Binocular microscope

The Binocular microscopes used were the Olympus SZH10 and the ZEISS (Axioskop) with a Photometrics COOLSNAP^{TM}*cf* (Roper Scientific Inc) colour digital camera attached. The captured images were processed using Open*lab* 3.1.1 software and the Abode Photoshop 7.0.

2.18 Yeast Two Hybrid Interactions

The yeast strains AH109 and Y187 were used in this study.

2.18.1 Small-scale yeast transformations

The small-scale yeast transformations were carried out based to the protocol described by Causier and Davies, 2002. From a freshly grown plate of either AH109 or Y187 one colony was inoculated into 10 ml of liquid media YPAD (10g/L tryptone, 10g/L yeast extract, adenine hemisulphate 100mg/L, 2% (w/v) glucose, pH 5.8) and incubated overnight at 30°C/ 200 rpm. An appropriate amount of the overnight culture was inoculated into 100 ml YPAD to give an OD_{600} of 0.2 and incubated for 4h and 30 min at 30°C/ 200 rpm. The cells were pelleted at 1000g for 5 min and washed in 100 ml sterile water. The cells were washed in 1.5 ml 1 x Li/TE and resuspended in 0.5 ml 1 x Li/TE. 1 x Li/TE was prepared from autoclaved 10 x TE (100 mM Tris-Cl, pH7.5; 10 mM EDTA, pH 7.5) and 10 x LiAc (4M LiAc, pH 7.5) solutions (TE- LiAc-H_2O; 1:1:8). Each transformation was consisted of the followings components:1 µg plasmid DNA, 160 µg ssDNA (disperse salmon sperm DNA at 10 mg/ml in TE), 100 µl yeast cell suspension, 10 µl DMSO, 600 µl 1 x PEG/Li/TE. 1 x PEG/Li/TE was prepared by making 1x Li/TE using an autoclaved 50% (v/v) polyethylene glycol solution instead of H_2O. The transformation components were mixed gently and incubated in 30°C for 30 min and then at 42°C for 30 minutes.

The cells were pelleted, and resuspended in 1 ml sterile water. 100 µl were plated onto appropriate Synthetic Dropout selective media and incubated at 30°C for three days.

2.18.2 Synthetic Dropout (SD)

The SD medium was used for making the plates of amino acid selection based to the recipe described by the manual MATCHMAKER Library construction and screening kit (Clontech). It was composed by Difco Yeast Nitrogen base (4g); glucose 12g; Synthetic Dropout selection medium mix (0.4g); Difco Bacto Agar 10g and distilled water 600 ml; pH 5.6. The Synthetic Dropout Selection Medium Mix is constituted from: 30 mg/L Adenine hemisulfate; 20 mg/L Arginine HCl; 100 mg/L Glutamic Acid; 20 mg/L Histidine HCl, 33 mg/L Inositol, 30 mg/L Isoleucin, 30 mg/L Leucine, 30 mg/L Lycine HCl, 20 mg/L Methionine, 3 mg/L p-aminobenzaic acid, 50 mg/L Phenylalanine, 100 mg/L Homoserine, 40 mg/L Tryptophan, 30 mg/L Tyrosine, 20 mg/L Uracil, 150 mg/L Valine.

The appropriate components were omitted to prepare SD-Ade, SD-His, SD-Leu, SD-Trp, SD-Leu/Trp, and SD-His/Leu/Trp (- represents minus).

2.18.3 Yeast mating protocol

A single colony of the a-type strain was resuspended in 30 µl sterile water. A single colony of the α-type strain was resuspended in 30 µl sterile water. Onto a fresh YPAD plate (YPAD + 2% (w/v) bacteriological agar) 2.5 µl of the a-type yeast suspension was pipetted and allowed to become absorbed into the media. 2.5 µl of the α-type yeast suspension was pipetted on the dried a-type spot. The plate was incubated at room temperature until yeast growth is present (about 2 days). A small amount of the yeast growth was streaked onto SD –W, -L plates to select single colonies of diploid yeast. The yeast cells were grown at 30°C.

Single colonies were then resuspended in 30µl sterile H_2O and 3µl were spotted onto reporter gene selective media to check for protein-protein interactions.

2.18.4 Yeast glycerol stocks

The remaining 27µl of the resuspended colony into sterile water was inoculated in 3 ml YPAD + 2% (v/v) glycerol. The mixture was grown at 30°C for 1-2 days. The cells were then centrifuged at 1000g for 5 min and the pellet was resuspended in YPAD + 2% (v/v) glycerol medium. The glycerol stocks were let to freeze slowly at –80°.

2.18.5 *LacZ* assay

Filter paper (Whatman) was placed on top of transformant colonies growing on selective medium. The filter paper with the colonies attached was removed from the plate and placed colony side up in a pool of liqiud nitrogen for 15 sec. Then it was allowed to thaw at room temperature. Another filter paper (Whatman) was soaked in Z buffer supplemented with X-Gal. (Z buffer per litre: 16.1 g $Na_2HPO_4.7H_2O$; 5.5g NaH_2PO_4. H_2O; 750 mg KCl, 246 mg $MgSO_4$. $7H_2O$; pH 7.0.) The stock solution of X-Gal (5-bromo-4-chloro-3-indolyl-β-D-galactopyranoside) was made by dissolving 1g X-Gal in 50 ml of N,N-dimethylformamide and stored at –20°C. The in Z buffer + X-Gal solution was made fresh by adding 270 µl of β-mercaptoethanol and 1.67ml of X-Gal stock solution to 100 ml of Z buffer. The first filter, yeast colonies up, was placed onto the filter paper soaked in Z buffer + X-Gal. The filter papers were incubated at room temperature overnight.

Chapter 3

AtMAP65 Homologues and Consensus Motifs

3.1 Introduction

The objectives of this chapter is collection of Bioinformatics data on AtMAP65s, an initial step approaching the protein regulating factors (such as post-translation modifications, hormonal and environmental stimuli). The MAP65 proteins are abundant throughout the plant kingdom. A search in genome database at NCBI (http://www.ncbi.nlm.nih.gov/) revealed that there are nine *AtMAP65* genes in *Arabidopsis*. MAP65 homologues also exist in insects, vertebrates and yeast. In this study the diversity of the MAP65 proteins from *Arabidopsis* and other various species is investigated, constructing a MAP65 phylogenetic tree (Fig. 3.1). The MAP65 phylogenetic tree will give an indication of which MAP65 members belong in the same group based on their similarity of their deduced amino acids and potentially on their functional diversity.

In literature there are examples of MAP functions (such as MT binding and interaction with other proteins) to be controlled by phosphorylation (Hoshi *et al.*, 1992, Verde *et al.*, 1990, Diaz-Nido *et al.*, 1990; Mandelkow *et al.*, 1993). The presence of phosphorylation sites in AtMAP65s will be a primary indication that this could be the case in AtMAP65s function as well. Identification of phosphorylation sites in AtMAP65 genes suggest that the expression and activity of AtMAP65s are potentially under post-translation modification control. Searching in phosphorylation prediction servers Prosite (http://npsa-pbil.ibcp.fr/cgi-bin/npsa_automat.pl?page=npsa_prosite.html) and NetPhos 2.0 (www.cbs.dtu.dk/services/NetPhos) putative phosphorylation sites were found in all nine

AtMAP65 protein sequences. In addition, the search in Prosite revealed putative post-translation modification sites in AtMAP65 sequences.

Promoters contain transcriptional factors/motifs affected by hormones and/or environmental stimuli (such as temperature, light) and play a regulatory role in gene transcription. Identifying the promoter motifs in *AtMAP65* promoters will indicate the hormonal and environmental factors that possibly regulate *AtMAP65* expression. The regions 1.5 kb upstream the *AtMAP65* genes first translation codon have been selected as putative promoter regions. The plant *cis*-acting regulatory element web site (http://oberon.fvms.ugent.be:8080/PlantCARE/http://oberon.fvms.ugent.be:8080/PlantCARE/) has been used for identifying transcription regulatory motifs within the putative *AtMAP65* promoter regions.

3.2 *Arabidopsis MAP65* family

A search in NCBI revealed nine *MAP65* genes in the *Arabidopsis* genome. The deduced amino acid *Arabidopsis* MAP65 sequences show 28-81% identity and the predicted molecular weight varies from 62.7 to 80.3 kDa (table 3.1). The AtMAP65 molecular weights were calculated using the Protein Molecular Weight tool in the http://bioinformatics.org/sms/index.html web site. The coding sequences of *AtMAP65-1* (Smertenko *et al.*, 2004), *AtMAP65-5* (Smertenko *et al.*, unpublished data), *AtMAP65-3* (Muller *et al.*, 2004) and *AtMAP65-6* (Kaloriti D., unpublished data; chapter 5) have been cloned and were identical to the predicted sequences in the NCBI.

Table 3.1: AtMAP65 homology

	AtMAP65-1	AtMAP65-2	AtMAP65-3	AtMAP65-4	AtMAP65-5	AtMAP65-6	AtMAP65-7	AtMAP65-8	AtMAP65-9	Molecular weight (kDa)
AtMAP65-1	100									65.8
AtMAP65-2	81	100								65.2
AtMAP65-3	44	43	100							80.3
AtMAP65-4	36	37	46	100						73.5
AtMAP65-5	45	45	39	35	100					62.7
AtMAP65-6	44	41	37	34	41	100				69.4
AtMAP65-7	44	42	36	34	41	78	100			72.5
AtMAP65-8	40	39	33	28	37	35	35	100		68.3
AtMAP65-9	39	38	53	42	34	37	36	33	100	65.9

3.3 MAP65 Phylogenetic Tree

The PAUP (phylogenetic analysis using parsimony; Shwofford *et al.*, 1991) programme (version 4.0b10) was used to construct a MAP65 phylogenetic tree using MAP65 protein sequences from various plant, yeast, vertebrate and insect species (figure 3.1). The MAP65 phylogenetic tree was constructed working in co-operation with Dr Andrei Smertenko. The PAUP programme parameters were adjusted so that the only clades retained in the tree had bootstrap value over 60%. For determination of bootstrap values, 1000 replicas of the tree were performed.

The bootstrap value is calculated as following. Let there be m sequences, each with n amino acids. A phylogenetic tree is reconstructed from these sequences using some tree building method. From each sequence, n amino acids are then randomly chosen with

Figure 3.1
MAP65 Phylogenetic Tree

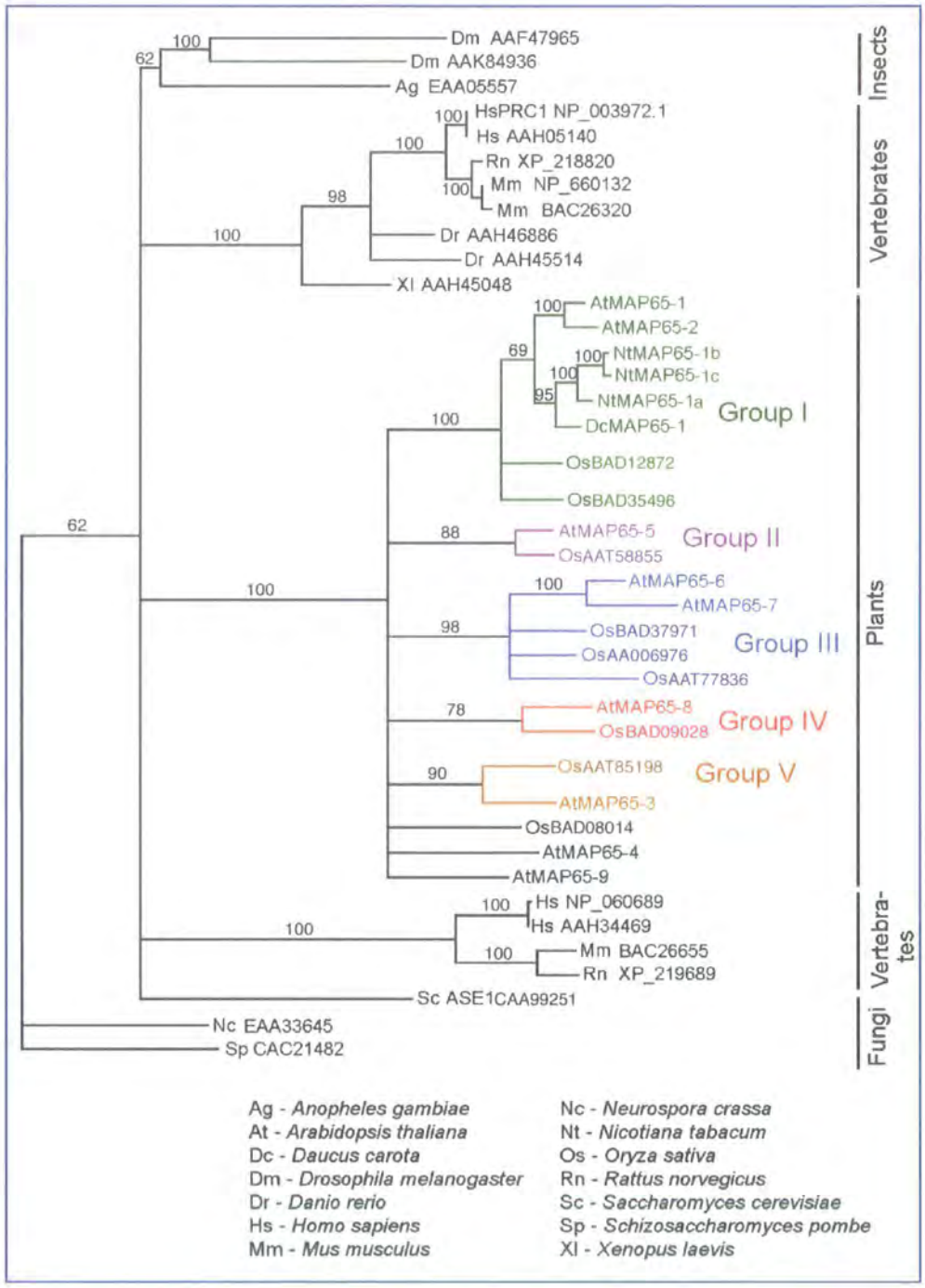

Figure 3.1: Phylogenetic tree of the AtMAP65 proteins and their homologues in various species.

replacement, giving rise to *m* rows of *n* columns each. These now constitute a new set of sequences. A tree is then reconstructed with these sequences using the same tree building method as before. The topology of this tree is compared to that of the original tree. Each interior branch of the original tree that is different from the bootstrap tree in terms of the sequences it partitions is given a score of 0; all other interior branches are given the value 1. This procedure of resampling the sites and subsequent tree reconstruction is repeated several hundred times, and the percentage of times each interior branch is given a value 1 is noted. This is known as the bootstrap value (http://www.megasoftware.net).

The plant MAP65 sequences used to construct the phylogenetic tree were nine from *Arabidopsis*, nine from rice, three from tobacco and one from carrot. The accession numbers of the AtMAP65, NtMAP65 and DcMAP65 proteins are listed in appendix A. The accession numbers of the rice, vertebrate, yeast and insect MAP65s homologues were obtained in NCBI and indicated on the phylogenetic tree. The vertebrate proteins used were homologues to the PRC1 protein. Specifically, the PRC1 sequences used were four from *Homo sapiens*, two from *Rattus norvegicus*, three from the *Mus musculus*, two from the *Danio rerio* and one from *Xenopus laevis*. The insect proteins used, also PRC1 homologues, were two from the *Droshophila melanogaster* and one from *Anopheles gambiae*. In addition, the yeast Ase1 protein sequence was used from *Saccharomyces cerevisiae*. The sequences were first aligned into Clustal W (http://www.ebi.ac.uk/clustalw), exported into NEXUS format and downloaded to PAUP programme. The tree was processed using Adobe Photoshope 7.0. Two distant MAP65 isoforms from yeast (NcEAA33645 and SpCAC21482) were used as the tree out-group. AtMAP65-1 has 12% and 16% with NcEAA33645 and SpCAC21482 respectively.

3.3.1 Plant AtMAP65 homologues

Plant MAP65 proteins comprise five groups based to their homology with each other. At "group I" belongs the AtMAP65-1, the AtMAP65-2, the three tobacco MAP65 proteins, the DcMAP65-1 (carrot) and two rice MAP65s (table 3.2).

Table 3.2: Homology of the MAP65 phylogenetic tree group I

	AtMAP65-1	AtMAP65-2	NtMAP65-1a	NtMAP65-1b	NtMAP65-1c	DcMAP65-1	OsBAD12872	OsBAD35496
AtMAP65-1	100							
AtMAP65-2	81	100						
NtMAP65-1a	74	70	100					
NtMAP65-1b	69	66	85	100				
NtMAP65-1c	70	68	85	98	100			
DcMAP65-1	72	71	80	76	77	100		
OsBAD12872	58	57	61	57	57	60	100	
OsBAD35496	64	61	64	61	61	65	57	100

At "group II" belongs AtMAP65-5 with another MAP65 from rice, OsAAT58855. The homology between them is 39%. The group III is constituted by AtMAP65-6, -7 and three rice proteins (table 3.3).

Table 3.3: Homology of the MAP65 phylogenetic tree group III

	AtMAP65-6	AtMAP65-7	OsBAD37971	OsAA006976	OsAAT77836
AtMAP65-6	100				
AtMAP65-7	78	100			
OsBAD37971	56	54	100		
OsAA006976	53	53	53	100	
OsAAT77836	45	40	44	53	100

"Groups IV" consists of AtMAP65-8 together with OsBAD09028, which share 43% identity to each other. "Group V" consists of AtMAP65-3 together with OsAAT85198 which have 54% identity between them. AtMAP65-4 and -9 do not group with any of the examined MAP proteins.

3.3.2 Animal and Yeast AtMAP65 homologues

The Anaphase Spindle Elongation factor, Ase1, (Pellman *et al.*, 1995) from *Saccharomyces cerevisiae* and the vertebrate Protein Regulating Cytokinesis, PRC1, (Jiang *et al.*, 1998) show 13% and 17% identity with AtMAP65-1. Ase1 and PRC1 show 15% identity with each other. Neither Ase1 nor any of the PRC1 homologues examined from insects and vertebrates integrated into the plant MAP65 groups formed in the phylogenetic tree.

3.4 AtMAP65 Protein Phosphorylation Sites

Two prediction servers were used to identify putative phosphorylation sites within AtMAP65 protein sequences, Prosite and NetPhos.

3.4.1 Search in Prosite

Based on the Prosite search (web site: http://npsa-pbil.ibcp.fr/cgi-bin/npsa_automat.pl?page=npsa_prosite.html) the AtMAP65 proteins have highly conserved phosphorylation sites for four protein kinases: cGMP- and cAMP-dependent protein kinases, protein kinase C, casein kinase II and tyrosine kinase (figure 3.2). The alignment of the AtMAP65 proteins in figure 3.2 was made using clustal X, SeqVu and Adobe Acrobat 4.0 programmes.

3.4.1.1 cAMP- and cGMP-dependent protein kinase

All AtMAP65 proteins except AtMAP65-5 have potential cAMP- and cGMP-dependent protein kinase phosporylation sites. Both cAMP- and cGMP-dependent protein kinases have a preference for the phosphorylation of serine or threonine residues found close to at least two consecutive N-terminal basic residues; however, there are exceptions in this rule (Glass *et al.*, 1986; Pinkse *et al.*, 2004). The motif used from the Prosite was (R/K)-x-x-(pS/pT), prosite access number: PS00004, and the randomised probability of the findings was 1.527×10^{-3} (figure 3.2). The randomised probability is the probability of the pattern occurring in the sequence by chance (http://genamics.com/expression/proscan.htm).

3.4.1.2 Protein Kinase C

The Prosite search revealed all AtMAP65 proteins have potential protein kinase C motifs. The consensus pattern the site used for the search was (pS/pT)-x- (R/K) and the randomised probability for the outcome was 1.423×10^{-3}, prosite accession number PS00005 (figure 3.2).

Figure 3.2
AtMAP65 Phosphorylation Sites predicted by Prosite

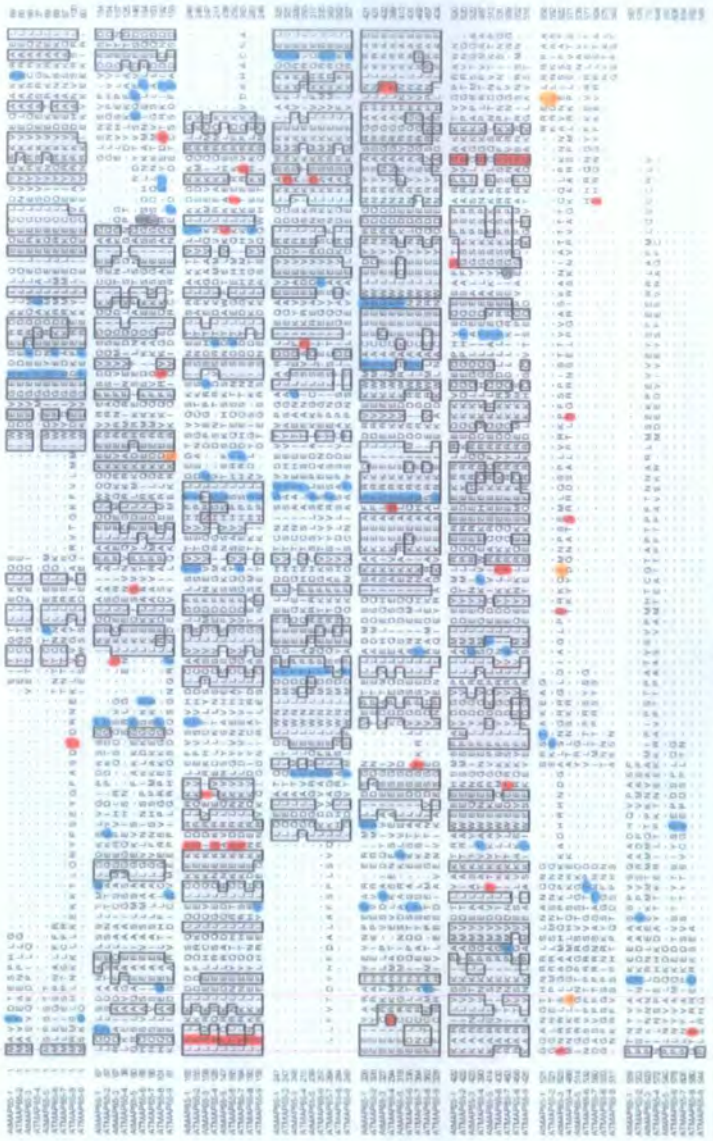

Figure 3.2:
The cAMP- and cGMP-dependent protein kinase phosphorylation sites are in orange colour. The protein kinase C phosphorylation sites are in red. The casein kinase II phosphorylation sites are in blue and the tyrosine kinase phosphorylation sites are in dark grey.

3.4.1.3 Casein Kinase II

Based to the Prosite search all AtMAP65s have casein kinesin II phosphorylation sites. Casein kinase II is a protein serine/threonine kinase. The consensus pattern found in most of the known physiological substrates is (pS/pT)-x-x-D /E) (Pinna *et al.*, 1990; Daniel *et al.*, 2004). This motif was used by Prosite Web Site for searching casein kinase II phosphorylation sites, accession number PS:00006, and the randomised probability given was 1.482 x 10^{-3} (figure 3.2)

.

3.4.1.4 Tyrosine Kinase

AtMAP65-6 and AtMAP5-7 contain tyrosine kinase phosphorylation sites in their sequences. Substrates of tyrosine protein kinases are generally characterised by a lysine or an arginine seven residues to the N-terminal side of the phosphorylated tyrosine. An acidic residue (Asp or Glu) is often found at either three or four residues to the N-terminal side of the tyrosine (Cooper *et al.*, 1984; Mandal *et al.*, 1999). The motifs used by Prosite Web Site were (R/K)-x-x-(D/E)-x-x-x-pY or (R/K)-x-x-x-(D/E)-x-x-pY , PS:00007, and the randomised probability given was 4.083 x 10^{-4} (figure 3.2)

3.4.2 Identification of cdk phosphorylation motifs

A search in previous publications revealed the cdk phosphorylation consensus motif is (S/T)-P-x-(K/R) (Archambault *et al.*, 2004). In addition, Chang *et al.*, 2000, suggested the minimal cdk consensus phosphorylation motif is (S or T)-P. Both the motifs (pS/pT)-P-x-(K/R) and (S/T)-P were used to identify putative cdk phosphorylation sites in AtMAP65 proteins (figure 3.3).

Figure 3.3
AtMAP65 predicted sites of cdk,
PKA and casein kinase I phosphorylation sites

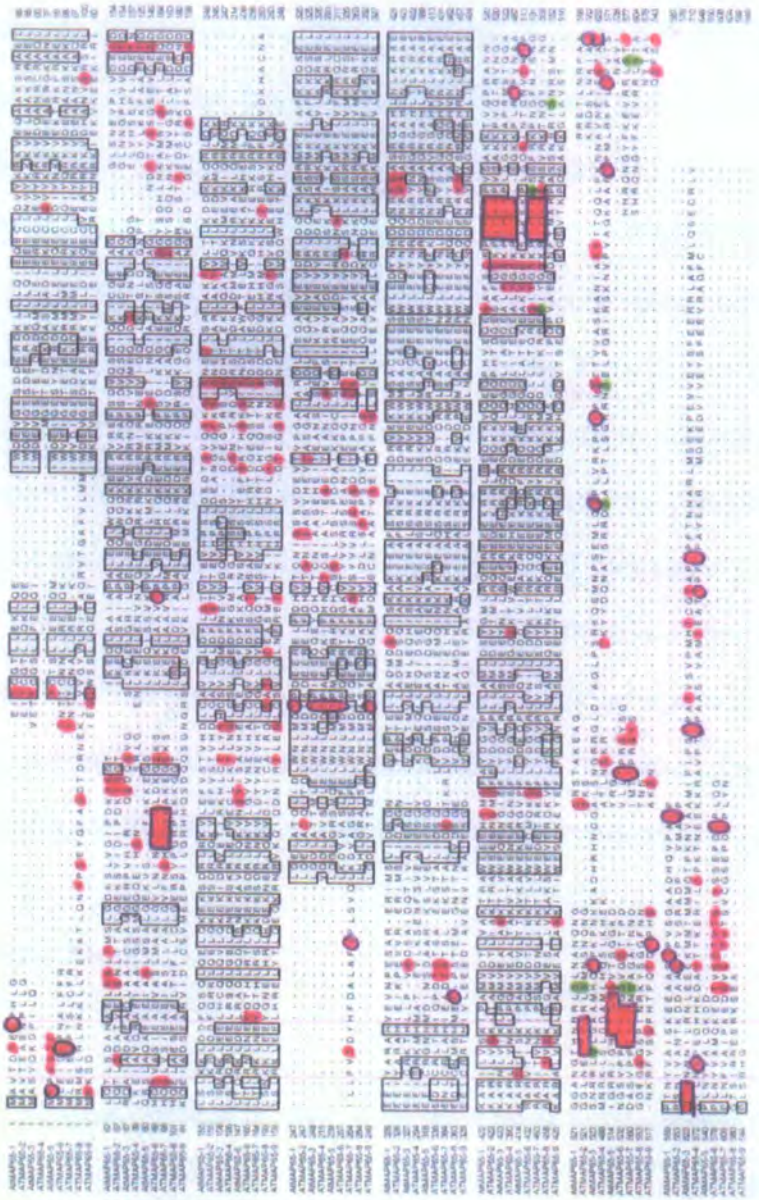

Figure 3.3:
The cdk phosphorylation sites are in pink colour within blue border lines. Where the motif (S/T)-P-x-(K/R) was used for the cdk phosphorylation sites prediction all the four motif residues are marked. Where the motif (S/T)-P was used only the S/T residues are marked. The predicted PKA phosphorylation sites are in green colour and the casein kinase I phosphorylation sites are in purple colour.

3.4.3 Identification of PKA phosphorylation motifs

Search in previous publications revealed the consensus motif of PKA is R-R-X-(pS/pT) (Loog *et al.*, 2000). This motif was used to identify putative PKA phosphorylation motifs in AtMAP65 protein sequences (figure 3.3).

3.4.4 Identification of casein kinase I phosphorylation motifs

The casein kinase I (ckI) consensus motif has been proposed to be (pS/pT /pY)-X_{1-2}-(S/T/Y) (Flotow *et al.*, 1990; Liu *et al.*, 2003). This motif was used for identifying putative ckI phosphorylation sites in AtMAP65 sequences (figure 3.3).

3.4.5 NetPhos search

The phosphorylation sites found searching in Prosite and in previous publications were compared to the results obtained searching in the phosphorylation prediction server NetPhos (www. cbs.dtu.dk/services/NetPhos). NetPhos, in contrast to Prosite, does not use consensus patterns for each kinase but the phosphorylation site search is carried out using sequence logos generated for each of the three acceptor residues, tyrosine, serine and threonine (Blom *et al.*, 1999). The NetPhos output scores had a value in the range 0.000 to 1.000 and the threshold was 0.500. Only the outputs with score value above the threshold were analysed. Some phosphorylation sites identified by the Prosite were excluded by the NetPhos search as their score were below the threshold. NetPhos search revealed some new phosphorylation sites in AtMAP65 protein sequences. All the phosphorylation sites predicted by NetPhos are illustrated in figure 3.4 and the novel sites found in addition to the sites predicted by Prosite are marked. Figure 3.5 also illustrates the phosphorylation sites found by search in NetPhos. However, in figure 3.5 the information obtained from Prosite

Figure 3.4
AtMAP65 Phosphorylation Sites predicted by NetPhos

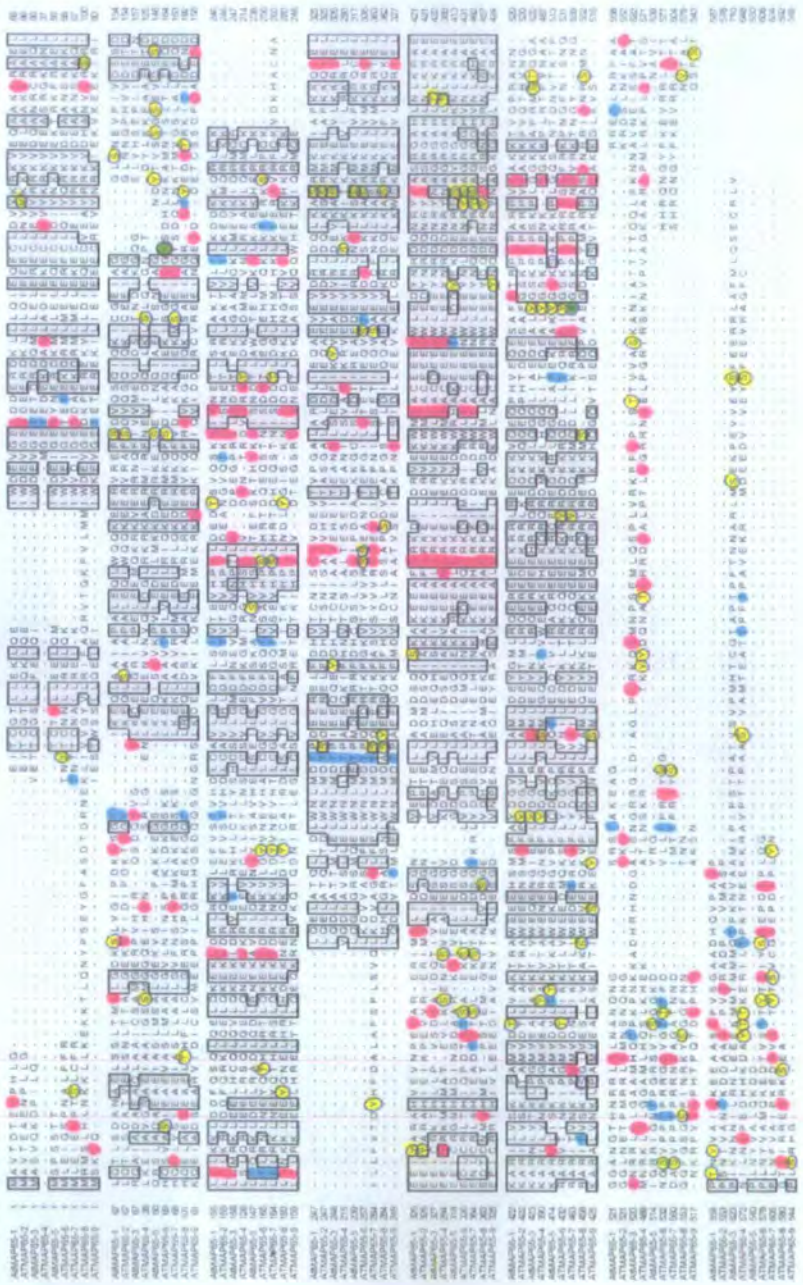

Figure 3.4:
In pink colour are marked the putative phosphorylated serine residues (S), in blue the threonine residues (T), and in green the tyrosine residues (Y). The sites predicted by NetPhos, which have not been predicted by Prosite, are marked in yellow colour.

Figure 3.5
Summary of the predicted MAP65 phosphorylation sites

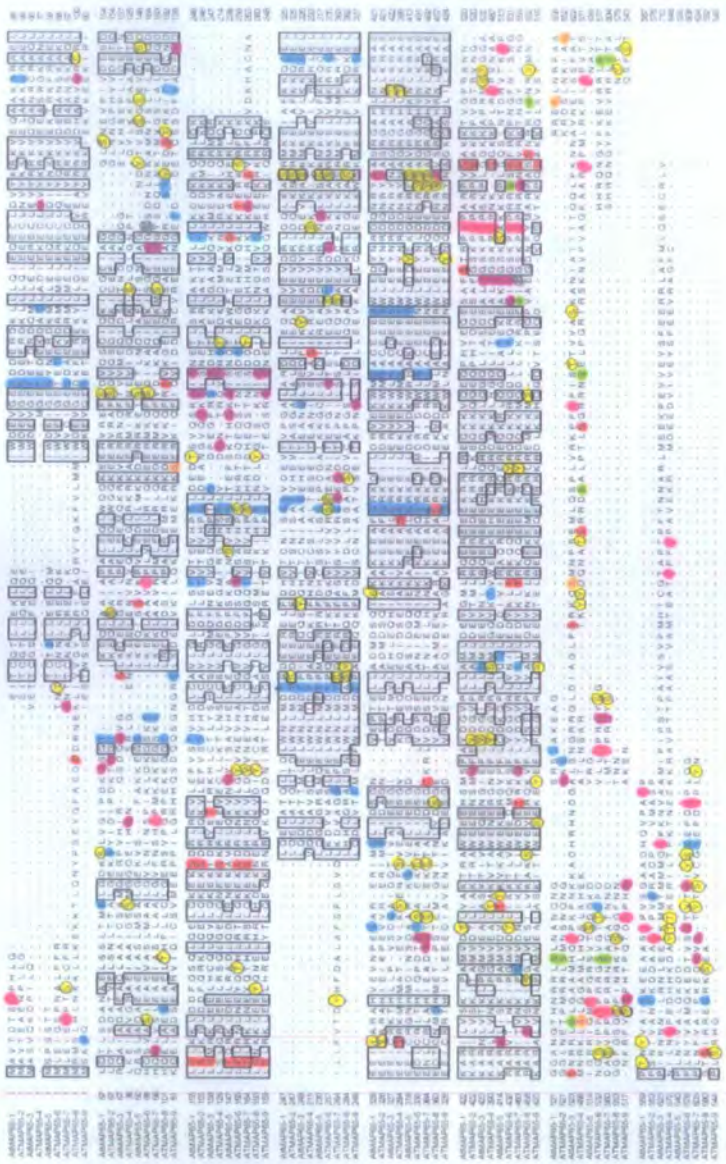

Figure 3.5:
All the S, T and Y residues marked were predicted as phoshorylation sites by the search in NetPhos. The results from the search for phosphorylation sites in Prosite and in previous publications are used in this table to indicate the protein kinases involved. Based to the Prosite search the phoshorylation sites of casein kinesin II are in blue colour, the tyrosine kinase phosphorylation sites are in dark grey, the PKC phosphorylation sites are in red and the cAMP- , cGMP- dependent protein kinase phosphorylation sites are in orange. Based to the motifs described in previous publications the phosphorylation sites of casein kinase I are in purple, of cdk are in pink and of PKA are in green. The sites predicted only from NetPhos are in yellow colour.

and from previous publications are also used as an indication for which protein kinase could phosphorylate the tyrosine, serine and threonine residues.

3.5 AtMAP65 Protein Motifs

3.5.1 N-glycosylation

All the AtMAP65 proteins contain N-glycosylation (Gavel *et al.*, 1990) sites as it was shown by the Prosite search, accession number PS00001. N-glycosylation sites are specific to the consensus sequence Asn-X-Ser/Thr. However, the presence of the consensus tripeptide is not sufficient to conclude that an asparagine residue is glycosylated and the protein folding should be taken into account. The presence of proline and aspartic acid between Asn and Ser/Thr inhibits N-glycosylation (Lerouge *et al.*, 1998). In addition, 50% of the sites that have a proline C-terminal to Ser/Thr are not glycosylated. The randomised probability for the search outcome was 5.138×10^{-3}. The results are illustrated in figure 3.6.

The presence of N-glycosylation motifs was also examined using the NetNGlyc prediction server (www.cbs.dtu.dk/services/NetNGlyc). The results obtained were similar to those from the Prosite search. The only differences were one site in AtMAP65-6 and one site in AtMAP65-8, which were excluded from the NetNGlyc as the site scores were below the threshold (threshold value: 0.500). These two sites are marked in figure 3.6 in yellow colour.

3.5.2 N-myristoylation

All the AtMAP65 proteins contain N-myristoylation sites based to the Prosite search (figure 3.6). The consensus pattern used by the Prosite Web Site is: G-(any residue except E,D,R,K,H,P,F,Y,W)- X-X-(S/T/A/G/C/N)-(any residue except P), accession number

PS:00008. G is the N-myristoylation site. The randomised probability given for the search outcome was 1.397×10^{-2}.

3.5.3 Amidation

AtMAP65-1, -3, -4, and -5 protein sequences contain amidation sites (figure 3.6). The amidated peptides are directly followed by a glycine residue and most often by at least two consecutive basic residues (Arg or Lys) (Bradbury *et al.*, 1987, Marco *et al.*, 2003). All amino acids can be amidated. However, neutral hydrophobic residues such as Val or Phe are good substrates, while charged residues such as Asp or Arg are less reactive. The C-terminal amidation consensus pattern used by Prosite was x-G-(RK)-(RK), accession number PS00009, and the randomised probability for the search outcomes was 8.636×10^{-4}. Amidation has not yet been shown to occur in plants.

3.5.4 EF-hand calcium binding domain

The motif search in AtMAP65 proteins using the Prosite Web Site had also shown that AtMAP65-9 protein at position 356-368 aa contains a consensus EF-hand calcium-binding domain (figure 3.6), which is found in many calcium binding proteins (Kawasaki *et al.*, 1995). The consensus pattern of the site is D-x-(DNS)-(any residue except: ILVFYW)-(DENSTG)-(DNQGHRK)-(any residue except: GP)-(LIVMC)-(DENQSTAGC)-x-x-(DE)-(LIVMFYW), prosite accession number PS:00018. The randomised probability of the search results was 3.074×10^{-6}.

3.6 AtMAP65 Promoter motifs

The *AtMAP65* putative promoter regions, 1.5 Kb upstream of the beginning of the coding sequence, were investigated for presence of conserved signal motifs using the plant *Cis*-

Figure 3.6
Prediction of AtMAP65 sites of N-glycosylation, N-myristoylation, amidation and EF-hand calcium domains

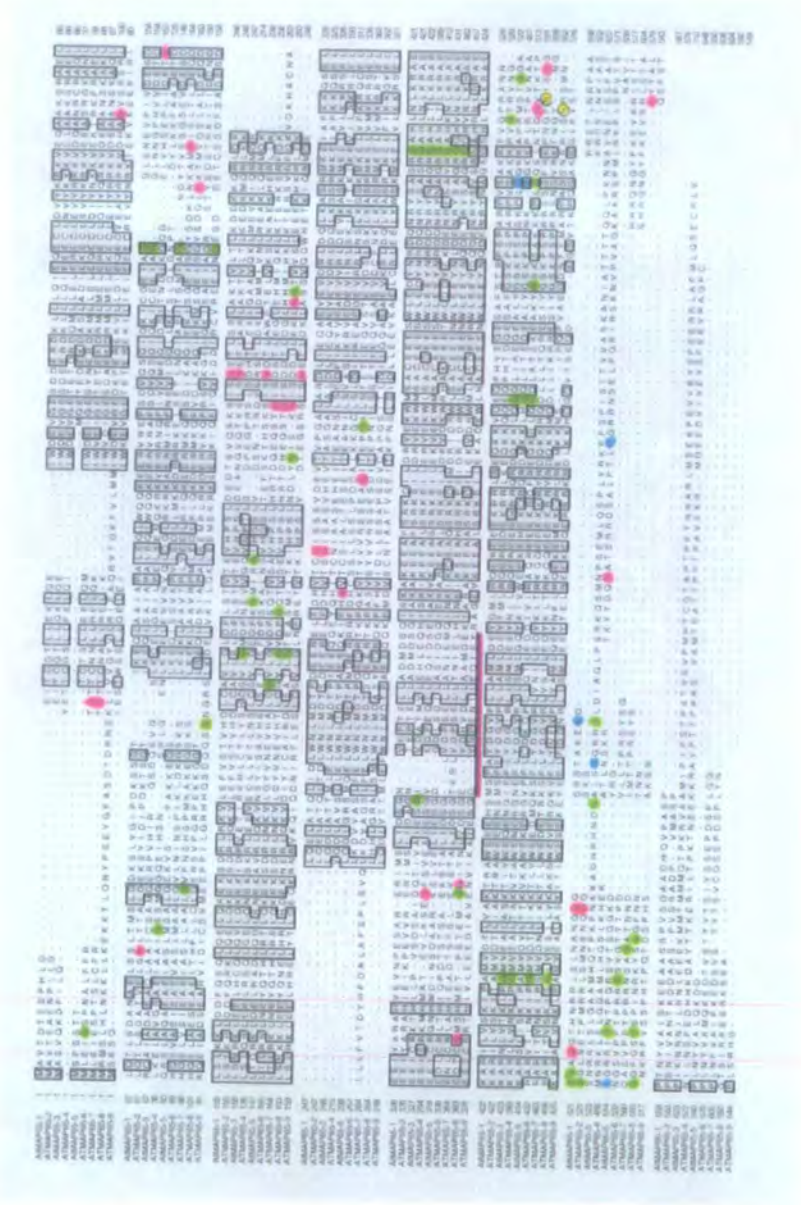

Figure 3.6:
The prediction of the N-glycosylation sites (in pink), of the N-myristoylation sites (in green), and of the amidation sites (in blue) is based to the Prosite search. The search in NetNGlyc for N-glycosylation sites revealed similar results to the Prosite search, with only exception one site in AtMAP65-6 and one site in AtMAP65-8, which were excluded from the NetNGlyc as the site scores were below the threshold (these two sites are marked with yellow colour). Based to the Prosite search AtMAP65-9 contains an EF-hand calcium domain, which is underlined.

acting regulatory element web site (*PlantCare*; http://oberon.fvms.ugent.be:8080/PlantCARE/) (Rombauts *et al.*, 1999). *PlantCare* for each prediction gives the core and the matrix percentage identity between the motif sequence and the promoter site. All the motifs listed in this study have 100% core identity. The matrix identity for all motifs found in each *AtMAP65-9* promoter, is shown in appendices B-I. Some motifs could be present more than once in a *AtMAP65* promoter. In this case the lowest and highest value of the matrix percentage identity is shown.

3.6.1 TATA- and CAAT- box

All *AtMAP65* promoters contain the core promoter element TATA-box found around –30 bp prior the transcription start (Pasquali *et al.*, 1999) and the CAAT-box which is a common *cis*-acting element in promoter regions (appendix B).

3.6.2 Light responsive elements

In addition, all *AtMAP65* promoter regions contain several *cis*-acting elements involved in light responsiveness. The light responsive elements found are the ACE (Feldbrugge *et al.*, 1996); the GT1-motif and AAGAA-motif (Bruce *et al.*, 1991); the AE box, ATC-motif, ATCC-motif, CATT-motif (Park *et al.*, 1996) and the AAAC-motif, ATCT, GA-motif, GAG motif, GATA motif, I-box, LAMP-element, TCCC-motif, TCT-motif, Chs-CMA1a, Chs-CMA2a, sbp-CMA1a elements and G-box (Arguello-Astorga *et al.*, 1996). The G-box has also been proposed as a putative methyl jasmonate (MeJa) responsive element (Rouster *et al.*, 1997). The light responsive element tables are shown in appendix C.

3.6.3 Hormone responsive elements

The *AtMAP65* promoters also contain several *cis*-acting elements involved in hormones responsiveness. The *AtMAP65-5, -6, -7* and *–9* promoters contain the A-box, which is a putative regulatory sequence found in gibberellin acid inducible genes (Kim *et al.*, 1992). Two other gibberelin-responsive elements, P-box and TATC-box (Washida *et al.*, 1999), found in the *AtMAP65* promoters (appendix D). The *AtMAP65-2, -4, -5, -7* and *–9* promoters contain the ABRE *cis*-acting element involved in abs*cis*ic acid responsiveness (Vanyushin B.F., 2004). A regulatory element involved in auxin responsiveness, the AuxRR-core (Sakai *et al.*, 1996), was found in the *AtMAP65-1, -4, -7* and *–8* promoter sequences. Another auxin responsive element, TGA (Pastuglia *et al.*, 1997), found in the *AtMAP65-8* promoter (appendix D). Two MeJa (methyl jasmonate)-responsiveness motifs, CGTCA and TGACG described by Rouster *et al.*, 1997, found in the *AtMAP65* promoter regions. All the *AtMAP65* promoters contain an ethylene responsive element ERE (Itzhaki *et al.*, 1994). The MeJa and ethylene responsive elements table is shown in appendix D.

3.6.4 Elicitor responsive elements

Some of the *AtMAP65* promoters also contain elicitor responsive elements. The Box-W1, fungal elicitor responsive motif described by Rushton *et al.*, 1996, found in *AtMAP65-7* promoter region. Another elicitor responsive element, ELI-box 3 (Pastuglia *et al.*, 1997), found in *AtMAP65-1, -2, -3, -4* and *–5* promoters (appendix E). In addition, EIRE, a responsive element of salicylic acid, which is believed to play an important role in disease resistance (Shah and Klessig, 1996) found in some of the *AtMAP65* promoters. Another motif involved in salicylic acid responsiveness, TCA-element (Pastuglia *et al.*, 1997), is present in *AtMAP65-1, -4, -6, -8* and *–9* promoters. The salicylic acid responsive elements table is illustrated in appendix F.

3.6.5 Environmental stress responsive elements

The *AtMAP65* promoters also found to contain environmental stress responsive motifs, such as the HSE, which is involved in heat stress responsiveness (Pastuglia *et al.*, 1997). *AtMAP65-1*, *-3* and *–5* promoters also contain a low-temperature responsiveness motif, LTR (Dunn *et al.*, 1998). All the *AtMAP65* promoters contain a wound-responsive element in their sequences, the WUN-motif (Pastuglia *et al.*, 1997). The MBS motif involved in drought-inducibility (Yamagucki-Shinozaki and Shinozaki, 1994) found in the *AtMAP65-1* promoter region. In addition, *AtMAP65-1*, *-2*, *-3*, *-5*, *-8* and *–9* contain a light responsive element, MRE, (Feldbrugge *et al.*, 1997). The environmental stress motif tables are shown in appendix G.

3.6.6 Cell cycle regulated elements

AtMAP65-3, *-4*, *-8* and *–9* contain E2Fa and/or E2Fb motifs (appendix H). The two E2F elements were involved in uperegulation of the ribonucleotide reductase promoter at the G1/S transition and mutation of these elements prevented any significant induction of the promoter (Chaboute *et al.*, 2000).

3.6.7 Endosperm expression and circadian clock motifs

Some of the *AtMAP65* promoters also contain the GCN4_motif and Skn_motif (Washida *et al.*, 1999), which are involved in endosperm expression (appendix I). *AtMAP65-1* and *–9* promoter regions contain a circadian clock motif, a *cis*-acting regulatory element involved in circadian control (Piechulla *et al.*, 1998). In particular, *AtMAP65-1* and *–9* promoters contain one circadian clock motif each with 100% core identity. The matrix percentage identity of the motif is 90% and 87.5% respectively in each sequence.

3.7 Summary

The completion of the *Arabidopsis* genome sequence has allowed the identification of nine *Arabidopsis MAP65* genes. The deduced amino acid *Arabidopsis* MAP65 sequences show 28-81% identity to each other and the predicted molecular weight varies from 62.7 to 80.3 kDa. The plant MAP65 proteins share some identity with PRC1 homologues from insects and vertebrates and the yeast Ase1. However, the yeast Ase1 and the PRC1 homologues examined do not integrate into the five groups that the plant MAPs from carrot, rice, tobacco and *Arabidopsis* create in the MAP65 phylogenetic tree.

The AtMAP65 proteins have highly conserved phosphorylation sites for various protein kinases: cAMP- and cGMP-dependent protein, protein kinase C, protein kinase A, casein kinase I, casein kinesin II, tyrosine kinase and cyclin dependent kinase. The positioning of these sites in AtMAP65 proteins alignment reveals that some of these sites are among conserved regions between the AtMAP65 protein sequences.

In addition, all AtMAP65 protein sequences contain N-glycosylation and N-myristoylation sites, putative regions of post-translation modifications. AtMAP65-9 sequence contains a consensus EF-hand calcium binding domain found at calcium binding proteins.

All putative *AtMAP65* promoter regions, 1.5 kb upstream the beginning of the coding sequence, contain the common promoter motifs TATA-box and CAAT-box. All *AtMAP65* promoters also contain several *cis*-acting elements involved in light and hormone responsiveness. Motifs associated with response to elicitors and environmental stress are also found in *AtMAP65* promoter sequences. In addition, the promoters of *AtMAP65-3*, *-4*, -

8 and *-9* contain putative cell regulation elements and *AtMAP65-1* and *-9* promoter sequences have a circadian clock motif.

3.8 Limitations of the Bioinformatics search

The results discussed above using various bioinformatic servers are primary indications for the presence of the putative post-translation modification motifs identified within the AtMAP65 protein sequences and the potential regulatory regions found in *AtMAP65* promoter regions. The web servers generate the predictions using logarithms and the motifs found do not always have functional significance. Further experimental research is required to confirm the presence of the predicted regions. The bioinformatics data obtained in this chapter are not used to draw conclusions but they could be used as a guide in experimental studies. The putative post-translation modification motifs found in conserved regions among the MAP65 sequences are the most probable to have functional significance and could be for example the first targets of phosphorylation assays. A way to utilise the prediction information of the promoter motifs is to place *Arabidopsis* plants transformed with *AtMAP65::GUS* fusions under the relevant hormonal and environmental stimuli and investigate the alternations in *AtMAP65* expression.

Chapter 4

Expression Programme of all *AtMAP65* genes

4.1 Introduction

The aim of this thesis is comparison of the properties of different AtMAP65 isoforms and potentially the identification of the functional role of each of them. This chapter is focused on the comparison of *AtMAP65* expression pattern. The results will indicate at which organs and/or tissues each of the *AtMAP65* is expressed, allowing us to investigate if the *AtMAP65* isoforms are differentially expressed and if any of them has an organ/tissue specific expression and potentially play a distinct role from the rest family members. The expression programme of the nine *AtMAP65*s was investigated by transforming *Arabidopsis* with an *AtMAP65::GUS* reporter gene transcriptional fusion construct for each of the AtMAP65 members. A section of approximately 1.5 Kb upstream of the start of the coding sequence was generated by PCR for each of the *AtMAP65* genes and used to drive the expression of the *GUS* (β-glucuronidase) reporter gene. The abundance of each of the *AtMAP65* transcripts was examined by Reverse Transcription- PCR (RT-PCR) in various tissues of wild type *Arabidopsis* Col-0 plant. The RT-PCR primers were designed to amplify each of the *AtMAP65s* specifically.

4.2 Investigating the expression of *AtMAP65* genes using the *GUS* reporter gene

The putative *AtMAP65* promoters were cloned from wild type Col-0 *Arabidopsis* genomic DNA and were used for the generation of *AtMAP65::GUS* expressing plants. The transgenic plants were used to examine the promoter activity in various organs.

4.2.1 Cloning of the *AtMAP65* putative promoters into the pΔ-GUS-Bin19

As most of the transcription regulatory elements are found within 1 kb upstream of the start of the coding sequence, 1.5 kb upstream of the coding sequence of the *AtMAP65* genes was selected as putative promoter region. The *AtMAP65::GUS* constructs were made using the pΔ-GUS-Bin19 vector, which was gift from Professor Keith Lindsey. The pΔ-GUS-Bin19 vector contains the pUC19 multiple cloning site and the *GUS* coding sequence followed by the *nos* terminator.

The *AtMAP65-1* promoter fragment was amplified using a forward and a reverse primer, which both included a *Bam*H1 site (appendix J-1). The PCR fragment was ligated into the pGEM-T Easy vector and introduced into competent *E.coli*, strain DH5α. The transformed plasmids were digested with *Bam*HI to check if the cloning was successful. DNA sequencing with the universal primers *M13F* and *M13R* and internal primers revealed that the cloned fragment sequence was identical to the DNA sequence in the GeneBank database. The promoter fragment was sub-cloned into the pΔ-GUS-Bin19 vector (Topping *et al.*, 1991). The transformed plasmids were digested with *Bam*HI to check if the cloning was successful. The digestions revealed that the *AtMAP65-1* putative promoter fragment was cloned into pΔ-GUS-Bin19 vector. As one restriction enzyme was used for the cloning, the promoter was checked if it was cloned in the correct orientation. DNA sequencing with the reverse primer (*nested 1*; CGT AAG TCA GAC CTA GCG), which is specific to the *GUS* gene, revealed that the insert was in the correct orientation.

The procedure of making the *AtMAP65-1::GUS* construct is summarised in figure 4.1. The same procedure was followed for the other eight *AtMAP65* promoters with the exception that the forward primer for *AtMAP65-2, -3, -4* and *-9* included an *Hin*dIII site. The

Figure 4.1:
AtMAP65-1::GUS construct

The *AtMAP65-1* putative promoter fragment was amplified by PCR with a *Bam*H1 site in both 5' and 3' primers

↓

The putative promoter fragment was then cloned into the pGEM-T Easy vector and digested with *Bam*HI

↓

The putative promoter fragment was ligated into *Bam*H1 digested p-Δ-GUS-Bin19 (the uncut p-Δ-GUS-Bin19 version is drawn below)

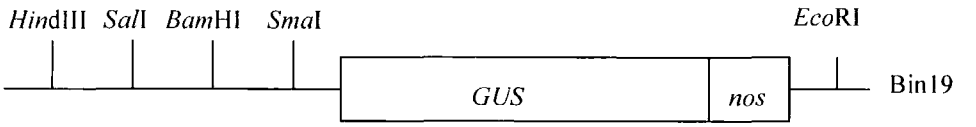

Orientated version selected by sequencing

↓

AtMAP65-1 Promoter::GUS

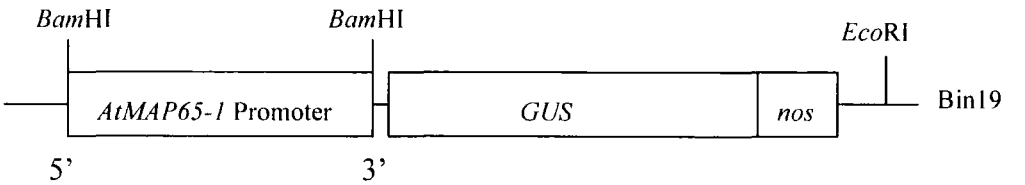

sequences of the nine *AtMAP65* promoters and the primers used for their amplification are shown in appendices J1 to J9. All the *AtMAP65* promoters are about 1.5 Kb in size and DNA sequencing with internal primers revealed that they are identical to the DNA sequences in the GeneBank database.

4.2.2 Transforming *Arabidopsis* with the *AtMAP65::GUS* constructs

The *AtMAP65::GUS* constructs were transformed into *Agrobacterium tumefaciens* strain C58C3 by electroporation. *Arabidopsis thaliana* plants were transformed using the "dipping method" (Clough and Bent, 1998). The seeds were surface sterilised and plated on 1/2 MS medium containing 0.6% (w/v) agar, 50 μg/ml kanamycin and 200 μg/ml augmentin. The kanamycin-sensitive plants became white 10 days after germination. The T1 (transformants of 1st generation) plants, which remained green, were selected and planted in soil. T2 seeds were selected individually from each T1 plant.

The T2 seeds were surface sterilised and plated on 1/2 MS medium in the presence of 50 μg/ml kanamycin. The ratio of kanamycin resistant seedlings to kanamycin sensitive was counted and the number of *AtMAP65::GUS* construct insertions in the T2 lines was calculated based on the segregation analysis (table 4.1). (The kanamycin segregation data and the number of T-DNA loci for the *AtMAP65::GUS* lines are illustrated in appendix K). The T2 lines with more than one *AtMAP65::GUS* construct insertion were not analysed. The T2 lines with one insertion of the *AtMAP65::GUS* construct were selected and used for identifying the histochemical localisation of the *GUS* activity.

Table 4.1: Segregation Analysis

Ratio of Kan sensitive to Kan resistant plants	Number of *AtMAP65::GUS* construct insertions
1:3	1
1:15	2
1:63	3

The transformant seedlings were vacuum-infiltrated for 30 minutes with GUS substrate solution and incubated at 37^{0}C for 12 hours. Stained tissues were subsequently fixed overnight in 2.5 % (v/v) glutaraldehyde at 4°C to prevent diffusion of the GUS staining during the subsequent incubation in chlorallactophenol (Barthels *et al.*, 1997). Incubation in chlorallactophenol removed plant pigments and brown phenolics, resulting in transparent tissues, which were examined for *GUS* activity using Leica MZ125 and Zeiss Axioscope microscopes equipped with a Photometrics COOLSNAP^{TM}*cf* colour digital camera.

T2 plants of each line were also planted in soil and their flowers were examined for GUS staining following the same procedure as for seedlings.

4.2.3 Analysis of the *AtMAP65::GUS* fusions

AtMAP65-1::GUS

Seven T2 lines out of 10 examined had one insertion of the *AtMAP65-1:GUS* construct. These seven lines were analysed for *GUS* activity. The *AtMAP65-1:GUS* stained all tissues in leaves, hypocotyl and roots of *Arabidopsis* seedlings (figure 4.2). *GUS* was also expressed in the flower with the exception of sepals, anthers and pollen. All seven lines had this pattern of expression with some variability in the level of staining.

Figure 4.2
AtMAP65-1::GUS staining

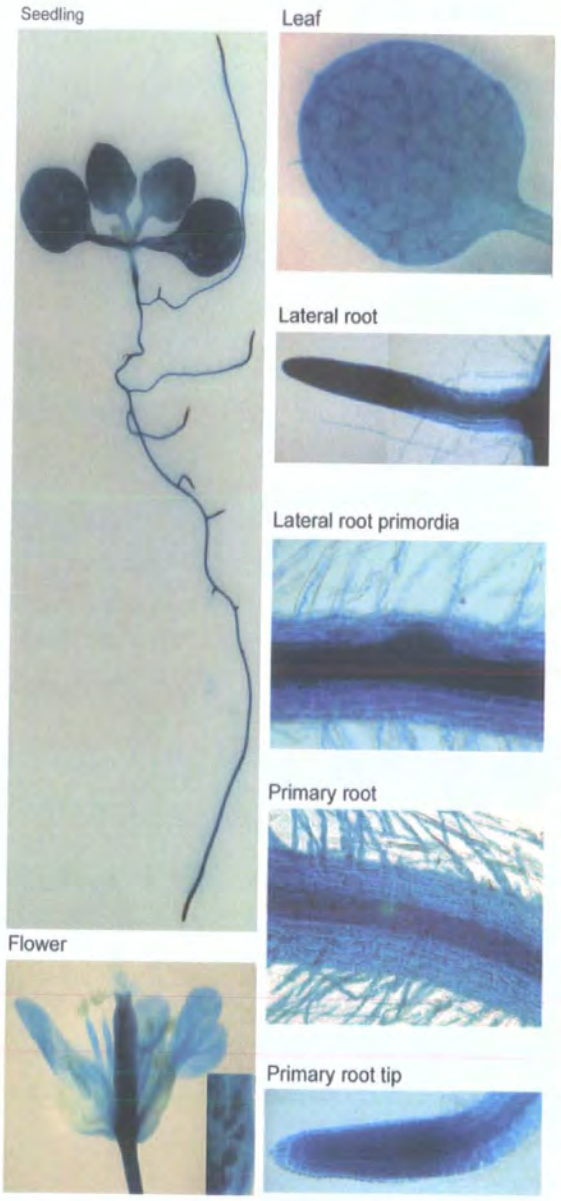

Figure 4.2:
AtMAP65-1:: GUS staining in *Arabidopsis* seedling. *GUS* was expressed in all tissues in leaves, hypocotyl and roots. Staining was also observed in the flower.

AtMAP65-2::GUS

From the fifteen T2 lines examined, twelve had one insertion of the *AtMAP65-2::GUS* construct. These twelve lines were analysed for *GUS* histochemical activity, and two of them showed no staining at all. The other ten lines had similar staining in leaves, hypocotyl and roots. *GUS* expression was observed in mesophyll cells of both cotyledons and leaves. Staining was also observed in hypocotyls and in vascular tissues of roots. In addition, *GUS* expressed in primary and lateral root tips (figure 4.3). In the flower, all the lines stained the ovules/embryos and the stamens (figure 4.4). Six of the lines also showed slight staining in petals while the other four did not.

AtMAP65-3::GUS

From the 10 T2 lines examined, eight had one insert of the *AtMAP65-3::GUS* construct. One of them showed no staining in any organ. The other seven lines showed similar staining in leaves and roots. The cotyledons veins and the mesophyll cells of leaves were stained. Staining was also observed in vascular tissues of hypocotyls and roots. In addition, *GUS* expression was observed at root initiation points. The primary and lateral root tips were stained also (figure 4.5). In the flower, all seven lines had staining in the ovules/embryos and five of the seven lines also stained the pollen (figure 4.6). Only one of the seven lines stained both the pollen and stamens.

AtMAP65-4::GUS

From the ten T2 lines examined, nine lines were shown to have one insert of the *AtMAP65-4::GUS* construct. Four of them showed no GUS staining in any *Arabidopsis* organ or tissue.

Figure 4.3
AtMAP65-2::GUS staining

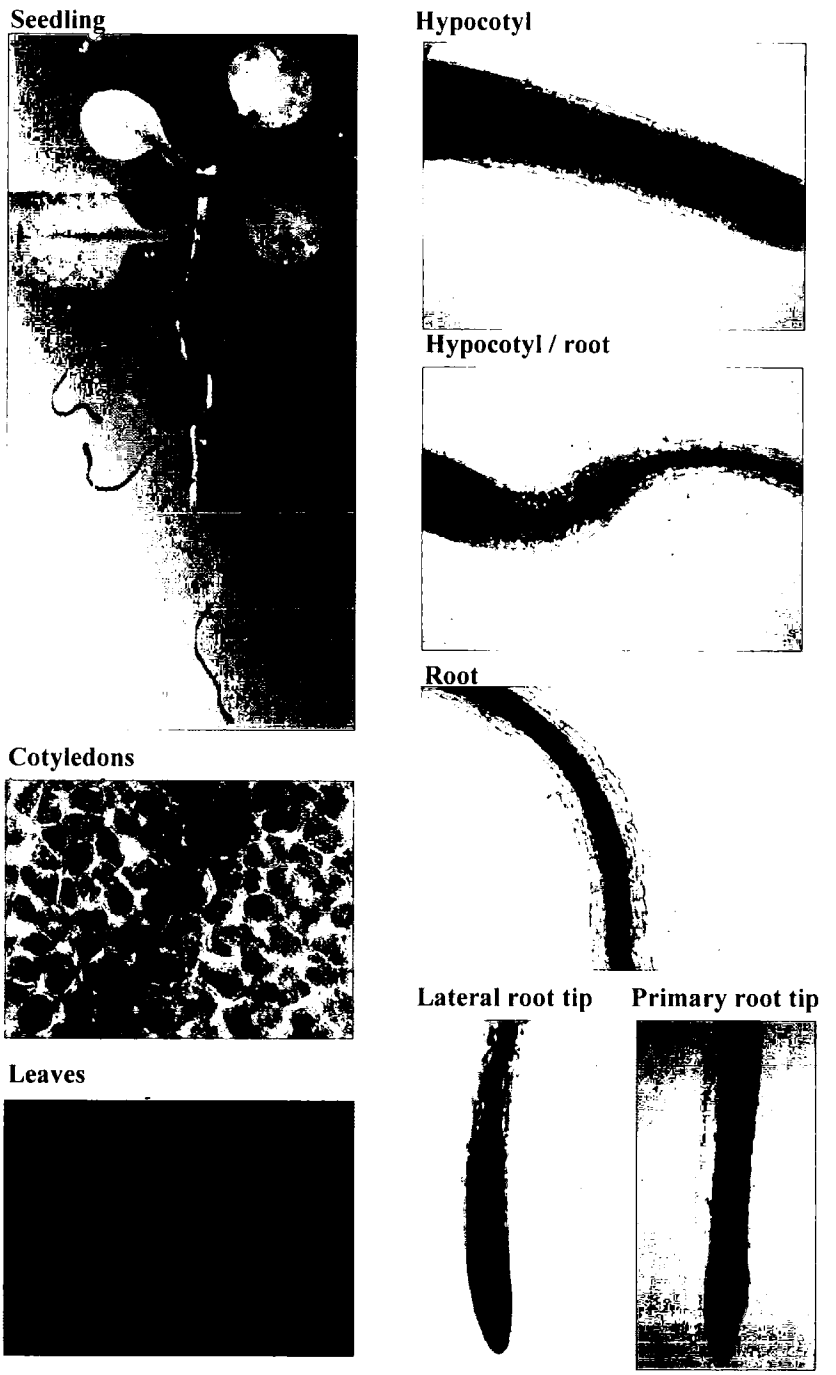

Figure 4.3:
AtMAP65-2:: GUS staining in *Arabidopsis* seedling. *GUS* was expressed in mesophyll cells and veins of leaves. Staining was also observed in root vascular tissues and tips.

Figure 4.4
AtMAP65-2::GUS staining in the flower

Flower

Figure 4.4:
AtMAP65-2:: GUS staining in the *Arabidopsis* flower. *GUS* was expressed in embryo-ovules and stamens.

Figure 4.5
AtMAP65-3::GUS staining

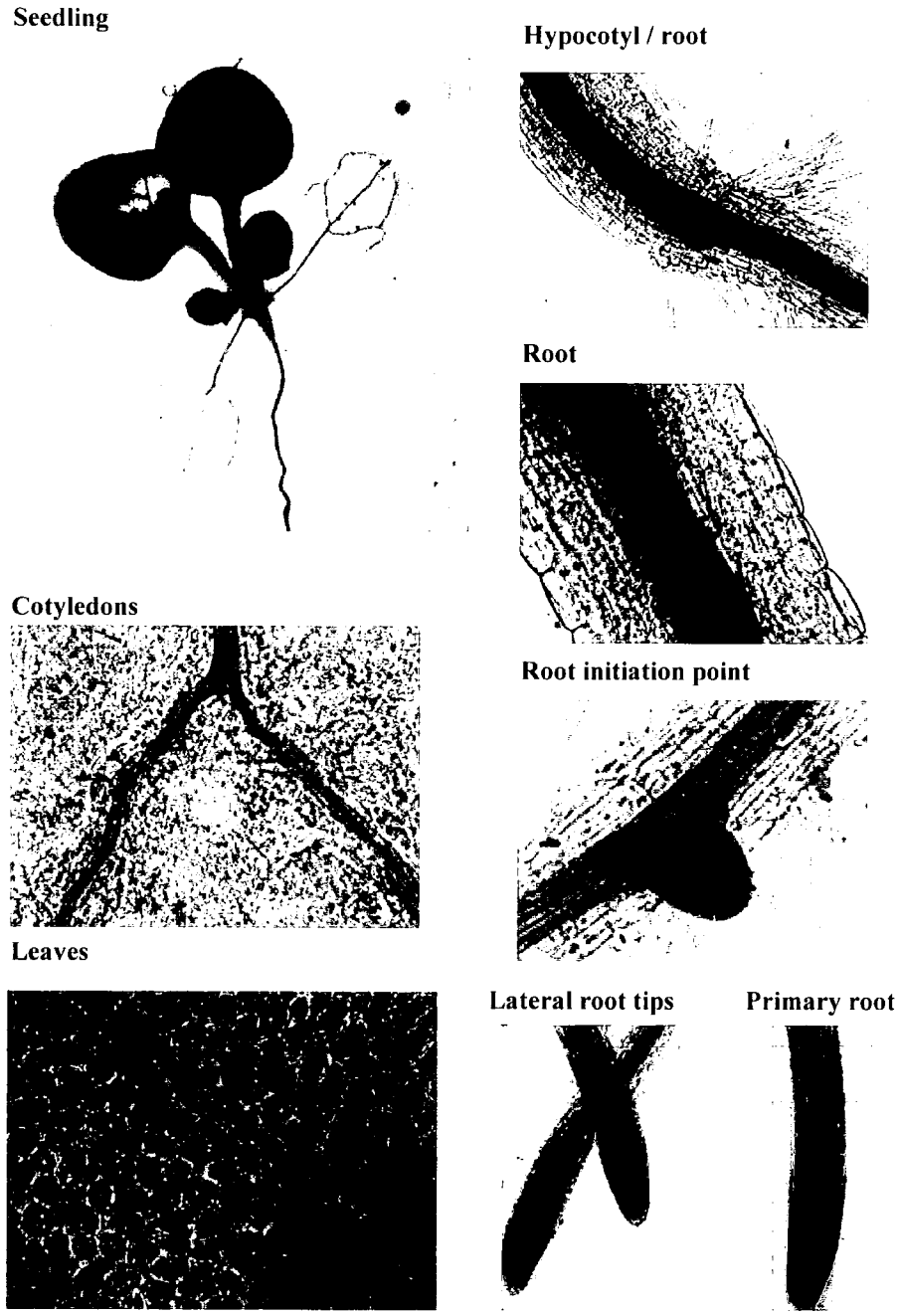

Figure 4.5:
AtMAP65-3:: GUS staining in *Arabidopsis* seedling. *GUS* was expressed in veins of cotyledons and in mesophyll cells of leaves. Staining was also observed in hypocotyl and root vascular tissues and in root tips.

Figure 4.6
AtMAP65-3::GUS staining in the flower

Flower

Figure 4.6:
AtMAP65-3:: GUS staining in the *Arabidopsis* flower. *GUS* was expressed in embryo-ovules and pollen.

The other five weakly stained in the vascular root, the lateral root initiation point and the primary root tip and the lateral root tip cap (figure 4.7).

AtMAP65-5::GUS

From the twelve T2 lines examined, ten had one insert of the *AtMAP65-5::GUS* construct. Three of these ten lines did not show any staining. The other seven lines showed week staining in roots. In particular, the vascular root tissues, the root tip initiation points and the primary and lateral root tip caps were stained (figure 4.8). Two of the lines stained the pollen in flowers (figure 4.9).

AtMAP65-6::GUS

Nine T2 lines from the ten examined had a single insert of the *AtMAP65-6::GUS* construct. Eight lines had similar staining in leaves, hypocotyl, roots and the flower with variability in the level of staining The *GUS* was expressed in mesophyll cells, root vascular tissues, lateral root initiation points and primary and lateral root tips (figure 4.10). In the flower the *GUS* was expressed in ovules/embryos, petals and stamens. An exception was found: one line showed staining similar to the *AtMAP65-1::GUS* construct, in which almost all the plant tissues were stained.

AtMAP65-7::GUS

Nine *AtMAP65-7::GUS* T2 lines were processed by segregation analysis. Eight T2 lines had a single *AtMAP65-7::GUS* insertion and were analysed. None of these lines showed GUS staining in either *Arabidopsis* seedlings or flowers.

Figure 4.7
AtMAP65-4::GUS staining

Root

Lateral root tip

Primary root tip

Figure 4.7:
AtMAP65-4:: GUS staining in *Arabidopsis* roots. *GUS* was expressed weakly in root vascular tissues and tips.

Figure 4.8
AtMAP65-5::GUS staining

Root iniation point

Lateral root tip

Figure 4.8:
AtMAP65-5:: GUS staining in *Arabidopsis* roots. *GUS* was weakly expressed in root initiation points and tips.

Figure 4.9
***AtMAP65-5::GUS* staining in the flower**

Figure 4.9:
AtMAP65-5:: GUS staining in the *Arabidopsis* flower. *GUS* was expressed in pollen.

Figure 4.10
AtMAP65-6::GUS staining

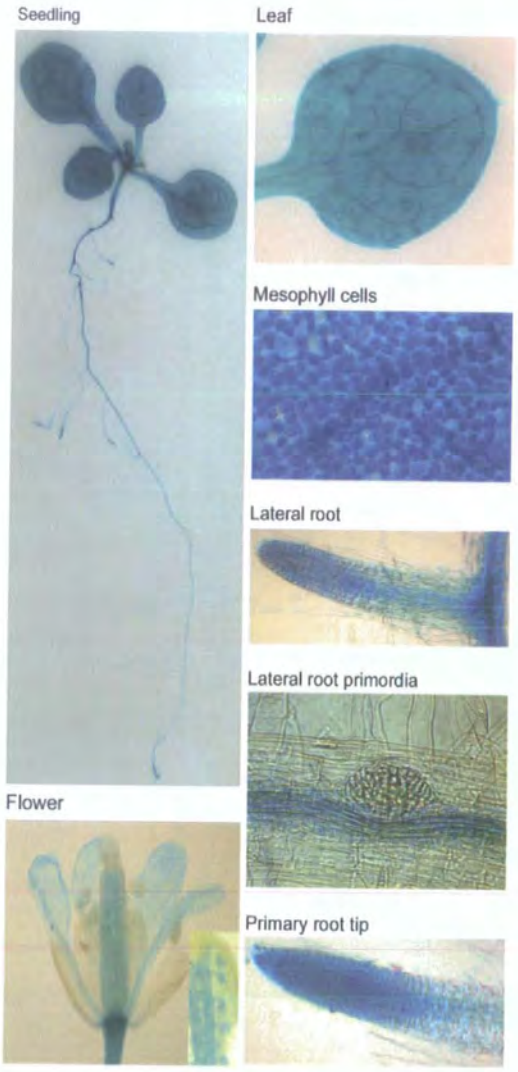

Figure 4.10:
AtMAP65-6:: GUS staining in *Arabidopsis* seedling and flower.
GUS was expressed in leaves, root vasculat tissues and tips. In the flower, *GUS* stained embryo-ovules and sepals.

AtMAP65-8::GUS

From the eight T2 lines tested by segregation analysis, seven had a single insertion of the *AtMAP65-8::GUS* construct. All the seven lines had similar staining in leaves and roots with variations in signal level (figure 4.11). The *GUS* was expressed in the root vascular tissues, lateral root initiation points and primary and lateral root tips. The *GUS* staining was also concentrated in stipules. None of the seven T2 lines showed staining in the flower.

AtMAP65-9::GUS

Nine of the eleven lines examined by segregation analysis had one *AtMAP65-9::GUS* construct. All these nine lines had a pollen-specific staining in the flower (figure 4.12). Six of these lines, in addition to the pollen staining, also had weak staining in primary and lateral root tips and in the lateral root initiation point (figure 4.13).

4.3 Investigating the expression of *AtMAP65* genes by RT-PCR

Total RNA was extracted from *Arabidopsis* tissue culture cells and various *Arabidopsis* tissues: seedlings, roots, stem, leaves, flowers and siliques using the Qiagen plant RNAeasy kit. The extracted RNA from each sample was treated with DNAase and subsequently the enzyme was removed by running the RNA extracts through Qiagen plant RNAeasy mini kit columns.

0.6 μg total RNA from each *Arabidopsis* sample were used in reverse transcription for cDNA production using the SuperScript™ II Rnase H⁻ Reverse Transcriptase (Invitrogen). The cDNA produced was treated with RNAase and the enzyme was removed by using the

Figure 4.11
***AtMAP65-8::GUS* staining**

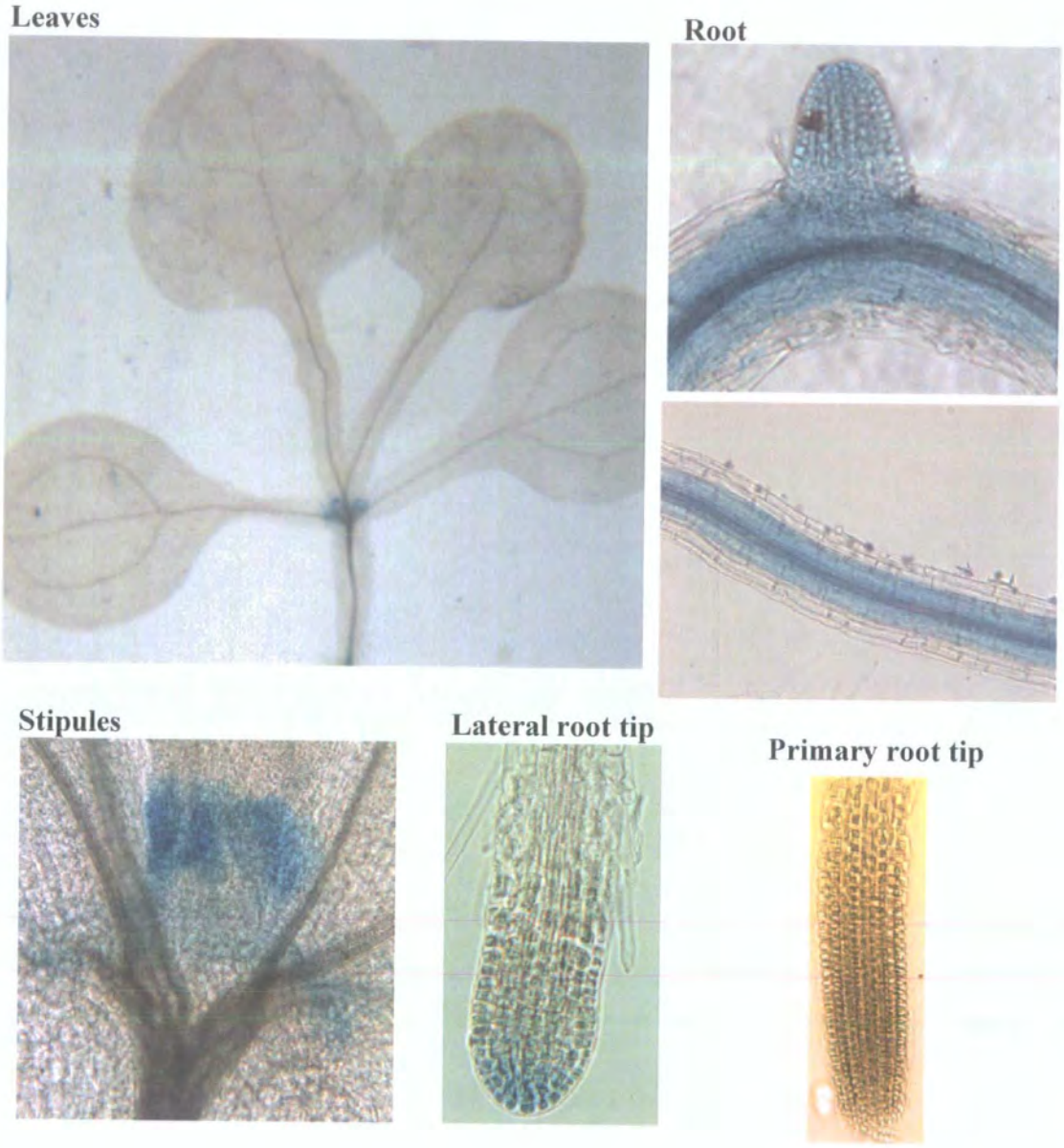

Figure 4.11:
AtMAP65-8::GUS staining in *Arabidopsis* seedling. *GUS* staining was concentrated in stipules. Staining was also observed in root vascular tissues and root tips.

Figure 4.12
AtMAP65-9::GUS staining in the flower

flower

Pollen

Figure 4.12:
AtMAP65-9:: GUS staining in the *Arabidopsis* flower.
GUS was specifically expressed in pollen.

Figure 4.13
AtMAP65-9::GUS staining in roots

Lateral root Initiation point

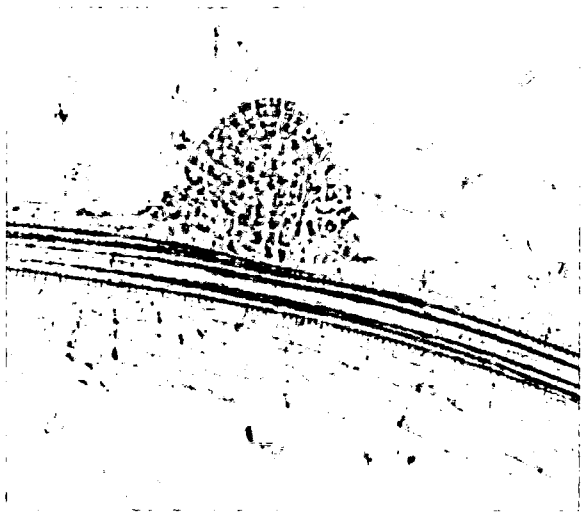

Lateral root tip

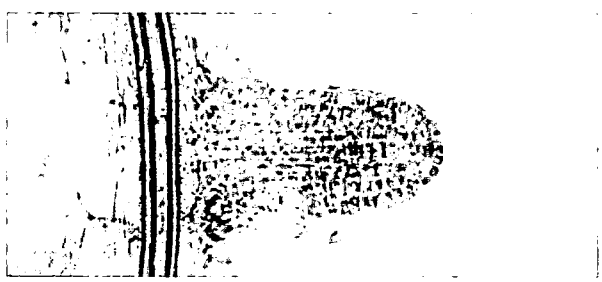

Figure 4.13:
AtMAP65-9:: GUS staining in *Arabidopsis* roots. *GUS* was weakly expressed in root initiation points and tips.

plant RNAeasy mini kit columns. (The above RNA extractions and *Arabidopsis* cDNA samples were prepared working together with Andrej Hlavacka and Tim Hawkins.)

Specific primers were designed for each *AtMAP65*. Their protein sequences were aligned and regions of low homology were selected. The primers were based on the corresponding nucleotide sequences and were specific for each *AtMAP65* (see appendices L and M).

The RT-PCR reaction was performed with each of the *Arabidopsis* cDNA samples prepared from tissue culture cells, seedlings, roots, stem, leaves, flowers and siliques. 100ng and 10ng of cDNA were used for each RT-PCR. All the RT-PCRs were repeated once.

The RT-PCR samples were run in 1% (w/v) agarose gels and visualised by U.V. light. The gel images were scanned and their bands were analysed using Photoshop 7.0. The light intensity of each band was measured for each replica gel. The light-intensity of the background was substracted from each band light-intensity. Then, the data from the replicates were normalised by mean: the intensity for each band in a particular replicate was divided by the mean intensity for all bands in the replicate. Next, the data were averaged across the replicates and histograms were plotted based on the average values from each set of RT-PCR gel replicates. (The data of each histogram are illustrated in appendix N)

4.3.1 RT-PCR results

AtMAP65-1 RT-PCR

The RT-PCR of *AtMAP65-1* using 100ng cDNA as template from each sample revealed that the *AtMAP65-1* transcript is very abundant in *Arabidopsis* tissue culture cells and all the *Arabidopsis* tissues examined; seedlings, roots, stem, leaves, flowers and siliques. The RT-

PCR using 10ng cDNA as template from each sample also showed that the *AtMAP65-1* gene is highly expressed in all *Arabidopsis* tissues (figure 4.14).

AtMAP65-2 RT-PCR

RT-PCR of *AtMAP65-2* using 100ng cDNA as template from each sample showed that *AtMAP65-2* is present in all tissues examined. *Arabidopsis* tissue culture cells, roots and flowers gave the higher signal. In RT-PCR using 10ng cDNA as template from each tissue, the signal remained the higher for tissue culture cells, roots and flowers (figure 4.15).

AtMAP65-3 RT-PCR

The *AtMAP65-3* RT-PCR with 100ng cDNA as template from each sample revealed *AtMAP65-3* is present in all tissues examined. The signal was higher in tissue culture cells, roots and flowers. In RT-PCRs with 10ng cDNA as template from each sample the signal in flowers was the highest. Signal in tissue culture cells and roots was also observed (figure 4.16).

AtMAP65-4 RT-PCR

The RT-PCR for *AtMAP65-4* with 100ng cDNA from each sample as template revealed the signal was higher in tissue culture cells, roots and flowers. In RT-PCR with 1:10 diluted cDNA the signal remained higher only in tissue culture cells and roots (figure 4.17).

AtMAP65-5 RT-PCR

Using *AtMAP65-5* primers the RT-PCRs with 100ng cDNA from each sample, the signal was higher in tissue culture cells, roots and flowers. In the RT-PCRs with 1:10 diluted

Figure 4.14
AtMAP65-1 RT-PCR

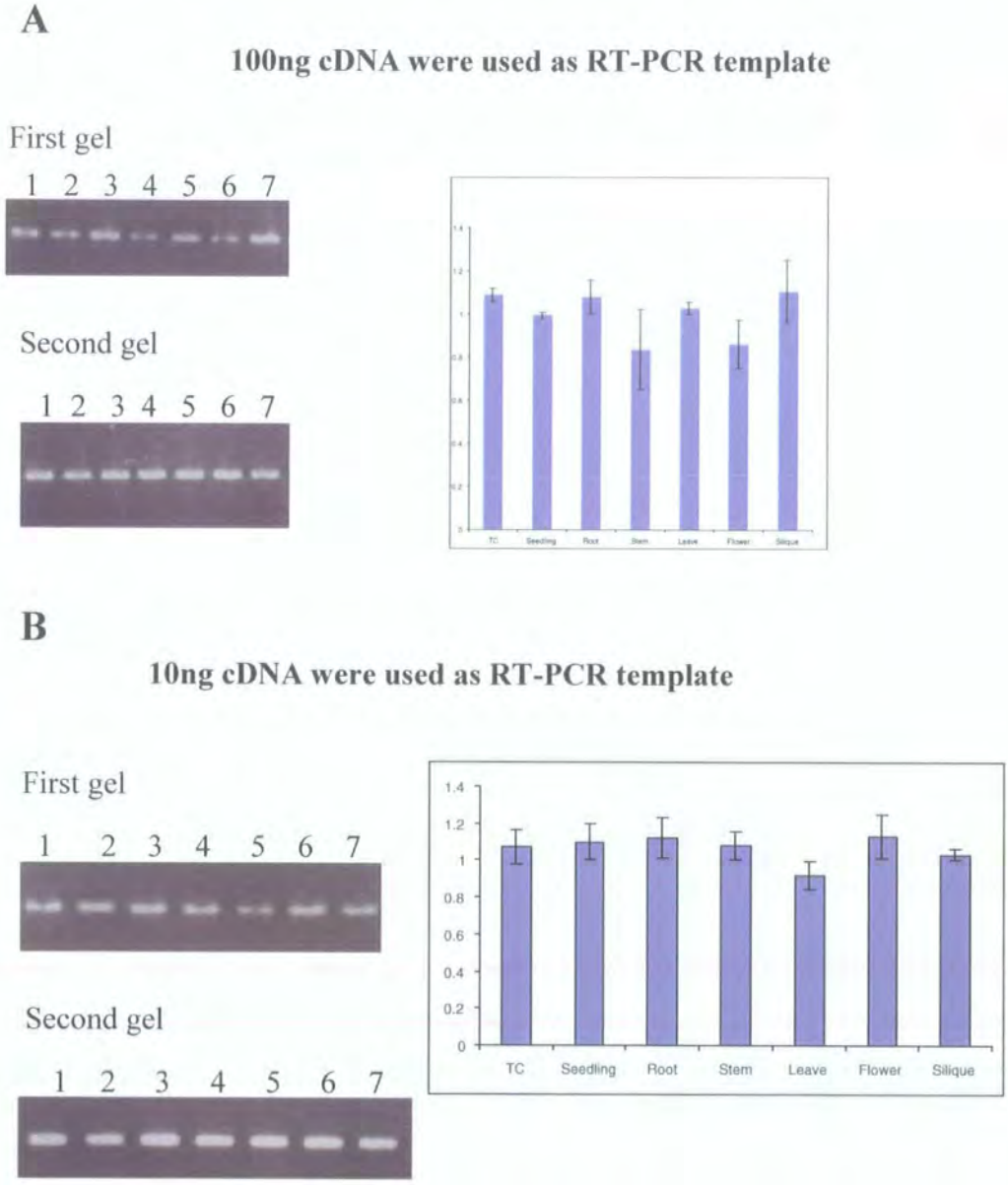

Figure 4.14: *AtMAP65-1* RT-PCR with cDNA samples prepared from 1. Tissue Culture cells, 2. Seedlings, 3. Roots, 4. Stem, 5. Leaves, 6. Flowers, 7. Siliques. **A.** RT-PCR using 100 ng cDNA as template for each of the seven samples. A repeat RT-PCR was carried out and a histogram was produced based on average values. **B.** RT-PCR using 10 ng cDNA as template for each of the seven samples. A repeat RT-PCR was carried out and a histogram was produced based on average values.

Figure 4.15
AtMAP65-2 RT-PCR

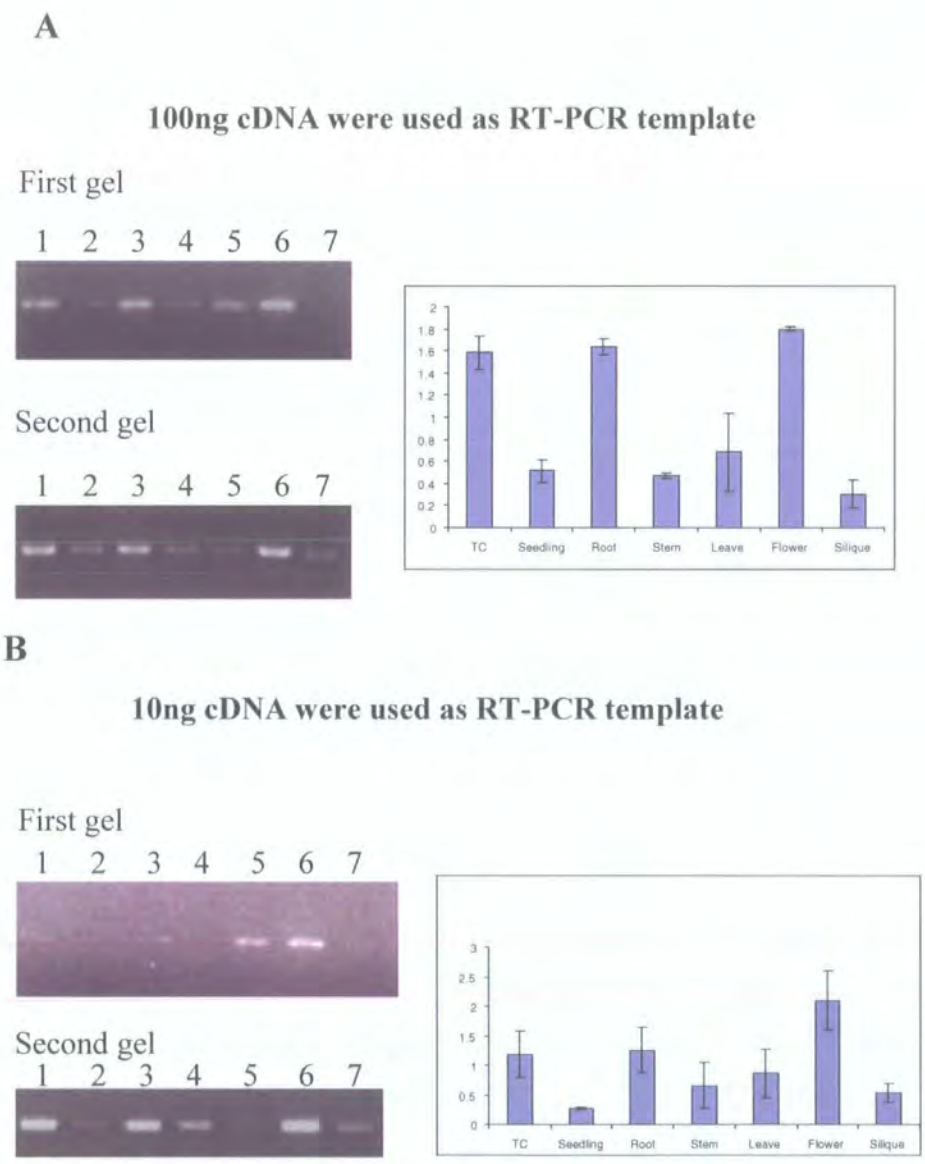

Figure 4.15: *AtMAP65-2* RT-PCR with cDNA samples prepared from 1. Tissue Culture cells, 2. Seedlings, 3. Roots, 4. Stem, 5. Leaves, 6. Flowers, 7. Siliques. **A.** RT-PCR using 100 ng cDNA as template for each of the seven samples. A repeat RT-PCR was carried out and a histogram was produced based on average values. **B.** RT-PCR using 10 ng cDNA as template for each of the seven samples. A repeat RT-PCR was carried out and a histogram was produced based on average values.

Figure 4.16
AtMAP65-3 RT-PCR

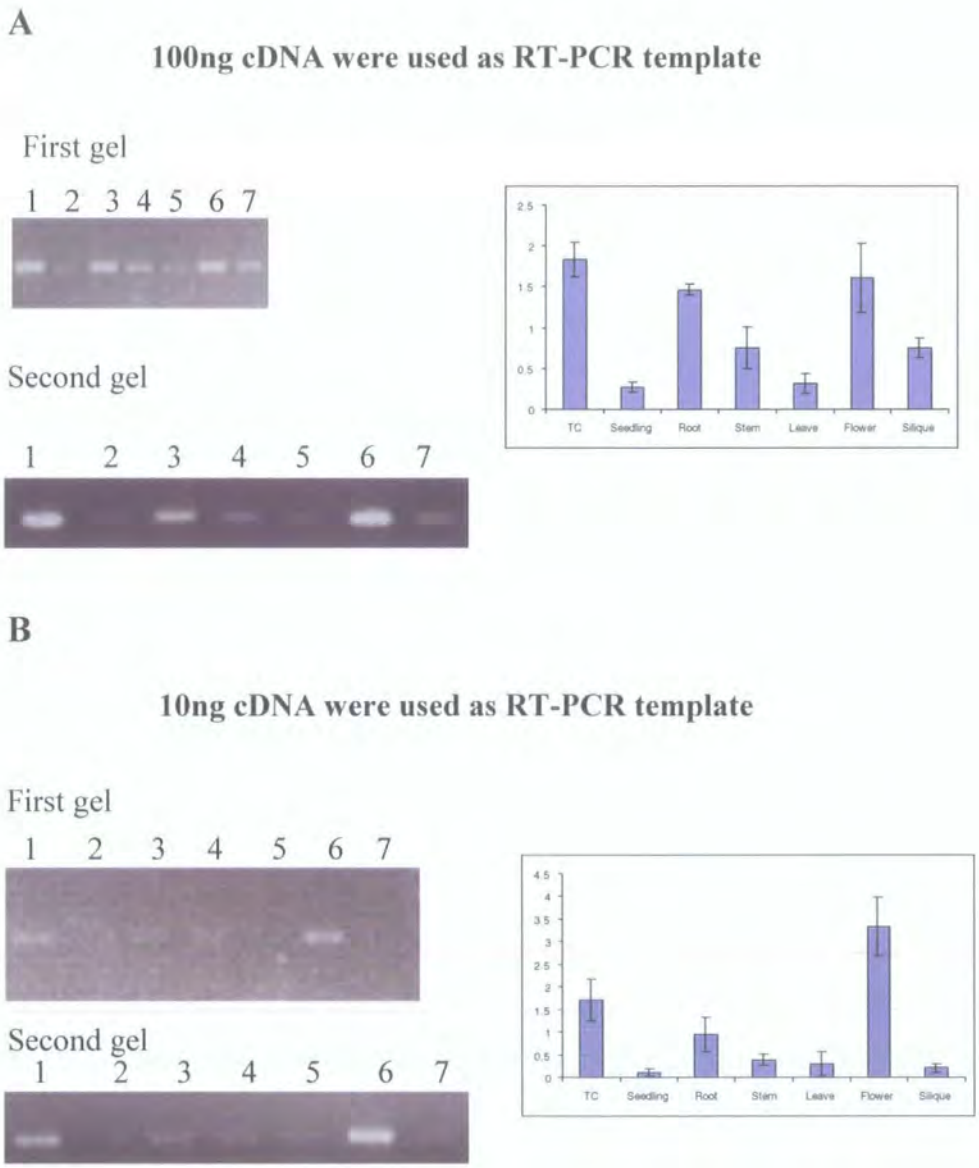

Figure 4.16: *AtMAP65-3* RT-PCR with cDNA samples prepared from 1. Tissue Culture cells, 2. Seedlings, 3. Roots, 4. Stem, 5. Leaves, 6. Flowers, 7. Siliques. **A.** RT-PCR using 100 ng cDNA as template for each of the seven samples. A repeat RT-PCR was carried out and a histogram was produced based on average values. **B.** RT-PCR using 10 ng cDNA as template for each of the seven samples. A repeat RT-PCR was carried out and a histogram was produced based on average values.

Figure 4.17
AtMAP65-4 RT-PCR

A

100ng cDNA were used as RT-PCR template

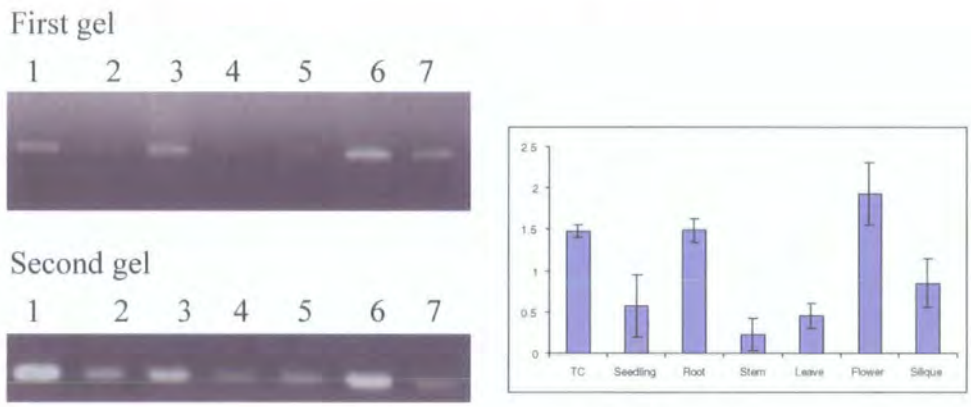

B

10ng cDNA were used as RT-PCR template

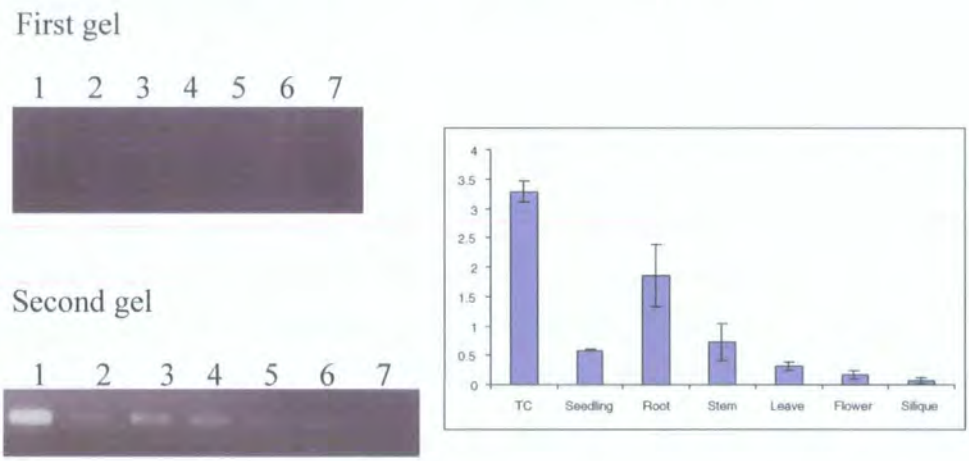

Figure 4.17: *AtMAP65-4* RT-PCR with cDNA samples prepared from 1. Tissue Culture cells, 2. Seedlings, 3. Roots, 4. Stem, 5. Leaves, 6. Flowers, 7. Siliques. **A.** RT-PCR using 100 ng cDNA as template for each of the seven samples. A repeat RT-PCR was carried out and a histogram was produced based on average values. **B.** RT-PCR using 10 ng cDNA as template for each of the seven samples. A repeat RT-PCR was carried out and a histogram was produced based on average values.

cDNA as template, the average signal between the replicate gels remained high only in tissue culture cells (figure 4.18).

AtMAP65-6 RT-PCR

The *AtMAP65-6* RT-PCR gels with 100ng cDNA as a template revealed the *AtMAP65-6* transcript is abundant in *Arabidopsis* tissue culture cells and in all the *Arabidopsis* tissues examined. In *AtMAP65-6* RT-PCRs with 1:10 diluted cDNA as template, the average signal remained high for the tissue culture cells, roots, stem and siliques (figure 4.19).

AtMAP65-7 RT-PCR

The *AtMAP65-7* RT-PCRs did not give any band using as a template either of the cDNA samples. Control PCR with genomic DNA as template revealed the *AtMAP65-7* primers could amplify the *AtMAP65-7* sequence.

AtMAP65-8 RT-PCR

The RT-PCRs of *AtMAP65-8* using 100ng cDNA as template from each sample revealed high signal in roots, stem and flowers. The signal in roots and stem remained high in RT-PCRs with 1:10 diluted cDNA as template (figure 4.20).

AtMAP65-9 RT-PCR

The RT-PCRs of *AtMAP65-9* primers with 100ng cDNA from each sample gave higher signal in roots, stem and flowers (figure 4.21). The RT-PCRs of *AtMAP65-9* primers with 1:10 diluted cDNA did not give any signal.

Figure 4.18
AtMAP65-5 RT-PCR

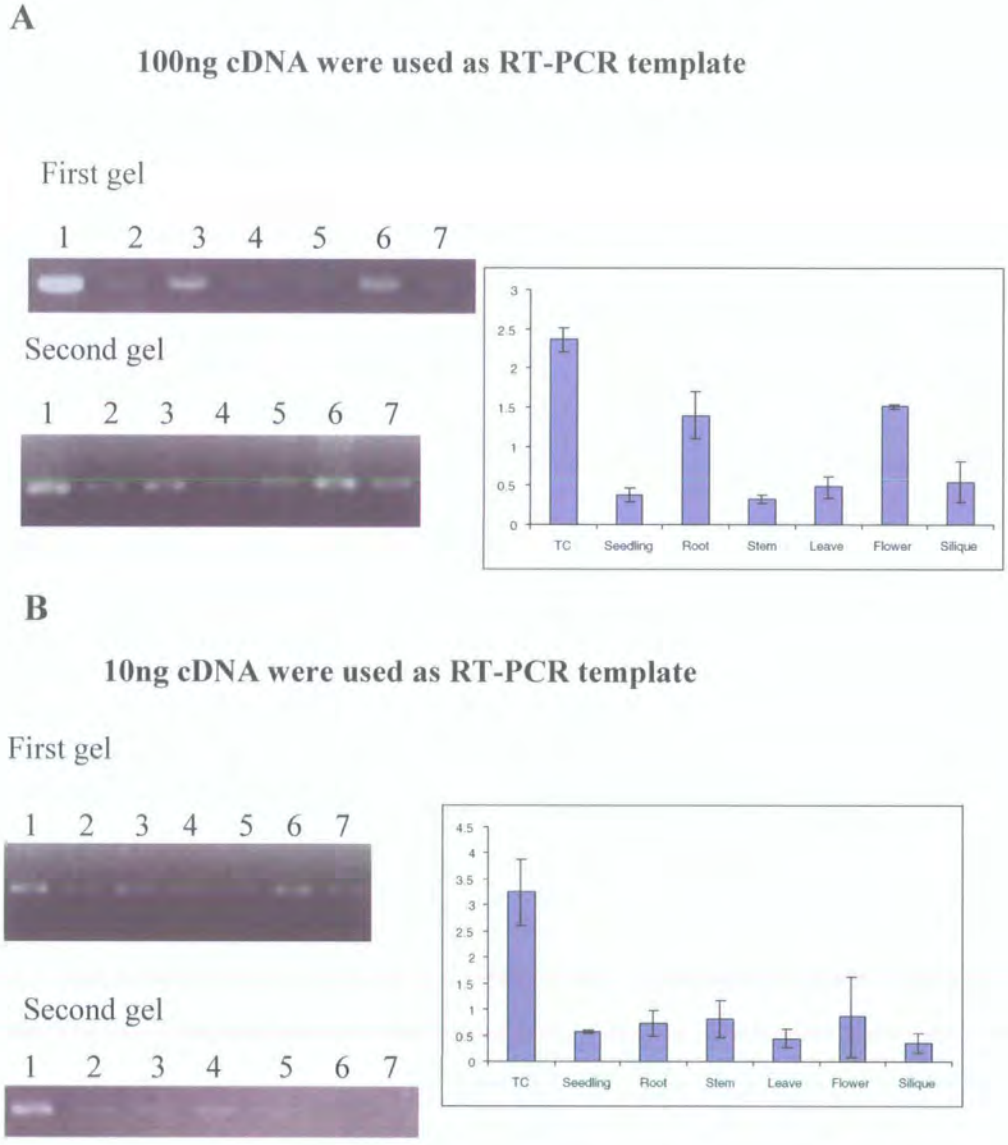

Figure 4.18: *AtMAP65-5* RT-PCR with cDNA samples prepared from 1. Tissue Culture cells, 2. Seedlings, 3. Roots, 4. Stem, 5. Leaves, 6. Flowers, 7. Siliques. **A.** RT-PCR using 100 ng cDNA as template for each of the seven samples. A repeat RT-PCR was carried out and a histogram was produced based on average values. **B.** RT-PCR using 10 ng cDNA as template for each of the seven samples. A repeat RT-PCR was carried out and a histogram was produced based on average values.

Figure 4.19
AtMAP65-6 RT-PCR

A

100ng cDNA were used as RT-PCR template

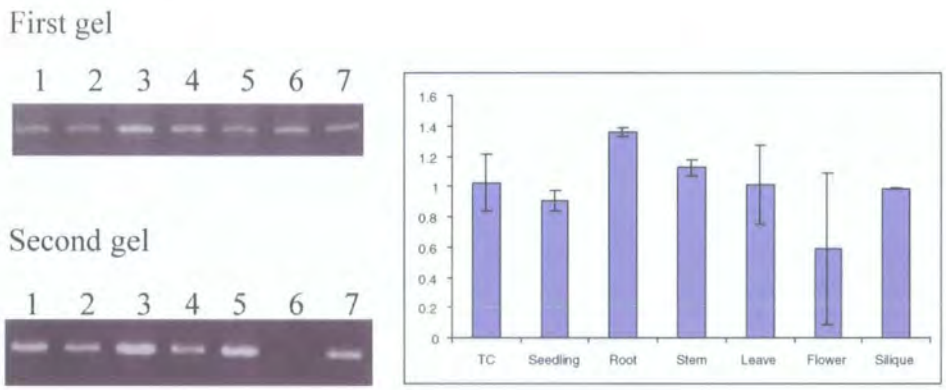

B

10ng cDNA were used as RT-PCR template

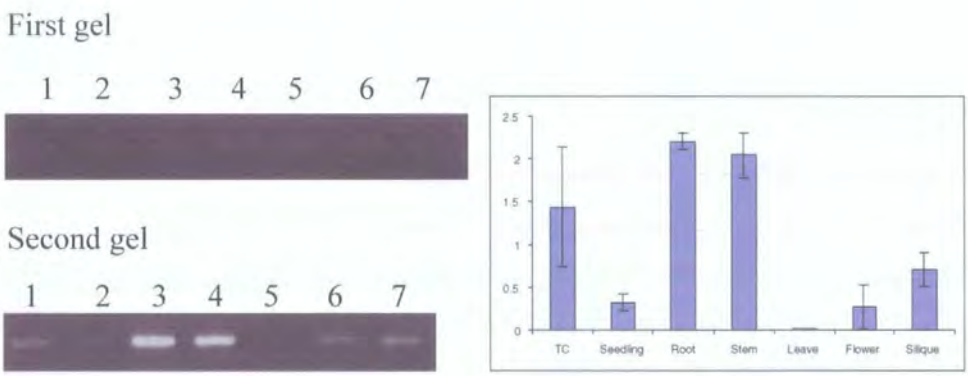

Figure 4.19: *AtMAP65-6* RT-PCR with cDNA samples prepared from 1. Tissue Culture cells, 2. Seedlings, 3. Roots, 4. Stem, 5. Leaves, 6. Flowers, 7. Siliques. **A.** RT-PCR using 100 ng cDNA as template for each of the seven samples. A repeat RT-PCR was carried out and a histogram was produced based on average values. **B.** RT-PCR using 10 ng cDNA as template for each of the seven samples. A repeat RT-PCR was carried out and a histogram was produced based on average values.

Figure 4.20
AtMAP65-8 RT-PCR

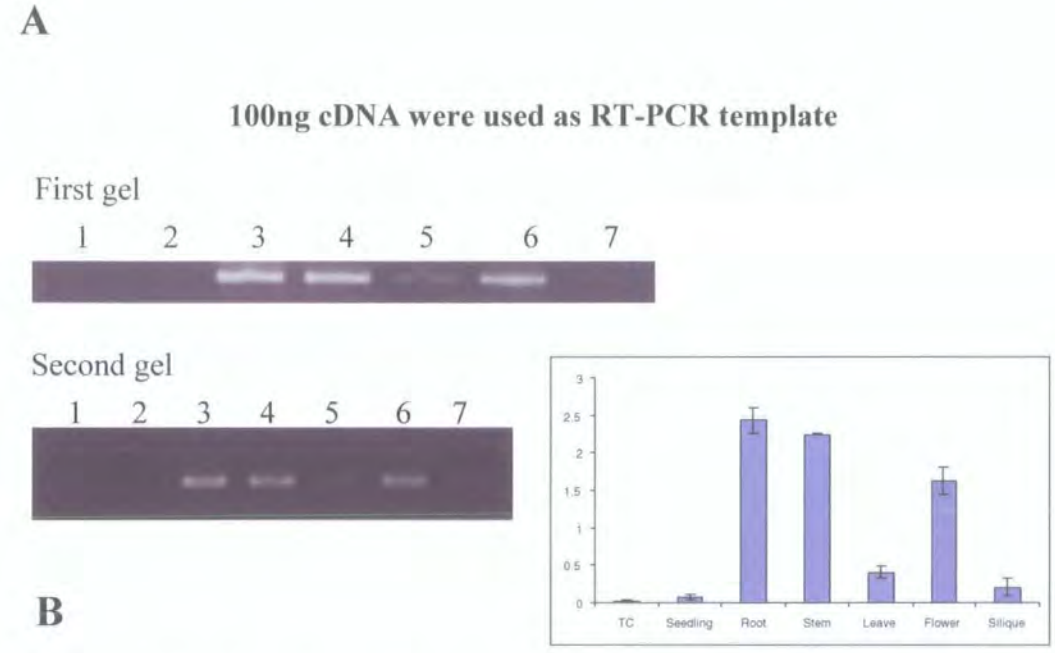

Figure 4.20: *AtMAP65-8* RT-PCR with cDNA samples prepared from 1. Tissue Culture cells, 2. Seedlings, 3. Roots, 4. Stem, 5. Leaves, 6. Flowers, 7. Siliques. **A.** RT-PCR using 100 ng cDNA as template for each of the seven samples. A repeat RT-PCR was carried out and a histogram was produced based on average values. **B.** RT-PCR using with 10 ng cDNA as template for each of the seven samples. A repeat RT-PCR was carried out and a histogram was produced based on average values.

Figure 4.21
AtMAP65-9 RT-PCR

100ng cDNA were used as RT-PCR template

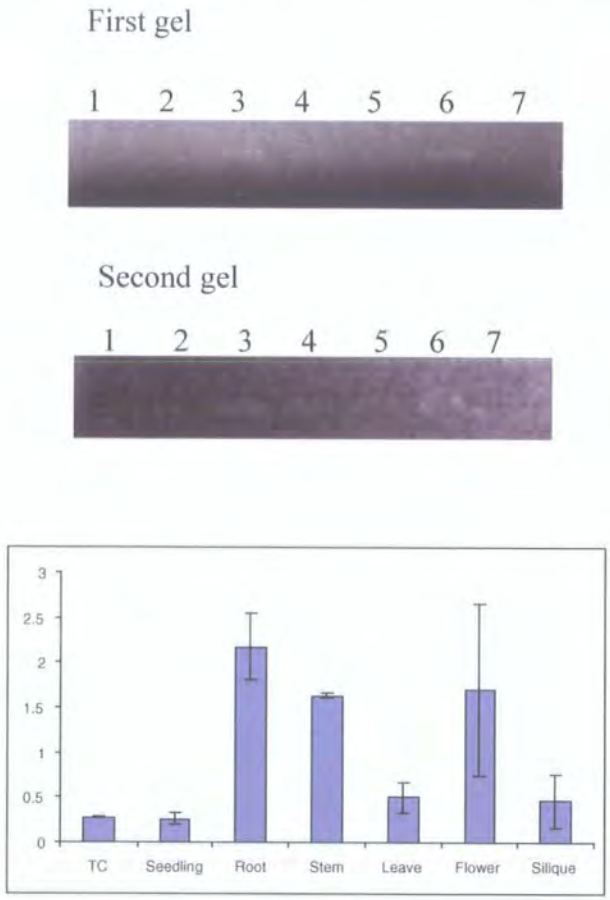

Figure 4.21:
AtMAP65-9 RT-PCR with cDNA samples prepared from 1. Tissue Culture cells, 2. Seedlings, 3. Roots, 4. Stem, 5. Leaves, 6. Flowers, 7. Siliques.
RT-PCR using 100 ng cDNA as template for each of the seven samples. A repeat RT-PCR was carried out and a histogram was produced based on average values.
RT-PCR using 10 ng cDNA as template for each of the seven samples gave no bands.

4.4 Summary

The expression programme of each of the *AtMAP65* genes was investigated using Promoter::GUS reporter gene fusions in transgenic *Arabidopsis* and RT-PCR of cDNA samples prepared from various *Arabidopsis* tissues.

GUS histochemical analysis for the *AtMAP65-1::GUS* reporter gene fusion revealed that *AtMAP65-1* was expressed in all *Arabidopsis* organs and tissues examined, leaves, hypocotyl, roots and flower with exception the sepals, anthers and pollen. RT-PCT using specific primers to *AtMAP65-1* and cDNA from variours *arabidopis* tissues confirmed that *AtMAP65-1* transcript was abundant in all *Arabidopsis* samples prepared from tissue culture cells, seedlings, roots, leaves, flowers and siliques.

GUS expression for the *AtMAP65-2* fusion revealed *AtMAP65-2* was present in *Arabidopsis* leaves, hypocotyl and roots but it did not stain all the tissues. The mesophyll cells and veins were more strongly stained in cotyledons than leaves. In hypocotyls and roots the vascular tissues were stained. Strong staining was also shown in primary and lateral root tips. In the flower, the embryo and stamens were stained. *AtMAP65-2* RT-PCR also revealed *AtMAP65-2* transcript to be present in roots, leaves and flowers.

The *AtMAP65-3::GUS* fusion was expressed in mesophyll cells and veins of leaves. GUS staining was also observed in root vascular tissues, root initiation points and primary and lateral root tips. RT-PCR also showed that *AtMAP65-3* is expressed in leaves and roots, roots giving a particularly high signal. In the flower, *AtMAP65-3::GUS* stained the embryo and some lines stained the pollen as well. RT-PCR also showed that *AtMAP65-3* transcript is present in flowers.

The *AtMAP65-4::GUS* fusion resulted in weak GUS staining in vascular root tissues, lateral root initiation points and primary and lateral root tip caps. RT-PCR confirmed that the *AtMAP65-4* transcript is most abundant in roots. In addition, RT-PCR gave a hint of the presence of *AtMAP65-4* transcript in flowers but the GUS signal was not observed in *AtMAP65-4::GUS* plant flowers.

The *AtMAP65-5::GUS* fusion resulted in weak GUS staining in leaf mesophyll cells. GUS staining was also observed in vascular root tissues, root tip initiation points and primary and lateral root tip caps. RT-PCR confirmed that the *AtMAP65-5* transcript was present in roots. In addition, RT-PCR revealed that the *AtMAP65-5* transcript is present in flowers. Some *AtMAP65-5::GUS* lines also showed staining in the pollen. From the RT-PCR of *AtMAP65-5* using 10ng cDNA as template from each sample, only tissue culture cells gave high signal. These data agree with the *AtMAP65-5::GUS* fusion results where weak staining in *Arabidopsis* seedlings was observed.

The *AtMAP65-6::GUS* fusion showed high expression in leaf mesophyll cells and vascular tissues of hypocotyl and roots. Primary and lateral root tips were also stained. RT-PCR confirmed that *AtMAP65-6* transcript is abundant in *Arabidopsis* seedlings, roots and leaves. In addition, GUS was present in flower embryos, petals and stamens. RT-PCR also indicated the presence of *AtMAP65-6* transcript in flowers.

GUS expression for the *AtMAP65-7* fusion was not observed in either seedlings tissues or flowers. In addition, RT-PCR for *AtMAP65-7* transcript did not give any signal. *AtMAP65-7*

expression could be too low to be detected and/or its expression could be activated under certain conditions, like under hormonal treatment or pathogen attack.

The *AtMAP65-8::GUS* staining in leaves was concentrated in stipules. In roots the vascular tissues and the lateral root initiation points were stained. *GUS* was also expressed in primary and lateral root tips. RT-PCR confirmed that the *AtMAP65-8::GUS* transcript is present in leaves and roots. It also indicated *AtMAP65-8* is present in flowers but *AtMAP65-8::GUS* staining was not observed in flowers.

The *AtMAP65-9::GUS* fusion resulted in a pollen specific GUS staining in the flowers. It also weakly stained the primary and lateral root tips and the lateral root initiation points. *AtMAP65-9* RT-PCR using 100ng cDNA as template confirmed *AtMAP65-9* expression in *Arabidopsis* flowers and roots. However, the RT-PCR using 10ng cDNA as template did not give any signal and this result confirms the weak expression of *AtMAP65-9::GUS* in *Arabidopsis* seedling (Fig 4.13).

Chapter 5

Cloning and characterisation of the AtMAP65-6 isoform

5.1 Introduction

In previous research the biochemical properties of AtMAP65-1 (Smertenko *et al.*, 2004), AtMAP65-3 (Muller *et al.*, 2004) and AtMAP65-5 (Dr Smertenko, unpublished data) have been identified. In order to continue the functional dissection of the *Arabidopsis* MAP65 proteins, cDNA libraries were screened with *AtMAP65* probes. As a result the full length coding sequence of the *AtMAP65-6* was obtained and in this chapter, the biochemical properties and the *in vivo* pattern of AtMAP65-6 expression are investigated. The AtMAP65-6 coding sequence was cloned into the expression vector pET28α (Amersham Pharmacia) and subsequently, the recombinant protein AtMAP65-6 was expressed and purified. The ability of AtMAP65-6 to bind MTs was tested *in vitro* and compared to AtMAP65-1 and AtMAP65-5. AtMAP65-1, -5 and -6 protein-protein interactions were tested in a Yeast Two Hybrid system. AtMAP65-6 localisation was also examined through the cell cycle.

5.2 Cloning of AtMAP65 genes by screening cDNA libraries

5.2.1 cDNA library screening procedure

Three cDNA libraries, CD4-14, CD4-15 and CD4-6, obtained from the *Arabidopsis* Biological Resource Center (ABRC, Columbus, USA), were used for this study. The CD4-14 and CD4-15 libraries were constructed from poly(A)$^+$mRNA isolated from *Arabidopsis* seedlings and hypocotyls. Both the libraries were size fractionated and CD4-15 contained inserts of average size 2-3 Kb and CD4-14 contained inserts of average size 1-2 Kb. The

CD4-6 library was constructed from poly(A)$^+$mRNA isolated from *Arabidopsis* flowers and it contained inserts of average size 1.2 Kb.

5.2.2 *AtMAP65-6* full length Cloning

Through the screening of CD4-15 *Arabidopsis* cDNA, the full length *AtMAP65-6* was cloned. An *AtMAP65-6* Expression Sequence Taq (*EST*) obtained from *Arabidopsis* Biological Resource Center (ABRC, Columbus, USA) was used as probe for screening the *Arabidopsis* library CD4-15, which contained inserts of average size 2-3 Kb and was prepared using RNA isolated from seedlings and hypocotyls. The size of the cDNA was predicted to be 2.3- 2.4 Kb long.

The titer of the CD4-15 library was 1 x 10^{10} plaques/ ml = 1x 10^7 plaques/ µl. The titer is calculated as: plaques x dilution factor / volume plated. 750,000 plaques were the desired amount of plaques for the first screening. So the library was diluted 1 x 10^7 / 7.5 x 10^5, 13 times in SM buffer. The XL1-Blue cells, grown overnight were resuspended and diluted in 10 mM $MgSO_4$ to obtain OD_{550} of 0.5. To infect the XL1-Blue cells with the library, 2 µl of the diluted library were mixed with 10 µl of the diluted XL1-Blue cells, and their mixture was incubated at 37°C for 2 hours. The screening procedure followed was as described in Materials and Methods chapter (section 2.6). In summary the steps followed were: plaques grown on NZY plates, their DNA transferring onto nitrocellulose membrane, DNA denaturation and crosslinking with the membranes, prehybridisation, hybridisation with P^{32} radiolabelled *AtMAP65-6* probe, signal detection by autoradiography. The screening gave 100 positives and the strongest 20 were taken through the subsequent screening. The plaques of interest were transferred into SM buffer with chloroform and vortexed to release the phage particles into the SM buffer. The desired ratio of plaque/plate for the second screening

was selected to be 5,000 plaques. The titer of phage solution was calculated and based on this, the plating dilution for the next screening was determined. For example, 1 µl of 10^4 phage solution gave 30 plaques. Hence, in order to have about 5000 plaques per plate, this phage solution had to be diluted 10^2 times and 2 µl to be plated. In this way the plating dilutions were selected for each phage solution. The second screening was successful and the 10 strongest positives were selected for the third round. From the plates of the second screening, it was calculated that roughly 16 plaques gave 1 positive. For the third screening the target was 500 plaques per plate. The titer and the plating dilutions for each phage solution were calculated as above. For example, 1 µl of 10^4 times diluted phage solution gave 10 plaques. So, in order to achieve 500 plaques at the next round, the phage solution was diluted 10^3 times and 5 µl was plated.

From the third screening, single positives were isolated and were used for *in vivo* excision into pBluescript. The phagemids were digested with *Eco*RI enzyme. Based on the gene-bank database, the AtMAP65-6 gene has an *Eco*RI enzyme site at about 800 bp from the beginning of the coding sequence. Consequently, the *Eco*RI digestion in the case of full length cloning was expected to release two fragments, one about 800 bp and one about 1.5 Kb making together the estimated 2.5 Kb cDNA size. From the four tested positives, one proved to have the correct insert size (Figure 5.1, panel A). Sequencing of the excised positive No 4 from both 5' and 3' ends proved that the full length AtMAP65-6 cDNA had been cloned (the *AtMAP65-6* coding sequence and translation are illustrated in appendix O). The *AtMAP65-6* sequence cloned was identical to the sequence in the NCBI Genebank database (http://www.ncbi.nlm.nih.gov/Genbank/index.html).

5.2.3 Cloning of AtMAP65-3 gene

A part of the AtMAP65-3 cDNA, recovered by PCR from the CD4-14 library by Safina Khan, was used as a probe for cDNA library screening. The AtMAP65-3 cDNA based on the database is about 2.5 Kb and as CD4-14 contains inserts 1-2 Kb in average, the CD4-15 library was used instead. The CD4-15 cDNA library was constructed from mRNA from the same tissues as CD4-14 and contained larger sizes of inserts, about 2-3 Kb. However, the CD4-15 library did not give any positives and as a result the CD4-6 library was used. The CD4-6 is a floral cDNA library, which has inserts of average size 1.2 Kb.

The CD4-6 library titer was 3.9 x 10^{11} plaques per ml = 3.9 x 10^{8} plaques / µl. For the screening 75,000 plaques are needed in total so the library was diluted 3.9 x 10^{8} / 7.5 x 10^{5}, 520 times. The XL1-Blue cells were prepared in the same way as previously described and 2 µl of the diluted library were mixed with 10 µl of diluted XL1-Blue cells in SM buffer at OD_{550}: 0.5.

The strongest 13 positives were taken through the subsequent 2nd screening. It was calculated from the first screening plates that roughly 750 plaques gave 1 positive. The target of plaques /plate for the second screening was selected to be 5,000 plaques. The titer and plating dilution of each phage solution were calculated. For example, one phage solution had a titer of about 2 x 10^{5}. Hence, it was diluted 10^{2} times and 2.5 µl were plated on NZY plates in order to give 5,000 plaques per plate at the next round. The second screening was successful and the 10 strongest positives were selected for the third round. For the third screening the target was 500 plaques per plate. The phages soluion titer and plating dilutions were calculated. For example, 1 µl of 10^{3} diluted phage solution gave 10 plaques. So, the

phage solution was diluted 10^3 times and 1 µl was plated in order that 500 plaques could be achieved.

The screening of the CD4-6 library with the AtMAP65-6 probe was successful and a 1.4 Kb part of the AtMAP65-3 C-terminus was cloned through three rounds of screening. The excised phagemid contained the truncated version of the AtMAP65-3 cDNA as illustrated at Figure 5.1, panel B.

Reverse Transcription - Polymerase Chain Reaction (RT-PCR) was performed to clone the missing 5' end of the AtMAP65-3 gene. The primers were designed, according to the database sequence, at the 5' end of the AtMAP65-3 coding sequence and at a region about 1.9 Kb downstream of the start, where there is an *Eco*RI enzyme site (see appendix P, panel A for the *AtMAP65-3* primers). The region where the *Eco*RI enzyme site overlaps with the already cloned C-terminus part of AtMAP65-3 from the CD4-6 library. Total RNA extract from *Arabidopsis* tissue culture cells was used as a template. The RT-PCR was successful and a 1.5 to 2.0 Kb part of AtMAP65-6 gene was produced as shown at Figure 5.1, panel C.

5.2.4 Cloning of AtMAP65-9 gene

cDNA libraries were also used for *AtMAP65-9* cloning. A part of *AtMAP65-9*, cloned by PCR from the CD4-14 library by Safina Khan, was used as a probe. All the CD4-14, CD4-15 and CD4-6 libraries were screened but the *AtMAP65-9* clone was not obtained.

Figure 5.1
Cloning of *AtMAP65-1* and *AtMAP65-3*

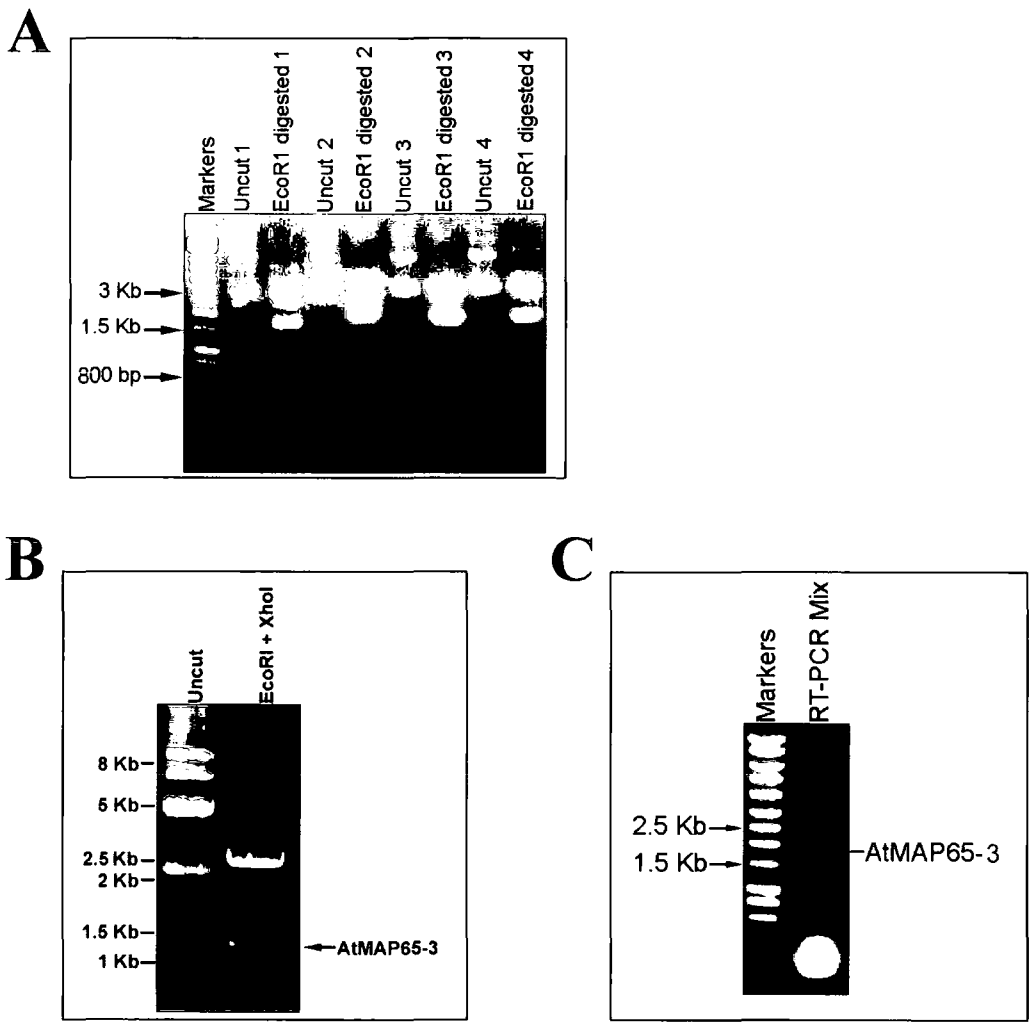

Figure 5.1:

A. *Eco*RI digestion of *AtMAP65-6* pBluescript phagemids after four rounds of cDNA screening. Plasmid 4 released two bands around 1.5 Kb and 800 bp, which their sum corresponded to the size of the predicted *AtMAP65-6* gene. DNA sequencing confirmed plasmid 4 contained an *AtMAP65-6* full length clone identical to the *AtMAP65-6* sequence in the gene-bank database.

B. *Eco*RI digestion of *AtMAP65-3* pBluescript phagemid after four rounds of cDNA screening. The plasmid releases an *AtMAP65-3* truncated version of 1.4 Kb missing the 5' end. The *AtMAP65-3* full length gene was estimated from the gene-bank database to be about 2.5 Kb.

C. *AtMAP65-3* truncated version obtained from RT-PCR.

The primers were designed at the 5' end of *AtMAP65-3* in the beginning of the coding sequence and 1.9 Kb downstream, where an *Eco*RI site is located. The section where the *Eco*RI site is, overlaps with the AtMAP65-3 section cloned by the cDNA screening.

5.3 AtMAP65-6 expression in *E.coli*

5.3.1 AtMAP65-6 cloning into an expression vector

AtMAP65-6 coding sequence was cloned into pGEM-T Easy vector. DNA sequencing proved that the PCR did not introduce any mutation and AtMAP65-6 coding sequence was then sub-cloned into the expression vector pET28α using *Nde*I and *Xho*I restriction sites at the 5' and 3' end respectively (see appendix P, panel B for the *AtMAP65-6* primers). DNA sequencing proved that the AtMAP65-6 coding sequence was inserted, in frame, into pET 28α.

5.3.2 Expression and purification of AtMAP65-6 recombinant protein

The recombinant plasmid was transformed into BL21 (DE3), BL21 (DE3) PLysS and BL21 (DE3) Star *E.coli* strains. AtMAP65-6 was better expressed in BL21 (DE3) pLysS cells. The recombinant protein was then purified using a nickel affinity column and four protein aliquots of 1ml each were eluted in 250mM immidazole buffer. Protein concentration was measured by the Bradford assay. The readings of the spectophotometer were 0.067, 0.088, 0.071 and 0.015 for the first, second, third and fourth elution respectively. The Bradford Standard Curve had a rate: y = 0.0538 x, where y is the absorbance at 595 nm and x the protein quantity at μg (Figure 5.2, panel A). For the Bradford assay, 5μl of each of the four elutions were used and it was calculated that they contained 1.245, 1.635, 1.32 and 0.275 μg of protein respectively (x = y/0.0538). So, the concentration of AtMAP65-6 was 0.249 mg/ml, 0.327 mg/ml, 0.264 mg/ml and 0.055 μg/μl (or mg/ml) at each of the four elutions respectively. The above calculations required the presence of pure AtMAP65-6 recombinant protein in the elution extracts. The one dimensional polyacrylamide (1D PAGE) gel proved that AtMAP65-6 extracts were not contaminated with high concentrations of other proteins

Figure 5.2
AtMAP65-6 Biochemical Analysis

A

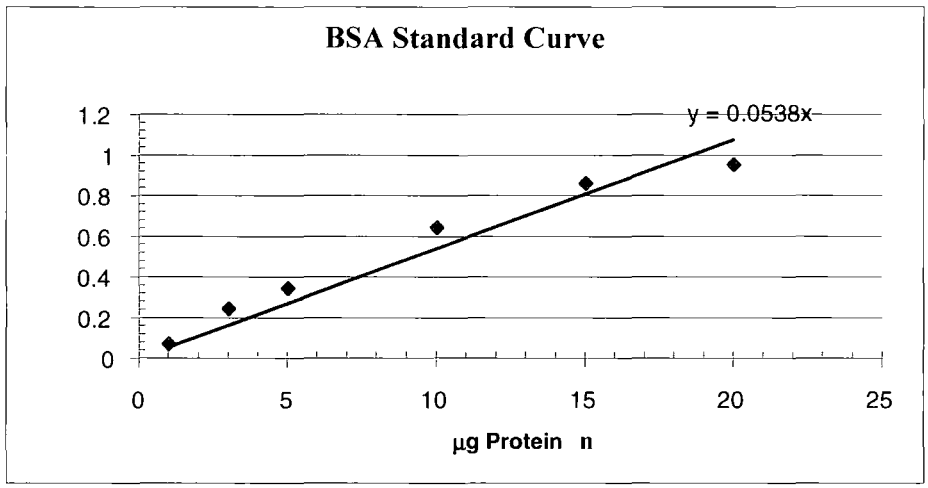

B

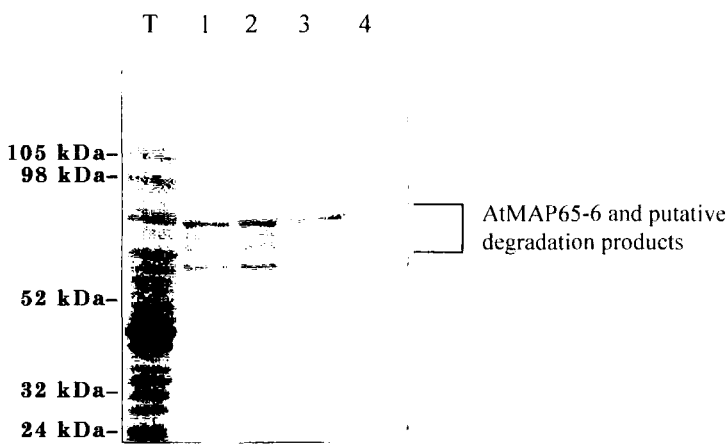

Figure 5.2:
A. The Bradford assay graph used to determine the concentration of the recombinant AtMAP65-6. The y axis is the Absorbance at 595 nm and the x axis, the protein quantity µg.
B. One dimension SDS-PAGE gel of AtMAP65-6 recombinant protein elutions after nickel affinity column purification. Lane T: 5µl of total protein extract run prior purification. Lanes 1, 2, 3 and 4: 10µl protein of protein elutions 1, 2, 3 and 4 run respectively. Based to the calculations in paragraph 5.3.2, 0.498, 0.654, 0.528 and 0.11µg of AtMAP65-6 protein were approximately loaded in lanes 1, 2, 3 and 4 respectively.

(Figure 5.2, panel B). AtMAP65-6 protein runs at about the 65 kD point on 1 D PAGE gel as it was predicted from its molecular weight.

5.4 Biochemical analysis of AtMAP65-6

5.4.1 MT co-sedimentation assay

The MT co-sedimentation assay was used to investigate if recombinant AtMAP65-6 could bind to MTs *in vitro*. The tubulin used was purified from porcine brain by Dr Andrei Smertenko. The MTs were stabilised by taxol and mixed with AtMAP65-6 recombinant protein (1:2 molar ratio) and centrifuged at 100,000 x g for 30 min. AtMAP65-6 protein was found to bind MTs and the tubulin::AtMAP65-6 complex was sedimented. In the control experiment the AtMAP65-6 protein, on its own, remained in the supernatant (Figure 5.3, panel A). A MT co-sedimentation assay with AtMAP65-1 as positive control was also performed. AtMAP65-1 also bound MTs (Figure 5.3, panel B).

5.4.2 MT turbidometric assay

The effect of AtMAP65-6 on MT polymerisation was assessed using a turbidimetric assay. AtMAP65-6 was added to a MAP-free porcine brain tubulin solution (final concentration 30 μM) at a molar ratio of 1:2. The turbidity of the mixture was monitored at 350 nm and 32°C. AtMAP65-6 induced an increase in the turbidity of the polymerising MT mixture compared to control (figure 5.4). AtMAP65-1 and AtMAP65-5 activity was assessed at the same time and both of them increased the turbidity of the MT solution. (AtMAP65-1 and AtMAP65-5 recombinant proteins were offered from Dr Andrei Smertenko).

Figure 5.3
AtMAP65-6 and AtMAP65-1 tubulin co-sedimentation assay

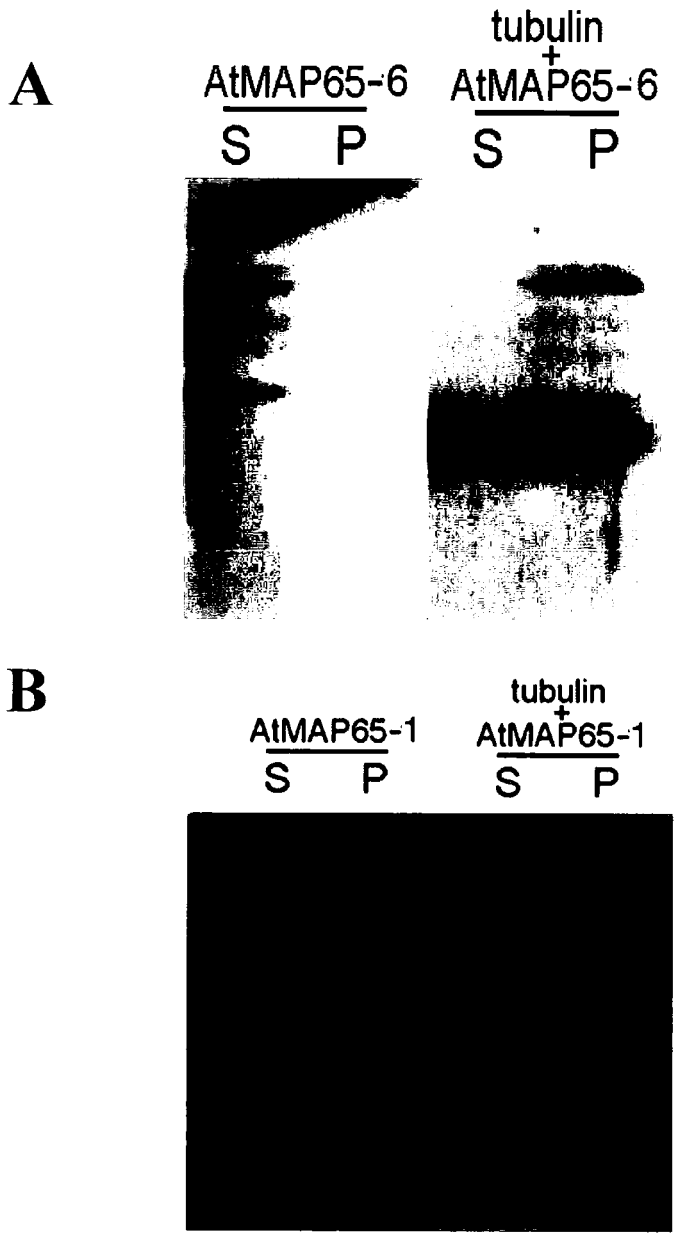

Figure 5.3: Tubulin co-sedimentation assay for AtMAP65-6 and AtMAP65-1.
A. In the control experiment AtMAP65-6 remains in the supernatant after centrifugation at 100,000 rpm for 30 min. When AtMAP65-6 is mixed with taxol stabilised MTs in 1:2 molar ratio, binds to MTs and the tubulin-AtMAP65-6 complex sediments.
B. AtMAP65-1 also binds to taxol-stabilised MTs (mixed in 1:2 molar ratio) and their complex is present in pellet. At the control experiment in absence of tubulin, AtMAP65-1 remains in the supernatant.

Figure 5.4
MT turbidometric assay in presence of AtMAP65-1, AtMAP65-6 and AtMAP65-5

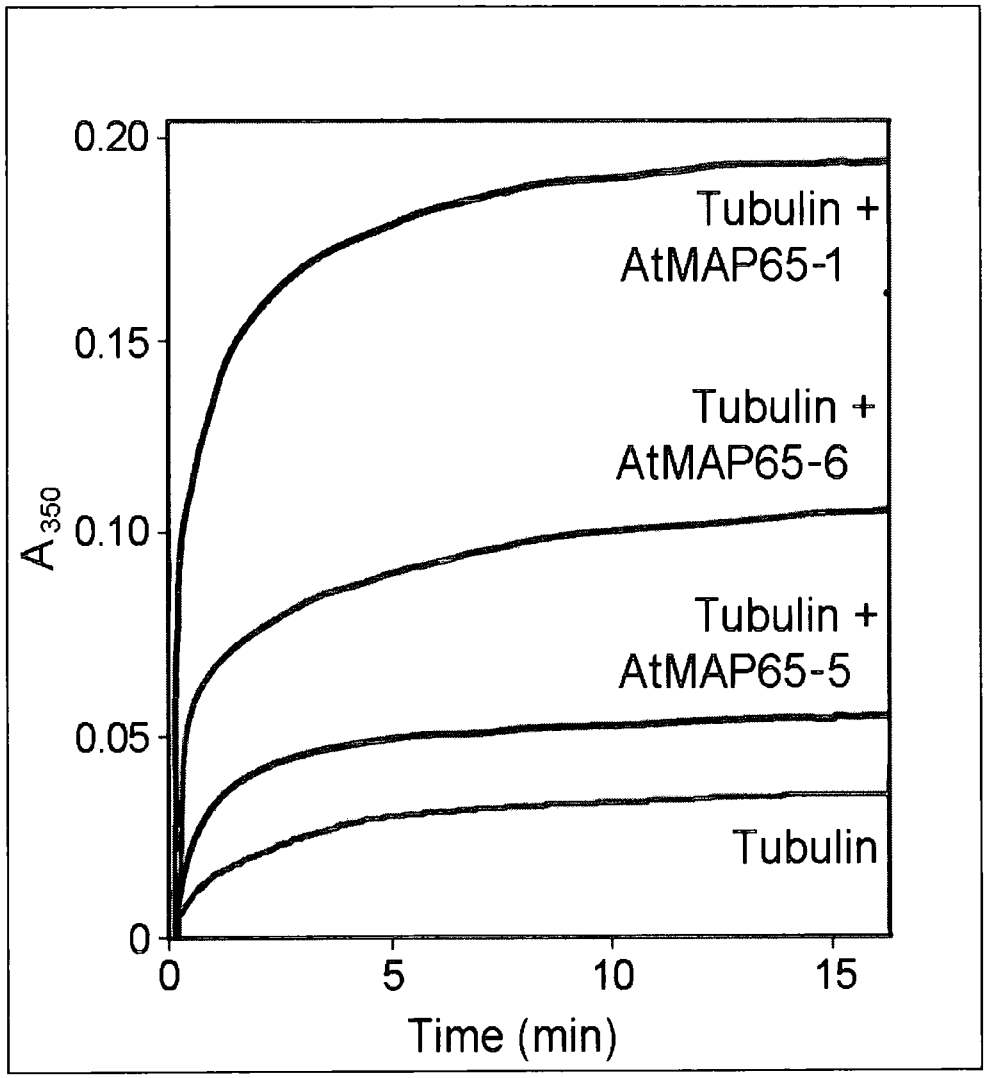

Figure 5.4:
Turbidometric assay of 30 μM tubulin solution of its own and after the addition of AtMAP65-1, AtMAP65-6 and AtMAP65-5 in 1:2 molar ratio monitored at 350 nm and 32°C.

5.5 Assessing AtMAP65-1, AtMAP65-6 and AtMAP65-5 interactions with Yeast Two Hybrid assays

5.5.1 Overview of the Yeast Two Hybrid procedure

The yeast two hybrid system is based on the fact that many eukaryotic transcription factors have separable DNA-binding and transcription activation domains. The fusion of "test proteins" to each separate domain reconstitutes an active transcription factor providing that the "test proteins" interact. The expression of reporter genes, which contain upstream elements to which the DNA-binding domain (BD) binds, can be monitored to detect the interaction. The yeast strains used for two hybrid experiments carry mutations in a number of genes required for amino acid biosynthesis, such as *TRP1*, *LEU2*, *HIS3* and *URA3* (review by Causier and Davies, 2002). Hence, if these amino acids are not added into the growth medium the yeast strain does not grow. Many of the two-hybrid plasmids carry genes that complement these mutations and provide selection of the transformant yeast.

Two plasmids needed to be constructed in order to test the possible interaction between two proteins, for example A and B. One plasmid encoded the *GAL4* DNA binding domain (BD), fused to the coding sequence of protein A. The BD vector used was the GATEWAY version of pAS2-1 (Ketelaar *et al*,2004) which carries the *TRP1* gene for selection in yeast. The second plasmid encoded the *GAL4* transcription activation domain (AD) fused to coding sequence of protein B. The AD vector used was the GATEWAY version of pACT-2 (Ketelaar *et al*, 2004) which carries the *LEU2* gene for selection in yeast (The maps of pAS2-1 and pACT2-1 vectors are illustrated in Appendix Q).

The yeast strain used for the Y2H system contain integrated reporter gene constructs; for example, the selectable yeast genes *HIS3*, *ADE2* and the *E.coli LacZ* gene. Interaction between BD and AD fusion proteins A and B stimulates transcription of the reporter genes. Transcription and translation of *HIS3* and *ADE2* allows selection on yeast growth medium lacking Histidine and Adenosine hemisulphate respectively. The His- and Ade-positive yeast colonies have also β-galactosidase activity and turn blue in the presence of 5-bromo-4-chloro-3 indolyl-β-D-galactopyranoside (X-Gal).

Haploid yeast strains of opposing mating type (a and α), one containing the DNA-binding domain fusion construct and the other the activation domain fusion construct can be mated to obtain the diploid yeast containing both constructs (review by Causier and Davies, 2002). The yeast strains used for the experiments were AH109 and Y187. AH109 contains the reporter genes *LacZ*, *HIS3*, *ADE2* and *MEL1*. Y187 contains the *LacZ* reporter gene.

First, *GAL4* BD fusion plasmids with each of AtMAP65-1, AtMAP65-6 and AtMAP65-5 were constructed by cloning their coding sequence into the GATEWAY version of pAS2-1. The constructs were transformed into AH109 and Y187. The AH109 strains were tested for auto-activation of some of the reporter genes. Then *GAL4* AD fusion plasmids with each of AtMAP65-1, AtMAP65-6 and AtMAP65-5 were constructed by cloning their coding sequence into the GATEWAY version of pACT-2. The constructs carrying the *GAL4* activating domain were transformed into AH109. The yeast colonies that grew on synthetic dropout (SD) medium without tryptophan (W) for Y187 strain and without Leucine (L) for AH109 strain were used for mating. The mating occurred in YPAD plates at room temperature for about 2 days until yeast growth. The diploids were selected on SD plates without Trp and Leu. Then the diploids were plated onto reporter gene selective media,

without Adenine hemisulfate (A) and/ or Histidine (H), and were also tested for β-galactosidase activity.

5.5.2 GATEWAY cloning of *AtMAP65-1*, *AtMAP65-6* and *AtMAP65-5* coding sequences into pAS2-1 and pACT-2

PCR was performed to amplify AtMAP65-1, AtMAP65-6 and AtMAP65-5 coding sequences with GATEWAY primers using PFU turbo enzyme. The *AtMAP65-1* and *AtMAP65-6* coding sequences cloned into pet28α vector were used as DNA templates for *AtMAP65-1* and *AtMAP65-6* PCR. The DNA template for *AtMAP65-5* PCR was the *AtMAP65-5* coding sequence in pGEM-T Easy vector. (see Appendix R for *AtMAP65-1*, *-5* and *–6* GATEWAY primers).

AtMAP65-1, AtMAP65-6 and AtMAP65-5 coding sequences were cloned into pDONR using the BP reaction. Subsequently, AtMAP65-1, AtMAP65-6 and AtMAP65-5 clones in pDNOR were cloned into pAS2-1 and pACT-2 vectors using the LR reaction.

5.5.2.1 *AtMAP65-1* cloning into Y2H vectors

Candidate plasmids containing the AtMAP65-1 coding sequence cloned into pDONR by BP reaction were selected based on pDONR gentamycin resistance. Presence of insert was checked with *Apa*I and *Sac*I double digestion (Figure 5.5, A). The plasmid which released the correct size of insert was sent for DNA sequencing, which proved the AtMAP65-1 coding sequence was cloned into pDONR without any point mutation. Then, the plasmid was subsequently used for gateway cloning into pAS2-1 and pACT-2 vectors by LR reaction. The cloning was successful and the constructs of the AtMAP65-1 coding sequence

into pAS2-1 and pACT-2 were confirmed by restriction enzyme digestions (Figure 5.5, A) and DNA sequencing.

5.5.2.2 *AtMAP65-6* cloning into Y2H vectors

The AtMAP65-6 coding sequence was cloned into both pAS2-1 and pACT-2 following the same procedure as for AtMAP65-1. First, AtMAP65-6 was cloned into pDONR by BP reaction and the construct was confirmed by *Apa*I and *Sac*I double digestion (Figure 5.5, B) and DNA sequencing. DNA sequencing proved that the amplified AtMAP65-6 coding sequence was free of mutations. LR reaction followed and the AtMAP65-6 coding sequence was cloned into pAS2-1 and pACT-2 destination vectors. These constructs were also checked by restriction enzyme digestions (Figure 5.5, B) and DNA sequencing.

5.5.2.3 AtMAP65-5 cloning into Y2H vectors

AtMAP65-5 coding sequence was cloned into pDONR using the BP reaction in a similar way to *AtMAP65-1* and *AtMAP65-6*. The construct was checked by *Hind*III and *Nhe*I double digestion (Figure 5.5, C). DNA sequencing proved that there were no mutations in the construct. Subsequently, the AtMAP65-5 coding sequence was cloned into pAS2-1 and pACT-2 yeast-two-hybrid vectors. The constructs were examined by restriction enzyme digestion (Figure 5.5, C) and DNA sequencing.

5.5.3 Transformation of BD plasmids into AH109 yeast strain for auto-activation control experiments

The BD fusion plasmids were tested in yeast to ensure that the constructs do not auto-activate the reporter gene(s). The constructs of *AtMAP65-1*, *-6* and *-5* in pAS2-1 were

Figure 5.5
Yeast Two Hybrid Cloning

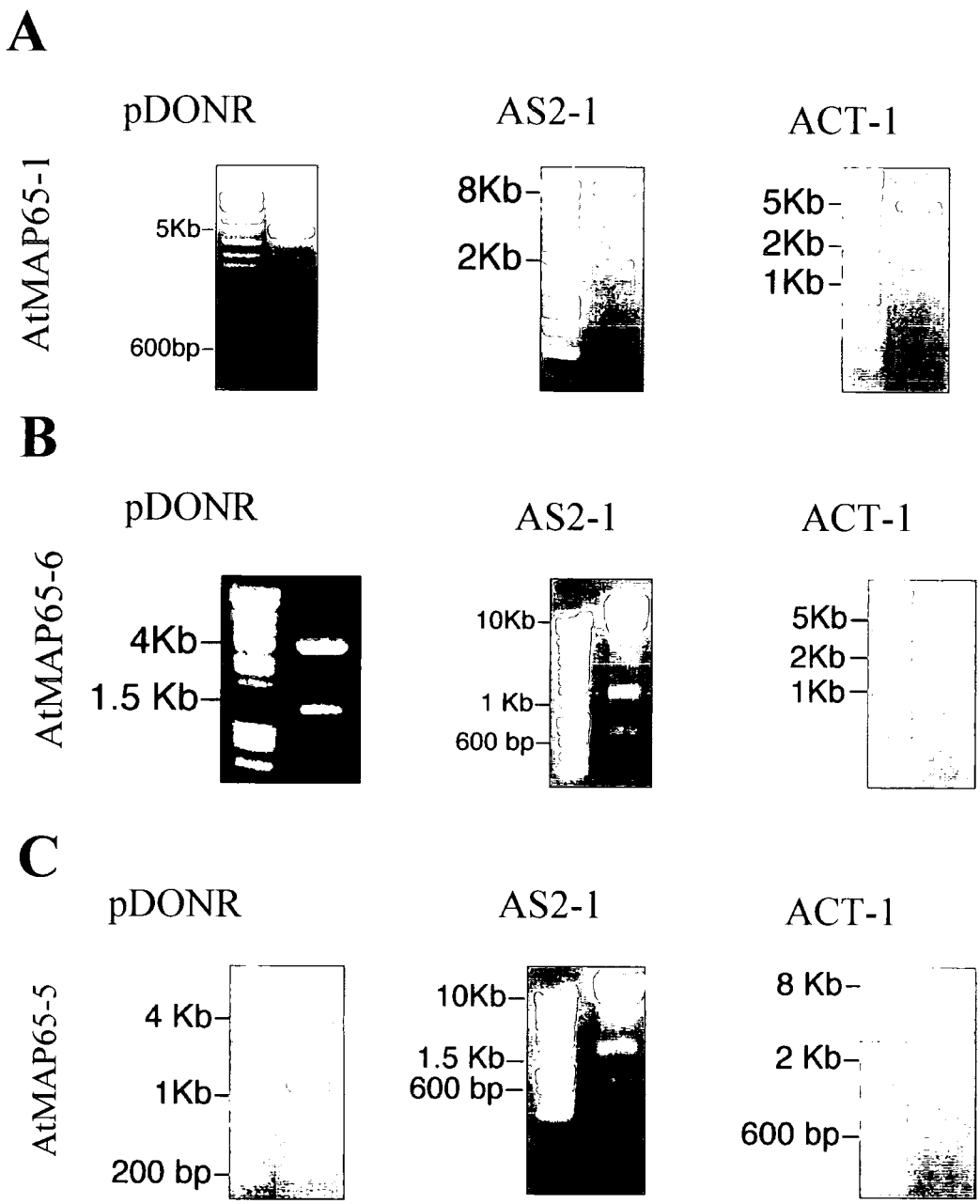

Figure 5.5:
A. Confirmation of cloning of AtMAP65-1 coding sequence into pDNOR, AS2-1 and ACT-1 vectors after double digestion with *Apa*I/ *Sac*I, *Nde*I/ *Sal*I and *Nde*I/ *Xho*I respectively.
B. Confirmation of cloning of AtMAP65-6 coding sequence into pDNOR, AS2-1 and ACT-1 vectors after double digestion with *Apa*I/ *Sac*I, *Nde*I/ *Sal*I and *Nde*I/ *Xho*I respectively.
C. Confirmation of cloning of AtMAP65-5 coding sequence into pDNOR, AS2-1 and ACT-1 vectors after double digestion with *Hin*dIII/ *Nhe*I, *Nde*I/ *Sal*I and *Nhe*I/ *Xho*I respectively.

transformed into AH109 yeast strain. The pAS2-1 vector carries the *GAL4* DNA-Binding Domain (BD) and contains the *TRP1* (W) gene. The Trp-positive transformants, containing the BD:AtMAP65 fusion plasmid, were selected on SD medium without tryptophan (Figures 5.6, 5.7 and 5.8, panel A). The Trp-positive transformants appeared as colonies after 3 days incubation at 30°C and then were plated out onto reporter gene selective media. AtMAP65-1, -6 and –5 fusion proteins with *GAL4* binding domain were tested for auto-activation of *HIS3* and *ADE2* reporter genes. Their growth was assessed after three days at 30°C on SD-TRP-HIS and SD-TRP-ADE respectively.

All AtMAP65-1, -6 and –5 fusion proteins with *GAL4* binding domain did not auto-activate the *ADE2* reporter gene. Hence, these plasmids can be used for testing interactions between them by monitoring *ADE2* reporter gene transcription (Figures 5.6, 5.7 and 5.8, panel B).

The AtMAP65-1 fusion protein with *GAL4* binding domain did not auto-activate the *HIS3* reporter gene (Figure 5.6, panel C). The AtMAP65-6 fusion protein, on the other hand, auto-activated the *HIS3* reporter gene (Figure 5.7, panel C). The *HIS3* reporter gene is leaky in most strains (Gietz *et al.*, 1997). The growth of AtMAP65-5: *GAL4* BD transformants was negligible after three to four days at 30°C and hence the plasmid could be used for testing yeast-two-hybrid interactions by monitoring *HIS3* reporter gene transcription (Figure 5.8, panel C).

BD: AtMAP65-1 and AtMAP65-6 plasmids were tested for auto-activation of the *lacZ* reporter gene, which results in expression of β-galactosidase activity. The β-galactosidase activity was detected by the filter assay. The transformants tested by this protocol were grown on SD-Trp medium as colonies grown on YPAD medium all develop blue colour

Figure 5.6
AtMAP65-1 auto-activation test

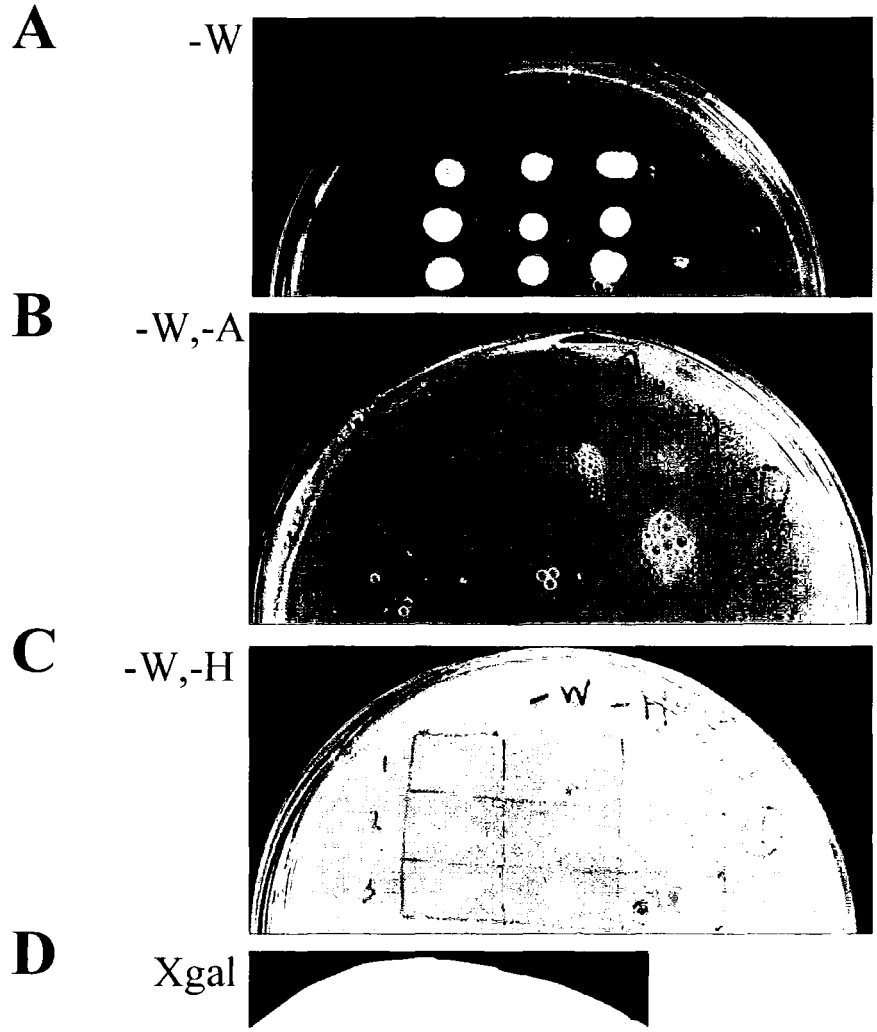

Figure 5.6:
A. AtMAP65-1 Trp-positive transformants containing the BD: AtMAP65-1 fusion plasmid were selected in SD medium without Trp. **B.** AtMAP65-1: BD Trp-positives were plated onto SD medium plate in absence of Trp and Ade. AtMAP65-1 did not auto-activate the *Ade 2* reporter gene. **C.** AtMAP65-1: BD Trp-positives were plated onto SD medium plate in absence of Trp and His. AtMAP65-1 did not auto-activate the *His 3* reporter gene.
D. AtMAP65-1 BD plasmids were tested for auto-activation of the *Lac Z* reporter gene, which results in expression of β-galactosidase activity. The yeast colonies were transferred onto filter paper and incubated overnight in Xgal buffer. AtMAP65-1 did not auto-activate *Lac Z*.

(Gietz *et al.*, 1997). Strong activation of *lacZ* gene gives a blue colour in a few hours. In case of AtMAP65-1, faint blue colouration developed following an overnight incubation at room temperature (Figure 5.6, panel D). This colouration was considered negligible and further experiments on AtMAP65-1 protein-protein interactions were followed by monitoring *lacZ* reporter gene expression.

The AtMAP65-6 fusion with *Gal4* Binding Domain gave stronger blue colour than AtMAP65-1 case after overnight incubation, indicating that the plasmid could auto-activate to a small degree the *lacZ* reporter gene (Figure 5.7, panel D). The X-gal staining for AtMAP65-6 came up within one hour incubation, much quicker than for AtMAP65-1 (the filter paper of AtMAP65-1 was blank after three hours of incubation and coloration was detected after overnight incubation.

5.5.4 Transformation of BD plasmids into Y187 yeast strain and of AD plasmids into AH109 yeast strain

AtMAP65-1, -6 and –5 fusion proteins in BD cloning vector were transformed into Y187 yeast strain. AtMAP65-1, -6 and –5 fusion proteins in AD cloning vector were transformed into AH109 yeast strain. The transformants were plated on YPAD medium plates in the presence of 2% (w/v) glucose and without Tryptophan and Leucine in the case of *GAL4* BD plasmids and *GAL4* AD plasmids respectively.

Figure 5.7
AtMAP65-6 auto-activation test

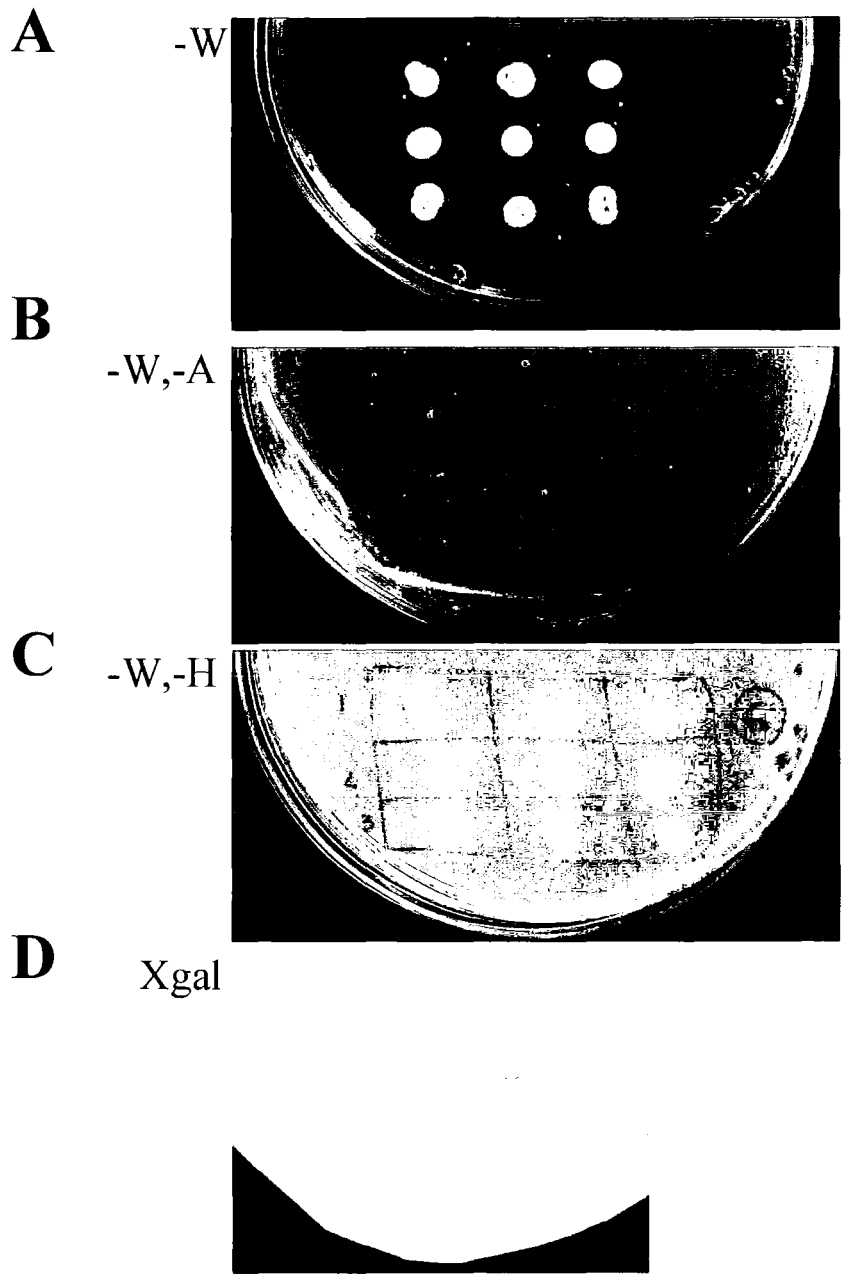

Figure 5.7:
A. AtMAP65-6 Trp-positive transformants containing the BD: AtMAP65-6 fusion plasmid, were selected in SD medium without Trp. **B.** AtMAP65-6: BD Trp-positives were plated onto SD medium plate in absence of Trp and Ade. AtMAP65-6 did not auto-activate the *Ade 2* reporter gene. **C.** AtMAP65-6: BD Trp-positives were plated onto SD medium plate in absence of Trp and His. AtMAP65-6 auto-activated the *His 3* reporter gene.
D. AtMAP65-6 BD plasmids were tested for auto-activation of the *Lac Z* reporter gene, which results in expression of β-galactosidase activity. The yeast colonies were transferred onto filter paper and incubated overnight in Xgal buffer. AtMAP65-6 auto-activated *Lac Z* at some level.

Figure 5.8
AtMAP65-5 auto-activation test

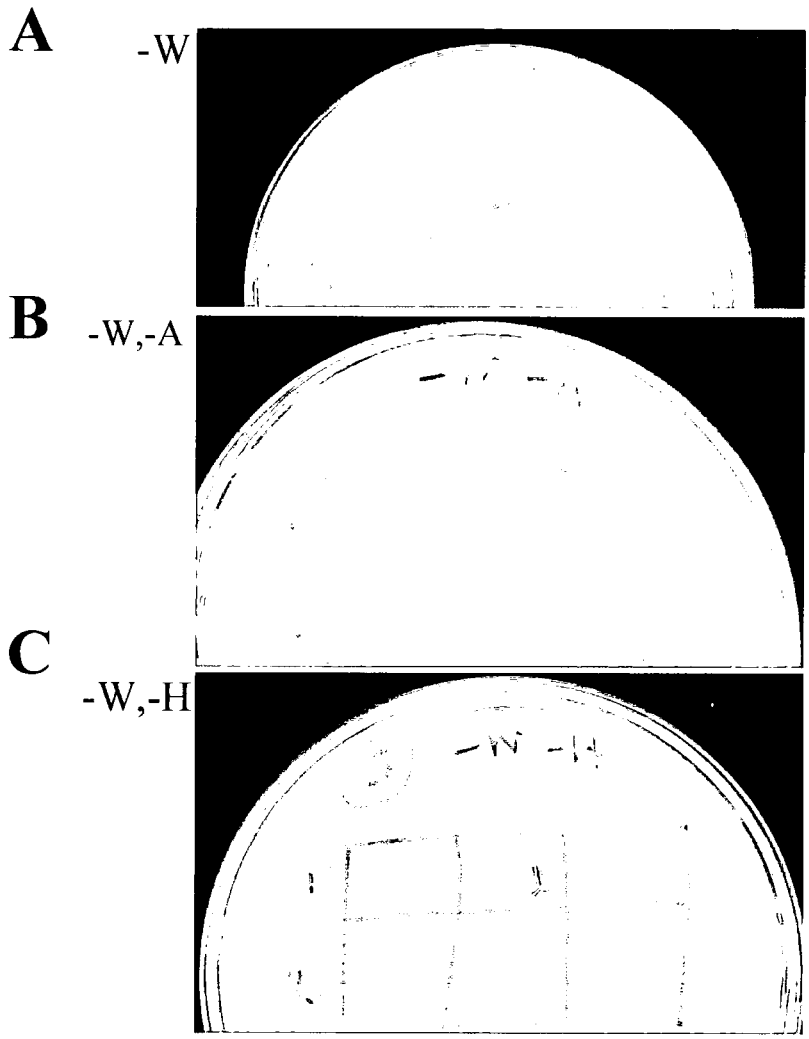

Figure 5.8:
A. AtMAP65-5 Trp-positive transformants containing the BD: AtMAP65-5 fusion plasmid, were selected in SD medium without Trp. **B.** AtMAP65-5: BD Trp-positives were plated onto SD medium plate in absence of Trp and Ade. AtMAP65-5 did not auto-activate the *Ade 2* reporter gene. **C.** AtMAP65-5: BD Trp-positives were plated onto SD medium plate in absence of Trp and His. AtMAP65-5 did not auto-activate the *His 3* reporter gene.

5.5.5 Mating between Y187 and AH109 yeast strains carrying the *GAL4* BD plasmids and *GAL4* AD plasmids respectively

Colonies from each construct were re-suspended in water and applied to a YPAD medium plate. First, the transformants of one type of yeast were applied and after their absorption, the transformants of the second yeast strain were added on the top of the dried spots of the previous strain. The plate was incubated at room temperature for two days for yeast mating to occur.

5.5.6 Diploid Selection

Mating yeast grew as colonies on YPDA medium plates and then were streaked to SD plates without Tryptophan and Leucine to get single colonies of diploid yeast. The plates were incubated at 30°C for three days.

5.5.7 Testing for protein-protein interactions monitoring *HIS3* and *ADE2* transctription

The colonies grown on SD plates minus Trp and Leu indicated diploid yeast with both the BD and AD plasmids. The colonies were then transferred onto reporter gene selective media to check for protein-protein interactions. The transformants were checked for activation of the Histidine and Adenine reporter genes on SD-Trp-Leu medium plates without also Histidine and Adenine hemisulfate respectively. The transformants were also transferred to SD -Trp- Leu plates for control.

5.5.8 Testing for protein-protein interactions monitoring *lacZ* reporter gene expression

The colonies grown on the diploid selection plate were transferred onto filter paper. The filter paper was frozen in liquid nitrogen. Another filter paper was soaked in Z buffer + X-Gal solution. The filter paper with the colonies attached was placed onto the filter paper soaked in Z buffer with X-Gal. The two filters were incubated at room temperature overnight. Blue colour developing indicated protein-protein interaction.

5.5.9 Assessing AtMAP65-1: AtMAP65-1 Interaction

Two AtMAP65-1 clones A and B each of them fused with the transcription Activation Domain, were mated with three AtMAP65-1 Binding Domain clones 1,2 and 3. The results of the Y2H interactions for AtMAP65-1 AD clone A are illustrated in Figure 5.9. The mating between AD clone A and BD clones 1, 2 and 3 was successful and diploid yeast colonies were selected on a SD plate without Tryptophan and Leucine. The diploid positives failed to activate the *Ade2*, *His 3* and *lacZ* reporter genes, indicating absence of interaction between AtMAP65-1 proteins. The AtMAP65-1 AD clone B gave the same results as AtMAP65-1 AD clone A in testing its possible interaction with AtMAP65-1 BD clones 1,2 and 3 (Figure 5.10).

5.5.10 Assessing AtMAP65-6: AtMAP65-6 Interaction

Three AtMAP65-6 Activating Domain clones were mated with three AtMAP65-6 Binding Domain clones. From the nine mating combinations, seven gave yeast positives at diploid selection plate (Figure 5.11). The AtMAP65-6 yeast positives were tested for activation of only *Ade2* and *LacZ* reporter genes as AtMAP65-6 auto-activate *His3* reporter gene (Figure 5.7). The diploid AtMAP65-6 positives activated the *Ade2* and *lacZ* reporter genes, indicating interaction between AtMAP65-6 proteins.

Figure 5.9
AtMAP65-1: AtMAP65-1 assay for AD clone A

A

AtMAP65-1 AD clone A (in AH109 strain) + AtMAP65-1 BD clone **1** (in Y187 strain)	AtMAP65-1 AD clone A (in AH109 strain) + AtMAP65-1 BD clone **2** (in Y187 strain)	AtMAP65-1 AD clone A (in AH109 strain) + AtMAP65-1 BD clone **3** (in Y187 strain)

B

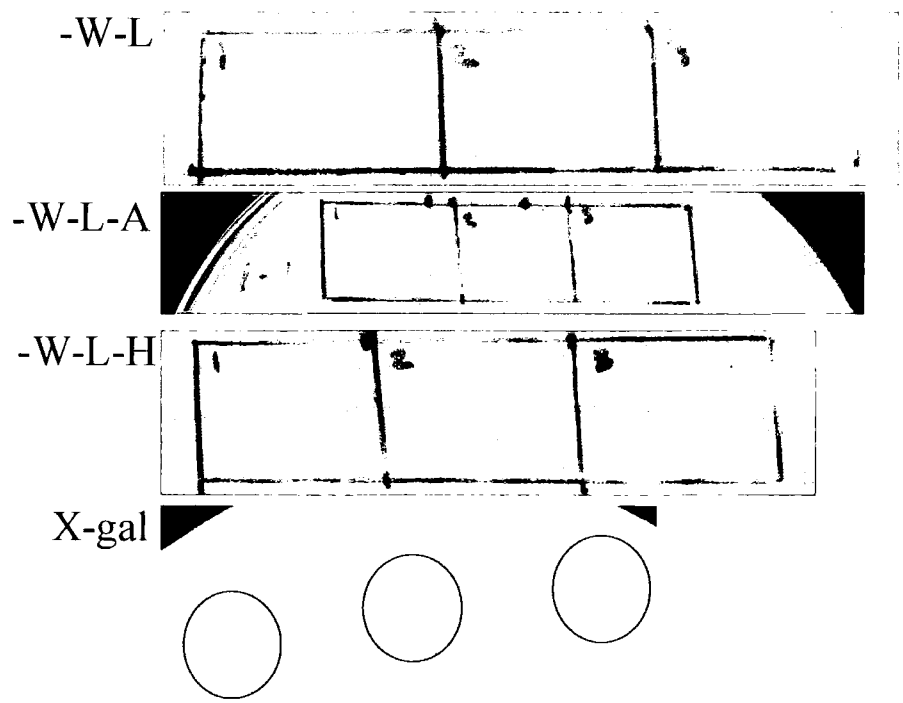

Figure 5.9:
A. The mating combinations. The AtMAP65-1 AD clone A was mated with three AtMAP65-1 BD clones 1, 2, 3.
B. Diploid yeast colonies were spotted onto a SD plate without Tryptophan and Leucine (-W, -L plate) in parallel to selection tests. The diploid positives failed to activate the *Ade2* (in -W, -L, -A plate), *His 3* (in -W, -L, -H plate), and *lacZ* reporter genes (by Xgal incubation), indicating absence of interaction between AtMAP65-1 with itself.

Figure 5.10
AtMAP65-1: AtMAP65-1 assay for AD clone B

A

AtMAP65-1 AD clone B (in AH109 strain) + AtMAP65-1 BD clone **1** (in Y187 strain)	AtMAP65-1 AD clone B (in AH109 strain) + AtMAP65-1 BD clone **2** (in Y187 strain)	AtMAP65-1 AD clone B (in AH109 strain) + AtMAP65-1 BD clone **3** (in Y187 strain)

B

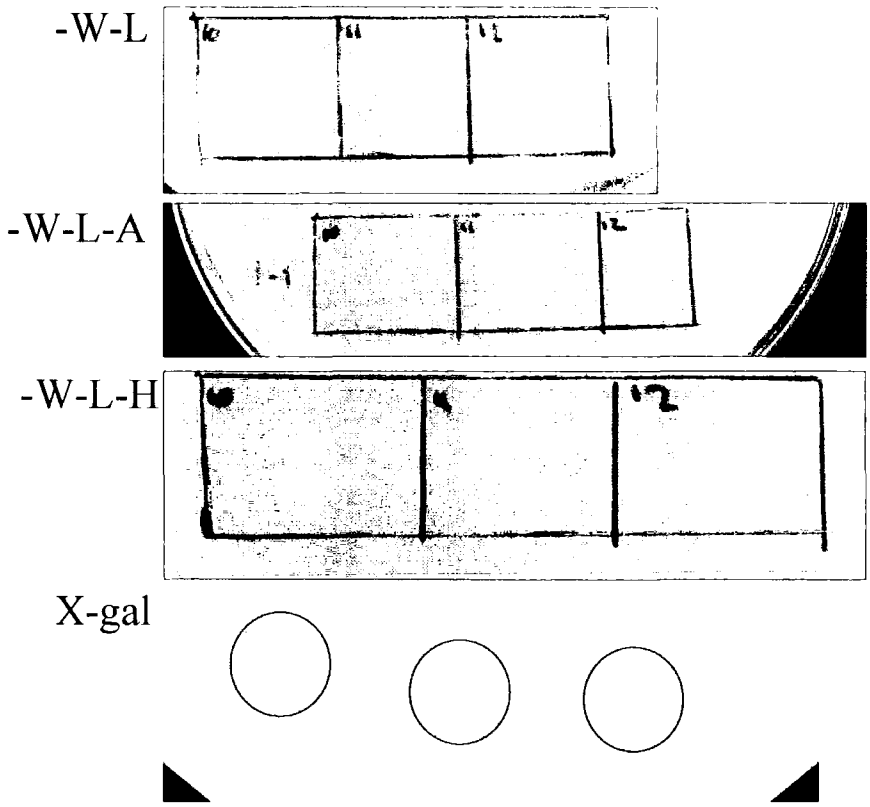

Figure 5.10:
A. The mating combinations. The AtMAP65-1 AD clone B was mated with three AtMAP65-1 BD clones 1, 2, 3.
B. The diploid yeast colonies were spotted onto a SD plate without Tryptophan and Leucine (-W, -L plate) in parallel to selection tests. The diploid positives failed to activate the *Ade2* (in -W, -L, -A plate), *His 3* (in -W, -L, -H plate), and *lacZ* reporter genes (by Xgal incubation), indicating absence of interaction between AtMAP65-1 with itself.

Figure 5.11
AtMAP65-6: AtMAP65-6 Y2H Interactions

A

AtMAP65-6 AD clone A (in AH109 strain) + AtMAP65-6 BD clone **A** (in Y187 strain)	AtMAP65-6 AD clone B (in AH109 strain) + AtMAP65-6 BD clone **A** (in Y187 strain)	AtMAP65-6 AD clone C (in AH109 strain) + AtMAP65-6 BD clone **A** (in Y187 strain)
AtMAP65-6 AD clone A (in AH109 strain) + AtMAP65-6 BD clone **B** (in Y187 strain)	AtMAP65-6 AD clone B (in AH109 strain) + AtMAP65-6 BD clone **B** (in Y187 strain)	AtMAP65-6 AD clone C (in AH109 strain) + AtMAP65-6 BD clone **B** (in Y187 strain)
AtMAP65-6 AD clone A (in AH109 strain) + AtMAP65-6 BD clone **C** (in Y187 strain)	AtMAP65-6 AD clone B (in AH109 strain) + AtMAP65-6 BD clone **C** (in Y187 strain)	AtMAP65-6 AD clone C (in AH109 strain) + AtMAP65-6 BD clone **C** (in Y187 strain)

B

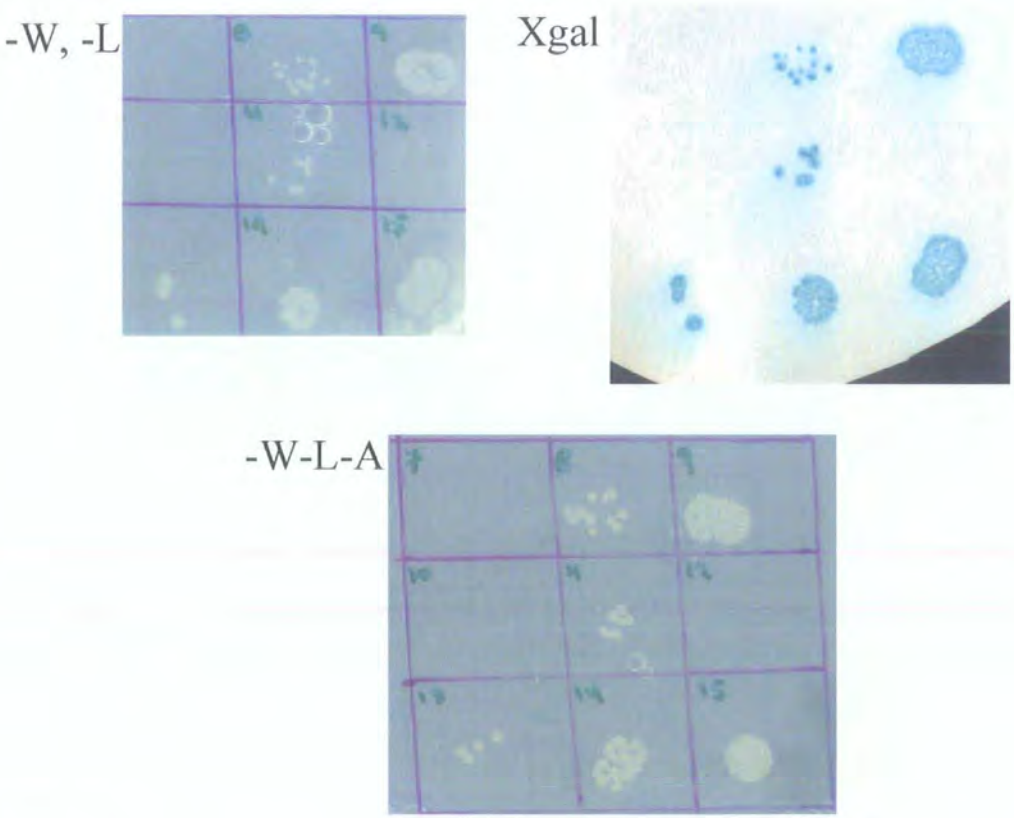

Figure 5.11:
A. The mating combinations of three AtMAP65-6 AD clones with three AtMAP65-6 BD clones.
B. From the nine mating combinations, seven gave positives at the -W. -L plate. The diploid AtMAP65-6 transformants activated the *Ade2* (-W, -L, -A) and *LacZ* (by Xgal incubation), indicating interaction between AtMAP65-6 and itself. The activation of *His3* reporter gene was not checked as AtMAP65-6 BD fusion protein auto-activate *His3* (see Figure 5.7).

5.5.11 Assessing AtMAP65-1: AtMAP65-6 Interaction

5.5.11.1 AtMAP65-1 AD: AtMAP65-6 BD

One AtMAP65-1 clone fused to the transcription Activation Domain was mated with three AtMAP65-6 DNA-Binding Domain clones. The selected diploid positives failed to activate the *ADE2* and *LacZ* reporter genes (Figure: 5.12). The activation of *HIS3* was not tested for the AtMAP65-1: AtMAP65-6 protein interaction as the AtMAP65-6: DNA-binding domain fusion protein auto-activate *HIS3*.

5.5.11.2 AtMAP65-1 BD: AtMAP65-6 AD

One AtMAP65-1 clone fused to the DNA- Binding Domain was mated with three clones of AtMAP65-6: fused to Activation Domain. The selected diploid positives failed to activate the *ADE2* and *LacZ* reporter genes but activated the *HIS3* reporter gene (Figure: 5.13). As *HIS3* transcription is often leaky and the experiment was performed in absence of 3-AT, *HIS3* activation is most probably an artefact and as the other two reporter genes were not activated, AtMAP65-1 does not seem to interact with AtMAP65-6 using the Y2H system.

5.5.12 Assessing AtMAP65-1: AtMAP65-5 Interaction

AtMAP65-1 protein was tested in the Y2H assay for interaction with AtMAP65-5. Two clones of AtMAP65-5 fused to Activation Domain were mated with three clones of AtMAP65-1 fused to DNA-Binding domain. The diploid yeast colonies were selected on a SD plate without Tryptophan and Leucine. The diploid positives failed to activate the *Ade2*, *His 3* and *lacZ* reporter genes, indicating absence of interaction between AtMAP65-1 and AtMAP65-5 (data not shown).

Figure 5.12
AtMAP65-1 AD: AtMAP65-6 BD

A

AtMAP65-1 AD clone A (in Y187 strain)	AtMAP65-1 AD clone A (in Y187 strain)	AtMAP65-1 AD clone A (in Y187 strain)
+	+	+
AtMAP65-6 BD clone A (in HF01 strain)	AtMAP65-6 BD clone B (in HF01 strain)	AtMAP65-6 BD clone C (in HF01 strain)

B

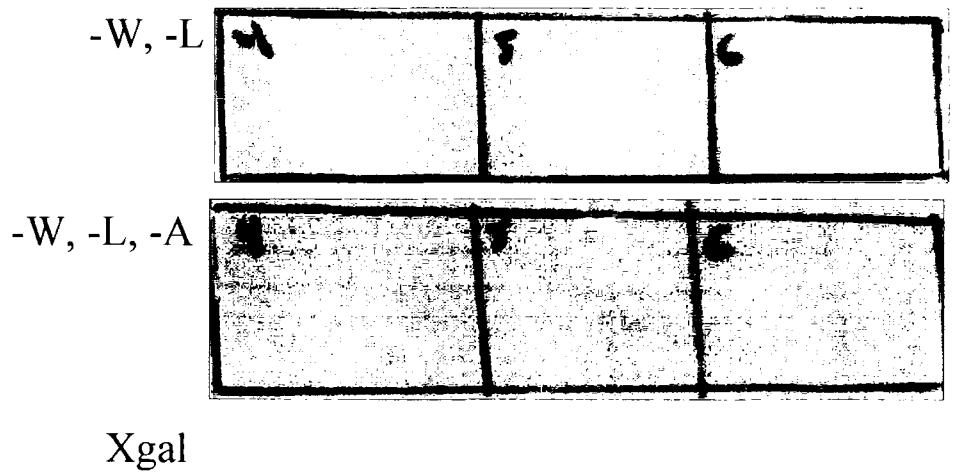

Figure 5.12:
A. The mating combinations. The AtMAP65-1 AD clone A was mated with three AtMAP65-6 BD clones.
B. The selected diploid positives (-W, -L plate) failed to activate the *ADE2* (-W, -L, A) and *LacZ* (by Xgal incubation). The activation of *HIS3* was not tested for the AtMAP65-1: AtMAP65-6 protein interaction as the AtMAP65-6: DNA-binding domain fusion protein auto-activate *HIS3*.

Figure 5.13
AtMAP65-1 BD: AtMAP65-6 AD

A

AtMAP65-1 BD clone A (in pGBT9 plasmid) + AtMAP65-6 AD clone A (in pGAD424 plasmid)	AtMAP65-1 BD clone A (in pGBT9 plasmid) + AtMAP65-6 AD clone B (in pGAD424 plasmid)	AtMAP65-1 BD clone A (in pGBT9 plasmid) + AtMAP65-6 AD clone C (in pGAD424 plasmid)

B

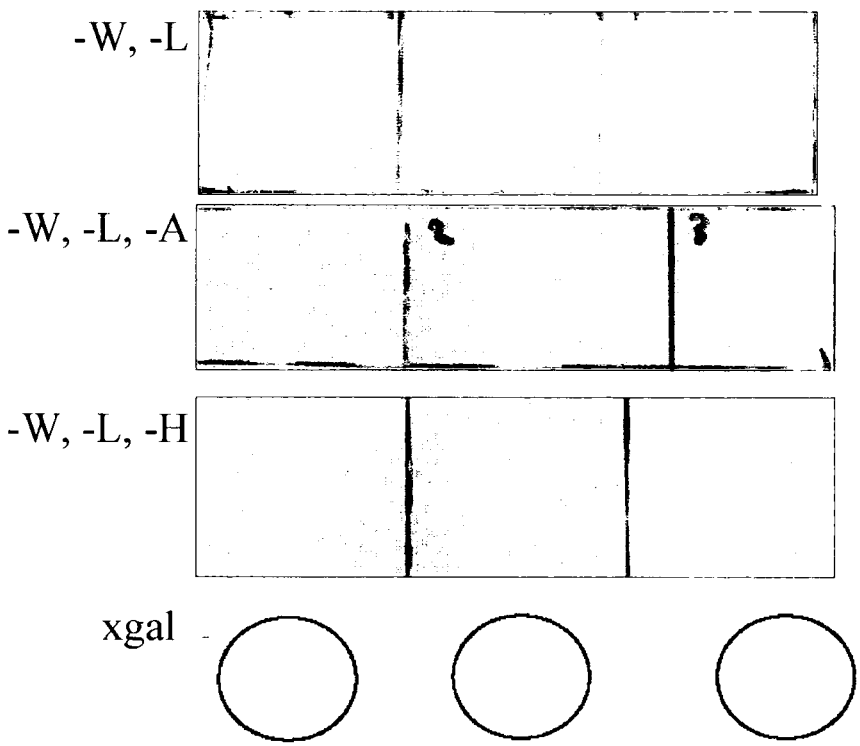

Figure 5.13:
A. The mating combinations of the AtMAP65-1 BD clone A and three AtMAP65-6 AD clones.
B. The diploid positives (-W, -L) failed to activate the *ADE2* (-W, -L, A) and *LacZ* (by Xgal incubation) but activated the *HIS3* reporter gene (-W, -L, -H). As *HIS3* transcription is often leaky and the experiment was performed in absence of 3-AT, *HIS3* activation is most probably an artefact and as the other two reporter genes were not activated, AtMAP65-1 does not seem to interact with AtMAP65-6.

5.5.13 Assessing AtMAP65-6: AtMAP65-5 Interaction

AtMAP65-6 was also tested in the Y2H system for interaction with AtMAP65-5. Two clones of AtMAP65-5 fused to Activation Domain were mated with three clones of AtMAP65-6 fused to DNA-Binding domain. The diploid yeast colonies were selected on a SD plate without Tryptophan and Leucine. The diploid positives failed to activate the *Ade2* and *lacZ* reporter genes, indicating absence of interaction between AtMAP65-6 and AtMAP65-5 (data not shown). The activation of *HIS3* was not tested for the AtMAP65-6 BD: AtMAP65-5 AD, protein: protein, interaction as the AtMAP65-6: DNA-binding domain fusion protein auto-activate *HIS3*.

Table 5.1: Results table of yeast 2 hybrid assays (+ represents interaction, - represents non-interaction)

	AtMAP65-1	**AtMAP65-5**	**AtMAP65-6**
AtMAP65-1	-	-	-
AtMAP65-5	-	Not examined	-
AtMAP65-6	-	-	+

5.6 Preparation of Antibody against AtMAP65-6

The recombinant AtMAP65-6 protein was used to immunise mice and was administrated in three fortnightly injections of 100 µg protein. Anti AtMAP65-6 antibody recognises three isoforms on western blot of 2D SDS-PAGE gel of total protein extract from *Arabidopsis* tissue culture cells (Figure 5.14, A). The specificity of the anti AtMAP65-6 antibody was examined by probing a two dimension SDS–PAGE gel with AtMAP65-1, AtMAP65-5 and AtMAP65-6 antibodies (Dr Fenyk and Dr Smertenko, figure 5.14, B).

Figure 5.14
AtMAP65-6 2D SDS-PAGE electrophoresis gel

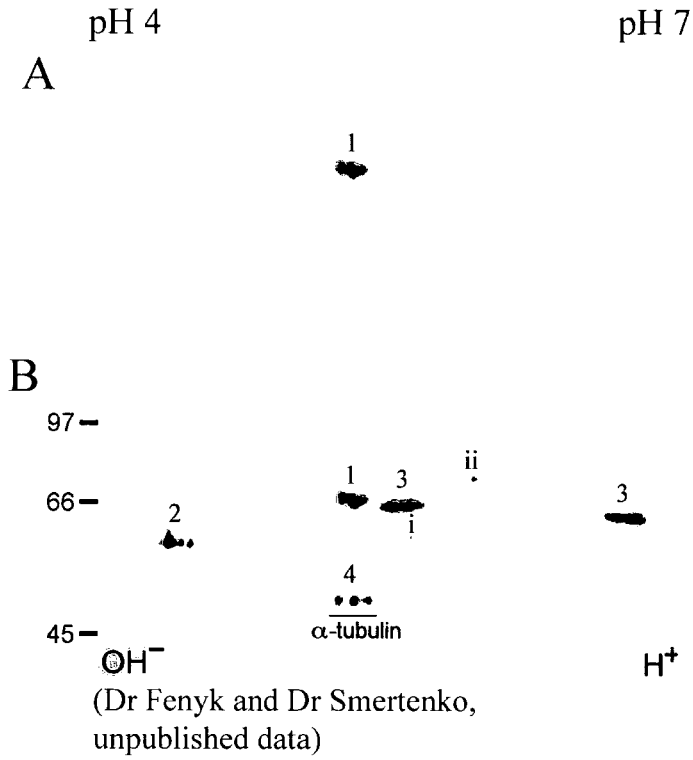

(Dr Fenyk and Dr Smertenko, unpublished data)

Figure 5.14:
A. Anti MAP65-6 antibody recognises three isoforms on a Western blot of 2D SDS-PAGE gel of total protein extract from *Arabidopsis* tissue culture cells.

B. The membrane was also blotted with AtMAP65-5 antibody which produced the spots under the number 2 and AtMAP65-1 antibody which produced the spots under the number 3. α-tubulin was blotted as a positive control and produced the spots under the number 4. The spots i and ii are artefacts most probably produced due to the secondary antibody during α- tubulin staining.

5.7 Localisation of AtMAP65-6 in the cell cycle

The localisation of AtMAP65-6 was studied through the cell cycle in *Arabidopsis* tissue culture cells at both interphase and mitotic stages (figure 5.15). During interphase, AtMAP65-6 exhibits a mainly cytoplasmic/vesicular staining (Figure 5.15,A-B). However, it decorates MTs in the preprophase band (Figure 5.15, C-F). AtMAP65-6 is present in the metaphase spindle but does not appear to decorate MTs (Figure 5.15, G-J). In anaphase spindle localises at the midzone and has a broader staining along phragmoplast MTs (Figure 5.15, K-N and O-R).

5.8 Summary

The full length of the coding sequence of *AtMAP65-6* was cloned by screening an *Arabidopsis* Col-0 cDNA library, constructed from mRNA isolated from seedlings and hupocotyls. Two truncated versions of *AtMAP65-3* were cloned. The C-terminal half of the protein was obtained by screening a floral cDNA library from *Arabidopsis* Col-0. The N-terminal half of AtMAP65-3 was obtained by RT-PCR. The template used for RT-PCR was RNA extracted from tissue culture cells. *AtMAP65-9* cloning was unsuccessful by screening cDNA libraries isolated from either seedlings/ hypocotyls or flowers, suggesting AtMAP65-9 is expressed at low levels in the tissues from which the libraries were made.

The coding sequence of *AtMAP65-6* was subcloned into the bacterial expression vector pET28α and the recombinant protein purified by virtue of a His-tag on the N-terminus. The interaction of recombinant AtMAP65-6 with MTs was investigated and a co-sedimentation assay showed that AtMAP65-6 binds to taxol stabilised brain MTs. The MT interaction properties of the MAP65 isoforms AtMAP65-6, -1 and –5 were assessed by turbidometric

Figure 5.15
AtMAP65-6 localisation through the cell cycle

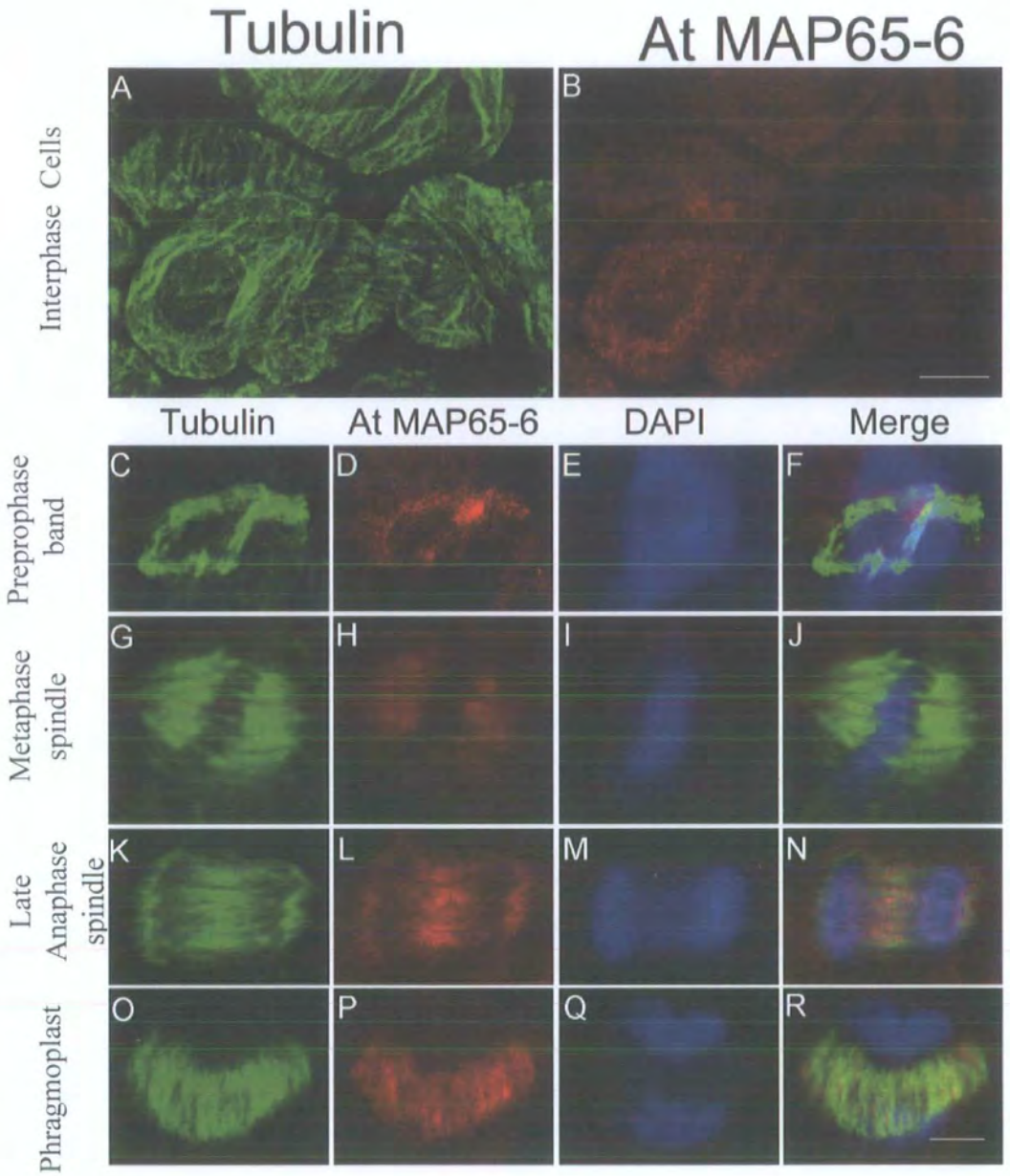

Figure 5.15:
Localisation of AtMAP65-6 at the different cell cycle stages.
Scale bars correspond to 10 μm.

assay. It was shown that all three MAP65 recombinant proteins increased the turbidity of MAP-free porcine brain tubulin *in vitro*.

AtMAP65-1, -5 and –6 were tested in a Yeast Two Hybrid system to investigate possible protein-protein interactions. AtMAP65-1 and AtMAP65-5 did not interact with themselves in this system. In contrast, the Yeast Two Hybrid results for AtMAP65-6 indicate the protein can make dimers. The possibility of AtMAP65-1, 5 and 6 to form heterodimers was also investigated by the Yeast Two Hybrid assay. However, all the AtMAP65-1::AtMAP65-6, AtMAP65-1::AtMAP65-5, AtMAP65-6::AtMAP65-5 combinations did not show interaction.

AtMAP65-6 localisation was examined in interphase and mitotic cells. AtMAP65-6 does not bind to interphase cortical MTs but it decorates the PPB. Its localisation in the metaphase spindle is very weak, however it has a preferentially midzone staining in the anaphase spindle. During cytokinesis AtMAP65-6 has a broad staining along phragmoplast MTs.

Chapter 6

General Discussion

6.1 Plant MAPs

Most of the plant MAPs studied until now have homologues in other eukaryotes (Spiral and MAP190 seem to be an exception), but not all animal MAPs are present in plants (Lloyd *et al.*, 2004). Plant cells lack the well-characterised animal MAPs tau, MAP1, MAP2 and MAP4. Plant MTs are structurally similar to their eukaryotic counterparts but they differ in their organisation and dynamics. For instance, plant cells have three distinct microtubule assemblies (the interphase cortical array, the preprophase band and the phragmoplast) and plant MTs are more dynamic remaining in the treadmilling state longer than animal MTs (Shaw *et al.*, 2003). In plants, as in animal cells, MAPs must be involved in regulating MT structure and function. Hence, studying plant MAPs would aid the understanding of the mechanisms which regulate plant MT organisation.

6.2 MAP65 proteins

MAP65 is a family of MT-associated proteins with molecular weight of approximately 65 kDa. Biochemically isolated MAP65 proteins from tobacco and carrot (Smertenko *et al.*, 2000; Chan *et al.*, 2002) and a recombinant MAP65 from *Arabidopsis*, AtMAP65-1, form 25-30 nm cross-bridges between brain/plant MTs (Smertenko *et al.*, 2004), similar to those observed in electron microscopic analysis of plant cells (Lancelle *et al.*, 1986). Hence, MAP65 proteins have been proposed to be involved in maintaining the parallelism between cortical MTs. However, the MAP65 immunofluoresence staining in all the MT arrays through the cell cycle (Jiang and Sonobe, 1993; Chan *et al.*, 1996; Smertenko *et al.*, 2000 and 2004) gave an indication that MAP65 proteins are also involved in MT organisation

beyond interphase. In addition, the *Arabidopsis ple* mutants caused by mutations in *AtMAP65-3/PLE* revealed an essential role of *AtMAP65-3/PLE* in cytokinesis (Muller *et al.*, 2002 and 2004). Interestingly, AtMAP65-3/PLE does not localise to the interphase cortical array, indicating that each MAP65 isoform could have distinct functions from each other in MT organisation through the cell cycle.

6.3 The MAP65 proteins in group I of the phylogenetic tree

Searching the *Arabidopsis* genome has revealed nine *AtMAP65* isoforms (Hussey *et al.*, 2002). Phylogenetic analysis using the Paup programme (version 4.0b10) has shown that the plant AtMAP65 isoforms from *Arabidopsis*, tobacco, carrot and rice can be classified into five groups. In group I there are three tobacco proteins (NtMAP65-1a,b and c; Smertenko *et al.*, 2000), two from *Arabidopsis* (AtMAP65-1 and -2; Smertenko *et al.*, 2004) and one from carrot (Chan *et al.*, 2003).

The properties of NtMAP65-1a have been described in Smertenko *et al.*, 2000. It was shown that NtMAP65-1a binds along MTs and increases the turbidity of tubulin solutions. The NtMAP65-1b (Wicker-Planquart *et al.*, 2004) and AtMAP65-1 (Smertenko *et al.*, 2004) isoforms have similar biochemical properties to NtMAP65-1a. They bind and bundle MTs but do not have effect on MT dynamics and do not promote tubulin polymerisation. Thermal dilution experiments showed that MAP65 proteins do not affect the stability of MTs. Another indication that MAP65 proteins do not effect MT dynamics *per se* comes from *in vivo* experiments. That is, in the re-assembly of MTs in BY-2 cells after cold-treatment, NtMAP65-1a associates with MTs after they are assembled. These data show that NtMAP65-1a is unlikely to be involved in the initial promotion of MT polymerisation.

The biochemical properties of the AtMAP65-2 isoform, which also belongs in group I of the MAP65 phylogenetic tree, has not yet been characterised. However, as it has high identity to the other MAP65 members of group I, it could have similar biochemical properties. (*AtMAP65-2* encodes a protein, which shows 70% similarity to tobacco NtMAP65-1a, 66% to NtMAP651b, 81% to AtMAP65-1 and 71% to DcMAP651.)

Immunofluoresence studies revealed that NtMAP65-1a binds to the cortical array but not necessarily just stabilised MTs as NtMAP65-1a does not bind all MTs that are stabilised by taxol. NtMAP65-1 antibody also stained the PPB and the line of MT overlap in the mitotic spindle and the cytokinetic phragmoplast (Smertenko *et al.*, 2000). AtMAP65-1 immunofluoresence studies revealed that AtMAP65-1 also localises to the MT arrays through the cell cycle (Smertenko *et al.*, 2004) and its localisation is similar to that described for NtMAP65-1a (Smertenko *et al.*, 2000). AtMAP65-1 located to cortical MTs, to the PPB and at the midzone of the anaphase spindle and the phragmoplast.

6.4 AtMAP65-6 in comparison with other MAPs

In this study, the full length coding sequence of the *AtMAP65-6* gene was obtained by screening an *Arabidopsis* cDNA library prepared from seedlings and hypocotyls. The open reading frame encodes a 608 amino acid protein of 69.4 kDa molecular weight and a pI of 6.87. The protein sequences of AtMAP65-1 and AtMAP65-6 show 44% identity with eachother. The AtMAP65-6 belongs to group III MAP65s on the phylogenetic tree together with AtMAP65-7 and three rice MAP65 isoforms.

The *AtMAP65-6* full length coding sequence was inserted into the expression vector pET28a and the recombinant AtMAP65-6 was expressed in bacteria and purified by virtue of a His-

tag on the N-termini. Using an high-speed MT co-sedimentation assay, it was shown that the recombinant AtMAP65-6 protein could bind MTs *in vitro*. The effect of AtMAP65-6 on MT polymerisation was assessed using a MT turbidometric assay. The effect of AtMAP65-1 and AtMAP65-5 proteins was also tested. All three proteins were found to increase MT turbidity. The increased turbidity indicates that the proteins are capable of promoting the assembly of tubulin and/or inducing MT bundling. Smertenko *et al.*, 2004 proved the increase in tubulin turbidity by AtMAP65-1 is due to MT bundling and that AtMAP65-1 does not induce MT polymerisation (Smertenko *et al.*, 2004). In addition, both AtMAP65-6 and AtMAP65-5 proteins were shown to bundle MTs in dark field microscopy analysis (Smertenko A., unpublished data).

An antibody was raised against AtMAP65-6 and its localisation to MT arrays was examined by immunofluoresence studies. AtMAP65-6 in contrast to AtMAP65-1 does not localise to cortical MTs. Other MAP65 homologues that do not bind the interphase cortical array are AtMAP65-3 and the human and yeast MAP65 isoforms PRC1 (Jiang *et al.*, 1998) and Ase1 (Pellman *et al.*, 1995) respectively. However, AtMAP65-6, like AtMAP65-1 and AtMAP65-3, decorates the PPB. The AtMAP65-6 immunofluoresence data in interphase cells suggest, that AtMAP65-6 is not involved in the organisation of the cortical array. Its presence in the PPB, together with other MAP65 isoforms, indicates that the presence of structural MAPs could be essential for the accumulation of MTs in the PPB, most possibly by creating MT bundles.

In the metaphase spindle, the AtMAP65-6 localisation is very weak and is similar in this respect to AtMAP65-1. However, AtMAP65-6 staining is observed on anaphase spindle, where it localises preferentially at the spindle midzone. The AtMAP65-1 and –3 stain

specifically the anaphase spindle midzone and remain at the overlapping zone of anti-parallel MTs at cytokinesis as indicated by their specific staining at the phragmoplast midzone. AtMAP65-6 is also present in the phragmoplast but in contrast of AtMAP65-1 and –3 is not only present in phragmoplast midzone but also stains the region of no overlapping MTs.

Plus-end motor proteins have seen shown to localise to the spindle and phragmoplast midzones. For example, in animal cells members of the BimC kinesin motors family have been shown to cross-link MTs within interpolar MT bundles (Sharp *et al.*, 2000). In plants, the BimC orthologues, TKRP125 (tobacco kinesin-related polypeptide of 125 kDa) and DcKRP120-2 could play a similar role in maintaining the integrity of the anaphase spindle midzone (Barroso *et al.*, 2000). Another plus end-directed kinesin related protein, AtPAKRP1 (*Arabidopsis thaliana* phragmoplast-associated kinesin-related protein 1) is possibly also involved in establishing the anaphase spindle and phragmoplast bipolar structures (Lee and Liu, 2000). This kinesin concentrates at the spindle midzone during late anaphase and at the phragmoplast mid-line during cytokinesis.

Another structural plant MAP that stains the areas of overlapping MTs in the anaphase spindle and the phragmoplast in *Arabidopsis* cells is MOR1/GEM1. MOR1/GEM1 is a member of the XMAP125 family of MAPs and members of this family have been shown to bind and bundle MTs raising the possibility that MOR1/GEM1 could stabilise the phragmoplast midzone by bundling MTs. MOR1/GEM1 in the *gem1* and *gem2* mutants is truncated at the C-terminus. It has been shown that this C-terminus contains a MT-binding domain. The lost microtubule-binding capability of the GEM1 and GEM2 proteins were proposed to cause the cytokinesis defects resulting in the aberrant cell plate formation

observed in the *gem1* and *gem2* phenotypes (Twell *et al.*, 2002). In addition, the MOR1/GEM 1 tobacco homologue was shown to participate in the formation of MT bundles in phragmoplasts (Yasuhara *et al.*, 2002). It was proposed NtMAP65-1 could interact with proteins capable of localising the MT plus ends and form complexes to stabilise the overlapping MT ends (Smertenko *et al.*, 2000). These interacting proteins could be other members of the MAP65 family, the tobacco homologue of MOR1/GEM1 or kinesin-like proteins.

The AtMAP65 isoforms 1 and 3 could stabilise the MTs in the anaphase spindle and phragmoplast midzone by creating bundles and/ or interacting with other structural MAPs, such as MOR1/GEM1 and EB1, and plus-end kinesins located at the spindle and phragmoplast midzone. It has been suggested that the absence of AtMAP65-3/PLE could abolish MT crosslinking between antiparallel MTs resulting in the two circlet of MT in the phragmoplast moving apart. A second scenario proposed was that in the absence of AtMAP65-3 the flux of tubulin through the plus ends (possibly through MOR1/GEM1 and EB1) is increased resulting in a broader phragmoplast midzone which is observed in the *ple* mutants (Muller *et al.*, 2004).

The AtMAP65 animal and yeast orthologues, PRC1 and Ase1, probably have an equivalent function to MAP65 proteins. However, AtMAP65-1 also stains the cortical MTs while Ase1, PRC and AtMAP65-3 localise specifically to the anaphase spindle and the phragmoplast midzone. However, PRC1 is able of binding interphase MTs on overexpression resulting in perinuclear MT staining (Jiang *et al.*, 1998). Ase1 bundles antiparallel MTs during anaphase, is required for spindle elongation and is immobile within the spindle midzone. A model proposed was that a network of immobile MAPs, like Ase1-related proteins, by

creating static cross-bridges within a highly organise MT lattice, could work in concert with highly dynamic motor proteins to maintain spindle bipolarity and promote spindle elongation (Schuyer *et al.*, 2003). PRC1 is present in the late anaphase spindle midzone and its complete suppression causes failure of MT interdigitation between the overlapping spindle MT sets (Mollinary *et al.*, 2002). Ase1, as PRC1, binds and bundles MTs *in vitro*, localises to the antiparallel spindle MTs during anaphase and its absence results in premature spindle collapse in mid anaphase (Schuyler *et al.*, 2003).

AtMAP65-6 is present in the anaphase spindle midzone but its localisation in the phragmoplast is broader from the MT overlapping region. Hence, AtMAP65-6 may be involved in other functions in the phragmoplast than the other MAP65 proteins that localise specifically to the phragmoplast midzone. Possibly, AtMAP65-6 could also interact with motor proteins in phragmoplast or bundling phragmoplast MTs to create the tracks for motor proteins transferring cargo to the phragmoplast midzone. An example of a motor protein proposed to transport Golgi-derived vesicles in the phragmoplast is the AtPAKRP2 (*Arabidopsis thaliana* phragmoplast associated kinesin related protein 1). This could explain why AtMAP65-6 staining is broad within the phragmoplast and not exclusive in the midzone.

6.5 AtMAP65 dimerisation

It has been proposed that MAP65 proteins are involved in the organisation of all MT arrays by bundling and crosslinking MTs (Jiang and Sonobe, 1993). AtMAP65-1, NtMAP65 1b and DcMAP65 62kDa were shown to bundle MTs (Smertenko *et al.*, 2004; Wicker-Planquart *et al.*, 2004; Chan *et al.*, 1999). In addition, using dark field microscopy it has been shown that AtMAP65-5 and AtMAP65-6 also bundle MTs (Smertenko A., unpublished data). The

putative interactions between AtMAP65-1, -5 and –6 were investigated in yeast two hybrid assays to test if the MAP65 proteins could form homodimers and/or heterodimers. Of all the combinations tested, AtMAP65-1::AtMAP65-1, AtMAP65-1::AtMAP65-6, AtMAP65-1::AtMAP65-5, AtMAP65-6:AtMAP65-6, AtMAP65-6::AtMAP65-5, only the AtMAP65-6 protein showed an interaction with itself. Further experiments could be done to confirm this interaction, such as western blot of the diploid yeast checking if expresses both BD:MAP65-6 and AD:MAP65-6.

The Y2H results for AtMAP65-1 come in contradiction with the Smertenko *et al.*, 2004, data which prove that AtMAP65-1 forms dimers (Smertenko *et al.*, 2004). A reason that AtMAP65-1 interaction with itself failed in Y2H system could be that in the Y2H vector systems the DNA-binding domain and the activation domain are fused to the N-terminal end of the test protein. When interactions occur at the N-terminus of the test protein(s), the presence of the DNA binding and/or activation domain could cause problems (Causier and Davies, 2002). Smertenko *et al.*, 2004, showed the AtMAP65-1 dimerisation domain is at the N-terminus of the protein and this is probably why MAP65-1 interactions failed in the Y2H.

The dimerisation region (aa 151-339) of AtMAP65-1 is conserved in AtMAP65-6 (Smertenko *et al.*, 2004). So why are AtMAP65-6 interactions successful in Y2H if a dimerisation domain is present at the N-terminus, as is the case for AtMAP65-1. A possible answer is that AtMAP65-6 is correctly folded in the yeast system: AtMAP65-1 and AtMAP65-6 have different sizes (65.8 kDa and 69.4 kDa respectively) and pIs. AtMAP65-1 has pI 4.72 and AtMAP65-6 6.87.

6.6 MT-binding domain

There are many indications that the MT binding region of MAP65 proteins lies in the C-teminus (Mollinari *et al.*, 2002; Schuyler *et al.*, 2003; Wicker-Planquart *et al.*, 2004; Smertenko *et al.*, 2004). The amino acid sequence alignment of Ase1, PRC1, NtMAP65-1a, 1b, 1c, *C.elegans* SPD-1, *S.pompe* CAC21482 and *D.melanogaster* AAK84936 and AAF47965 share a conserved motif (CM) of 16 amino acids located in the C-terminus (Mollinari *et al.*, 2002; Schuyler *et al.*, 2003). It has been shown that the CM is involved in PRC1 binding to MTs *in vitro* (Mollinari *et al.*, 2002) and is required for the proper localisation of Ase1 *in vivo* (Schuyler *et al.*, 2003). This motif is present in the *Arabidopsis*, tobacco and carrot MAP65s (see table 6.1). The motif consensus sequence is NLKRAEKARILVNKIP. Hence, the CM motif could also be important in the MT binding activity of the plant MAP65 proteins. However, an AtMAP65-1 fragment containing amino acids 340-494, which includes the CM motif, could not induce MT bundling alone, indicating that the dimerisation region is necessary to produce MT crossbridges (Smertenko *et al.*, 2004).

Table 6.1: The CM motif locates in a highly conserved region between Ase1, PRC1 and the MAP65 isoforms from *Arabidopsis*, tobacco and carrot.

AtMAP65-1	NLKRAEKARILVSKIP
AtMAP65-2	NLKRAEKARILVSKIT
AtMAP65-3	TLKRAEKARNLVTKLP
AtMAP65-4	TLKRAEKARLLVNKLP
AtMAP65-5	NLKRAEKARSLISKIP
AtMAP65-6	NLKRAERARVTINKIP
AtMAP65-7	NLKHAERARITVNKIP
AtMAP65-8	NLRRAERARITVSKIS
AtMAP65-9	ILKRAEKARALVNKLP
NtMAP65-1a	NLKRAEKARILVNKIP
NtMAP65-1b	NLKRAEKARILVNKIP
NtMAP65-1c	NLKRAEKARILVNKIP
DcMAP65-1	NLKRAEKARILVNKIP
PRC1 Hs	LLKEEKQRAKLQKMLP
Ase1	LLTEEKMRKRITRHFP

6.7 Cell cycle dependent regulation of the MAP65 proteins

The AtMAP65-6 protein does not bind cortical MTs, it locates to the PPB, and is present in the metaphase spindle but does not appear to decorate the MTs. AtMAP65-6 localises to the anaphase spindle and also to phragmoplast MTs. The switching on and off of AtMAP65-6 binding to MT arrays indicates a cell-cycle dependent regulation of AtMAP65-6 function. A cell cycle regulated expression of MAP65 isoforms has been shown. For example, the triplet of the carrot MAP65 proteins of 60, 62 and 68 kDa identified on blots of dividing populations is reduced to one band of 62 kDa when the cells enter interphase (Chan *et al.*, 2003). In addition, the AtMAP65-1 does not appear to bind MTs in the metaphase spindle, although its transcript has been proven to be present throughout the cell cycle (Smertenko *et al.*, 2004). Similarly, AtMAP65-3 does not localise to the metaphase spindle MTs although it is present in the cell at these stages, as suggested by the cytoplasmic staining of the anti-AtMAP65-3 antibody (Muller *et al.*, 2003).

The MAP65 binding activity could be under post-translation modification control. For the search of putative phosphorylation sites in AtMAP65 seguences the Prosite (http://npsa-pbil.ibcp.fr/cgi-bin/npsa_automat.pl?page=npsa_prosite.html) and NetPhos (www.cbs.dtu.dk/services/NetPhos) prediction servers were used in addition to search in previous publications. The search revealed the AtMAP65 proteins have highly conserved phosphorylation sites for various protein kinases: cyclin dependent protein kinases (cdk), cAMP- and cGMP-dependent protein kinase, protein kinase A, protein kinase C, casein kinase I, casein kinase II and tyrosine kinase.

PRC1, the human ortholoque of AtMAP65, has two cdk phosphorylation sites. It was shown that mutations of the two cdk phosphorylated threonine residues to alanine suppresses PRC1 bundling activity (Mollinari *et al.*, 2002). However, a phosphorylation mimic where the cdk sites were mutated to glutamic acid, bound and bundled MTs in the same manner as the non-phosphorylated protein (Mollinari *et al.*, 2002). These data indicate that phosphorylation on its own cannot effect the MT binding properties of MAPs. The same conclusion arose from the observation that phosporylated AtMAP65-1 was still capable of binding MTs and increasing the turbidity of tubulin solutions (Smertenko *et al.*, 2004).

Other post-translation modifications could be involved, together with phosphorylation, in regulating MAP65 function. A search in Prosite web site revealed that there are three other post-translation modification possibilities for AtMAP65: N-glycosylation, N-myristoylation and C-terminal amidation sites. C-terminal amidation has not yet been shown to occur in plants. The most abundant of these sites in the AtMAP65 protein sequences was the N-glycosylation. Some N-glycosylation sites were conserved between the AtMAP65 members.

The anti-AtMAP65-6 antibody recognises three isoforms on a western blot of 2D SDS-PAGE gel of a total protein extract from *Arabidopsis* tissue culture cells. These AtMAP65-6 isoforms could be the result of post-translation modifications. Based on the motifs found in the bioinformatics search, the three isoforms could be products of AtMAP65 phosphorylation, glycosylation or myristoylation.

Interestingly, in the AtMAP65-9 protein sequence a consensus EF-hand calcium-binding domain was found. This domain is present in many calcium binding proteins (Kawasaki *et al.*, 1995). This observation indicates that AtMAP65-9 expression and function could be regulated through calcium. It has been reported that the calcium/ calmodulin complex affects MT stability via MAPs (Cyr *et al*, 1991a). In addition, calcium, through calmodulin, has been shown to inhibit the interaction of KCBP (kinesin-like calmodulin binding protein) with MTs and the extent of inhibition was found to be dependent on calcium and calmodulin concentration (Deavours *et al*, 1998). Vos *et al.*, 2000, also proposed that ER systems close to the spindle and phragmoplast could regulate calcium concentrations in a cell cycle dependent manner, affecting KCBP activity. The AtMAP65-9 immunofluoresence studies show that AtMAP65-9 does not localise to MT arrays in tissue culture cells (Smertenko A., unpublished data). The presence of an EF-hand motif in its sequence may indicates that AtMAP65-9 functions in a cell type specific manner: for example it may only bind to MTs in the cells where it is expressed (see below, table 6.2) and in a calcium/calmodulin dependent manner.

6.8 Expression programme of all the *AtMAP65* genes

The expression of the nine *AtMAP65* genes was analysed by transforming *Arabidopsis* with an *AtMAP65::GUS* reporter gene transcriptional fusion construct for each of the AtMAP65 members. The abundance of each of the *AtMAP65* transcripts in various *Arabidopsis* tissues was examined by Reverse Transcription-PCR (RT-PCR). The results of the two techniques were compared for each of the *AtMAP65* genes. The staining of the GUS in *Arabidopsis* organs for each *AtMAP65* in most cases was confirmed by the RT-PCR results. The advantage of GUS fusions was that the pattern of each *AtMAP65* expression could be observed for individual tissues. On the other hand, RT-PCR proved to be more sensitive in the case of *AtMAP65-4* and *AtMAP65-8* and revealed presence of their transcripts in cDNA prepared from flowers, where GUS staining was not observed.

AtMAP65-1 expression is the most abundant amongst the *AtMAP65* isoforms in the *Arabidopsis* plant. AtMAP65-1::GUS staining was observed throughout the *Arabidopsis* seedlings and flowers; anthers, sepals and pollen were the only exception. *AtMAP65-2* was also expressed in all *Arabidopsis* organs but not in all the tissues. The expression programme observed for all *AtMAP65s* is summarised in table 6.2.

Table 6.2: GUS staining for each *AtMAP65::GUS* fusion. (+) represents that staining found in all the lines examined; (-) represents no staining; when the staining pattern between lines was different the percentage of lines where staining was observed is noted.

	AtMAP 65-1	AtMAP 65-2	AtMAP 65-3	AtMAP 65-4	AtMAP 65-5	AtMAP 65-6	AtMAP 65-7	AtMAP 65-8	AtMAP 65-9
leaves	++	++	++	-	-	++	-	-	-
Vascular tissue	++	++	++	++	+	++	-	++	-
Root tips	++	++	++	+	+	++	-	++	+
Root tip initiation point	++	++	++	+	+	++	-	++	+
Petals	++	-	-	-	-	-	-	-	-
Sepals	-	60%	-	-	-	++	-	-	-
Stamens	++	++	14%	-	-	++	-	-	-
Ovule/ embryo	++	++	++	-	-	++	-	-	-
pollen	-	-	71%	-	29%	-	-	-	++

6.8.1 AtMAP65 proteins in plant tissues

After embryo development, plant growth is concentrated in meristems, which are localised regions of perpetuating embryonic tissues (Raven *et al.*, 1992). The meristems located at root and shoot tips are called apical meristems and are involved in the extension of the plant body. The apical meristems of the shoot are usually protected by leaves and the whole complex forms a bud. Certain meristematic cells are able to divide repeatedly. After each division, one of the sister cells remains in the meristem while the other becomes a new body cell. The cells that remain in the meristem are called initials, while their sister cells are called derivatives. Usually, the derivatives divide one or more times before they begin to differentiate into specific types of cells.

Growth of the body of the plant involves both cell division and cell enlargement. The overall size of cells increases from younger to older meristematic tissues. Cell differentiation often begins while the cell is still enlarging. At maturity, when differentiation is complete, some cell types have live protoplasts and others dead (eg tracheid elements). In roots the region of cell elongation is followed by the region of maturation. The principal plant tissues, which are established by early meristematic activity and influenced by both cell division and cell enlargment, are organised into three tissue systems in all plant parts; into the ground tissue system or cortex, the vascular tissue system and the dermal tissue system.

All *AtMAP65* genes, except *AtMAP65-7* that is not expressed in any tissue examined, are expressed in the meristematic region of the main root tip of the seedling, indicating the involvement of AtMAP65s in cell division. Root hairs are produced in the root maturation region. Lateral roots arise in the pericycle, which surrounds the vascular tissues and is composed of parenchyma cells. The pericycle divisions occur some distance beyond the

region of elongation. The derivatives of both the pericycle and the endodermis contribute to the development of the new root. The *AtMAP65s* are present in lateral root initiation points and are probably involved in organising the MT mitotic and cytokinetic arrays in the pericycle cell divisions. The young root, early in its formation, develops a root cap and an apical meristem and the AtMAP65 genes are also expressed there.

In addition, the *AtMAP65* genes are expressed in the vascular tissues. The vascular system has two major components, the xylem through which water moves upward through the plant body and the phloem, through which food manufactured in photosynthetic regions is transported to non-photosynthetic parts of the plant. The xylem consists of tracheids, vessel members, parenchyma cells and schlerenchyma cells. The phloem consists of sieve cells, albuminous cells, parenchyma and schlerenchyma cells. Of the above cell types the parenchyma cells and sieve cells are living at maturity and the schlerenchyma cells can be alive or dead. *AtMAP65* genes are probably organising the MT arrays in the living cells of the vascular system. Parenchyma cells are also capable of cell division and this could explain the presence in vascular tissues of AtMAP65-6 and –3, which localise in mitotic MT arrays.

Initially the vascular systems of the parent and lateral roots are not connected to each other but are joined later, when derivatives of parenchyma cells differentiate into xylem and phloem. Cell differentiation involves cell division and cell enlargement. AtMAP65 proteins are expressed in lateral root vascular tissues and hence are good candidates for regulating these processes by organising the MT arrays. The vascular root system of leaves and flower is a continuation of the stem vascular tissue.

AtMAP65-1 is expressed throughout the seedling ground tissue system, where the plant cells are in a state of elongation and/or maturation. More specifically, it is expressed in the cortex

of roots, in the elongating hypocotyl that pushes up the cotyledons during germination and seedling development, and in leaves. The leaf cortex is called mesophyll and is composed of parenchyma cells. In addition to *AtMAP65-1*, AtMAP65-*2*, *-3* and *–6* are expressed in mesophyll cells. AtMAP65-2 is also present in the hypocotyl cortex. *AtMAP65-1* is also expressed in the epidermal cells, where it could bundle and crosslink MTs.

6.8.2 Correlation of GUS staining with AtMAP65 immunolocalisation

The *AtMAP65s* expression in meristematic regions indicates that AtMAP65 proteins are involved in cell division. Confirmation of this indication comes from AtMAP65-1, -3 and –6 immunolocalisation to MT mitotic arrays and from the cytokinetic defects in the *pleiade* mutants. The *AtMAP65-3::GUS* fusion express in the organs where the *ple* mutant phenotype is observed. The recessive mutations in the *AtMAP65-3/PLE* gene resulted in defective root cells and embryos: both tissues that stained for GUS.

AtMAP65-1 is expressed throughout the seedling even in cell tissues where only cortical MTs are present, such as the epidermis. This observation, in conjunction with the AtMAP65-1 immunolocalisation to MT cortical arrays and its ability to crosslink MTs, indicates that AtMAP65-1 could be involved in mediating MT cortical array changes during root cell elongation and also in maintaining the MTs parallelism when cells have matured. AtMAP65-2 could have the same function, as it is present in elongating hypocotyl cortex and immunolocalisation studies show it locates to both cortical and mitotic arrays.

AtMAP65-5 also localises to MTs in both cortical and mitotic arrays. AtMAP65-5 has been shown to bind and bundle MTs *in vitro* (Smertenko *et al.*, unpublished data) and it has been also shown to increase the turbidity of a tubulin solution (Chapter 5). The antibody against

AtMAP65-5 identifies specifically the AtMAP65 protein on a western blot of tissue culture cells. However, the anti-AtMAP65-5 antibody fails to identify the AtMAP65-5 protein on western blots of any other *Arabidopsis* tissues. RT-PCR of cDNA prepared from various *Arabidopsis* tissues using specific primers against AtMAP65-5 showed that the *AtMAP65-5* transcript is present in *Arabidopsis* tissues. The weak staining for GUS in AtMAP65-5::GUS plants indicates that the *AtMAP65-5* promoter has low activity. The function of AtMAP65-7 and AtMAP65-8 is still unknown and immunofluorescence data show both proteins do not bind MTs in tissue culture cells, but the cytoplasm is stained with the respective antibodies.

The specific expression of *AtMAP65-9* in pollen and the weak GUS staining in root tips and root tip initiation points, indicates low expression in *Arabidopsis* seedlings and flowers and could explain why its cDNA could not be cloned by screening the cDNA libraries used. In addition, RT-PCR using *AtMAP65-9* primers with 10ng cDNA from various *Arabidopsis* tissues did not give any signal, indicating also low abundance of *AtMAP65-9* transcripts in *Arabidopsis* tissues. The anti-AtMAP65-9 antibody has a cytoplasmic staining and does not stain the MT arrays through the cell cycle. (The immunolocalisation of AtMAP65-2, -4, -5, -7, -8 and –9 was investigated by Dr Smertenko A., unpublished data.)

6.9 Hormonal regulation of gene expression

Promoters contain regions that play a regulatory role in gene transcription. Proteins called regulatory transcription factors can bind directly to regions within promoters, activating or repressing gene transcription. Transcription factors can be activated by hormones and/or environmental influences such as light, temperature and environmental stress. By controlling gene expression hormonal and environmental stimuli are known to be involved in cell differentiation. Several plant genes that are either activated or repressed in such ways have been found and sequence motifs involved in environmental and hormonal regulation of their

expression have been identified. A search in the *AtMAP65* promoter regions using the Plant *cis*-acting regulatory element (*PlantCare*) web site (http://oberon.fvms.ugent.be:8080/PlantCARE/) revealed several regulatory elements (motifs) involved in environmental or hormonal responsiveness.

The hormonal motifs found include auxin, gibberellin, abs*cis*ic acid, ethylene, methyl jasmonate (MeJa), and salicylic acid responsive elements. Auxin stimulates cell division and elongation (Friml J., 2003), however it is also involved in apical dominance (inhibitory effect of the growth of the lateral buds by the apical bud). This is an example where the same hormone can cause different responses in different tissues or in the same tissue at different times. Gibberelin, like auxin, enhances the rate of cell division and elongation (Thomas and Sun, 2004). Abs*cis*ic acid has a negative effect on cell division and elongation and it has been shown to induce and stimulate apoptosis (Vanyushin B.F., 2004). Ethylene is commonly synthesised in response to stress, especially in tissues undergoing senescence or ripening and it is also involved in disease resistance (Conrath *et al.*, 2002). Ethylene's effect on cell division and cell expansion could be either positive or negative. MeJa has several effects on plants like promoting leaf senescence and ethylene formation. Plants that are attacked by insects or that are mechanically damaged produce higher levels of MeJa in the wounded parts of the plant and MeJa role seems to be involved in the production of defence proteins (Conrath *et al.*, 2002). Salicylic acid also seems to promote disease resistance and ethylene synthesis and has a positive effect on plant growth. However, large concentrations of salicylic acid have a negative effect (see www.alumni.ca/~mcleo31/).

Plants have the ability to respond to environmental changes and adjust their pattern of growth respectively. Environmental stimuli usually influences hormone activity and modifies plant behaviour. For example, both phototropism and gravitropism involve auxin

function under the influence of light. Moreover, photoperiodism controls the onset of flowering in many plants and gibberellin has been described as a flowering stimulator. Also, calcium has been proposed to be involved in the gravitropic response of both shoots and roots, through the calcium-binding protein calmodulin. In addition light, drought and temperature stress can alter plant growth, as the plant adjusts its rate of growth in order to survive (Raven, *et al.*, 1992).

Several environmental motifs have been found in *AtMAP65* promoters, including light and temperature responsive elements (Arguello-Astorga *et al.*, 1996; Dunn *et al.*, 1998). Some motifs involved in wound and elicitor responsiveness (Pastuglia *et al.*, 1997) were also found. The parenchyma cells play an important role in regeneration and wound healing because of their capability to divide. Interestingly, all *AtMAP65s* are expressed in vascular tissues where parenchyma cells are located and all *AtMAP65s* have a wound regulatory motif in their promoters. The categories of hormone and environmental regulatory motifs found in *AtMAP65s* by searching in *PlantCare* web site are summarised in table 6.3.

Some other motifs found are cell cycle (Chaboute *et al.*, 2000) and endosperm expression regulatory elements (Washida *et al.*, 1999). Also, *AtMAP65-1* and *–9* contain a regulatory element involved in circadian rhythm control (Piechulla *et al.*, 1998). The circadian rhythms are cycles of activity that occur in an organism under constant environmental conditions. For example, the expression of light-harvesting complexes is under the control of the circadian clock.

Table 6.3: Summary of all the categories of motifs found in *PlantCare* web site. (+ represents presence of motif and – absence)

	AtMAP 65-1	AtMAP 65-2	AtMAP 65-3	AtMAP 65-4	AtMAP 65-5	AtMAP 65-6	AtMAP 65-7	AtMAP 65-8	AtMAP 65-9
TATA CAAT	+	+	+	+	+	+	+	+	+
light	+	+	+	+	+	+	+	+	+
gibberellin acid	+	+	+	+	+	+	+	+	+
abs*cis*ic acid	-	+	-	+	+	-	+	-	+
auxin	+	-	-	+	-	-	+	+	-
MeJa	-	-	-	+	+	+	+	+	-
ethylene	+	+	+	+	+	+	+	+	+
salicylic acid	+	+	+	+	-	+	-	+	+
elicitor	+	+	+	+	+	-	+	-	-
heat stress	-	+	+	+	+	+	+	+	+
low temp.	+	-	+	-	+	-	-	-	-
wound	+	+	+	+	+	+	+	+	+
drought	+	-	-	-	-	-	-	-	-
cell cycle	-	-	+	+	-	-	-	+	+
endosperm expression	+	+	-	+	+	+	+	+	-
Circadian control	+	-	-	-	-	-	-	-	+

To further analyse the motifs listed in table 6.3, future experiments will involve placing *Arabidopsis* plants transformed with the *AtMAP65::GUS* fusions under hormonal and environmental stress treatments and investigating alternations in *AtMAP65* expression. It will be interesting to investigate if *AtMAP65-7*, that as both *GUS* fusion and RT-PCR data indicate does not express under normal conditions, will be expressed under treatment with gibberellin acid, abs*cis*ic acid, auxin, MeJa and ethylene to whose regulatory motifs are present in its promoter. Some environmental stress regulation motifs have also been identified in its promoter region in addition to elicitor and wound responsive elements.

6.10 Conclusion

The search in the *Arabidopsis* genome has revealed the presence of nine MAP65 isoforms. In this study the expression programme of each of the *AtMAP65* genes was analysed by both *GUS* fusion constructs and RT-PCR. The data showed the *AtMAP65* isoforms were differentially expressed in *Arabidopsis* tissues. For example, *AtMAP65-9* proved to be pollen specific. *AtMAP65* expression could be regulated by hormonal or environmental stimuli and/ or post translation modifications, as indicated from the consensus motifs present in *AtMAP65* promoters and in AtMAP65 proteins. In this study AtMAP65-6, as AtMAP65-1 and AtMAP65-5, were shown to bind MTs and to increase the turbidity of MT solutions. The immunolocalisation studies reveal that AtMAP65-6 comparing to other AtMAP65 proteins, binds MTs differentially in some MT arrays and similarly to other MT arrays. For example, AtMAP65-6 does not bind the interphase cortical MTs in contrast to AtMAP65-1. However, both proteins show a similar localisation in the anaphase spindle. AtMAP65 proteins could have co-operative function at certain stages but they also express at different levels, at different times and in different tissues, depending on the way the plant cell uses the microtubule associated proteins in order to respond immediately to developmental needs and environmental stimuli.

Appendix A

Accession number of AtMAP65, NtMAP65 and DcMAP65 proteins

AtMAP65-1	AA042887
AtMAP65-2	AAM62657
AtMAP65-3	BAB08676
AtMAP65-4	CAB82688
AtMAP65-5	AAC67346
AtMAP65-6	AAD21782
AtMAP65-7	AAF79248
AtMAP65-8	AAG26947
AtMAP65-9	NP_201031
NtMAP65-1a	CAC17794
NtMAP65-1b	CAC17795
NtMAP65-1c	CAC17796
DcMAP65-1	CAD58680

Appendix B

The TATA-box and CAAT-box motifs in *AtMAP65* promoters

	TATA-box		CAAT-box	
	motifs number	**matrix identity (%)**	**motifs number**	**matrix identity (%)**
AtMAP65-1	14	85.7-100	13	85.7-100
AtMAP65-2	11	87.2-100	14	85.7-100
AtMAP65-3	24	85.7-100	27	85.7-100
AtMAP65-4	13	87.2-100	31	100
AtMAP65-5	20	85.7-100	30	85.7-100
AtMAP65-6	23	85.7-100	15	85.7-100
AtMAP65-7	10	87.6-100	15	85.7-100
AtMAP65-8	14	85.7-100	17	85.7-100
AtMAP65-9	11	86.9-100	20	88.6-100

Appendix C

Light responsive elements in *AtMAP65* promoters

	ACE		GT1-motif		AE box	
	motif number	matrix identity (%)	motif number	matrix identity (%)	motif number	matrix identity (%)
AtMAP65-1	-	-	-	-	2	85.2-88.6
AtMAP65-2	2	90.1-97.5	2	85.7	2	92.8-95.8
AtMAP65-3	-	-	-	-	2	85.2
AtMAP65-4	1	86.4	-	-	2	85.2
AtMAP65-5	1	88.9	2	85.7	2	85.2
AtMAP65-6	2	89.5-93.8	-	-	-	-
AtMAP65-7	2	93.5	2	85.7	2	85.2
AtMAP65-8	1	86.7	3	85.7-100	-	-
AtMAP65-9	1	85.2	1	85.7	1	85.2

	ATC-motif		ATCC-motif		CATT-motif	
	motif number	matrix identity (%)	motif number	matrix identity (%)	motif number	matrix identity (%)
AtMAP65-1	1	88.9	1	87.5	1	100
AtMAP65-2	-	-	-	-	-	-
AtMAP65-3	-	-	-	-	-	-
AtMAP65-4	-	-	1	87.5	-	-
AtMAP65-5	4	87.5-90.3	-	-	-	-
AtMAP65-6	-	-	-	-	-	-
AtMAP65-7	1	87.5	-	-	-	-
AtMAP65-8	1	87.5	-	-	1	100
AtMAP65-9	4	87.5-95.1	1	100	-	-

	ATCT		GA-motif		GAG motif	
	motif number	matrix identity (%)	motif number	matrix identity (%)	motif number	matrix identity (%)
AtMAP65-1	-	-	3	87.5-100	1	87.5
AtMAP65-2	-	-	3	87.5	5	87.5
AtMAP65-3	1	90	3	87.5	1	100
AtMAP65-4	-	-	1	87.5	8	87.5-100
AtMAP65-5	-	-	6	87.5	5	87.5
AtMAP65-6	-	-	1	87.5	2	87.5
AtMAP65-7	-	-	2	87.5	5	87.5
AtMAP65-8	1	90	2	87.5	5	87.5-100
AtMAP65-9	-	-	5	87.5	18	87.5

	GATA motif		I-box		LAMP-element	
	motif number	matrix identity (%)	motif number	matrix identity (%)	motif number	matrix identity (%)
AtMAP65-1	1	87.5	15	88.3-100	1	87.5
AtMAP65-2	-	-	12	85-98	1	100
AtMAP65-3	1	87.5	24	86.3-95.1	2	85.4-95.8
AtMAP65-4	1	87.5	22	85-100	4	85.4-100
AtMAP65-5	1	87.5	27	85-100	-	-
AtMAP65-6	1	87.5	27	88.3-100	2	85.4-87.5
AtMAP65-7	1	87.5	15	86.3-97.2	-	-
AtMAP65-8	-	-	32	88.3-100	2	87.5
AtMAP65-9	1	87.5	29	86.3-100	-	-

	TCCC-motif		TCT-motif		Chs-CMA1a	
	motif number	matrix identity (%)	motif number	matrix identity (%)	motif number	matrix identity (%)
AtMAP65-1	2	85.7	-	-	1	87.5
AtMAP65-2	6	85.7	1	100	-	-
AtMAP65-3	5	85.7	-	-	1	87.5
AtMAP65-4	6	85.7	-	-	3	87.5
AtMAP65-5	1	85.7	1	100	3	87.5
AtMAP65-6	3	85.7	-	-	1	87.5
AtMAP65-7	5	85.7	-	-	1	87.5
AtMAP65-8	4	85.7-100	-	-	-	-
AtMAP65-9	2	85.7-100	1	100	1	87.5

	AAGAA		AAAC-motif		G-box	
	motif number	matrix identity (%)	motif number	matrix identity (%)	motif number	matrix identity (%)
AtMAP65-1	5	90.3-93.5	1	100	-	-
AtMAP65-2	5	90.3-96.8	-	-	11	85.4-100
AtMAP65-3	2	87	-	-	2	90.4-92.2
AtMAP65-4	1	87	-	-	2	90.7-100
AtMAP65-5	4	87-93.5	1	87.8	3	87.4-90.7
AtMAP65-6	4	87-93.5	-	-	4	87.4-95.2
AtMAP65-7	3	87	-	-	3	88.1-100
AtMAP65-8	7	87-93.5	-	-	3	88.9-93.7
AtMAP65-9	6	87-96.8	-	-	3	85.5-100

	Chs-CMA2a		sbp-CMA1a	
	motifs number	**matrix identity (%)**	**motifs number**	**matrix identity (%)**
AtMAP65-1	1	87.5	-	-
AtMAP65-2	-	-	-	-
AtMAP65-3	-	-	1	86.7
AtMAP65-4	-	-	-	-
AtMAP65-5	-	-	-	-
AtMAP65-6	-	-	-	-
AtMAP65-7	1	87.5	-	-
AtMAP65-8	-	-	-	-
AtMAP65-9	-	-	-	-

Appendix D
Hormone responsive elements in *AtMAP65* promoters

	Abox		P-box		TATC-box	
	motif number	matrix identity (%)	motif number	matrix identity (%)	motif number	matrix identity (%)
AtMAP65-1	-	-	2	85.7	1	85.7
AtMAP65-2	-	-	4	85.7-100	1	85.7
AtMAP65-3	-	-	1	85.7	-	-
AtMAP65-4	-	-	1	85.7	-	-
AtMAP65-5	2	85.1-87.3	-	-	1	85.7
AtMAP65-6	2	85.1-87.3	1	85.7	1	85.7
AtMAP65-7	1	85.1	1	85.7	-	-
AtMAP65-8	-	-	2	85.7	2	85.7-100
AtMAP65-9	1	95.8	-	-	1	85.7

	ABRE		AuxRR-core		TGA-element	
	motif number	matrix identity (%)	motif number	matrix identity (%)	motif number	matrix identity (%)
AtMAP65-1	-	-	1	85.7	-	-
AtMAP65-2	6	85.1-100	-	-	-	-
AtMAP65-3	-	-	-	-	-	-
AtMAP65-4	1	85.1	1	85.7	-	-
AtMAP65-5	1	87.6	-	-	-	-
AtMAP65-6	-	-	-	-	-	-
AtMAP65-7	2	87.5-94.9	1	85.7	-	-
AtMAP65-8	-	-	1	85.7	1	100
AtMAP65-9	2	87.5-100	-	-	-	-

	CGTCA-motif		TGACG-motif		ERE	
	motif number	matrix identity (%)	motif number	matrix identity (%)	motif number	matrix identity (%)
AtMAP65-1	-	-	-	-	2	87.5-100
AtMAP65-2	-	-	-	-	2	87.5-100
AtMAP65-3	-	-	-	-	2	87.5
AtMAP65-4	2	100	1	100	4	87.5-100
AtMAP65-5	1	100	-	-	3	87.5
AtMAP65-6	1	100	-	-	2	87.5
AtMAP65-7	2	100	-	-	2	87.5-100
AtMAP65-8	1	100	-	-	3	87.5
AtMAP65-9	-	-	-	-	3	87.5-100

Appendix E

Elicitor responsive elements in *AtMAP65* promoters

	Box-W1		ELI-box 3	
	motifs number	matrix identity (%)	motifs number	matrix identity (%)
AtMAP65-1	-	-	1	88.9
AtMAP65-2	-	-	1	88.9
AtMAP65-3	-	-	1	100
AtMAP65-4	-	-	1	88.9
AtMAP65-5	-	-	1	88.9
AtMAP65-6	-	-	-	-
AtMAP65-7	1	100	-	-
AtMAP65-8	-	-	-	-
AtMAP65-9	-	-	-	-

Appendix F
Salicylic acid responsive elements in *AtMAP65* promoters

	EIRE		TCA-element	
	motifs number	**matrix identity (%)**	**motifs number**	**matrix identity (%)**
AtMAP65-1	1	85.7	5	85.6-91.4
AtMAP65-2	1	85.7		
AtMAP65-3	2	85.7		
AtMAP65-4	-	-	2	85.6-88.5
AtMAP65-5	-	-		
AtMAP65-6	2	85.7	2	85.6-91.4
AtMAP65-7	-	-		
AtMAP65-8	1	85.7	1	88.5
AtMAP65-9	-	-	1	85.6

Appendix G
Environmental stress motifs in *AtMAP65* promoters

	HSE		LTR		WUN-motif	
	motif number	matrix identity (%)	motif number	matrix identity (%)	motif number	matrix identity (%)
AtMAP65-1	-	-	1	100	3	89.5
AtMAP65-2	2	87.5-92.3	-	-	7	89.5-94.8
AtMAP65-3	3	87.4-97.8	1	100	3	94.8
AtMAP65-4	3	85.3-94.7	-	-	4	89.5-94.8
AtMAP65-5	4	87.4-90	1	100	4	89.5-94.8
AtMAP65-6	2	85.3-87.4	-	-	4	89.5-94.8
AtMAP65-7	2	87.4-93.2	-	-	4	89.5-94.8
AtMAP65-8	1	88.8	-	-	2	94.8
AtMAP65-9	2	93.4-94.7	-	-	4	89.5-100

	MBS		MRE	
	motif number	matrix identity (%)	motif number	matrix identity (%)
AtMAP65-1	1	100	1	85.7
AtMAP65-2			1	85.7
AtMAP65-3			3	85.7
AtMAP65-4			-	-
AtMAP65-5			5	85.7
AtMAP65-6			-	-
AtMAP65-7			-	-
AtMAP65-8			3	85.7
AtMAP65-9			1	85.7

Appendix H

Cell cycle regulating elements in *AtMAP65* promoters

	E2Fa		E2Fb	
	motifs number	**matrix identity (%)**	**motifs number**	**matrix identity (%)**
AtMAP65-1	-	-	-	-
AtMAP65-2	-	-	-	-
AtMAP65-3	1	87.5	-	-
AtMAP65-4	1	87.5	-	-
AtMAP65-5	-	-	-	-
AtMAP65-6	-	-	-	-
AtMAP65-7	-	-	-	-
AtMAP65-8	-	-	1	87.5
AtMAP65-9	1	87.5	1	87.5

Appendix I

Endosperm expression regulated motifs in *AtMAP65* promoters

	GCN4_motif		Skn_motif	
	motif number	matrix identity (%)	motif number	matrix identity (%)
AtMAP65-1	3	86.9-93.4	2	100
AtMAP65-2	2	90.1	-	-
AtMAP65-3	-	-	-	-
AtMAP65-4	2	90.1-100	2	100
AtMAP65-5	-	-	3	100
AtMAP65-6	2	86.9	1	100
AtMAP65-7	1	86.9	1	100
AtMAP65-8	1	93.4	3	100
AtMAP65-9	-	-	-	-

Promoter region for the *AtMAP65-1::Gus* construct

ATMAP65-1 Promoter

CAGCAATTCTCCGGAGAACTTTTCATCTATTTTGAATGCAAGACTATAATGTCA
AAGATGTCAATGTTTGATCTGAGTATTTCAAACTAACATTTATAATTCCAGTTTA
CTTTACAGATATCTGATAATTAATTTATGTGTTTATCTTTGTCAACTGTATTTGAT
ATTAATTCAAAATTCCTAAAAATGTTTTATCCTCTTGCATCATACTTTAAAACAA
ATATGAATTTCGACTGATAGCGATAATAAATATTTACAATATTGTAATTGGATA
ATATAAATCTAGTGATATATATATGGTCCCTAAAACTGGTAAACAACTTTGGTTG
TACAGTAAATGTTTTTGTAGAGCTACACATAACATTTACAGCTTTAAATAACCAT
AAGTTAACTTGGTTAGAGAAAACCAAAAACTATTGAAGCATCCGAGAATCTAGT
GGTGAATTATAACGATATTATTGCACTGTAAGAAAAGAAAAGAATTAAAAAAA
AAAGTAAATAACTTGTGTGGTCAAACAAGCAAAGAACCAAGTCAAGGAAGAGT
AAAAAAAGACACAAGTCTGTCTGTGAACAGTGTCATGTTTGTAAATAAAGAAGG
AAACTAGGGGTGAATATTTTGCTAATTGGAGTTTCCATCGTACTTCAAAAAAAA
AAAACGATTGGGTCCCACACTCACCTCTCCGTCTCTTCCACCTCCATAGATAGAT
TTTTTTTCCTTAAGCAAAAAAGATTTTATCTCACTCTCAATAGTGTTAGTATTGTC
ACAGAGAAAGCTTCAGATCTAGAAGAAGAAGCAGAGTTCATAAAGAGAAACCC
ATTTTAAACCCTAGAAATCAAGTGTCAATCTCGGTAATTAAAGTTTATGCCTTTT
TCTTTTTACTGTTAGATTTGATCAATTTTGAGGTCTTTAGTCTGTTCCTTAAGGTT
TTGATTGCTTTGGTTTTATCACCAATGCTGTCCGATTCTCTTGAAGATTCTGTTTT
TTTTGTTCAGAGATCTGCTTCTTCTTTCTGTGCTTTGCTTCTGCTTGATCGGATTTT
AGATATTGCATTCTGAGCTTGACTTCGTTTGCTTTCTGTGTCATGGTGAAAAAAG
GGTTTTTGAGCTTCGTAAGTCAAATTTTTTGTTTCCGATTCTTAATGTTTGGTCTG
TGGAGTTTAATCTTTGGTTAGAGTGATTAAGAGGTTTTAGATTCCGAAAAAGATT
CTAACTTTGATTGAGAATATCTACAGCGTATCTTTTGGTGTTTGTTATTGTTTTTT
CTTAGCTTCGTAATCTTAGTTCAGTTTCATTATAATCTGATGCAGAAGAAAGATC
TGATTTGAGCGATGTATAATTCATTCTTAGTTTAGTTTTAGTCTCTCATTGGTTTT
TGTTTTTGATATTTTCTGC**AGGAAACCTTCTGATTCCGC***AACAATG*

Forward primer (*M-1,5*): AA GGATCC CAGCAATTCTCCGGAGAACT (*Bam*HI site underlined)
Reverse primer (*M-1,3*) : TT GGATCC GCGGAATCAGAAGGTTTCCT (*Bam*HI site underlined)

The putative *AtMAP65-1* promoter sequence. The forward and reverse primers used for the promoter amplification by PCR using genomic DNA as template are in bold. Italicise sequence, not cloned but inserted to show relative position of the translation start codon (underlined).

Promoter region for the *AtMAP65-2::Gus* construct

AtMAP65-2 Promoter

CATTGTATAGATACCTCGCTTGATCGCCTGCGGTGTCGAATGCGAGCTGTTGG
AGAGCTAGGAGTATAATTGTAATCCCTTGGTGAATTAGGAATGTTGGGATAATG
GTTATCTCTCTGGTTATTAGTATTCATTCGAGACGTTGGTGTAGTAGGGTAACTA
GTATCCCTTAGCTTTCTAATCCGTGGAGAATTTGGACTGAGATCTTTCTCCATTG
CCATTGAGATCCCTAGGAAATGCTCTCAGTTCCTGGATTGAGTTCTTGAAATTCA
GTTAATCATGATGATCTGGGTTTCTTTATACATCCGAGGAAATGAATTTGGGGTT
GATCTATAATTTCAAAATGTCAACCATAACTCGAGCTTATACACGTCTTAATGAA
ACACACACATTGATATCTGATGAGAGATTACTTGTGTAACAAGCATATAATAGA
GGATTTAGATTTGAATGTGTAAGCCTAGAAATCTAAATGATTCATCAAAGCAAA
ACGTGATGATTCACATACAAAGGATAAATTTCATAAGTGAACATTGCAACAAAA
TGGGATCATGACAAGTAGAAAAAAGAGAATGAACTTACATTAACGAAAACGTG
GTGGGATGATGGTGATTGAAAATGCGAAACCCTAATTAATGAAAAGAAACGTG
AAGAAAGAAACTCAAAAGGTGAGGGAAGAAGGAGGAGGAGGAAGGTGGTGGA
TGAGCACTTAGCGGTGAGGTTTCATCAAATCATCGGAAGAGAGAACCAATAAAC
TATTCATGTCGCTGCTTCATGTTTAAACCCGGAATGAGTGACACGTGTTGTCTTG
ATCTGTTTGGGCTGGGTCAGATATTTAAGCCCATTAAGGAAAGCCTTTTAACTAT
TCAGACATGAGCATGAGGAGTCAACGAGGTCTGTGAGATCAGTGGTCAAATCA
GTAAATAACGCGAAAAGACAGGGTCTCTCACCTTTTTGCTGTTGTTTTTTCCTCA
TTAATTATTGAGTTCCGTAAAATGGGTCCCACTTTTCCCATTTCCCAACCTCCAT
AACCAAAGTTGGAGATTTCTCTGTTTCCTATGCTCTCTCTCTCTCTTACTCTCACA
GTGACTATTCGTCGCTTCAGATCTAAAAGAGAGGAAGATAAACCATTTGGATTC
AATATCGATTAAGGTAAGAAAGCCATCTTCTACTTGTTGGATTCGATTAGTTTCA
TTTCAGCTCATTGCCTCTTTACTTCTTCAATGTTGATTTCTTGCTTTGGCTTTGGTT
TTATCACCAATGCTGTTTGATTTCTTTGAAGTTCCTTTCGAGCTTTTCTTGAGCTT
AGTTTCACATTCTTAGCTTCACTAAGTTCTTTGATGTGTTTTTGTTCCCAAGTTCA
AAATGTTGTTTCTGATTCAATTTGGTTTTCTAAAAAAGATTGCAACTTTGGTTTCT
TTTAGTGTATAGTTAGTTTGGATCTTCACTAAATATGTTCGTTGTTTCTACTTTTG
TAG**GAAACCTTTTGACTTCACAAG***AATG*

Forward primer (*M-2,5*): AA AAGCTT CATTGTATAGATACCTCGCTT (*Hin*dIII site underlined)
Reverse primer (*M-2,3*) : TT GGATCC CTTGTGAAGTCAAAAGGTTTC (*Bam*HI site underlined)

The putative *AtMAP65-2* promoter sequence. The forward and reverse primers used for the promoter amplification by PCR using genomic DNA as template are in bold. Italicise sequence, not cloned but inserted to show relative position of the translation start codon (underlined).

Promoter region for the *AtMAP65-3::Gus* construct

AtMAP65-3 Promoter

CGCCATTGATTCACAGTGAAACAAGCAAGAAGGGGAAAGTAGAATACTGAGT
TGTTTTGTAATAAGTAACTTTCCAAAAGTAATTTAATTTACTCATACAAAAATAG
AAAATTTGGACGATATAGCAGTTTTCCAGTTTTTCAAAAACAGTAATTAAACAT
ATGACCAAAGGAAAACCAAACTGCCCATAGTAATTGTTGCCTGGGTGAATTGGA
TTAGACAGAACTTGATGGGACGGTGTTGCAGTAAATTTTTAAAAAGTTACACTC
TTCCCTACACAAAACCGCGGCAACATATAACTTTCCCCTCAAAAAAAGAAAAAA
TGATTACTCAAATGTTCGACACTTGGGATTAACAGATGTAGTGATGTATTATAA
AGCAGATTATTTTTTTTTTTAGTATAAATCAATCACATATGTCGTTTGTAAAATT
ATAAAGCAGATTATTTATAAACCTGATGTAGTGATGAGATCAAATACTTCTTCAT
TCGACAGAGATGTTTATGCTTATTGAATCATCGGATTATGAGATTCTTTAAATGT
TTCAAATTATTTGTAACTCGCCAGACGCATACTGTATATCAGTATATGCATGTAA
TTTCCCGTCTATGTTCGATTATTTTGGTTCAATATATAATCATACCACGCCCAAA
CCAAAACTAAATTTTGAATTCCATATATTAAACCAATTAGTTACCTTAATCATAT
ATTCTTCATCAGAGTAGGATTTCTAAGGAACATTTAATCATATATTAAACCGATC
TCTGTTAGATTGACTACACTGATCATTGACAAACAGAGAAAGTCTGGTTTGGAT
AGGCGTGGTATGACTACTACACCGAAATAATTAAAATTAGACCGGTTCAGACCA
AAGATCGGCTTAACACAATTTATGCTAGATTTTCGTTTTTGAGATCTGAACCGTT
CATAGGGAATAAGAATATCTCAACGGTAGGGATCTATTCGTCTACTGTAAGCAC
GATGCACTGGATTCTAAAGCCTTAAATCAGATTTTTGAAATTCAAAAGTTCGAA
AAAGTAAAAGCCCAAATATACAAAAATAGTTTGAGCTGGTTGGGGTAACGGAC
GAAATTCCCAATCTCATCATCATCATCTCTCTCTCTACCCAAAACCTTTTACTTCT
TCGTAACGGCTCTATTTCTCTTCTCTCTTCTCTCCACACACAGAAATATCTCGATC
TAGGTTTCTAAAATTGGATTCTCTATCTCAAACGCTAATCGAAGAGTTTTCTCTG
AATCGTTTTCTTAAATCTAATCTCGCGAAGTTTCAGTGACAGATTCAATCAAACT
TCAAAATCATCATCAGTTCTGGAAAATTTACGAGAAATCTCCCGTTTCAGGCAA
GTTTTCTCTCAATTTGTTGCTTCGCAATGTCAAAATCAATCATATAGGCTTTCAA
TCAATTGCTTCGAATTTAGCTTCTAATTTTGAGAATGACATAGTTAGGGTTTCGT
TTTCCCT**GTTACAGGCTTAAGCATTTCG***AAATG*

Forward primer (*M-3,5*): AA AAGCTT CGCCATTGATTCACAGTGAAA (*Hin*dIII site underlined)
Reverse primer (*M-3,3*) : TT GGATCC CGAAATGCTTAAGCCTGTAAC (*Bam*HI site underlined)

The putative *AtMAP65-3* promoter sequence. The forward and reverse primers used for the promoter amplification by PCR using genomic DNA as template are in bold. Italicise sequence, not cloned but inserted to show relative position of the translation start codon (underlined).

Promoter region for the *AtMAP65-4::Gus* construct

AtMAP65-4 Promoter

TGAAGAGAGAGAGAGAGAGATTTTTCAGAAATTTTTATGTGTTTTGTTTTAATT
AATTTTATTTTCAATTATTAAGAAGCTCAGGCTTTGCTCTGACAATACTGATAAG
TCCCAGGGGTATTATTTTATTTGTCTCTCTCCACATATTTTAGTTTTGTTTTAATTT
CTCTTTCCAGAAGAAATTCAGACAAGCCTTTGGTTCGTCGTCCTTTATCCACTTC
CCCAATCATCATTAACAATTTGGTTTGTACGATTACAATAGATGTGGTGATTACT
AATGATTTTACTTACGTTAACCAATATGACCATTGTCCATATGTATAGACTATAG
ACGACCAAAACCAATGTTAAATTTATATTAGTTTTGTGATTGAACTATAGACTAT
ATACTATGTCCACTTCTGTTTTTTACATAATGTTTGAAAGGTTTTTAAAACTTTTT
ACACAAAATTTAAGTTTATTTGAACGATGTATCATACTTTTATGATTACAGATAA
CGCATGTTTTAACTTTAAAAGCAATGTAGTTACTGTAACATTTTGTTGACGAAAT
AAAAGTTCTAAACAAAATATTAGAGTCTCATTCTATAGTTGCAAAAATAGTTAT
TTTGCGTTTATTCTTTACATTCTCTTATCATATGCATGGATCAGTTCAAAGTCAAA
GAGTATATCAATGTCAAAGTAATAGAGATGTCAATGCAGTCATTATCCATTTTTT
TTTTTTTTTACTATGAAAAGATTTTGATAATTTATGTGCTTTTTGAAAATATATT
TTAGTTGTTTAACTGGCCTACATTTTTATTTTATTTAAGATATCATTATGGAGCCA
ATTATATTTCAAAAAAATCCATTTCGAAATTCAAGGCTTTATTGCTTACTAAATC
TGGTCCGTCAAATAAAAAGGAGAAAAGCAAAAAACGGAAAGAGGAATTTAATA
CAACGGCTCAGATGATTCCACGTCAAAATAAATCGTGAGACTCGGATCGTAACG
GACCCTCCTCCCGCTCCTTGTTCAAATTTCAATTTCACATCCGTTATACTCACAA
CACTTATAAACCCTAATTTTGCTCTCTCTCTCTCTTTGATCAATTCTTCACAACAT
CTTCTTCTTGGCGCTGATCCTCAAACCAGGTAGTTTCTAATTTCTCGCTCTTTTCT
CTTGTAGATGTTAAAAATCTTCTTGAACTTTTCATGAGTCATCGCGATTTTGTAA
TTTAACTCTGCGGAGAAAACAGAGAAAATTCTGTATCTGTTTCCGAATAATTTG
GTATTTGTGTAATCGAGAATCGGAGTCACGAAACAATTCAGCTGTGATGTTGAT
AATTGGGAATTTTTGTCTATAGGTTTTAATCACCATGATACGGAATTCAACAGAG
CAGTTTTCGAGAATCGAGACTACATGTGGATTGTTACTTCGCCAATTGCAGGTCT
TTTCTTGAAGAAGATTCACATCCTCGTTTTCTTTGTTTATGTTCAAAATTGGGAAT
TTACCAATTTTGA**TGATATCAGGAAATATGGAATG***AAATG*

Forward primer (*M-4,5*): AA AAGCTT TGAAGAGAGAGAGAGAGAGA (*Hin*dIII site underlined)
Reverse primer (*M-4,3*) : TT GGATCC CATTCCATATTTCCTGATATCA (*Bam*HI site underlined)

The putative *AtMAP65-4* promoter sequence. The forward and reverse primers used for the promoter amplification by PCR using genomic DNA as template are in bold. Italicise sequence, not cloned but inserted to show relative position of the translation start codon (underlined).

Promoter region for the *AtMAP65-5::Gus* construct

AtMAP65-5 Promoter:

CAGATCGTCCGTTCAATAGTACTCTATCCAAATTCCAAACAAAGAGAATTACA
AAAAAATGCATACTTTGAGAAAGATTCAAACTTGCATGTCATAACACAAGCAAG
GAAAAAAACTTACTGATTGGCCTCTTCAAAGGCAGGTGGTGGAGTCTCTTCATT
GTTGTAGTGAGAGACCAAAGTGTCGAAACAGTAAACAGCCATTTCTCTGTTCGC
CGACACCATTGTTGCTTGGAAGAGAAAACCGCAGATGAAAAAAATCCAAATCA
GCAAGTAATGTGAACCTGAAATAACCAAAATCTTATTATGCTTAAAGATACCAA
TTTTTAAACACTACCCAGAGCTAACTATCAAAAGCAACTCACAAATCAAATACC
AAATTGCACAAATTAGCAATAGCAGTATTAAAAAATTGAAAATTTAAAAGTGAT
GGTCGACGATGAAATTGATCTGTTTTGTATGAGGGAAATCAATTAAAAGCTATG
GAATCTAAAAGGTTATGGATCGATCTGTAAGAAGAATTGAAACCAAAAGAGAT
AAGGAATCAATTCTGAGTATGAAGAAGAGAGCGGAGAAAACCTGAGTAAAGAA
AAGCGCAGGAGAGAGAGGAAGATGAAGTGTCTACGTTTTGTTTAATTAGAAAG
CTTTGTTGTTTGATTTTGAGTATAGTGACAATTTTTTTGGTTGGTGTGTCTTTTTC
TCAAAGACTTGTTAACTAAACTATTTGAGCTTAGTTACGGCCGCAGCTAGTTTTT
GTTTTTCTCCATATATATACGTCGCCCTAGCTAGATTCACAAAAGATTTTTTTTTT
TCAAAAGTAAAAAAAGATTAAAAGTTATCGATTCAATATATAATCTATTTAACTT
ATTTTGTCATTACTACATAATAGAAAAATTAAATTATTCGATATAAACTAATTTT
ATAAGACAAGAATTTTGGTCTTACCGAAAAAAAAAGACAAGATATAAACATATT
TATCAAAACATATATGGTTATAGTATTTGTTAAAAAGATAATTTATCTTTCCTAA
AAACTAGGTTAGTAATCGTCTAATTTTGTTTAGACGGTTTACTTTACATAAAAAA
TAAAATGCAATATACAACCAAATATAAAATAATAATAACAATTTTTACATATAG
TCAAATGCAAAGCAAAGGAAAATTTTAAATAAGAATTTTTATTTATTCAACATA
AATAGATACATTTTTTTTTGGTTACTAAATCAAGTTTGATTATTCTCTAGAATATT
GGTATTTTTGTAACCTCTCTAGAATTTCAACAAAGAAAATGGCAAAAAAAAAAAA
ACATTCGGACTTCCCCGGGCACGAAATTCGAGAGGGATACTAATTTTTTTTATAG
TTTACCGCCAAAAACACATTCTTTCCAAAATCGACATTTGCTCTCGTCCTTCAAA
ACAATATCTCTCGGGATCTTCACGCTGTAACCAGATAAGCCTTCTAGGGTTTCTG
AGCAACGTC**ATTTTCACTACTCGCCGGCG***GCGTGAACAAAATG*

Forward primer (*M-5,5*): AA GGATCC CAGATCGTCCGTTCAATAGT (*Bam*HI site underlined)
Reverse primer (*M-5,3*) : TT GGATCC CGCCGGCGAGTAGTGAAAAT (*Bam*HI site underlined)

The putative *AtMAP65-5* promoter sequence. The forward and reverse primers used for the promoter amplification by PCR using genomic DNA as template are in bold. Italicise sequence, not cloned but inserted to show relative position of the translation start codon (underlined).

Promoter region for the *AtMAP65-6::Gus* construct

AtMAP65-6 Promoter:

GACCAAATTGGCATCTTTCTTGTTATTAAGAGGGGTACATAGTATCATCATCAT
CCTTAATTAATTAGAGTCCACGCAATAACAATAGAAGACTCTGTCCTCCCCATTT
GTGGTAAATCCTCTTCTCATGATTATTGTTTGGTTGAGTATATGTTTTATTCTATT
ACTACTCACCAGAAGAACATTTTCATATGTGATTCGAATACAATGTTACATTTCT
AATATGAGAGATAACATATGCACCTACTTTTTATACATGCAGTTGTATATTGTGT
GATGTATAGTTATATATTTTCGTCTAATTTCTGTTGAGTTCATATGTCATACCTAA
TTTGCTATAGGATTTTATTGACTGAACAAAAAAAAATGTATACATGGTCTTTATC
TTAGAATAATGGATATATCTATTTCTTTTATTTGATTTGCTTCGCAAATGTACGA
ATATTCGATCTTTCTAAATCGAATTGAATCAAATAACAGATCGAAACAAATCTA
ACGAATATTTTGTCCAACCCTAATATTTTTTTTAAAAAAAAATGTTAGTTGTTTAA
TTATATTACTAAAATCATGAAAATATAATAAATGTTGTAAATGATAGAAAAAAA
AATTGAAAGAACGTTTTTCTGAAGAGTTTATATACCTTGTATACAAACATCTTTT
AATAAAAAAAAACAAATAATTCATATTAATGGTGACATAGACTGCACCCAAAACC
GCAGCGCAACAGTGCTGTAACAGTATTAAAATCTTTACATATACATATGTATCT
ATGTATTTTTGTTACTATTCGAACCGTATCGCACTTTTTCGTAAAACGCAGTTAC
TAGTCAGAAATTAAAAATATATAATTTTAAATGAAAGCAAAAAAATTATCGTAAA
GTTTACACTTCACCGTCAAAACACAGCTACTTATGTCAGTGACTCTTCTTCTATC
ACCACTACACGACACCAAAGAAAAACACTAACACACTCTCTCTGATAACTCTCG
CGTGACTCTCCTCCTTCAACTCTAACTGGTTCGTACCCTTCACGCTCCATTACCG
GCAACGCGCTTATCGTCTGGCACACTCACCCGCACCGTACCCGTCGTCGGTCTTT
TCGCCAATTTATCGTATTTTTCCGTGAAAGAGAATAATATAATACTCTAATAAAG
TGTTATAATAAATTACAACGTTACTATTTACAACGATTTTTAAAAGAAGCTGATT
ATTATTTCTTCTGTAACTCTCTTCTCTGTTGCTCTACCTGTTCTTTTCTCTCTGTTC
ATTCTCTTTTCTTTAGCTTAATTCAGCAAAAAATTTATCTTTGTTTCTCTCTTTTGT
TTCTTTCCTCTGCAAAGTAAAGTTATGAGAGCTTAATAATGTTTGTCTCATCTTC
AAGCTTCAGATCTGATTCCTTGTTTCTACAAGTAATTGTCTCTTTCTTTTTCGATT
AACCACCATTTCTGTGAAGAAAACCTTTTTGCTTGCTTCAAGATTCGAGT**GAGG**
AAAATTTTAGCTGAAA*ATG*

Forward primer (*M-6,5*): AA GGATCC GACCAAATTGGCATCTTTCT (*Bam*HI site underlined)
Reverse primer (*M-6,3*) : TT GGATCC TTTCAGCTAAAATTTTCCTC(*Bam*HI site underlined)

The putative *AtMAP65-6* promoter sequence. The forward and reverse primers used for the promoter amplification by PCR using genomic DNA as template are in bold. Italicise sequence, not cloned but inserted to show relative position of the translation start codon.

Promoter region for the *AtMAP65-7::Gus* construct

AtMAP65-7 Promoter:

AAATAGTTTCTCCGTTCCGTTGAGGCTTAGTTTTCCTCTTTTGGGCTTAGTTTTT
GGAGACATTTAGTTGGTCTGCCGGCGTTTGTATTTCAAATGGTATTCTACCTTGG
GTTTTTAATAAAATTCAGACAACAAAAAAAAAAAATTAGCAGTTGTGGCAAGCA
ATAATGAAAGGTTTGGATAATGATACTAATTTTTTTGCTGATTAAATTAAATATA
GAAATAAGATTTTCAACTTATTCTTAATGAAATTAGTGGAGTGGAGTGACATTG
GCCACCACCACTTCCTTGCTTTTGATTAGACCAATTTGGCATATTTTTCTTGTAAA
ATATACACACATCTTCTATTAATTTTAGCTTCACTCAAAACAAATACTATTTCTG
CATTTCATCATTCAAAAGTGATTTACCTCTTTATTCTCATGATTAAAGGTTCATTT
CAACGTCGATAGTAGTATTTAAATTACAATTTTTTTTTTTGGATGCATAAGACTA
ATTCTAAAAAATTTGGTTGGTCCAAAAGGTCGTCATGCAACGTACAAATACGAT
ATACCTAAACAATTGAGTACTCTATAAATACTTTTATACATCTGATCATCAAAGA
AGACAAATCTTATTCTCTTTATTCTATTGGGACGTGTTACCAACGCTCCTCTAAA
ACCCACGCGCTCCCGAGAATCCGTCACTTTAATTACTTTATTTTATCGTATTTTCA
TGAAGACGAATAAATACTACTAATATCAGAGAATAACAAGATAAAGTAGGTGA
CAAAAGAAAATTAGAAAAGAGAATAACAAAATAATAAATAACATTAATGTAGT
ATAAATTTTTAATAGTGTAAATATGACAAAAAGAAGCTCAGTTTTATTCAGACTT
TTTTTCTCTCCACATTCTTCTTCTTTCTTTAGTGTTTCCAACTTAACCCTCTCTCTT
TTCTTGCAAACTTTTGCTCGGAATTCTATGCTTTGCTGATCTATTGTTTTCTCTCT
GCAAAAGTAATGAGAAGCTTTTTGCTATGTTAAGCTTTAGATCTGCTATTATTTG
TTCCTGTGAGTCTTTTATATCTTGTGTGGTTTCTTTGAGACCTTAAGCAGCCATTG
TCACAAGCTGAGCTCTCTTTCTTTCTCTCTAGTTCAAGATTCTAACTTTGGAGCA
AGTAAGCAAGTCAGAGAGAGGACAAATTAGCTGAAATGCTGGAGATTGAAAGC
CCTACGAGTCTCTGTTTCCGTACAAACACTACTTGTAATGCTCTGCTTCGAGAGC
TTCAGGTTTTTCTTTCACCCTCTTCTTCTCTGTTTCTTGGAAAATTTAGGGTTTCTT
GATAATGATGCTTCAAGGACAAATTTAGGGTCTTTATAGGTAAAGTCTTCTCCTT
TTTTTCTGTCAACTATAGGTTTAAGGGTTACTGTGAATTTTGGTACCTCTTCTTAG
TTTCTGAGACTTCTTTTGACCTGTTTTTCTACAAGTATCTGATTTTTATGTTT**GGA**
GTATCTATATATTTCATGG*TTTAATG*

Forward primer (*M-7,5*): AA GGATCC AAATAGTTTCTCCGTTCCGTT (*Bam*HI site underlined)
Reverse primer (*M-7,3*) : TT GGATCC CCATGAAATATATAGATACTCC(*Bam*HI site underlined)

The putative *AtMAP65-7* promoter sequence. The forward and reverse primers used for the promoter amplification by PCR using genomic DNA as template are in bold. Italicise sequence, not cloned but inserted to show relative position of the translation start codon (underlined).

Promoter region for the *AtMAP65-8::Gus* construct

AtMAP65-8 Promoter:

TGTGGGCCAGTGGTCTTAGTCCATTGGTTGTCTCTCTGTCACCGGGTTCGAGT
GGACTCGGTTGATGTAAGAAGTTTATCGTCAGCCATATTTTCTTAGCATGTGTAC
TGTGTACTGTTGACAAATGACAATGCATTCGATGTCAAAAAAAAAGGCTACATAT
TGTAGTAAATAGTAATATTGTCTTCCTTTTTTAATTACCGAATGTTCTAGGAATT
ATAATTTAAAAATAAACCAAAATGATGGTCATTGGTTTAATTTTGAAATGTTGGT
AAAAAGAATTAGTTAAATATGAATAAATCGACTCTGATTTGTAGTCATTTTATAT
TATTTTGAATTGAACTTTAAATCTATAGTACTGAAACACTAATGTTTGAATTTGT
GTAGAGGGAGAGTTGAAAGAGATTTGCCGACTTCGACGGCCGACACGCGCCGA
CAATACATGCATATGTCGGCTATTTAGATCTCTACATTGAATATCCTAAATTACA
ATAATACCTTCTCCCTTACTAATATTCTTTGAATCAACCTTTATTATTTTTTGTTTT
TTATGTTTTTTTCAGAAATTATTTGTTGGCAACCATGTTCGCTTTTTTTTTGAATT
ATTATATCCCAAAATTTATAATGATTTAGACATTATTTTCCAGTTTTGCCATAAA
ATATTAAATTAATCCACAGATAATATTTAAAAACTTTTAAAGGTTAACATTGTCG
TTTTTTTTTTAAAGGTTAACATTGTCCTTTTTTTTTGTAAATATAAATGAACTATC
GCCTATTAGCAACAAAAAAGTTGAGTTTGGTCTGAGAATCGTTTAGAACTTTTG
GTTTGTTGGATCGTACATATATAGGACTGCAAATTTATTACTATTTGTTAATTAG
TTGAGGCTCTCCTCTTCTTATTTATTTATGAGACGTACCAAATAAGTCATTATAA
AGTGTACTAACGTCCGGAAATTTGTCCACGAGTAACAATTTAAACCTCAGATGT
GGTCAATGAAAAATACAAGAATTTTAAAACGACGGCTAAAATAATATAAATTTT
GTAAGGACATATTGATCTATCACTGATACTAAAACAGAGGAATTAGTTTTAATG
ATAATGAGCATATGCAAATCTATCACTGATACAAAAAAAAAAACAGAGGAATTTT
AAGGGGGGGGGGGGGGAAATTCAGAAAGAACTTGATAACCAAAATCTAAGCCA
CAAAGAAAAAGAAGCTATGTTGTAAGAACCCACATGGTGAAGAATCTCTGTCTA
TTTCGATTTTGTGTTCAGATAAAACAGTAATAAGCAAAAAAGTTAGCACTACAG
GTTTGCTTACGAATCAAGTTTTGTGTAGTATATACAAAAAAAAAACATCTCTCTCT
GGCTTTTCATACAGCAGAAGCAAACGCATCAGCACAAAAGCGACTTCTAAGCTT
TACCAAATTCAGATGAAGTTGAGAGAGAGAAAGAGAAAGAGACATAAACTGAA
GAATCAA**AGAGGAGGAGGGAGATGCGG***ATG*

Forward primer (*M-8,5*): AA GGATCC TGTGGGCCAGTGGTCTTAGTC (*Bam*HI site underlined)
Reverse primer (*M-8,3*) : TT GGATCC CCGCATCTCCCTCCTCCTCT (*Bam*HI site underlined)

The putative *AtMAP65-8* promoter sequence. The forward and reverse primers used for the promoter amplification by PCR using genomic DNA as template are in bold. Italicise sequence, not cloned but inserted to show relative position of the translation start codon.

Promoter region for the *AtMAP65-9::Gus* construct

AtMAP65-9 Promoter:

ACTCTGATATGGTGTTTGTAATTTGCTTAAATGGCTCAAATTTCCAATTGAACT
TTGGGCTAAAAGCTGAGATAAATCACACAAATACATAAATAATATGAATAGTAA
AGAGAATCGTTGAAGATGAATGTGTGTTCTTACGTGAAGGAGGATAGTTTCCAG
AGGATTGAAACCAGATTTCGATTTCTTCAGTCTCGGAATAAAGCTCAGGTCTAG
AGAAATCATAGAACCTCGGTGCATCGAATTCGAAATCAATATCGAATTCGAAAT
CATCGCCAGAAAAACTCATTATCCTCGATGATGATTCGGGAACCATTATCAATC
CTCGATGATAACTCCGATCTCAGACGACGGGAATCAAGTAGGAGCGTTTCACAT
CAATCGAATCGAAAATGTCCTTCTCCTTCTCTCCCTCCTCCTCCTCCTCCTCC
TCCTCGAGAATCGGAGAATCTCTGGAAAAAATCGCCAGAGGATAAGAGCGAAG
GAGAGAGAGAGAGAGAAATTGGAGATGAGAGAAGAGCTCTAACTTTTCTTGTG
GACAAGAAGAGAGAGAGAGAGAGAGAAGGTAACGGCCCTAAAATTCAGTTGGC
GCGGATGTATAACAATAACAGCTCATATTTTTAGTATTCTCAATTTGGTTCTTCA
GTTTTCTAAAATCACAAATTAGACCCCAATTTATATTTTTTTGAACCACAACACC
AGTTCATCTAATAATTTATGTTCTTTAGTTTCTATATATTAAATTTTGCACATGTT
TTCTACTTCGGTTCTTGGTATTGGCAAGAATTTTAGTTACTTTACTAGATGTAAA
TTCAAATCTTAAATATATGAAAATAGTGTTTTAATTTGTGAATTAAATTATGGTA
ATTTCGTGGTTAAAGATAGTTAAAGCGTATCTAGGAAATTAGAATTTGTTTTTCT
TCTATAATTTCAACTTGTCGTAACGCTCTTAAATATGAGATATATTTGGCGCATC
ATATATCTTTCTATTGTTAAAAAAACATGACAACAAGAAAATCTATGTATCATG
AAGCAAAAGGAAACTAATATCTACAAAGTTTTATTAGGGGAGAAAGGAGAGAT
TTCAAAAGATTAGGGGGAAGCAAACAAATATACGAAATAAGCGTTTTCCCTCTG
CCTGTAATTTTTTTGTTTACAATTAACAACTTACCTGTAATTTTTTTTTGACTAGA
TTATTTTTATTTGATTCCTAAATTTTATCCGAATTTTTTTCAAGGAAAAACCAACG
GCTGTGTCCTTCAATCCAGGTAAAGAATCTCGTATTTCTTCCAGGAAAATTCAAA
AGAAAAAAGTTTCAGCAATTAAAATGATTATCATTTAGAAAGAAAAAAATTCTT
GTGTTTTCTAAAAAGATTTTGTTATCGTTTGAGAAATTTTATGAAGTAACCTATT
GAGGAAAAAAAACATCCTCATAGGATTGAATAAGATAACGAATGTGGAAGAAT
TTTGAATTTATT**TGCAGAGTTTGGAGATAAATA***ATG*

Forward primer (*M-9,5*): AA AAGCTT ACTCTGATATGGTGTTTGTAAT (*Hin*dIII site underlined)
Reverse primer (*M-9,3*) : TT GGATCC TATTTATCTCCAAACTCTGCAA (*Bam*HI site underlined)

The putative *AtMAP65-9* promoter sequence. The forward and reverse primers used for the promoter amplification by PCR using genomic DNA as template are in bold. Italicise sequence, not cloned but inserted to show relative position of the translation start codon.

Appendix K

Kanamycin segregation data and number of T-DNA loci for AtMAP65::GUS lines

AtMAP65-1::GUS

Line	Kan sensitive	Kan resistant	T-DNA loci	Line	Kan sensitive	Kan resistant	T-DNA loci
1	122	370	1	**6**	5	334	3
2	132	408	1	**7**	101	319	1
3	93	287	1	**8**	86	263	1
4	23	365	2	**9**	18	288	2
5	138	429	1	**10**	139	421	1

AtMAP65-2::GUS

Line	Kan sensitive	Kan resistant	T-DNA loci	Line	Kan sensitive	Kan resistant	T-DNA loci
1	68	216	1	**6**	94	308	1
2	103	321	1	**7**	79	253	1
3	85	256	1	**8**	3	203	3
4	142	432	1	**9**	9	145	2
5	129	398	1	**10**	123	372	1

Line	Kan sensitive	Kan resistant	T-DNA loci
11	124	381	1
12	81	246	1
13	15	243	2
14	139	448	1
15	135	422	1

AtMAP65-3::GUS

Line	Kan sensitive	Kan resistant	T-DNA loci	Line	Kan sensitive	Kan resistant	T-DNA loci
1	105	324	1	**6**	100	317	1
2	232	626	1	**7**	136	424	1
3	138	423	1	**8**	97	302	1
4	17	269	2	**9**	144	450	1
5	21	318	2	**10**	92	319	1

AtMAP65-4::GUS

Line	Kan sensitive	Kan resistant	T-DNA loci	Line	Kan sensitive	Kan resistant	T-DNA loci
1	151	463	1	**6**	35	101	1
2	79	239	1	**7**	13	216	2
3	83	256	1	**8**	161	484	1
4	95	194	1	**9**	142	449	1
5	25	78	1	**10**	129	383	1

AtMAP65-5::GUS

Line	Kan sensitive	Kan resistant	T-DNA loci	Line	Kan sensitive	Kan resistant	T-DNA loci
1	137	421	1	**7**	57	184	1
2	86	267	1	**8**	176	534	1
3	5	89	2	**9**	83	258	1
4	123	385	1	**10**	20	319	2
5	128	379	1	**11**	106	325	1
6	93	282	1	**12**	158	491	1

AtMAP65-6::GUS

Line	Kan sensitive	Kan resistant	T-DNA loci	Line	Kan sensitive	Kan resistant	T-DNA loci
1	94	289	1	**6**	157	483	1
2	128	393	1	**7**	119	362	1
3	75	232	1	**8**	62	191	1
4	99	319	1	**9**	9	145	2
5	113	355	1	**10**	125	384	1

AtMAP65-7::GUS

Line	Kan sensitive	Kan resistant	T-DNA loci	Line	Kan sensitive	Kan resistant	T-DNA loci
1	121	364	1	**6**	76	236	1
2	114	347	1	**7**	128	399	1
3	89	251	1	**8**	133	406	1
4	107	339	1	**9**	14	227	2
5	142	438	1				

AtMAP65-8::GUS

Line	Kan sensitive	Kan resistant	T-DNA loci	Line	Kan sensitive	Kan resistant	T-DNA loci
1	74	229	1	**6**	113	344	1
2	149	456	1	**7**	121	360	1
3	10	164	2	**8**	85	258	1
4	96	278	1				
5	102	317	1				

AtMAP65-9::GUS

Line	Kan sensitive	Kan resistant	T-DNA loci	Line	Kan sensitive	Kan resistant	T-DNA loci
1	86	262	1	**7**	107	335	1
2	123	374	1	**8**	126	382	1
3	97	305	1	**9**	93	281	1
4	16	256	2	**10**	118	361	1
5	12	191	2	**11**	131	399	1
6	119	365	1				

Appendix L

RT-PCR primer positions in AtMAP65 protein sequences alignment

Alignment of MAP65 protein sequences.
RT-PCR primers were designed to nucleotide sequence in areas with low protein sequence homology. The blocks in yellow indicate the conserved regions. The blocks in purple indicate the positions were the RT-PCR primes designed.

Appendix M
AtMAP65 RT-PCR primer sequences

AtMAP65-1
Forward: GATACCAGTGTCCAGTCTAAG
Reverse: AGCAGATTCCGGGTTAACTTC

AtMAP65-2
Forward: GCAAATGGTGTTCAAACCAAG
Reverse: AACAACCTCTGGTTTTATTTC

AtMAP65-3
Forward: AAAGCACCTGTGTACTCTGTAT
Reverse: GGTAATATGCTGATACTCTTG

AtMAP65-4
Forward: TGTTTGCTGAAAACGCTTAAC
Reverse: AGACTCAGTCAAAGCGATGCT

AtMAP65-5
Forward: ACTGTTAGTTCTGGTTCAGAA
Reverse: GCATCCTTTTTTCAAGGGATC

AtMAP65-6
Forward: GCCATGAACATTTCATTGACT
Reverse: GCTAGGTTGAATGTGAGTTAG

AtMAP65-7
Forward: ACGATGGCTGGTTCTTTGGCT
Reverse: GTCAGCCTCAATGTGAGCCAA

AtMAP65-8
Forward: GACTCAACTAGAAAGATAACC
Reverse: CGACATGTTGCACGTATCTTC

AtMAP65-9
Forward: GTGAAACAGATTCAAGATAAT
Reverse: TTCAAGAACAATGTGTGTTCT

AtMAP65-1 RT-PCR 100 ng cDNA

First gel

band	background	band minus background	(band-backgroung)/ mean:
206,3	96,8	109,5	1,05848236
201,67	99,94	101,73	0,98337361
211,31	107,8	103,51	1,00057999
213,78	108,08	105,7	1,02174964
215,93	112,53	103,4	0,99951667
214,89	114,38	100,51	0,97158047
207,22	107,41	99,81	0,96481392
		mean: 103,451429	

Second gel

band	background	band minus background	(band-backgroung)/ mean
180,8	93,59	87,21	1,12167203
172,98	94,63	78,35	1,00771704
189,22	99,06	90,16	1,15961415
148,07	97,34	50,73	0,65247588
179,23	97,01	82,22	1,05749196
161,38	103,11	58,27	0,74945338
204,91	107,63	97,28	1,25118971
		mean: 77,7457143	

1st and 2nd gels average values		error bar values:
1,09007719	TC	0,03159483
0,99554533	Seedling	0,01217172
1,08009707	Root	0,07951708
0,83711276	Stem	0,18463688
1,02850432	Leave	0,02898764
0,86051692	Flower	0,11106355
1,10800182	Silique	0,1431879

Analysis of the light intensity of each band of two replicas AtMAP65-1 RT-PCRs using 100 ng cDNA from various At tissues. From the light intensity of each band the light intensity of the background was substracted. Then the values were nornalised by mean; the intensity for each band in each replicate was divided by the mean intensity for all bands in the replicate. The data were averaged across the two replicates and a histogram plotted based on the average values. The formula for calculating the error bar values was: ABS (1st gel value-2nd gel value)/2

AtMAP65-1 RT-PCR 10 ng cDNA

First gel

band	background	band minus background	(band-backgroung)/ mean:
205,08	94,21	110,87	0,97794831
205,07	91,7	113,37	1
212,19	97,6	114,59	1,01076122
214,21	100,31	113,9	1,00467496
218,28	105,81	112,47	0,99206139
216,66	102,2	114,46	1,00961454
209,95	96,02	113,93	1,00493958
		mean: 113,37	

Second gel

band	background	band minus background	(band-backgroung)/ mean
194,47	113,63	80,84	1,16701073
186,14	103,07	83,07	1,19920313
197,09	111,69	85,4	1,23283914
188,91	108,74	80,17	1,15733857
162,17	103,59	58,58	0,84566413
194,85	108,45	86,4	1,24727519
180,31	106,84	73,47	1,060617
		mean: 78,2757143	

1st and 2nd gels average values		error bar values:
1,07247952	TC	0,09453121
1,09960156	Seedling	0,09960156
1,12180018	Root	0,11103896
1,08100676	Stem	0,07633181
0,91886276	Leave	0,07319863
1,12844487	Flower	0,11883033
1,03277829	Silique	0,02783871

Analysis of the light intensity of each band of two replicas AtMAP65-1 RT-PCRs using 10 ng cDNA from various At tissues. From the light intensity of each band the light intensity of the background was substracted. Then the values were nornalised by mean; the intensity for each band in each replicate was divided by the mean intensity for all bands in the replicate. The data were averaged across the two replicates and a histogram plotted based on the average values. The formula for calculating the error bar values was: ABS (1st gel value-2nd gel value)/2

AtMAP65-2 RT-PCR 100 ng cDNA

First gel

band	background	band minus background	(band-backgroung)/ mean:
158,14	92,69	65,45	1,43072618
102,53	83,67	18,86	0,41227648
173,77	95,55	78,22	1,70987627
109,82	89,33	20,49	0,44790801
145,37	97,82	47,55	1,03943514
187,93	106,31	81,62	1,78419971
104,16	96,13	8,03	0,17553447

mean: 45,7457143

Second gel

band	background	band minus background	(band-backgroung)/ mean:
192,46	84,03	108,43	1,7394164
121,38	83,01	38,37	0,61552529
181,18	83,23	97,95	1,57129795
109,94	79,22	30,72	0,49280524
101,63	81,23	20,4	0,32725348
197,33	84	113,33	1,8180214
106,33	79,17	27,16	0,4356963

mean: 62,3371429

1st and 2nd gels average values		error bar values:
1,58507129	TC	1,58507129
0,51390089	Seedling	0,51390089
1,64058711	Root	1,64058711
0,47035662	Stem	0,47035662
0,68334431	Leave	0,68334431
1,80111056	Flower	1,80111056
0,30561538	Silique	0,30561538

Analysis of the light intensity of each band of two replicas AtMAP65-2 RT-PCRs using 100 ng cDNA from various At tissues. From the light intensity of each band the light intensity of the background was substracted. Then the values were nornalised by mean; the intensity for each band in each replicate was divided by the mean intensity for all bands in the replicate. The data were averaged across the two replicates and a histogram plotted based on the average values. The formula for calculating the error bar values was: ABS (1st gel value-2nd gel value)/2

AtMAP65-2 RT-PCR 10 ng cDNA

First gel

band	background	band minus background	(band-backgroung)/ mean:
107,63	96,59	11,04	0,79066103
95,06	90,95	4,11	0,29434935
101,49	89,49	12	0,85941417
94,01	90,31	3,7	0,26498603
119,99	102,23	17,76	1,27193297
139,57	103,23	36,34	2,60259257
100,27	95,03	5,24	0,37527752
		mean: 12,8842857	

Second gel

band	background	band minus background	(band-backgroung)/ mean:
210,86	102,34	108,52	1,56675907
109,49	93,16	16,33	0,23576461
206,95	92,91	114,04	1,64645415
162	90,13	71,87	1,03762416
123,35	92,46	30,89	0,44597482
202,6	92,31	110,29	1,59231347
131,05	82,75	48,3	0,69733195
	mean	mean: 71,4628571	

1st and 2nd gels average values		error bar values:
1,17871005	TC	0,38804902
0,26505698	Seedling	0,02929237
1,25293416	Root	0,39351999
0,6513051	Stem	0,38631906
0,85895389	Leave	0,41297907
2,09745302	Flower	0,50513955
0,53630473	Silique	0,16102721

Analysis of the light intensity of each band of two replicas AtMAP65-2 RT-PCRs using 10 ng cDNA from various At tissues. From the light intensity of each band the light intensity of the background was substracted. Then the values were nornalised by mean; the intensity for each band in each replicate was divided by the mean intensity for all bands in the replicate. The data were averaged across the two replicates and a histogram plotted based on the average values. The formula for calculating the error bar values was: ABS (1st gel value-2nd gel value)/2

AtMAP65-3 RT-PCR 100 ng cDNA

First gel

band	background	band minus background	(band-backgroung)/ mean:
196,35	82,75	113,6	2,04129306
91,64	79,51	12,13	0,21796554
168,08	90,48	77,6	1,39440441
111,83	83,9	27,93	0,50187777
96,13	85,45	10,68	0,1919103
201,86	89,07	112,79	2,02673806
118,68	83,85	34,83	0,62586476

mean: 55,6514286

Second gel

band	background	band minus background	(band-backgroung)/ mean:
203,34	152,16	51,18	1,62367945
154,5	144,09	10,41	0,33025602
202,59	154,17	48,42	1,53611878
186,29	154,33	31,96	1,01392722
171,05	157,43	13,62	0,43209289
205,8	168,34	37,46	1,18841407
193,68	166,08	27,6	0,87560674

mean: 31,5214286

1st and 2nd gels average values		error bar values:
1,83248626	TC	0,2088068
0,27411078	Seedling	0,05614524
1,4652616	Root	0,07085718
0,7579025	Stem	0,25602472
0,31200159	Leave	0,1200913
1,60757607	Flower	0,419162
0,75073575	Silique	0,12487099

Analysis of the light intensity of each band of two replicas AtMAP65-3 RT-PCRs using 100 ng cDNA from various At tissues. From the light intensity of each band the light intensity of the background was substracted. Then the values were nornalised by mean; the intensity for each band in each replicate was divided by the mean intensity for all bands in the replicate. The data were averaged across the two replicates and a histogram plotted based on the average values. The formula for calculating the error bar values was: ABS (1st gel value-2nd gel value)/2

AtMAP65-3 RT-PCR 10 ng cDNA

First gel

band	background	band minus background	(band-backgroung)/ mean:
172,04	103,23	68,81	2,16519824
106,98	100,77	6,21	0,19540592
126,95	108,45	18,5	0,58212712
126,77	110,71	16,06	0,50534928
129,8	111,72	18,08	0,56891126
205,48	120,26	85,22	2,68156073
127,08	117,5	9,58	0,30144745
		mean: 31,78	

Second gel

band	background	band minus background	(band-backgroung)/ mean:
94,73	89,28	5,45	1,24429224
84,72	84,58	0,14	0,03196347
94,81	88,99	5,82	1,32876712
85,21	84,07	1,14	0,26027397
85,43	85,29	0,14	0,03196347
102,99	85,49	17,5	3,99543379
79,01	78,53	0,48	0,10958904
		mean: 4,38142857	

1st and 2nd gels average values		error bar values:
1,70474524	TC	0,460453
0,11368469	Seedling	0,08172122
0,95544712	Root	0,37332
0,38281162	Stem	0,12253765
0,30043737	Leave	0,2684739
3,33849726	Flower	0,65693653
0,20551825	Silique	0,09592921

Analysis of the light intensity of each band of two replicas AtMAP65-3 RT-PCRs using 10 ng cDNA from various At tissues. From the light intensity of each band the light intensity of the background was substracted. Then the values were nornalised by mean; the intensity for each band in each replicate was divided by the mean intensity for all bands in the replicate. The data were averaged across the two replicates and a histogram plotted based on the average values. The formula for calculating the error bar values was: ABS (1st gel value-2nd gel value)/2

AtMAP65-4 RT-PCR 100 ng cDNA

First gel:

band	background	band minus background	(band-backgroung)/ mean:
202,04	82,86	119,18	1,5583159
152,39	79,71	72,68	0,95031381
184,51	81,47	103,04	1,34728033
112,34	79,72	32,62	0,42651674
127,65	81,49	46,16	0,60355649
197,28	78,65	118,63	1,55112448
118,16	75,11	43,05	0,56289226
		mean: 76,48	

Second gel:

band	background	band minus background	(band-backgroung)/ mean:
186,3	83,9	102,4	2,96356322
86,38	74,47	11,91	0,34468787
128,71	77,52	51,19	1,4814922
90,55	75,2	15,35	0,44424507
72,47	71,61	0,86	0,0248893
138,84	79,38	59,46	1,72083466
69,14	68,44	0,7	0,02025873
		mean: 34,5528571	

1st and 2nd gels average values		error bar values:
2,26093956	TC	0,70262366
0,64750084	Seedling	0,30281297
1,41438627	Root	0,06710593
0,4353809	Stem	0,00886417
0,31422289	Leave	0,28933359
1,63597957	Flower	0,08485509
0,2915755	Silique	0,27131676

Analysis of the light intensity of each band of two replicas AtMAP65-4 RT-PCRs using 100 ng cDNA from various At tissues. From the light intensity of each band the light intensity of the background was substracted. Then the values were nornalised by mean; the intensity for each band in each replicate was divided by the mean intensity for all bands in the replicate. The data were averaged across the two replicates and a histogram plotted based on the average values. The formula for calculating the error bar values was: ABS (1st gel value-2nd gel value)/2

AtMAP65-4 RT-PCR 10 ng cDNA

First gel:

band	background	band minus background	(band-backgroung)/ mean:
212,81	125,32	87,49	3,46824705
133,72	119,28	14,44	0,57242528
153,6	119,91	33,69	1,33552684
144,5	118,32	26,18	1,03781812
110,71	104,93	5,78	0,22912868
104,59	98,6	5,99	0,23745342
95,26	92,25	3,01	0,11932134

mean: 25,2257143

Second gel:

band	background	band minus background	(band-backgroung)/ mean:
90,41	80,63	9,78	3,10377658
83,77	81,88	1,89	0,59980958
92,55	85,04	7,51	2,38337036
89,59	88,28	1,31	0,41574103
88,37	87,12	1,25	0,39669946
90,91	90,64	0,27	0,08568708
83,65	83,6	0,05	0,01586798

mean: 3,15142857

1st and 2nd gels average values		error bar values:
3,28601181	TC	0,18223523
0,58611743	Seedling	0,01369215
1,8594486	Root	0,52392176
0,72677958	Stem	0,31103854
0,31291407	Leave	0,08378539
0,16157025	Flower	0,07588317
0,06759466	Silique	0,05172668

Analysis of the light intensity of each band of two replicas AtMAP65-4 RT-PCRs using 10 ng cDNA from various At tissues. From the light intensity of each band the light intensity of the background was substracted. Then the values were nornalised by mean; the intensity for each band in each replicate was divided by the mean intensity for all bands in the replicate. The data were averaged across the two replicates and a histogram plotted based on the average values. The formula for calculating the error bar values was: ABS (1st gel value-2nd gel value)/2

AtMAP65-5 RT-PCR 100 ng cDNA

First gel:

band	background	band minus background	(band-backgroung)/ mean:
212,94	119,66	93,28	2,51944685
114,16	103,66	10,5	0,28359983
167,03	104,08	62,95	1,70024849
107,9	94,08	13,82	0,37327139
103,72	90,83	12,89	0,34815255
152,46	97,43	55,03	1,48633319
100,8	90,1	10,7	0,28900173

mean: 37,0242857

Second gel:

band	background	band minus background	(band-backgroung)/ mean:
183,23	86,7	96,53	2,20478736
106,32	85,745	20,575	0,46994199
135,39	87,5	47,89	1,09382851
98,3	86,8	11,5	0,26266502
117,86	90,7	27,16	0,62034626
169,25	101,8	67,45	1,54058746
131,48	96,11	35,37	0,80786625

mean: 43,7821429

1st and 2nd gels average values		error bar values:
2,3621171	TC	0,15732974
0,37677091	Seedling	0,09317108
1,3970385	Root	0,30320999
0,31796821	Stem	0,05530318
0,48424941	Leave	0,13609686
1,51346032	Flower	0,02712713
0,54843399	Silique	0,25943226

Analysis of the light intensity of each band of two replicas AtMAP65-5 RT-PCRs using 100 ng cDNA from various At tissues. From the light intensity of each band the light intensity of the background was substracted. Then the values were nornalised by mean; the intensity for each band in each replicate was divided by the mean intensity for all bands in the replicate. The data were averaged across the two replicates and a histogram plotted based on the average values. The formula for calculating the error bar values was: ABS (1st gel value-2nd gel value)/2

AtMAP65-5 RT-PCR 10 ng cDNA

First gel:

band	background	band minus background	(band-backgroung)/ mean:
168,62	124,08	44,54	3,87035106
132	125,14	6,86	0,59610706
138,6	133,1	5,5	0,4779284
152,64	139,18	13,46	1,16962113
148,99	141,79	7,2	0,62565172
141,42	140,44	0,98	0,08515815
145,52	143,5	2,02	0,17553007

mean: 11,5085714

Second gel:

band	background	band minus background	(band-backgroung)/ mean:
152,27	99,66	52,61	2,61182545
100,14	89,27	10,87	0,53964156
108,2	88,8	19,4	0,96311374
97,54	88,37	9,17	0,455245
92,73	87,36	5,37	0,26659385
123,6	90,82	32,78	1,62736434
99,7	88,9	10,8	0,53616641

mean: 20,1428571

1st and 2nd gels average va	Average	error bar values:
3,24108825	TC	0,62926281
0,56787431	Seedling	0,02823275
0,72052107	Root	0,24259267
0,81243307	Stem	0,35718807
0,44612279	Leave	0,17952893
0,85626125	Flower	0,7711031
0,35584824	Silique	0,18031817

Analysis of the light intensity of each band of two replicas AtMAP65-5 RT-PCRs using 10 ng cDNA from various At tissues. From the light intensity of each band the light intensity of the background was substracted. Then the values were nornalised by mean; the intensity for each band in each replicate was divided by the mean intensity for all bands in the replicate. The data were averaged across the two replicates and a histogram plotted based on the average values. The formula for calculating the error bar values was: ABS (1st gel value-2nd gel value)/2

AtMAP65-6 RT-PCR 100 ng cDNA

First gel:

band	background	band minus background	(band-backgroung)/ mean:
182,32	70,92	111,4	1,2110012
160,59	70,64	89,95	0,97782368
200,51	73	127,51	1,38612893
170,98	72,53	98,45	1,07022502
193,96	76,79	117,17	1,2737254
78,28	70,03	8,25	0,08968366
165,54	74,34	91,2	0,99141211
	mean:	91,99	

Second gel:

band	background	band minus background	(band-backgroung)/ mean:
153,03	101,22	51,81	0,83420548
148,82	97,03	51,79	0,83388346
190,48	107,94	82,54	1,32899673
175,85	102,58	73,27	1,17973819
151,65	104,99	46,66	0,75128407
171,33	103,53	67,8	1,09166439
151,46	90,58	60,88	0,98024377
	mean:	62,1071429	

1st and 2nd gels average values		error bar values:
1,02260334	TC	0,18839786
0,90585357	Seedling	0,07197011
1,35756283	Root	0,0285661
1,12498161	Stem	0,05475658
1,01250474	Leave	0,26122067
0,59067402	Flower	0,50099036
0,98582794	Silique	0,00558417

Analysis of the light intensity of each band of two replicas AtMAP65-6 RT-PCRs using 100 ng cDNA from various At tissues. From the light intensity of each band the light intensity of the background was substracted. Then the values were nornalised by mean; the intensity for each band in each replicate was divided by the mean intensity for all bands in the replicate. The data were averaged across the two replicates and a histogram plotted based on the average values. The formula for calculating the error bar values was: ABS (1st gel value-2nd gel value)/2

AtMAP65-6 RT-PCR 10 ng cDNA

First gel:

band	background	band minus background	(band-backgroung)/ mean:
196,83	78,11	118,72	2,1330267
94,11	70,52	23,59	0,42383844
190,7	73,04	117,66	2,11398182
171,71	72,43	99,28	1,78375076
66,97	66,33	0,64	0,0114988
67,29	66,14	1,15	0,0206619
96,03	67,46	28,57	0,51331345
		mean: 55,6585714	

Second gel:

band	background	band minus background	(band-backgroung)/ mean:
118,01	81,01	37	0,73699307
91,57	80,47	11,1	0,22109792
204,81	89,46	115,35	2,29762569
205,62	89,61	116,01	2,31077205
74,71	74,2	0,51	0,01015855
110,41	84,28	26,13	0,52047646
125,24	79,91	45,33	0,9029161
		50,2042857	

1st and 2nd gels average values		error bar values:
1,43500988	TC	0,69801682
0,32246818	Seedling	0,10137026
2,20580375	Root	0,09182193
2,04726141	Stem	0,26351064
0,01082867	Leave	0,00067012
0,27056918	Flower	0,24990728
0,70811478	Silique	0,19480133

Analysis of the light intensity of each band of two replicas AtMAP65-6 RT-PCRs using 10 ng cDNA from various At tissues. From the light intensity of each band the light intensity of the background was substracted. Then the values were nornalised by mean; the intensity for each band in each replicate was divided by the mean intensity for all bands in the replicate. The data were averaged across the two replicates and a histogram plotted based on the average values. The formula for calculating the error bar values was: ABS (1st gel value-2nd gel value)/2

AtMAP65-8 RT-PCR 100 ng cDNA

First gel:

band	background	band minus background	(band-backgroung)/ mean:
85,61	85,21	0,4	0,00858259
91,94	86,8	5,14	0,11028623
204,55	99,38	105,17	2,25657641
196,58	91,7	104,88	2,25035403
104,29	81,95	22,34	0,47933742
175,83	91,55	84,28	1,80835086
86,25	82,22	4,03	0,08646955
		mean: 46,6057143	

Second gel:

band	background	band minus background	(band-backgroung)/ mean:
64,22	63,56	0,66	0,02725358
62,96	62,3	0,66	0,02725358
141,99	78,83	63,16	2,60808523
129,65	75,38	54,27	2,24098774
74,93	67,01	7,92	0,32704299
123,7	88,53	35,17	1,45228558
71,94	64,26	7,68	0,31713259
		mean: 24,2171429	

1st and 2nd gels average values		error bar values:
0,01791808	TC	0,0093355
0,06876991	Seedling	0,04151632
2,43233082	Root	0,17575441
2,24567088	Stem	0,00468315
0,40319021	Leave	0,07614722
1,63031822	Flower	0,17803264
0,20180107	Silique	0,11533152

Analysis of the light intensity of each band of two replicas AtMAP65-8 RT-PCRs using 100 ng cDNA from various At tissues. From the light intensity of each band the light intensity of the background was substracted. Then the values were nornalised by mean; the intensity for each band in each replicate was divided by the mean intensity for all bands in the replicate. The data were averaged across the two replicates and a histogram plotted based on the average values. The formula for calculating the error bar values was: ABS (1st gel value-2nd gel value)/2

AtMAP65-8 RT-PCR 10 ng cDNA

First gel:

band	background	band minus background	(band-backgroung)/ mean:
109,56	108,19	1,37	0,30573533
104,53	103,95	0,58	0,12943539
110,36	102,55	7,81	1,74291453
119,72	102,46	17,26	3,85181879
98,04	96,7	1,34	0,29904039
98	96,41	1,59	0,35483151
88,92	87,5	1,42	0,31689355

mean: 4,48142857

Second gel:

band	background	band minus background	(band-backgroung)/ mean:
63,32	63,2	0,12	0,06119327
64,06	64	0,06	0,03059663
64,46	64,04	0,42	0,21417644
72,22	65,88	6,34	3,23304437
71,15	65,78	5,37	2,73839878
64,81	64,56	0,25	0,12748598
63,84	63,29	0,55	0,28046915

mean: 1,87285714

1st and 2nd gels average values		error bar values:
0,1834643	TC	0,12227103
0,08001601	Seedling	0,04941938
0,97854548	Root	0,76436904
3,54243158	Stem	0,30938721
1,51871958	Leave	1,21967919
0,24115874	Flower	0,11367277
0,29868135	Silique	0,0182122

Analysis of the light intensity of each band of two replicas AtMAP65-8 RT-PCRs using 10 ng cDNA from various At tissues. From the light intensity of each band the light intensity of the background was substracted. Then the values were nornalised by mean; the intensity for each band in each replicate was divided by the mean intensity for all bands in the replicate. The data were averaged across the two replicates and a histogram plotted based on the average values. The formula for calculating the error bar values was: ABS (1st gel value-2nd gel value)/2

AtMAP65-9 RT-PCR 100 ng cDNA

First gel:

band	background	band minus background	(band-backgroung)/ mean:
178,03	176,1	1,93	0,26452851
173,92	172,49	1,43	0,19599781
180,61	167,47	13,14	1,80098684
174,53	162,85	11,68	1,60087719
162,8	160,37	2,43	0,33305921
167,34	148,02	19,32	2,64802632
155,27	154,13	1,14	0,15625

mean: 7,29571429

Second gel:

band	background	band minus background	(band-backgroung)/ mean:
168,69	167,8	0,89	0,2893368
170,06	169,07	0,99	0,32184655
179,88	172,04	7,84	2,54876463
182,32	177,22	5,1	1,6579974
184,73	182,68	2,05	0,66644993
191,17	188,87	2,3	0,74772432
194,3	191,94	2,36	0,76723017

mean: 3,07571429

1st and 2nd gels average values		error bar values:
0,27693265	TC	0,01240415
0,25892218	Seedling	0,06292437
2,17487574	Root	0,37388889
1,6294373	Stem	0,0285601
0,49975457	Leave	0,16669536
1,69787532	Flower	0,950151
0,46174008	Silique	0,30549008

Analysis of the light intensity of each band of two replicas AtMAP65-9 RT-PCRs using 100 ng cDNA from various At tissues. From the light intensity of each band the light intensity of the background was substracted. Then the values were nornalised by mean; the intensity for each band in each replicate was divided by the mean intensity for all bands in the replicate. The data were averaged across the two replicates and a histogram plotted based on the average values. The formula for calculating the error bar values was: ABS (1st gel value-2nd gel value)/2

Appendix O
AtMAP65-6 coding sequence

```
   1 CGGCCGCTAAAGTTATGAGAGCTTAATAATGTTTGTCTCATCTTCAAGCTTCAGATCTGATTCCTTGTTTCTACAAGTAATTGTCTCTTT

  91 CTTTTTCGATTAACCACCATTTCTGTGAAGAAAACCTTTTTGCTTGCTTCAAGATTCGAGTGAGGAAAATTTTAGCTGAAAATGCTGGAA
                                                                                M  L  E

 181 ATTGGAAGTCCCAATGCTCTGTTTTTCCGTACGAATACTACTTGTAATAATCTTCTCCGTGAGCTTCAGAAAATATGGGTTGAAATTGGT
   4  I  G  S  P  N  A  L  F  F  R  T  N  T  T  C  N  N  L  L  R  E  L  Q  K  I  W  V  E  I  G

 271 GAGACTGAGACTGAGAAAGATAGAATGCTTATGGAATTAGAGAGAGAATGTCTTCAAATCTATCAAAGAAAAGTTGATGAGGCTGCAAAT
  34  E  T  E  T  E  K  D  R  M  L  M  E  L  E  R  E  C  L  Q  I  Y  Q  R  K  V  D  E  A  A  N

 361 TCTAAGGCAAAGCTTCATCAGTCTGTTGCATCAATAGAAGCTGAAGTTGCTTCTTTAATGGCTGCCCTTGGTGTGTTAAACATCAACTCA
  64  S  K  A  K  L  H  Q  S  V  A  S  I  E  A  E  V  A  S  L  M  A  A  L  G  V  L  N  I  N  S

 451 CCGATTAAACTGGATAAAGGTTCAAAATCATTGAAAGAAAAGCTTGCAGCTGTGACACCTCTAGTTGAGGAATTGAGAATTCAAAAAGAG
  94  P  I  K  L  D  K  G  S  K  S  L  K  E  K  L  A  A  V  T  P  L  V  E  E  L  R  I  Q  K  E

 541 GAGAGAATGAAGCAGTTTTCCGATATAAAGGCGCAAATTGAGAAGATTAGTGGGGAAATCTCAGGATACAGTGACCATCTCAACAAGGCC
 124  E  R  M  K  Q  F  S  D  I  K  A  Q  I  E  K  I  S  G  E  I  S  G  Y  S  D  H  L  N  K  A

 631 ATGAACATTTCATTGACTCTTGAAGAACAAGACTTGACTTTGAGGAACCTTAACGAGTATCAAACACATCTCCGCACACTTCAAAAGGAA
 154  M  N  I  S  L  T  L  E  E  Q  D  L  T  L  R  N  L  N  E  Y  Q  T  H  L  R  T  L  Q  K  E

 721 AAGTCTGATCGTCTCAACAAAGTGTTGGGTTATGTCAACGAAGTCCACGCACTATGCGGTGTTCTTGGAGTTGACTTTAGTCAAACAGTT
 184  K  S  D  R  L  N  K  V  L  G  Y  V  N  E  V  H  A  L  C  G  V  L  G  V  D  F  S  Q  T  V

 811 AGTGCAGTTCATCCAAGCTTGCATAGAACAGACCAAGAGCAATCTACAAACATTAGTGATAGCACATTAGAGGGTCTTGAGCACATGATT
 214  S  A  V  H  P  S  L  H  R  T  D  Q  E  Q  S  T  N  I  S  D  S  T  L  E  G  L  E  H  M  I

 901 CAAAAGCTTAAAACTGAAAGAAAATCCCGATTTCAAAAGCTAAAGGATGTAGTGGCTTCACTCTTCGAGCTATGGAATCTAATGGACACA
 244  Q  K  L  K  T  E  R  K  S  R  F  Q  K  L  K  D  V  V  A  S  L  F  E  L  W  N  L  M  D  T

 991 CCACAGGAAGACAGAACTAAATTTGGGAAAGTTACTTATGTTGTAAGATCATCTGAAGCTAATATCACTGAGCCGGGAATCCTTTCGACC
 274  P  Q  E  D  R  T  K  F  G  K  V  T  Y  V  V  R  S  S  E  A  N  I  T  E  P  G  I  L  S  T

1081 GAAACAATTGAACAGGTATCTACGGAAGTGGACAGTCTCAGTAAACTGAAAGCAAGCAGAATGAAGGAGCTTGTAATGAAACGAAGATCC
 304  E  T  I  E  Q  V  S  T  E  V  D  S  L  S  K  L  K  A  S  R  M  K  E  L  V  M  K  R  R  S

1171 GAGTTAGAGGATCTTTGCAGACTAACTCACATTCAACCTGACACAAGCACTTCCGCTGAGAAATCAACGGCATTAATAGATTCTGGATTA
 334  E  L  E  D  L  C  R  L  T  H  I  Q  P  D  T  S  T  S  A  E  K  S  T  A  L  I  D  S  G  L

1261 GTGGACCCTTCAGAGCTTCTTGCAAATATTGAAATGCAAATAAACAAAATTAAAGACGAAGCACAGAGTCGAAAAGATATCATGGACAGA
 364  V  D  P  S  E  L  L  A  N  I  E  M  Q  I  N  K  I  K  D  E  A  Q  S  R  K  D  I  M  D  R

1351 ATTGACCGTTGGCTCTCTGCATGTGAAGAAGAAAATTGGCTGGAAGAGTATAATCTGGATGAGAACCGGTATAGTGCTGGAAGAGGGGGA
 394  I  D  R  W  L  S  A  C  E  E  E  N  W  L  E  E  Y  N  L  D  E  N  R  Y  S  A  G  R  G  G

1441 CATGTAAACCTCAAGCGTGCAGAGCGAGCTCGGGTTACAATCAATAAGATCCCCGGAATGGTTGACACTCTTATCAAGAAAACACTTGTG
 424  H  V  N  L  K  R  A  E  R  A  R  V  T  I  N  K  I  P  G  M  V  D  T  L  I  K  K  T  L  V

1531 TGGGAAGAAGACATGCAGAAGTCATTTCTATACGACGGTGTTCGATTGGTTAACATACTAGAAGACTATAAACTGACAAGGAAACAACAG
 454  W  E  E  D  M  Q  K  S  F  L  Y  D  G  V  R  L  V  N  I  L  E  D  Y  K  L  T  R  K  Q  Q

1621 GAAGAGGAAAAGAAAAGATACAGGGATCAAAAGAAGAGGCAGGATCTCCTACTAACCCAAAGGGAATCCATTTACGGATCAAAACCGAGT
 484  E  E  E  K  K  R  Y  R  D  Q  K  K  R  Q  D  L  L  L  T  Q  R  E  S  I  Y  G  S  K  P  S

1711 CCAAGAAGAAGCAGCAGCTTCAGAAAGCCCAATGGTTTCAACATTAGCAATGGGAATGGTTCAGTGCCTCCCACGCCTCGTAGAGGCTCG
 514  P  R  R  S  S  S  F  R  K  P  N  G  F  N  I  S  N  G  N  G  S  V  P  P  T  P  R  R  G  S

1801 GTAGGGACAACAACTCCTGACGTTCTTCTAACCCCAAGATCTTACTCTGGTCATCATCGCCAAAACGGGTATTTCAAAGAAGTTAGAAGA
 544  V  G  T  T  T  P  D  V  L  L  T  P  R  S  Y  S  G  H  H  R  Q  N  G  Y  F  K  E  V  R  R

1891 CTCTCTACTACTCCCTTAAACTATGTGGCCATGCAAAAGGAAGATACTGTTTCTACTACCTACACATCGATTTATAGCTCTGAGCCAGAC
 574  L  S  T  T  P  L  N  Y  V  A  M  Q  K  E  D  T  V  S  T  T  Y  T  S  I  Y  S  S  E  P  D

1981 TCGCCTCTCCAAGGCTGACTTGACTCTCTTTTCCACCGGATTTGTGGAGTAATGTTAATGGTAAAAAAAGAAGGAAGTGAAGAAGAAGGA
 604  S  P  L  Q  G  *
```

Appendix P

A. *AtMAP65-3* Primers for recovering full length clone

5' primer: ATG GCA AGT GTT CAA AAA GAT
3' primer: GAT ATT GAG AAT TCA TAC ACC

B. *AtMAP65-6* primers used for cloning into pET28α:

5'primer: AA CATATG CTG GAA ATT GGA

3' primer: TT CTCGAG TCA GCC TTG GAG

Appendix Q

GATEWAY vectors for the Yeast Two Hybrid assays

A

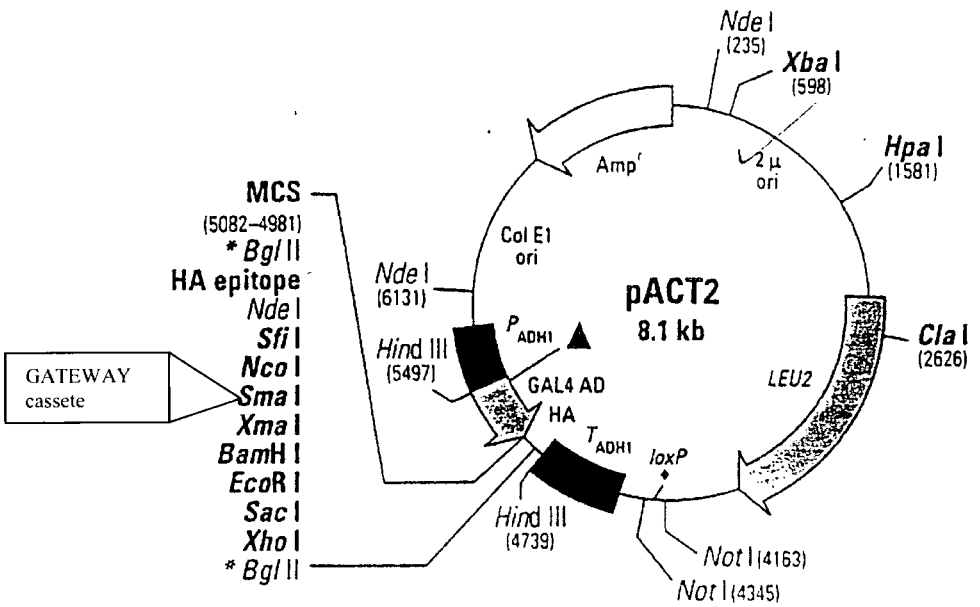

B

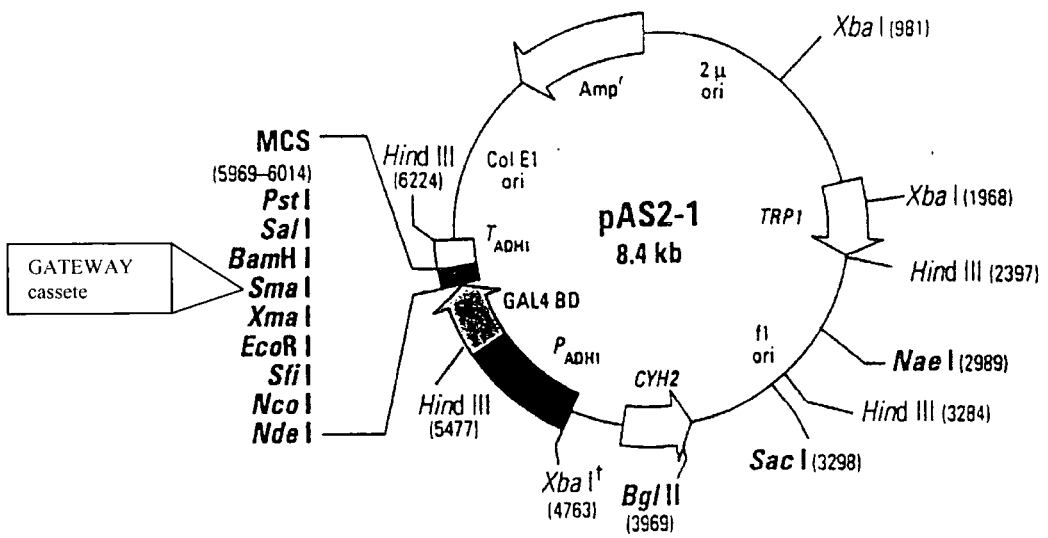

The GATEWAY vectors used for the Yeast two hybrids assays were made by Dr Anthony (Royal Holloway, University of London) by introducing the GATEWAY cassette within the *Sma*I cloning site of the (**A**) pACT2 and (**B**) pAS2-1 vectors supplied by Clontech Laboratories (Ketelaar *et al.*, 2004).

Appendix R

AtMAP65 GATEWAY primers for the Yeast Two Hybrid assays

At MAP65-1

*att*B1

GGGG ACA AGT TTG TAC AAA AAA GCA GGC TTG ACC ATG GCG GTG ACA GAT ACT GAA AGT CCT

*att*B2

GGGG AC CAC TTT GTA CAA GAA AGC TGG GTC TCA TGG TGA AGC TGG AAC TTG ATG ATC

At MAP65-5

*att*B1

GGGG ACA AGT TTG TAC AAA AAA GCA GGC TTG ACC ATG TCT CCG TCT TCA ACC ACT ACT TGC

*att*B2
GGGG AC CAC TTT GTA CAA GAA AGC TGG GTC TCA AGC TAT GCA TCC AAC GCG TTG GGA

At MAP65-6

*att*B1

GGGG ACA AGT TTG TAC AAA AAA GCA GGC TTG ACC ATG CTG GAA ATT GGA AGT CCC AAT GCT

*att*B2

GGGG AC CAC TTT GTA CAA GAA AGC TGG GTC TCA GCC TTG GAG AGG CGA GTC TGG CTC

References

Aizawa, H., Sekine, Y., Takemura, R., Zhang, Z.Z., Nangaku, M. & Hirokawa, N. (1992): Kinesin Family in Murine Central-Nervous-System. Journal of Cell Biology **119**, 1287-1296.

Alberts, B., Bray, D., Lewis, J., Raff, M., Roberts, K. & Watson, J. (1994): Molecular biology of the cell, third edition, 940.

Anthony, R.G., Waldin, T.R., Ray, J.A., Bright, S.W.J. & Hussey, P.J. (1998): Herbicide resistance caused by spontaneous mutation of the cytoskeletal protein tubulin. Nature **393**, 260-263.

Anthony, R.G. & Hussey, P.J. (1999): Double mutation in Eleusine indica alpha-tubulin increases the resistance of transgenic maize calli to dinitroaniline and phosphorothioamidate herbicides. Plant Journal **18**, 669-674.

Anthony, R.G., Reichelt, S. & Hussey, P.J. (1999): Dinitroaniline herbicide-resistant transgenic tobacco plants generated by co-overexpression of a mutant alpha-tubulin and a beta-tubulin. Nature Biotechnology **17**, 712-716.

Archambault, V., Chang, E.J., Drapkin, B.J., Cross, F.R., Chait, B.T. & Rout, M.P. (2004): Targeted proteomic study of the cyclin-Cdk module. Molecular Cell **14**, 699-711.

Arguello-Astorga, G.R. & HerreraEstrella, L.R. (1996): Ancestral multipartite units in light-responsive plant promoters have structural features correlating with specific phototransduction pathways. Plant Physiology **112**, 1151-1166.

Arioli, T., Burn, J.E., Betzner, A.S. & Williamson, R.E. (1998): A hot mutant for cellulose synthesis ... response: How many cellulose synthase-like gene products actually make cellulose? Trends in Plant Science **3**, 165-166.

Asada, T. & Shibaoka, H. (1994): Isolation of Polypeptides with Microtubule-Translocating Activity from Phragmoplasts of Tobacco by-2 Cells. Journal of Cell Science **107**, 2249-2257.

Asada, T., Kuriyama, R. & Shibaoka, H. (1997): TKRP125, a kinesin-related protein involved in the centrosome- independent organization of the cytokinetic apparatus in tobacco BY-2 cells. Journal of Cell Science **110**, 179-189.

Barrosso, C., Chan, J., Allan, V., Doonan, J., Hussey, P. & Lloyd, C. (2000): Two kinesin-related proteins associated with the cold stable cytoskeleton of carrot cells: characterization of a novel kinesin, DcKRP120-2. Plant Journal **24**, 869-968

Barthels, N., van der Lee F.M., Klap, J., Goddijn, O.J., Karimi, M., Puzio, P., Grundler, F.M., Ohl, S.A., Lindsey, K., Robertson, L., Robertson, W.M., Van Montagu, M., Gheysen, G, & Sijmons, P.C. (1997): Regulatory sequences of Arabidopsis drive reporter gene expression in nematode feeding structures. Plant Cell. **9**, 2119-2134.

Baskin, T.I. (2001): On the alignment of cellulose microfibrils by cortical microtubules: a review and a model. PROTOPLASMA **215**, 150-171

Bayley P,M., Sharma K.M. & Martin S.R. (1994): Microtubule Dynamics *in vitro*. Hyams J.S. & Lloyd C.W. (ed.), Wiley-Liss, Inc., 111-137

Blom. N., Gammeltoft, S., Brunak, S. (1999): Sequence and structure-based prediction of eukaryotic protein phosphorylation sites. Journal of Molecular Biology **294**, 1351-62.

Bokros, C.L., Hugdahl, J.D., Kim, H.H., Hanesworth, V.R., Vanheerden, A., Browning, K.S. & Morejohn, L.C. (1995): Function of the P86 Subunit of Eukaryotic Initiation-Factor (Iso)4f as a Microtubule-Associated Protein in Plant-Cells. Proceedings of the National Academy of Sciences of the United States of America **92**, 7120-7124.

Bouquin, T., Mattsson, O., Naested, H., Foster, R. & Mundy, J. (2003): The Arabidopsis lue1 mutant defines a katanin p60 ortholog involved in hormonal control of microtubule orientation during cell growth. Journal of Cell Science **116**, 791-801.

Bowser, J. & Reddy, A.S.N. (1997): Localization of a kinesin-like calmodulin-binding protein in dividing cells of Arabidopsis and tobacco. Plant Journal **114**, 1417-1417.

Bradbury AF, Smyth DG. (1987) Biosynthesis of the C-terminal amide in peptide hormones. Bioscience Reports **7**, 907-16.

Bruce, W.B., Deng, X.W. & Quail, P.H. (1991): A Negatively Acting DNA-Sequence

Element Mediates Phytochrome- Directed Repression of Phya Gene-Transcription. Embo Journal **10**, 3015-3024.

Burk, D.H., Liu, B., Zhong, R.Q., Morrison, W.H. & Ye, Z.H. (2001): A katanin-like protein regulates normal cell wall biosynthesis and cell elongation. Plant Cell **13**, 807-827.

Burk, D.H. & Ye, Z.H. (2002): Alteration of oriented deposition of cellulose microfibrils by mutation of a katanin-like microtubule-severing protein. Plant Cell **14**, 2145-2160.

Burns, R.G. & Surridge, C.D. (1994): Functional-Role of a Consensus Peptide Which Is Common to Alpha-Tubulin, Beta-Tubulin, and Gamma-Tubulin, to Actin and Centractin, to Phytochrome-a, and to the Tcp1-Alpha-Chaperonin Protein. Febs Letters **347**, 105-111.

Cai, G., Romagnoli, S., Moscatelli, A., Ovidi, E., Gambellini, G., Tiezzi, A. & Cresti, M. (2000): Identification and characterization of a novel microtubule- based motor associated with membranous organelles in tobacco pollen tubes. Plant Cell **12**, 1719-1736.

Camilleri, C., Azimzadeh, J., Pastuglia, M., Bellini, C., Grandjean, O. & Bouchez, D. (2002): The Arabidopsis TONNEAU2 gene encodes a putative novel protein phosphatase 2A regulatory subunit essential for the control of the cortical cytoskeleton. Plant Cell **14**, 833-845.

Causier, B. & Davies, B. (2002): Analysing protein-protein interactions with the yeast two-hybrid system. Plant Molecular Biology **50**, 855-870.

Chaboute, M.E., Clement, B., Sekine, M., Philipps, G. & Chaubet-Gigot, N. (2000): Cell cycle regulation of the tobacco ribonucleotide reductase small subunit gene is mediated by E2F-like elements. Plant Cell **12**, 1987-1999.

Chan, J., Rutten, T. & Lloyd, C. (1996): Isolation of microtubule-associated proteins from carrot cytoskeletons: A 120 kDa map decorates all four microtubule arrays and the nucleus. Plant Journal **10**, 251-259.

Chan, J., Jensen, C.G., Jensen, L.C., Bush, M., Lloyd, C.W. (1999): The 65-kDa carrot microtubule-associated protein forms regularly arranged filamentous cross-bridges between microtubules. Proc Natl Acad Sci U S A. **96**,14931-14936.

Chan, J., Calder, G.M., Doonan, J.H. & Lloyd, C.W. (2003): EB1 reveals mobile

microtubule nucleation sites in Arabidopsis. Nature Cell Biology **5**, 967-971.

Chan, J., Mao, G.J., Smertenko, A., Hussey, P.J., Naldrett, M., Bottrill, A. & Lloyd, C.W. (2003): Identification of a MAP65 isoform involved in directional expansion of plant cells. Febs Letters **534**, 161-163.

Chang, E.J., Archambault V., McLachlin D.T., Krutchinsky A.N. & Chait B.T. (2004): Analysis of Protein Phosphorylation by Hypothesis-Driven Multiple-Stage Mass Spectometry. Analytical Chemistry **76**, 4472-4483.

Chen, C.B., Marcus, A., Li, W.X., Hu, Y., Calzada, J.P.V., Grossniklaus, U., Cyr, R.J. & Ma, H. (2002): The Arabidopsis ATK1 gene is required for spindle morphogenesis in male meiosis. Development **129**, 2401-2409.

Cleary, A.L. & Smith, L.G. (1998): The Tangled1 gene is required for spatial control of cytoskeletal arrays associated with cell division during maize leaf development. Plant Cell **10**, 1875-1888.

Clough, S.J. and Bent A.F. (1998): Floral dip: a simplified method for *Agrobacterium*-mediated transformation of *Arabidopsis thaliana*. The plant journal **16**, 735-743.

Cohen, S.N., Chang A.C.Y and Hsu L (1972): Nonchromosomal antibiotic resistance in bacteria: Genetic transformation of *Escherichia coli* by R-factor DNA Proc. Natl. acad. Sci **69**, 2110

Conrath, U., Pieterse, C.M.J. & Mauch-Mani, B. (2002): Priming in plant-pathogen interactions. Trends in Plant Science **7**, 210-216.

Cooper, J.A., Esch, F.S., Taylor, S.S. & Hunter, T. (1984): Phosphorylation Sites in Enolase and Lactate-Dehydrogenase Utilized by Tyrosine Protein-Kinases Invivo and Invitro. Journal of Biological Chemistry **259**, 7835-7841.

Cyr, R.J. & Palevitz, B.A. (1989): Microtubule-Binding Proteins from Carrot .1. Initial Characterization and Microtubule Bundling. Planta **177**, 245-260.

Cyr, R.J. (1991a): Microtubule Associated Proteins in higher plants. Lloyd, C.W. (ed.), Academic Press Limited, 57-67.

Cyr, R.J. (1991b): Calcium Calmodulin Affects Microtubule Stability in Lysed Protoplasts. Journal of Cell Science **100**, 311-317.

Daniel, X., Sugano, S. & Tobin, E.M. (2004): CK2 phosphorylation of CCA1 is necessary for its circadian oscillator function in Arabidopsis. Proceedings of the National Academy of Sciences of the United States of America **101**, 3292-3297.

Day, I.S., Miller, C., Golovkin, M. & Reddy, A.S.N. (2000): Interaction of a kinesin-like calmodulin-binding protein with a protein kinase. Journal of Biological Chemistry **275**, 13737-13745.

Deavours, B.E., Reddy, A.S.N. & Walker, R.A. (1998): Ca2+/calmodulin regulation of the Arabidopsis kinesin-like calmodulin-binding protein. Cell Motility and the Cytoskeleton **40**, 408-416.

Desai, A., Verma, S., Mitchison, T.J. & Walczak, C.E. (1999): Kin I kinesins are microtubule-destabilizing enzymes. Cell **96**, 69-78.

Dhonukshe, P. & Gadella, T.W.J. (2003): Alteration of microtubule dynamic instability during preprophase band formation revealed by yellow fluorescent protein-CLIP170 microtubule plus-end labeling. Plant Cell **15**, 597-611.

Dhonukshe P., Laxalt A.M., Goedhart J., Gadella T.W. & Munnik T. (2003): Phospholipase d activation correlates with microtubule reorganization in living plant cells. Plant Cell, **15**, 2666-2679

Diaz-Nido, J., Serrano, L., Hernandez, M.A. & Avila, J. (1990): Phosphorylation of Microtubule Proteins in Rat-Brain at Different Developmental Stages - Comparison with That Found in Neuronal Cultures. Journal of Neurochemistry **54**, 211-222.

Dixit, R. & Cyr, R. (2002): Golgi secretion is not required for marking the preprophase band site in cultured tobacco cells. Plant Journal **29**, 99-108.

Dunn, M.A., White, A.J., Vural, S. & Hughes, M.A. (1998): Identification of promoter elements in a low-temperature- responsive gene (blt4.9) from barley (Hordeum vulgare L.). Plant Molecular Biology **38**, 551-564.

Durso, N.A. & Cyr, R.J. (1994): A Calmodulin-Sensitive Interaction between Microtubules

and a Higher-Plant Homolog of Elongation Factor-1-Alpha. Plant Cell **6**, 893-905.

Durso, N.A., Leslie, J.D. & Cyr, R.J. (1996): In situ immunocytochemical evidence that a homolog of protein translation elongation factor EF-1 alpha is associated with microtubules in carrot cells. Protoplasma **190**, 141-150.

Edelmann, W., Zervas, M., Costello, P., Roback, L., Fischer, I., Hammarback, J.A., Cowan, N., Davies, P., Wainer, B. & Kucherlapati, R. (1996): Neuronal abnormalities in microtubule-associated protein 1B mutant mice. Proceedings of the National Academy of Sciences of the United States of America **93**, 1270-1275.

Erhardt, M., Stoppin-Mellet, V., Campagne, S., Canaday, J., Mutterer, J., Fabian, T., Sauter, M., Muller, T., Peter, C., Lambert, A.M. & Schmit, A.C. (2002): The plant Spc98p homologue colocalizes with gamma-tubulin at microtubule nucleation sites and is required for microtubule nucleation. Journal of Cell Science **115**, 2423-2431.

Feldbrugge, M., Hahlbrock, K. & Weisshaar, B. (1996): The transcriptional regulator CPRF1: Expression analysis and gene structure. Molecular & General Genetics **251**, 619-627.

Filonova, L.H., Bozhkov, P.V. & Von Arnold, S. (2000): Developmental pathway of somatic embryogenesis in Picea abies as revealed by time-lapse tracking. Journal of Experimental Botany **51**, 249-264.

Filonova, L.H., Von Arnold, S., Daniel, G. & Bozhkov, P.V. (2002): Programmed cell death eliminates all but one embryo in a polyembryonic plant seed. Cell Death and Differentiation **9**, 1057-1062.

Flotow, H., Graves, P.R., Wang, A.Q., Fiol, C.J., Roeske, R.W. & Roach, P.J. (1990): Phosphate Groups as Substrate Determinants for Casein Kinase-I Action. Journal of Biological Chemistry **265**, 14264-14269.

Freudenreich, A. & Nick, P. (1998): Microtubular organization in tobacco cells: Heat-shock protein 90 can bind to tubulin in vitro. Botanica Acta **111**, 273-279.

Friml, J. (2003): Auxin transport - shaping the plant. Current Opinion in Plant Biology **6**, 7-12.

Furutani, I., Watanabe, Y., Prieto, R., Masukawa, M., Suzuki, K., Naoi, K., Thitamadee, S., Shikanai, T. & Hashimoto, T. (2000): The SPIRAL genes are required for directional central of cell elongation in Arabidopsis thaliana. Development **127**, 4443-4453.

Gardiner, J.C., Harper, J.D.I., Weerakoon, N.D., Collings, D.A., Ritchie, S., Gilroy, S., Cyr, R.J. & Marc, J. (2001): A 90-kD phospholipase D from tobacco binds to microtubules and the plasma membrane. Plant Cell **13**, 2143-2158.

Gavel, Y. & Von Heijne, G. (1990): Sequence Differences between Glycosylated and Nonglycosylated Asn-X-Thr Ser Acceptor Sites - Implications for Protein Engineering. Protein Engineering **3**, 433-442.

Gietz, R.D., TriggsRaine, B., Robbins, A., Graham, K.C. & Woods, R.A. (1997): Identification of proteins that interact with a protein of interest: Applications of the yeast two-hybrid system. Molecular and Cellular Biochemistry **172**, 67-79.

Glass, D.B., El-Maghrabi, M.R. & Pilkis, S.J. (1986): Synthetic Peptides Corresponding to the Site Phosphorylated in 6-Phosphofructo-2-Kinase Fructose-2,6-Bisphosphatase as Substrates of Cyclic Nucleotide-Dependent Protein-Kinases. Journal of Biological Chemistry **261**, 2987-2993.

Hable, W.E. & Kropf, D.L. (1998): Roles of secretion and the cytoskeleton in cell adhesion and polarity establishment in Pelvetia compressa zygotes. Developmental Biology **198**, 45-56.

Hashimoto, T. (2002): Molecular genetic analysis of left-right handedness in plants. Philosophical transactions of the Royal Society of London Series B-Biological Sciences **357**, 799-808.

Hertzer, K.M., Ems-McClung S.C. & Walczak C.E. (2003): Kin I kinesins: insights into the mechanism of depolymerization. Crit Rev Biochem Mol Biol **38**, 453-469.

Himmelspach, R., Wymer, C.L., Lloyd, C.W. & Nick, P. (1999): Gravity-induced reorientation of cortical microtubules observed in vivo. Plant Journal **18**, 449-453.

Homma, N., Takei, Y., Tanaka, Y., Nakata, T., Terada, S., Kikkawa, M., Noda, Y. & Hirokawa, N. (2003): Kinesin superfamily protein 2A (KIF2A) functions in suppression of collateral branch extension. Cell **114**, 229-239.

Hoshi, M., Ohta, K., Gotoh, Y., Mori, A., Murofushi, H., Sakai, H. & Nishida, E. (1992): Mitogen-Activated-Protein-Kinase-Catalyzed Phosphorylation of Microtubule-Associated Proteins, Microtubule-Associated Protein-2 and Microtubule-Associated Protein-4, Induces an Alteration in Their Function. European Journal of Biochemistry **203**, 43-52.

Hugdahl JD & Morejohn, LC. (1993): Rapid and reversible high-affinity binding of the dinitroaniline herbicide Oryzalin to tubulin from Zea-Mays L. PLANT PHYSIOLOGY **102**, 725-740.

Hunter, A.W., Caplow, M., Coy, D.L., Hancock, W.O., Diez, S., Wordeman, L. & Howard, J. (2003): The kinesin-related protein MCAK is a microtubule depolymerase that forms an ATP-hydrolyzing complex at microtubule ends. Molecular Cell **11**, 445-457.

Hussey, P.J., Haas, N., Hunsperger, J., Larkin, J., Snustad, D.P. & Silflow, C.D. (1990): The Beta-Tubulin Gene Family in Zea-Mays - 2 Differentially Expressed Beta-Tubulin Genes. Plant Molecular Biology **15**, 957-972.

Hussey, P.J. & Hawkins, T.J. (2001): Plant microtubule-associated proteins: the HEAT is off in temperature-sensitive mor1. Trends in Plant Science **6**, 389-392.

Hussey, P.J., Hawkins, T.J., Igarashi, H., Kaloriti, D. & Smertenko, A. (2002): The plant cytoskeleton: recent advances in the study of the plant microtubule-associated proteins MAP-65, MAP-190 and the Xenopus MAP215-like protein, MOR1. Plant Molecular Biology **50**, 915-924.

Hussey, P.J. (2002): Cytoskeleton - Microtubules do the twist. Nature **417**, 128-129.

Howard J, Hyman AA (2003): Dynamics and mechanics of the microtubule plus end NATURE **422**, 753-758

Igarashi, H., Orii, H., Mori, H., Shimmen, T. & Sonobe, S. (2000): Isolation of a novel 190 kDa protein from tobacco BY-2 cells: Possible involvement in the interaction between actin filaments and microtubules. Plant and Cell Physiology **41**, 920-931.

Itzhaki, H., Maxson, J.M. & Woodson, W.R. (1994): An Ethylene-Responsive Enhancer Element Is Involved in the Senescence-Related Expression of the Carnation Glutathione-S-Transferase (Gsti) Gene. Proceedings of the National Academy of Sciences of the United

States of America **91**, 8925-8929.

Jiang, C.J. & Sonobe, S. (1993): Identification and Preliminary Characterization of a 65-Kda Higher-Plant Microtubule-Associated Protein. Journal of Cell Science **105**, 891-901.

Jiang, W., Jimenez, G., Wells, N.J., Hope, T.J., Wahl, G.M., Hunter T. & Fukunaga, R. (1998): PRC1: a human mitotic spindle-associated CDK substrate protein required for cytokinesis. Mol. Cell, **2**, 877-885.

Job, D., Valiron, O. & Oakley, B. (2003): Microtubule nucleation. Current Opinion in Cell Biology **15**, 111-117.

Kawasaki, H. & Kretsinger, R.H. (1995): Calcium-Binding Proteins .1. Ef-Hands. Protein Profile **2**, 305-490.

Ketelaar, T., Voss, C., Dimmock, S.A., Thumm, M. & Hussey P.J. (2004): Arabidopsis homologues of the autophagy protein Atg8 are a novel family of microtubule binding proteins. FEBS Lett. **567**, 302-6

Kim, J.K., Cao, J. & Wu, R. (1992): Regulation and Interaction of Multiple Protein Factors with the Proximal Promoter Regions of a Rice High Pi Alpha-Amylase Gene. Molecular & General Genetics **232**, 383-393.

King, S.M. (2002): Dyneins motor on in plants. Traffic **3**, 930-931.

Kinoshita, K., Arnal, I., Desai, A., Drechsel, D.N. & Hyman, A.A. (2001): Reconstitution of physiological microtubule dynamics using purified components. Science **294**, 1340-1343.

Kline-Smith, S.L. & Walczak, C.E. (2002): The microtubule-destabilizing kinesin XKCM1 regulates microtubule dynamic instability in cells. Molecular Biology of the Cell **13**, 2718-2731.

Kopczak, S.D., Haas, N.A., Hussey, P.J., Silflow, C.D. & Snustad, D.P. (1992): The Small Genome of Arabidopsis Contains at Least 6 Expressed Alpha-Tubulin Genes. Plant Cell **4**, 539-547.

Kost, B., Mathur, J. & Chua, N.H. (1999): Cytoskeleton in plant development. Current

Opinion in Plant Biology **2**, 462-470.

Lambert, A.M. & Lloyd, C.W. (1994): The higher plant microtubule cycle. Hyams S.J. & Lloyd C.W. (ed.), Wiley-Liss, Inc., 325-341.

Lancelle, S.A., Callaham, D.A. & Hepler, P.K. (1986): A Method for Rapid Freeze Fixation of Plant-Cells. Protoplasma **131**, 153-165.

Lee, Y.R.J. & Liu, B. (2000): Identification of a phragmoplast-associated kinesin-related protein in higher plants. Current Biology **10**, 797-800.

Lee, Y.R.J., Giang, H.M. & Liu, B. (2001): A novel plant kinesin-related protein specifically associates with the phragmoplast organelles. Plant Cell **13**, 2427-2439.

Lerouge, P., Cabanes-Macheteau, M., Rayon, C., Fischette-Laine, A.C., Gomord, V. & Faye, L. (1998): N-glycoprotein biosynthesis in plants: recent developments and future trends. Plant Molecular Biology **38**, 31-48.

Liu, B., Marc, J., Joshi, H.C. & Palevitz, B.A. (1993): A Gamma-Tubulin-Related Protein Associated with the Microtubule Arrays of Higher-Plants in a Cell Cycle-Dependent Manner. Journal of Cell Science **104**, 1217-1228.

Liu, B., Cyr, R.J. & Palevitz, B.A. (1996): A kinesin-like protein, KATAp, in the cells of arabidopsis and other plants. Plant Cell **8**, 119-132.

Liu, W., Xu, Z.H., Luo, D. & Xue, H.W. (2003): Roles of OsCKI1, a rice casein kinase I, in root development and plant hormone sensitivity. Plant Journal **36**, 189-202.

Lloyd, C., Shaw, P.J., Warn, R.M. & Yuan, M. (1996): Gibberellic-acid-induced reorientation of cortical microtubules in living plant cells. Journal of Microscopy-Oxford **181**, 140-144.

Lloyd, C. & Hussey, P. (2001): Microtubule-associated proteins in plants - Why we need a map. Nature Reviews Molecular Cell Biology **2**, 40-47.

Lloyd, C. & Chan, J. (2002): Helical microtubule arrays and spiral growth. Plant Cell **14**, 2319-2324.

Lloyd C., Chan, J. & Hussey P.J. (2003): Microtubules and microtubule-associated proteins. Hussey P.J. (ed.), Blackwell Publishing Ltd., 3-31

Lloyd, C. & Chan, J. (2004): Microtubules and the shape of plants to come. Nature Reviews Molecular Cell Biology **5**, 13-22.

Loog, M., Toomik, R., Sak, K., Muszynska, G., Jarv, J. & Ek, P. (2000): Peptide phosphorylation by calcium-dependent protein kinase from maize seedlings. European Journal of Biochemistry **267**, 337-343.

Mandal, A., Naaby-Hansen, S., Wolkowicz, M.J., Koltz, K., Shetty, J., Retief, J.D., Conrod, S.A., Kinter, M., Sherman, N., Cesar, F., Flickinger, C.J. & Herr, J.C. (1999): FSP95, a testis-specific 95-kilodalton fibrous sheath antigen that undergoes tyrosine phosphorylation in capacitated human spermatozoa. Biology of Reproduction **61**, 1184-1197.

Mandelkow, E.M. & Mandelkow, E. (1993): Tau as a Marker for Alzheimers-Disease. Trends in Biochemical Sciences **18**, 480-483.

Mandelkow, E. & Mandelkow, E.M. (1995): Microtubules and Microtubule-Associated Proteins. Current Opinion in Cell Biology **7**, 72-81.

Marc, J., Sharkey, D.E., Durso, N.A., Zhang, M. & Cyr, R.J. (1996): Isolation of a 90-kD microtubule-associated protein from tobacco membranes. Plant Cell **8**, 2127-2138.

Marco, H.G., Hansen, I.A., Scheller, K. & Gade, G. (2003): Molecular cloning and localization of a cDNA encoding a crustacean hyperglycemic hormone from the South African spiny lobster, Jasus lalandii. Peptides **24**, 845-851.

Marcus AI, Ambrose JC, Blickley L, Hancock WO, Cyr RJ (2002): Arabidopsis thaliana protein, ATK1, is a minus-end directed kinesin that exhibits non-processive movement Cell Motility and the Cytoskeleton **52**, 144-150

McNally, F.J., Okawa, K., Iwamatsu, A. & Vale, R.D. (1996): Katanin, the microtubule-severing ATPase, is concentrated at centrosomes. Journal of Cell Science **109**, 561-567.

Mineyuki, Y. & Gunning, B.E.S. (1990): A Role for Preprophase Bands of Microtubules in Maturation of New Cell-Walls, and a General Proposal on the Function of Preprophase

Band Sites in Cell-Division in Higher-Plants. Journal of Cell Science **97**, 527-537.

Mitsui, H., Yamaguchishinozaki, K., Shinozaki, K., Nishikawa, K. & Takahashi, H. (1993): Identification of a Gene Family (Kat) Encoding Kinesin-Like Proteins in Arabidopsis-Thaliana and the Characterization of Secondary Structure of Kata. Molecular & General Genetics **238**, 362-368.

Mitsui, H., Nakatani, K., Yamaguchishinozaki, K., Shinozaki, K., Nishikawa, K. & Takahashi, H. (1994): Sequencing and Characterization of the Kinesin-Related Genes Katb and Katc of Arabidopsis-Thaliana. Plant Molecular Biology **25**, 865-876.

Mitsui, H., Hasezawa, S., Nagata, T. & Takahashi, H. (1996): Cell cycle-dependent accumulation of a kinesin-like protein, KatB/C, in synchronized tobacco BY-2 cells. Plant Molecular Biology **30**, 177-181.

Mollinari, C., Kleman, J.P., Jiang, W., Schoehn, G., Hunter T. & Margolis, R.L. (2002): PRC1 is a microtubule binding and bundling protein essential to maintain the mitotic spindle midzone. Journal of Cell Biology **157**, 1175-1186.

Moore, R.C. & Cyr, R.J. (2000): Association between elongation factor-1 alpha and microtubules in vivo is domain dependent and conditional. Cell Motility and the Cytoskeleton **45**, 279-292.

Morejohn, L.C., Fosket D.E. (1991): The biochemistry of compounds with anti-microtubule activity in plant cells. Pharmacol Ther. **51**, 217-230

Moscatelli, A., Delcasino, C., Lozzi, L., Cai, G., Scali, M., Tiezzi, A. & Cresti, M. (1995): High-Molecular-Weight Polypeptides Related to Dynein Heavy- Chains in Nicotiana-Tabacum Pollen Tubes. Journal of Cell Science **108**, 1117-1125.

Muller, S., Fuchs, E., Ovecka, M., Wysocka-Diller, J., Benfey, P.N. & Hauser, M.T. (2002): Two new loci, PLEIADE and HYADE, implicate organ-specific regulation of cytokinesis in Arabidopsis. Plant Physiology **130**, 312-324.

Muller, S., Smertenko, A., Wagner, V., Heinrich, M., Hussey, P.J. & Hauser, M.T. (2004): The plant microtubule-associated protein AtMAP65-3/PLE is essential for cytokinetic phragmoplast function. Current Biology **14**, 412-417.

Murray, J.W., Edmonds, B.T., Liu, G. & Condeelis, J. (1996): Bundling of actin filaments by elongation factor 1 alpha inhibits polymerization at filament ends. Journal of Cell Biology **135**, 1309-1321.

Nebenfuhr, A., Frohlick, J.A. & Staehelin, L.A. (2000): Redistribution of Golgi stacks and other organelles during mitosis and cytokinesis in plant cells. Plant Physiology **124**, 135-151.

Nick, P., Lambert, A.M. & Vantard, M., (1995): A microtubule-associated protein in maize is expressed during phytochrome-induced cell elongation. Plant Journal **8**, 835-844.

Nishihama, R., Soyano, T., Ishikawa, M., Araki, S., Tanaka, H., Asada, T., Irie, K., Ito, M., Terada, M., Banno, H., Yamazaki, Y. & Machida, Y. (2002): Expansion of the cell plate in plant cytokinesis requires a kinesin-like protein/MAPKKK complex. Cell **109**, 87-99.

Oppenheimer, D.G., Pollock, M.A., Vacik, J., Szymanski, D.B., Ericson, B., Feldmann, K. & Marks, M.D. (1997): Essential role of a kinesin-like protein in Arabidopsis trichome morphogenesis. Proceedings of the National Academy of Sciences of the United States of America **94**, 6261-6266.

Panteris, E., Apostolakos, P., Graf, R. & Galatis, B. (2000): Gamma-tubulin colocalizes with microtubule arrays and tubulin paracrystals in dividing vegetative cells of higher plants. Protoplasma **210**, 179-187.

Park, S.C., Kwon, H.B. & Shih, M.C. (1996): Cis-acting elements essential for light regulation of the nuclear gene encoding the A subunit of chloroplast glyceraldehyde 3-phosphate dehydrogenase in Arabidopsis thaliana. Plant Physiology **112**, 1563-1571.

Park S.K., Howden R., Twell D. (1998): The Arabidopsis thaliana gametophytic mutation gemini pollen1 disrupts microspore polarity, division asymmetry and pollen cell fate Development **125**, 3789-3799.

Pasquali, G., Erven, A.S.W., Ouwerkerk, P.B.F., Menke, F.L.H. & Memelink, J. (1999): The promoter of the strictosidine synthase gene from periwinkle confers elicitor-inducible expression in transgenic tobacco and binds nuclear factors GT-1 and GBF. Plant Molecular Biology **39**, 1299-1310.

Pastuglia, M., Roby, D., Dumas, C. & Cock, J.M. (1997): Rapid induction by wounding

and bacterial infection of an S gene family receptor-like kinase gene in Brassica oleracea. Plant Cell **9**, 49-60.

Pellman, D., Bagget, M., Tu, H. & Fink, G.R. (1995): 2 Microtubule-Associated Proteins Required for Anaphase Spindle Movement in Saccharomyces-Cerevisiae. Journal of Cell Biology **130**, 1373-1385.

Petrasek, J., Freudenreich, A., Heuing, A., Opatrny, Z. & Nick, P. (1998): Heat-shock protein 90 is associated with microtubules in tobacco cells. Protoplasma **202**, 161-174.

Piechulla, B., Merforth, N. & Rudolph, B. (1998): Identification of tomato Lhc promoter regions necessary for circadian expression. Plant Molecular Biology **38**, 655-662.

Pinkse, M.W.H., Uitto, P.M., Hilhorst, M.J., Ooms, B. & Heck, A.J.R. (2004): Selective isolation at the femtomole level of phosphopeptides from proteolytic digests using 2D-nanoLC-ESI-MS/MS and titanium oxide precolumns. Analytical Chemistry **76**, 3935-3943.

Pinna, L.A. (1990): Casein Kinase-2 - an Eminence-Grise in Cellular-Regulation. Biochimica Et Biophysica Acta **1054**, 267-284.

Popov, A.V., Severin, F. & Karsenti, E. (2002): XMAP215 is required for the microtubule-nucleating activity of centrosomes. Current Biology **12**, 1326-1330.

Preuss, M.L., Delmer, D.P. & Liu, B. (2003): The cotton kinesin-like calmodulin-binding protein associates with cortical microtubules in cotton fibers. Plant Physiology **132**, 154-160.

Ransom-Hodgkins, W.D., Brglez, I., Wang, X.M. & Boss, W.F. (2000): Calcium-regulated proteolysis of eEF1A. Plant Physiology **122**, 957-965.

Raven, P.H., Evert, R.F & Eichhorn, S.E. (1992): Biology of Plants, Fifth Edition, Worth Publishers, 453-469, 545-572.

Reddy, A.S. & Day, I.S. (2001): Kinesins in the Arabidopsis genome: a comparative analysis among eukaryotes. BMC Genomics **2**, Electronic publication

Reddy VS, Day IS, Thomas T, Reddy AS. (2003): KIC, a novel Ca2+ binding protein with one EF-hand motif, interacts with a microtubule motor protein and regulates trichome morphogenesis. Epub 2003. Plant Cell.**16**, (2004), 185-200.

Rogers, G.C., Rogers, S.L., Schwimmer, T.A., Ems-McClung, S.C., Walczak, C.E., Vale, R.D., Scholey, J.M. & Sharp, D.J. (2004): Two mitotic kinesins cooperate to drive sister chromatid separation during anaphase. Nature **427**, 364-370.

Rombauts, S., Dehais, P., Van Montagu, M. & Rouze, P. (1999): PlantCARE, a plant cis-acting regulatory element database. Nucleic Acids Research **27**, 295-296.

Rouster, J., Leah, R., Mundy, J. & CameronMills, V. (1997): Identification of a methyl jasmonate-responsive region in the promoter of a lipoxygenase 1 gene expressed in barley grain. Plant Journal **11**, 513-523.

Rushton, P.J., Reinstadler, A., Lipka, V., Lippok, B. & Somssich, I.E. (2002): Synthetic plant promoters containing defined regulatory elements provide novel insights into pathogen- and wound- induced signaling. Plant Cell **14**, 749-762.

Rutten, T., Chan, J. & Lloyd, C.W. (1997): A 60-kDa plant microtubule-associated protein promotes the growth and stabilization of neurotubules in vitro. Proceedings of the National Academy of Sciences of the United States of America **94**, 4469-4474.

Sakai, T., Takahashi, Y. & Nagata, T. (1996): Analysis of the promoter of the auxin-inducible gene, parC, of tobacco. Plant and Cell Physiology **37**, 906-913.

Sambrook, J., & Russel, D.W. (2001): Molecular Cloning, a laboratory manual, Cold Spring Harbor Laboratory Press.

Sawano, M., Shimmen, T. & Sonobe, S. (2000): Possible involvement of 65 kDa MAP in elongation growth of azuki bean epicotyls. Plant and Cell Physiology **41**, 968-976.

Saxton, W.M., Stemple, D.L. & McIntosh, J.R. (1984): Microinjection of Colchicine Bound Tubulin into Tissue-Culture Cells - Colchicine Acts as a Substoichiometric Microtubule Poison Invivo. Journal of Cell Biology **99**, A38-A38.

Schmit, A.C. & Lambert, A.M. (1990): Microinjected Fluorescent Phalloidin *In vivo* Reveals the F-Actin Dynamics and Assembly in Higher-Plant Mitotic Cells. Plant Cell **2**,

129-138.

Schmit, A.C. (2002): Acentrosomal microtubule nucleation in higher plants. In: International Review of Cytology - a Survey of Cell Biology, Vol 220, 257-289.

Schuyler, S.C., Liu, J.Y. & Pellman, D.J. (2003): The molecular function of Ase1p: evidence for a MAP-dependent midzone-specific matrix.. Journal of Cell Biology **160**, 517-528.

Sedbrook, J.C., Ehrhardt, D.W., Fisher, S.E., Scheible, W.R. & Somerville, C.R. (2004): The Arabidopsis SKU6/SPIRAL1 gene encodes a plus end-localized microtubule-interacting protein involved in directional cell expansion. Plant Cell **16**, 1506-1520.

Shah. J. & Klessig D.F. (1996): Identification of a salicylic acid-responsive element in the promoter of the tobacco pathogenesis-related beta-1,3-glucanase gene, PR-2d. Plant Journal **10**, 1089-1101.

Sharp, D.J., Brown, H.M., Kwon, M., Rogers, G.C., Holland, G. & Scholey, J.M. (2000): Functional coordination of three mitotic motors in Drosophila embryos. Molecular Biology of the Cell **11**, 241-253.

Shaw, J.P., Fairbairn, J.D. & Lloyd, W.,C. (1991): Cytoplasmic and nuclear intermediate filament antigens in higher plant cells. C.W. Lloyd, ed. (Academic Press Limited), pp. 69-81

Shaw, S.L., Kamyar, R. & Ehrhardt, D.W. (2003): Sustained microtubule treadmilling in Arabidopsis cortical arrays. Science **300**, 1715-1718.

Segui-Simarro, J.M., Austin II, J.R., White, E.A. & Staehelin, L.A. (2004): Electron tomographic analysis of somatic cell plate formation in meristematic cells of arabidopsis preserved by high-pressure freezing. The Plant Cell **16**, 836-856

Showfford, D.L. (1991): PAUP: Phylogenetic Analysis Using Parsimony, Version 3.1, Computer program distributed by the Illinois Natural History Survey, Champaign, Illinois.

Singh, H., LeBowitz, A.S., Baldwin J. & Sharp, P.A. (1988). Molecular cloning of an enhancer binding protein: Isolation by screening of an expression library with a recognition site DNA Cell **52**, 415

Smertenko, A.P., Lawrence, S.L. & Hussey, P.J. (1998): Immunological homologues of the Arabidopsis thaliana beta 1 tubulin are polyglutamylated in Nicotiana tabacum. Protoplasma **203**, 138-143.

Smertenko, A., Saleh, N., Igarashi, H., Mori, H., Hauser-Hahn, I., Jiang, C.J., Sonobe, S., Lloyd, C.W. & Hussey, P.J. (2000): A new class of microtubule-associated proteins in plants. Nature Cell Biology **2**, 750-753.

Smertenko, A.P., Bozhkov, P.V., Filonova, L.H., Von Arnold, S. & Hussey, P.J. (2003): Re-organisation of the cytoskeleton during developmental programmed cell death in Picea abies embryos. Plant Journal **33**, 813-824.

Smertenko, A.P., Chang, H.Y., Wagner, V., Kaloriti, D., Fenyk, S., Sonobe, S., Lloyd, C., Hauser, M.T. & Hussey, P.J. (2004): The Arabidopsis microtubule-associated protein AtMAP65-1: Molecular analysis of its microtubule bundling activity. Plant Cell **16**, 2035-2047.

Smirnova, E.A., Wawrowsky, K.A. & Bajer, A.S. (1992): Microtubule Nucleating Centers Reflect Microtubule Polarity in Interphase and Mitosis of Higher-Plant Haemanthus. Molecular Biology of the Cell **3**, A343-A343.

Smirnova, E.A., Reddy, A.S.N., Bowser, J. & Bajer, A.S. (1998): Minus end-directed kinesin-like motor protein, Kcbp, localizes to anaphase spindle poles in Haemanthus endosperm. Cell Motility and the Cytoskeleton **41**, 271-280.

Smith, H.M.S. & Raikhel, N.V. (1998): Nuclear localization signal receptor importin alpha associates with the cytoskeleton. Plant Cell **10**, 1791-1799.

Smith, L.G., Gertulla, S.M., Han, S. & Levy, J. (2001): TANGLED1: a microtubule binding protein required for the spatial control of cytokinesis in maize. Journal of Cell Biology **152**, 231-236.

Snustad, D.P., Haas, N.A., Kopczak, S.D. & Silflow, C.D. (1992): The Small Genome of Arabidopsis Contains at Least 9 Expressed Beta-Tubulin Genes. Plant Cell **4**, 549-556.

Sollner, R., Glasser, G., Wanner, G., Somerville, C.R., Jurgens, G. & Assaad, F.F. (2002): Cytokinesis-defective mutants of Arabidopsis. Plant Physiology **129**, 678-690.

Sorensen, A., Guerineau, F., Canales-Holzeis, C., Dickinson, H.G. & Scott, R.J. (2002): A novel extinction screen in Arabidopsis thaliana identifies mutant plants defective in early microsporangial development. Plant Journal **29**, 581-594.

Soyano, T., Nishihama, R., Morikiyo, K., Ishikawa, M. & Machida, Y. (2003): NQK1/NtMEK1 is a MAPKK that acts in the NPK1 MAPKKK-mediated MAPK cascade and is required for plant cytokinesis. Genes & Development **17**, 1055-1067.

Staiger, C.J. & Cande, W.Z. (1991): Microfilament Distribution in Maize Meiotic Mutants Correlates with Microtubule Organization. Plant Cell **3**, 637-644.

Stals, H., Bauwens, S., Traas, J., VanMontagu, M., Engler, G. & Inze, D. (1997): Plant CDC2 is not only targeted to the pre-prophase band, but also co-localizes with the spindle, phragmoplast, and chromosomes. Febs Letters **418**, 229-234.

Stoppin, V., Vantard, M., Schmit, A.C. & Lambert, A.M. (1994): Isolated Plant Nuclei Nucleate Microtubule Assembly - the Nuclear-Surface in Higher-Plants Has Centrosome-Like Activity. Plant Cell **6**, 1099-1106.

Stoppin-Mellet, V., Gaillard, J. & Vantard, M. (2002): Functional evidence for in vitro microtubule severing by the plant katanin homologue. Biochemical Journal **365**, 337-342.

Strompen, G., El Kasmi, F., Richter, S., Lukowitz, W., Assaad, F.F., Jurgens, G. & Mayer, U. (2002): The Arabidopsis HINKEL gene encodes a kinesin-related protein involved in cytokinesis and is expressed in a cell cycle- dependent manner. Current Biology **12**, 153-158.

Sugimoto, K., Williamson, R.E. & Wasteneys, G.O. (2001): Wall architecture in the cellulose-deficient rsw1 mutant of Arabidopsis thaliana: microfibrils but not microtubules lose their transverse alignment before microfibrils become unrecognizable in the mitotic and elongation zones of roots. Protoplasma **215**, 172-183.

Tamura, K., Nakatani, K., Mitsui, H., Ohashi, Y. & Takahashi, H. (1999): Characterization of katD, a kinesin-like protein gene specifically expressed in floral tissues of Arabidopsis thaliana. Gene **230**, 23-32.

Thitamadee S, Tuchihara K & Hashimoto,T. (2002): Microtubule basis for left-handed

helical growth in Arabidopsis. NATURE **417**, 193-196.

Thomas, S.G. & Sun, T.P. (2004): Update on gibberellin signaling. A tale of the tall and the short. Plant Physiology **135**, 668-676.

Tirnauer, J.S., Grego, S., Salmon, E.D. & Mitchison, T.J. (2002): EB1-microtubule interactions in Xenopus egg extracts: Role of EB1 in microtubule stabilization and mechanisms of targeting to microtubules. Molecular Biology of the Cell **13**, 3614-3626.

Topping, J.F., Wei, W.B. & Lindsey, K. (1991): Functional Tagging of Regulatory Elements in the Plant Genome. Development **112**, 1009-1019.

Tournebize, R., Popov, A., Kinoshita, K., Ashford, A.J., Rybina, S., Pozniakovsky, A., Mayer, T.U., Walczak, C.E., Karsenti, E. & Hyman, A.A. (2000): Control of microtubule dynamics by the antagonistic activities of XMAP215 and XKCM1 in Xenopus egg extracts. Nature Cell Biology **2**, 13-19.

Twell, D., Park, S.K., Hawkins, T.J., Schubert, D., Schmidt, R., Smertenko, A. & Hussey, P.J. (2002): MOR1/GEM1 has an essential role in the plant-specific cytokinetic phragmoplast. Nature Cell Biology **4**, 711-714.

Vale, R.D. and Fletterick, R.J. (1997): The design plan of kinesin motors. Annu Rev Cell Dev Biol. **13**, 745-777.

Vantard, M., Schellenbaum, P., Fellous, A. & Lambert, A.M. (1991): Characterization of Maize Microtubule-Associated Proteins, One of Which Is Immunologically Related to Tau. Biochemistry **30**, 9334-9340.

Vanyushin, B.F., Bakeeva, L.E., Zamyatnina, V.A. & Aleksandrushkina, N.I. (2004): Apoptosis in plants: Specific features of plant apoptotic cells and effect of various factors and agents. In: International Review of Cytology - a Survey of Cell Biology, Vol. 233, pp. 135-179.

Vasquez, R.J., Gard, D.L. & Cassimeris, L. (1994): Xmap from Xenopus Eggs Promotes Rapid Plus End Assembly of Microtubules and Rapid Microtubule Polymer Turnover. Journal of Cell Biology **127**, 985-993.

Verde, F., Labbe, J.C., Doree, M. & Karsenti, E. (1990): Regulation of Microtubule

Dynamics by Cdc2 Protein-Kinase in Cell-Free-Extracts of Xenopus Eggs. Nature **343**, 233-238.

Vinson, C.R., LaMarco, K.L., Johnson, W.H. & McKnight S.L. (1988): In situ detection of sequence-specific DNA binding activity specified by a recombinant bacteriophage. Genes Dev. **2**, 801

Von Arnold, S., Sabala, I., Bozhkov, P., Dyachok, J. & Filonova, L. (2002): Developmental pathways of somatic embryogenesis. Plant Cell Tissue and Organ Culture **69**, 233-249.

Vos, J.W., Safadi, F., Reddy, A.S.N. & Hepler, P.K. (2000): The kinesin-like calmodulin binding protein is differentially involved in cell division. Plant Cell **12**, 979-990.

Wadsworth, P. & Shelden, E. (1990): Microtubule Assembly in the Mitotic Spindle. Annals of the New York Academy of Sciences **582**, 312-313.

Walczak, C.E. & Mitchison, T.J. (1996a): Kinesin-related proteins at mitotic spindle poles: Function and regulation. Cell **85**, 943-946.

Walczak, C.E., Mitchison, T.J. & Desai, A. (1996b): XKCM1: A Xenopus kinesin-related protein that regulates microtubule dynamics during mitotic spindle assembly. Cell **84**, 37-47.

Wang, X.M. (1999): The role of phospholipase D in signaling cascades. Plant Physiology **120**, 645-651.

Washida, H., Wu, C.Y., Suzuki, A., Yamanouchi, U., Akihama, T., Harada, K. & Takaiwa, F. (1999): Identification of cis-regulatory elements required for endosperm expression of the rice storage protein glutelin gene GluB-1. Plant Molecular Biology **40**, 1-12.

Wasteneys, G.O. (2000): The cytoskeleton and growth polarity. Current Opinion in Plant Biology **3**, 503-511.

Wasteneys, G.O. (2002): Microtubule organization in the green kingdom: chaos or self-order? Journal of Cell Science **115**, 1345-1354.

Webb, M., Jouannic, S., Foreman, J., Linstead, P. & Dolan, L. (2002): Cell specification in the Arabidopsis root epidermis requires the activity of ECTOPIC ROOT HAIR 3 - a

katanin-p60 protein. Development **129**, 123-131.

Whittington, A.T., Vugrek, O., Wei, K.J., Hasenbein, N.G., Sugimoto, K., Rashbrooke, M.C. & Wasteneys, G.O. (2001): MOR1 is essential for organizing cortical microtubules in plants. Nature **411**, 610-613.

Wicker-Planquart, C., Stoppin-Mellet, V., Blanchoin, L. & Vantard, M. (2004): Interactions of tobacco microtubule-associated protein MAP65-1b with microtubules. Plant Journal **39**, 126-134.

Wymer, C. & Lloyd, C. (1996): Dynamic microtubules: Implications for cell wall patterns. Trends in Plant Science **1**, 222-228.

Yamaguchi-Shinozaki, K. & Shinozaki, K. (1994): A Novel Cis-Acting Element in an Arabidopsis Gene Is Involved in Responsiveness to Drought, Low-Temperature, or High-Salt Stress. Plant Cell **6**, 251-264.

Yasuhara, H., Muraoka, M., Shogaki, H., Mori, H. & Sonobe, S. (2002): TMBP200, a microtubule bundling polypeptide isolated from telophase tobacco BY-2 cells is a MOR1 homologue. Plant and Cell Physiology **43**, 595-603.